Unveiling Novel Participants in the DNA Damage Response



DPhil Candidate: Sujun Li

Supervisor: Prof. Martin Cohn

The Wolfson College

Department of Biochemistry

University of Oxford

Trinity Term 2023

Acknowledgements

I would like to take this opportunity to express my sincere gratitude to all those who have supported me throughout my DPhil journey. Their invaluable guidance, encouragement, and assistance played a pivotal role in the successful completion of this thesis.

First, I am grateful for the mentorship of my supervisor, Martin Cohn, for his expertise and invaluable guidance throughout this research endeavour. His insightful feedback, patience, and constant motivation have been instrumental in shaping the direction of my work. I would also like to thank my thesis committee members, Paul Elliott and Benoit Kornmann, as well as my confirmation examiners, Lars Jansen and Andre Furger, for their input and suggestions during the transfer and confirmation processes. Their insightful comments, constructive criticism, and intellectual discussions have been invaluable in broadening my perspective and enhancing the quality of my research. Additionally, I would like to express my gratitude to Professor Nicholas Proudfoot and Professor Tim Knott for their advice and guidance on my projects.

A special thank you goes to the China Scholarship Council - University of Oxford Scholarships, whose generous financial support, both in study fees and living expenses, enabled me to commence my study at Oxford and successfully complete my DPhil journey. Without their assistance, this achievement would not have been possible.

I would also like to express my gratitude to Professor Lidia Vasilieva for her patient guidance in teaching me the techniques required for Northern Blot analysis. Moreover, I extend my thanks to my lab members, Kelvin Yaprianto, Di Yang, Qiang Luo, Hannan Xu and Fengxiang Bai, for their kind guidance and support in imparting experimental skills. Their willingness to assist and patience in answering my countless questions have played an essential role in refining my experimental abilities and ensuring the success of my experiments.

Throughout my DPhil, the world faced an unprecedented challenge in the form of the COVID-19 pandemic. The emotional support and understanding I received from my family, friends, roommates, and lab members have been indispensable during this difficult time. Their constant encouragement, virtual gatherings, and unwavering belief in me provided the strength and resilience needed to persevere. In this regard, I want to express my special thanks to my parents,

Jie Li and Yan Gong, as well as my college advisor, Paul Aveyard, for their support that helped me navigate the difficulties faced during the pandemic.

Lastly, I would like to extend my deepest gratitude to all those who may not be named but have contributed in their own unique ways to the completion of this thesis. Whether it was through a kind word, a stimulating discussion, or a helping hand, your support made a significant impact on my journey. I am truly humbled and grateful for all the kindness and support I have received. Thank you for being integral to my academic and personal growth.

Abstract

The human genome is constantly challenged by DNA damage resulting from environmental factors and metabolic processes. To safeguard the integrity of the genome, a complex defence system known as the DNA damage response (DDR) has evolved. The DDR comprises intricate mechanisms, including DNA repair pathways, damage tolerance processes, cell cycle checkpoints and programmed cell death, together aimed at maintaining genomic stability. Among the various types of DNA lesions, interstrand crosslinks (ICLs) pose a significant threat as they impede DNA replication and transcription. Inadequate repair of ICLs is closely linked to Fanconi anaemia (FA), a genetic disorder associated with severe health consequences. Moreover, ICL-inducing agents have a broad clinical application in cancer therapy, although the emergence of drug resistance poses a challenge. Therefore, comprehending the mechanisms involved in ICL repair is critical for developing alternative treatment strategies and enhancing drug sensitivity.

The focus of this DPhil thesis is to investigate the participation and function of two novel proteins in the cellular response to ICL-induced DNA damage. Rapid accumulation of the first protein at ICL sites is observed, and its knockout results in heightened cellular sensitivity to ICL-inducing agents, indicating its positive contribution to cell survival against ICLs. Further investigations revealed that this protein operates independently of the established FA and NEIL3 pathway for ICL repair, suggesting its potential role in alternative repair mechanisms or early-stage DDR processes. The second novel protein exhibits a distinct relocation from the nucleoplasm to the peripheral nucleoli, forming a ring-shaped accumulation pattern in response to ICLs. Additional experiments demonstrate that this protein translocates into the nucleolar cap under nucleolar stress induced by various types of DNA damage and transcription inhibition. These findings support the notion that the nucleolus acts as a stress sensor, and the nucleolar translocation of this novel protein potentially contributes to cellular fate decisions or the interplay between DDR and nucleolar function. Together, the research presented in this thesis provides insights into the roles of two new protein players in preserving genomic stability. Understanding their interactions with established repair pathways and their potential therapeutic implications in FA and cancer treatment will pave the way for developing targeted interventions and improving patient outcomes.

Table of Contents

Acknowledgements **2**

Abstract **4**

Abbreviations **7**

Chapter 1. Introduction **13**

1.1 DNA Damage **13**

1.1.1 Sources of DNA Damage 13

1.1.2 Types of DNA Damage 15

1.1.3 DNA Damage and Disease 22

1.2 DNA Damage Response (DDR) **28**

1.2.1 DDR Proteins 28

1.2.2 DNA Repair Pathways 31

1.2.3 DNA Damage Tolerance 42

1.2.4 DNA Replication Stress 43

1.3 DNA Interstrand Crosslink (ICL) and ICL Repair **48**

1.3.1 Sources of ICL 48

1.3.2 Defective ICL Repair and Fanconi Anaemia (FA) 54

1.3.3 ICL Repair Pathways 56

1.4 The Nucleolus and Nucleolar Stress **71**

1.4.1 The Nucleolus and Its Function 71

1.4.2 Nucleolar Stress 73

1.4.3 The Nucleolus and DNA Damage Response 76

Chapter 2. Identification of Regulator of Chromatin Condensation 2 (RCC2) as a Novel Player in ICL Repair **79**

2.1 Introduction **79**

2.2 Results **89**

2.2.1 RCC2 knockout sensitises Hela cells to TMP/UVA and MMC treatments 89

2.2.2 RCC2 does not physically interact with DNA probes in vitro 92

2.2.3 RCC2 is not involved in the FA pathway for ICL repair 94

2.2.4 Exploring the connection between RCC2 and the NEIL3 repair pathway 98

2.2.5 Partial depletion of NEIL3 further sensitises RCC2-deficient cells to psoralen-induced ICLs 101

2.3 Discussion 104

Chapter 3. Exploring the Involvement of Zinc Finger Protein 638 (ZFN638) in DNA Damage Response 108

3.1 Introduction 108

3.2 Results 112

3.2.1 ZNF638 re-localises to nucleoli upon ICL formation 112

3.2.2 The presence of ICL diminishes the interaction between ZNF638 and DNA in vitro 116

3.2.3 The nucleolar re-localisation of ZNF638 is a general response to genetic instabilities 118

3.2.4 ZNF638 depletion increases HeLa cell sensitivity to DNA damage-inducing reagents 120

3.2.5 Exploration of factors affecting the ZNF638 nucleolar re-localisation 121

3.2.6 ZNF638 deficiency affects ribosomal RNA synthesis 125

3.2.7 Rapid reduction in ZNF638 protein level has no effect on rRNA synthesis 130

3.2.8 Identification of ZNF638 binding partners 133

3.3 Discussion 140

Chapter 4. Discussion 146

Chapter 5. Materials and Methods 156

Chapter 6. References 174

Abbreviations

3′ UTR	3′ untranslated region
5-EU	5-ethynyl uridine
53BP1	p53-binding protein 1
6-4 PP	6–4 photoproduct
8-oxo-dG	8-oxo-7,8-dihydroguanine
9-1-1 clamp	RAD9-RAD1-HUS1 clamp
A-T	Ataxia-telangiectasia
AA-ICL	acetaldehyde-induced ICL
Act D	actinomycin D
AlkB	Alkylation B
ALKBH	Alkylation Repair Homologs
alt-NHEJ	Alternative nonhomologous end-joining
AML	acute myeloid leukaemia
AP site	Apurinic/apyrimidinic site / Abasic site
APE1	AP endonuclease 1
ARF6	Adenosine 5′-diphosphate ribosylation factor 6
ATM	ataxia-telangiectasia mutated
ATR	ATM RAD3-related
BARD1	BRCA1 associated RING domain 1
BER	base excision repair
BLM	RecQ like helicase
BRCA1/2	Breast cancer type 1/2 susceptibility protein
BRD4	Bromodomain containing protein 4
BS	Bloom syndrome
C/EBP	CCAAT/enhancer-binding protein
CDC45	cell division cycle 45
CDK	cyclin-dependent kinase
CETN2	centrin 2
CHK1/2	checkpoint kinase 1/2
CK2	casein kinase 2
CLL	chronic lymphocytic leukaemia
CMG complex	CDC45-MCM2–7-GINS complex

co-IP	co-immunoprecipitation
CORO1C	coronin-1C
CPC	chromosomal passenger complex
CPD	Cyclobutane pyrimidine dimer
CPT	Camptothecin
CREB	cAMP response element binding protein
CRISPR	Clustered regularly interspaced palindromic repeats
CSA/CSB	Cockayne syndrome protein A/B
CtIP	CtBP-interacting protein
D-loop	displacement loop
DDR	DNA damage response
DEB	Diepoxybutane
DNA-PKcs	DNA-dependent protein kinase catalytic subunit
DNA2	DNA replication helicase/nuclease 2
DNL	*de novo* lipogenesis
DSB	double-strand break
dTAG	$FKBP12^{F36V}$ degron tag
EME1	Essential meiotic structure-specific endonuclease 1
EMSA	Electrophoretic Mobility Shift Assay
EMT	epithelial–mesenchymal transition
ERCC1	ERCC excision repair 1
ESCC	oesophageal squamous cell carcinoma
EXO1	exonuclease 1
FA	Fanconi anaemia
FAAP	Fanconi-associated protein
FAN1	FANCD2 and FANCI associated nuclease 1
FEN1	flap endonuclease 1
FH tag	Flag-HA tag
FHL2	four-and-a-half LIM-only protein 2
FTO	Fat Mass and Obesity associated
GEF	guanine nucleotide exchange factor
GG-NER	global genomic NER
GINS	go-ichi-ni-san

GSK3B	glycogen synthase kinase 3 beta
H2AK15ub	H2A Lys15 ubiquitylation
H4K20me2	dimethylated H4 Lys20
HDAC	histone deacetylase
HIF-1α	Hypoxia-inducible factor 1 alpha
HLA	human leukocyte antigen
hnRNP	heterogeneous nuclear ribonucleoprotein
HNSCC	head and neck squamous cell carcinoma
HR	homologous recombination
HSC	hematopoietic stem cell
HSC70	Heat shock cognate protein 70
HSCT	Hematopoietic stem cell transplantation
HUSH complex	human silencing hub complex
ICL	Interstrand crosslink
IGF2BP3	Insulin-like growth factor 2 mRNA-binding protein 3
ING1	Inhibitor of growth family member 1
IR	Ionizing radiation
IRBC	impaired ribosome biogenesis checkpoint
LCPAT1	lung cancer progression association transcript 1
LIG	DNA ligase
lncRNA	long non-coding RNA
MCL-1	Myeloma cell leukemia-1
MCM2–7	minichromosome maintenance 2–7
MDC1	DNA-damage Checkpoint Protein 1
MDM2/4	Mouse double minute 2/4
MECP2	methyl-CpG binding protein 2
MGMT	O^6-methylguanine-DNA methyltransferase
MHF	Histone-fold heterodimer
miRNA	MicroRNA
MLV	murine leukemia virus
MMC	Mitomycin C
MMEJ	microhomology-mediated end joining
MMR	mismatch repair

MRN complex	MRE11/RAD50/NBS1 complex
MS-MS	tandem mass spectrometry
MSH	MutS homologues
NBS	Nijmegen breakage syndrome
NCL	nucleolin
NEIL3	nei like DNA glycosylase 3
NER	nucleotide excision repair
NF-κB	Nuclear factor-κB
NHEJ	Non-homologous end joining
NOR	nucleolar organizer region
NPM	Nucleophosmin
NSCLC	non-small cell lung carcinoma
OGG1	8-oxo-guanine glycosylase 1
$p14^{ARF}$	ARF tumor suppressor
PAH	Polycyclic aromatic hydrocarbon
PAK4	P21-activated kinase 4
PALB2	Partner and Localizer of BRCA2
PARP	Poly (ADP-ribose) polymerase
PAXX	paralogue of XRCC4 and XLF
PCNA	proliferating cell nuclear antigen
PI3K	phosphoinositide-3-kinase
PIKK	phosphatidylinositol 3-kinase-like protein kinase
PKB/Akt	Protein kinase B
PLK1	polo-like kinase 1
PML	Promyelocytic leukaemia protein
PNKP	polynucleotide kinase/phosphatase
DNA/RNA Pol	DNA/RNA polymerase
PPAR	peroxisome proliferator-activated receptor
pre-rRNA	precursor ribosomal RNA
PRIMPOL	Primase and DNA directed polymerase
PSF	PTB-associated splicing factor
PTM	post-translational modification
rAAV	recombinant adeno-associated virus

RAD23B	Rad 23 homolog B
RAD51AP1	RAD51-associated protein 1
RALBP1	RAL binding protein-1
RCC2	Regulator of chromosome condensation 2
rDNA	ribosomal DNA
RFC	replication factor C
RIF1	Replication timing regulatory factor 1
RIR	replication-independent repair
RNAi	RNA interference
RNF	Ring finger protein
ROS	Reactive oxygen species
RP	ribosomal proteins
RPA	replication protein A
RRM	RNA recognition motif
RS domain	arginine/serine-rich domain
RUVBL1/2	RuvB like AAA ATPase 1/2
SAM	S-adenosylmethionine
SAN1	Senataxin-associated nuclease 1
SAPK	Stress-Activated map Kinase
SENP3	SUMO specific peptidase 3
SETDB1	SET Domain Bifurcated Histone Lysine Methyltransferase 1
SIRT7	sirtuin 7
SL-1	Selective factor 1
SLX	Structure-specific endonuclease subunit SLX
snoRNA	small nucleolar RNA
SSA	single-strand annealing
SSB	single-strand break
TC-NER	transcription-coupled NER
TCOF1/Treacle	Treacle Ribosome Biogenesis Factor 1
TCR	transcription-coupled repair
TD60	Telophase Disk-60
TDP1	tyrosyl DNA phosphatase 1
TFIIS	Transcription elongation factor IIS

TIF-IA	Transcription initiation factor-IA
TLS	translesion synthesis
TMP	trimethylpsoralen
TNF	Tumor necrosis factor
TOP1	DNA topoisomerase 1
TOPBP1	DNA topoisomerase 2-binding protein 1
TRAIP	TRAF Interacting Protein
TS	template switching
UAF1	USP1-associated factor 1
UBE2M/UBE2T	ubiquitin conjugating enzyme E2 M/T
UBF	Upstream binding factor
UHRF1/UHRF2	Ubiquitin-like with PHD and RING finger domains 1/2
USP	Ubiquitin specific peptidase
UV	Ultraviolet
VHL	von Hippel-Lindau tumor-suppressor protein
XAB2	XPA-binding protein-2
XLF	XRCC4-like factor
XPC/XPG/XPF	Xeroderma pigmentosum group C/G/F
XRCC	X-ray repair cross complementing
ZNF638	Zinc finger protein 638

Chapter 1. Introduction

1.1 DNA Damage

DNA is the fundamental unit of heredity, as it contains the genetic information necessary for the continuation of life. The integrity of DNA is of the utmost importance for all living organisms. As defined by Benjamin Lewin in his textbook "Genes", DNA damage is "Damage to DNA consisting of any change that introduces a deviation from the usual double-helical structure". Thus, any event that disrupts the structural integrity of the DNA molecule or alters the sequence of its building blocks constitutes DNA damage (Lewin, 2004). In humans, a significant proportion of cells are subject to continuous DNA damage resulting from environmental factors and normal metabolic processes within the body, with an estimated rate of 1×10^4 to 1×10^6 molecular lesions per cell per day (Friedberg, 2019). Although this accounts for only a small percentage of the human genome's approximately 6 billion base pairs, if left unrepaired or incorrectly repaired, DNA damage can result in severe genomic aberrations or mutations, compromising the function of afflicted cells (Jackson & Bartek, 2009).

1.1.1 Sources of DNA Damage

Sources of DNA damage can be broadly categorised into endogenous and exogenous agents. Both sorts of stressors are capable of causing diverse forms of DNA damage, as will be detailed in the next section. Endogenous factors typically involve replication errors, spontaneous base alterations, or the release of detrimental particles, such as free radicals, during metabolic processes or following the loss of cell membrane integrity (Alhmoud et al., 2020; De Bont & van Larebeke, 2004; N. Gupta et al., 2020). Exogenous factors, on the other hand, normally include environmental factors and chemotherapeutic agents. These agents have been found to cause base damage and DNA structural changes through mechanisms such as base modifications, helix-distorting bulky lesions, or cross-linking of DNA strands (Chatterjee & Walker, 2017).

Reactive oxygen species (ROS), a class of short-lived, highly reactive, oxygen-containing chemicals, are well-established endogenous DNA damaging particles. ROS are generated as byproducts of the electron transport chain during aerobic cellular respiration. They can also arise from catabolic oxidases, anabolic processes, and peroxisomal metabolism (Henle & Linn, 1997; Winterbourn, 2008). ROS directly oxidises DNA bases or insults the DNA sugar backbone, producing oxidatively generated base damage, tandem or clustered DNA lesions

(Arjunan et al., 2015; Cadet et al., 2012; Jaruga & Dizdaroglu, 2008; Srinivas et al., 2019). Another major group of endogenous factors are spontaneous DNA alterations. These base lesions can be caused by dNTP misincorporation during replication, bases deamination, DNA depurination, or modification of DNA bases by endogenous alkylators (Ciccia & Elledge, 2010). For example, spontaneous hydrolysis leads to DNA base deamination or an abasic site (Lindahl, 1993). Besides, non-enzymatic methylations are responsible for damaging thousands of DNA bases per cell every day (Holliday & Ho, 1998; Jackson & Bartek, 2009). S-adenosylmethionine (SAM), a methyl donor for methyl transferases during normal reactions, can spontaneously induce mutagenic base methylation in mammals (Rydberg & Lindahl, 1982).

Environmental factors, such as cigarette smoke, industrial chemicals, toxic heavy metals, ultraviolet (UV) and ionising radiation (IR), are common exogenous sources of DNA damage and mutation (Huang et al., 2018; Maremonti et al., 2020; Phillips et al., 1988; R. Wu et al., 2020). Among these, ionising radiation is a major cause of DNA damage (Smith et al., 2017). The energy released by IR when passing through cellular material can disrupt the DNA double helix and produces single-strand breaks (SSBs), double-strand breaks (DSBs), base/sugar damage or clustered damage sites of varying structural and chemical complexity (Lomax et al., 2013). In addition to direct damage, IR also causes secondary damage to DNA by generating oxygen-derived free radicals, including hydroxyl radicals, superoxide anion radicals, and hydrogen peroxide (Borek, 2004). ROS are formed when IR is absorbed by small molecules, primarily water, in the tissue environment, which subsequently induces oxidative damage to DNA (Smith et al., 2017).

Sunlight exposure is another environmental source of DNA damage, with the ultraviolet component causing significant DNA lesions in human cells (Hoeijmakers, 2009). The UV radiation can be categorised into UVC (190-290 nm), UVB (290-320 nm), and UVA (320-400 nm), with maximal absorption of UV radiation by DNA occurring at 260 nm (Moan & Peak, 1989). While the ozone layer filters out most of the hazardous UVC radiation, sunlight still contains 5.1% UVA and 0.3% UVB, which can damage DNA through photochemical alterations (Davies, 1995). The putative role of UVA in solar carcinogenesis is achieved by directly inducing DNA adduct formation or by exciting endogenous and exogenous photosensitisers (Douki et al., 1999). Additionally, UV radiation can cause DNA protein crosslinks, cyclobutane dimer accumulation, and DNA strand breakages, all of which induce

mutations and lead to skin cancers in humans (Kiefer, 2007; Moan & Peak, 1989; Peak & Peak, 1986; Rochette et al., 2003).

Bulky adducts on DNA molecules normally result from various environmental agents, particularly polycyclic aromatic hydrocarbons (PAHs) in cigarette smoke, or industrial pollution including vinyl chloride and styrene (Bolt, 2008; Hwa Yun et al., 2020; Laib et al., 1979). For instance, benzo[a]pyrene is present in coal tar, tobacco smoke, and grilled meats and, when consumed, can give rise to benzopyrene diol epoxide, a highly reactive metabolite that forms bulky adducts via binding to nucleophilic DNA at the exocyclic amine of guanine (Denissenko et al., 1998). If left unaddressed, DNA replication will typically result in adenine being placed across from the lesion in the daughter molecule, thereby causing a G to T transversion mutation upon subsequent adduct repair (Tretyakova et al., 2002). Other adduct-forming agents include a wide range of anticancer agents, such as platinum derivatives (Stornetta et al., 2017). Additionally, some commonly used compounds in polishing liquids, cleaning liquids, disinfectants, industrial solvents, as well as certain pesticides such as alachlor, diquat, chlorothalonil, and imidacloprid are all potent for forming DNA adducts (Chakarov et al., 2014).

The exogenous alkylating agent is another contributor to DNA damage. These agents are often found in dietary components, tobacco smoke, biomass burning, industrial processing, and chemotherapeutic agents (Grutzen & Andreae, 1990; N. Kondo et al., 2010; Lawley, 1966). Common examples of alkylating agents include haloalkanes (such as dichloromethane, trichloromethane or chloroform, and tetrachloromethane), alkyl sulfonates and nitrosoureas (De Bont & van Larebeke, 2004). These electrophilic agents preferentially react with the highly nucleophilic base ring nitrogens, particularly the N^7 of guanine and N^3 of adenine, as well as the oxygen atoms, leading to DNA base alkylation (N. Kondo et al., 2010). Many potent and widely used anticancer agents work by inducing DNA damage, which will be further discussed in section *1.1.3.2 DNA Damage and Cancer Therapies.*

1.1.2 Types of DNA Damage

Several forms of DNA damage can result from normal cellular processes or exposure to external DNA-damaging agents, as described above. These include oxidative damage and alkylation/deamination of DNA bases, loss of bases and generation of abasic sites, bulky adduct

formation, DNA crosslinking, and DNA strand breakage. This section provides an overview of different forms of DNA damage.

Oxidative damage

ROS is the leading cause of oxidative damage. At lower concentrations, ROS serve as essential cellular signalling messengers, enabling defence responses to invading pathogens by the immune system (Malle et al., 2007; Segal, 2005). However, excess ROS can lead to a wide spectrum of lesions, including non-bulky and bulky base modifications, abasic sites, non-conventional single-strand breaks, protein-DNA adducts, and intra/interstrand DNA crosslinks (Berquist & Wilson, 2012; Bjelland & Seeberg, 2003; Cadet et al., 2010; Ravanat et al., 2012). The most notable ROS species are superoxide radicals ($O2•^{-}$), hydrogen peroxide (H_2O_2), and hydroxyl radicals (•OH) (Cadet et al., 2011). Among these, hydroxyl radicals (•OH) are the most reactive and electrophilic among the ROS species and can be generated from enzymatic reactions or by exposure to IR (Book et al., 1988; Dizdaroglu et al., 1991). Hydroxyl radicals can interact with DNA bases by adding to their double bonds, abstracting hydrogen atoms from their methyl groups, or attacking the sugar residue in their immediate vicinity (Breen & Murphy, 1995).

Guanine is the most readily oxidised nucleic acid base due to its low ionisation potential. The hydroxyl radical can convert guanine residues to 8-oxo-7,8-dihydroguanine (8-oxo-dG), which is one of the most prevalent DNA lesions and a biomarker of oxidative stress (Cadet et al., 1999; Kasai & Nishimura, 1984). During DNA replication, adenine is frequently inserted opposite the 8-oxo-dG lesion, and then thymine is incorporated in lieu of the excised 8-oxo-dG during the repair process. Therefore, G to T transversion is the most common mutation from 8-oxo-dG (Cheng et al., 1992). Except for the formation of 8-oxopurines, purine base oxidation can produce fragmented purine structure formamidopyrimidine if the imidazole ring is opened (Berquist & Wilson, 2012; Chetsanga et al., 1981). Pyrimidine oxidation products typically include thymine glycol, uracil glycol, 5-hydroxycytosine, and dihydrouracil (van Loon et al., 2010).

Besides directly damaging DNA bases, ROS radicals can compromise the DNA backbone and cause single-strand breaks harbouring non-conventional termini, such as a 3′-phosphate or 3′-phosphoglycolate (Hennersg et al., 1983). In addition, the process of lipid peroxidation involves the oxidation of lipid molecules by hydroxyl radicals. This generates various aldehyde

products, such as malondialdehyde and 4-hydroxynonenal, capable of forming mutagenic adducts on DNA bases (Marnett, 2000). Furthermore, the former aldehydes (acrolein and croton aldehyde) can be converted to epoxy aldehydes by different oxidative processes, which subsequently modify DNA bases yielding etheno adducts such as 1, N^6-ethenoadenine (Barbin et al., 2003). Oxidative DNA damage accumulation, or oxidative stress, is thought to be a major mechanism in carcinogenesis, ageing and neurodegeneration (Maynard et al., 2009).

Alkylation of bases

Alkylated DNA bases are a major source of spontaneous DNA damage. The most common form of alkylation is methylation, which typically affects nitrogen or oxygen atoms in DNA bases, giving rise to major products such as N^7-methylguanine, N^3-methyladenine, and O^6-methylguanine. Other products of base methylation, such as N^1-methyladenine, N^3-methylcytosine, O^4-methylthymine, and methyl phosphotriesters, may also occur but to a lesser extent (De Bont & van Larebeke, 2004).

DNA alkylation often results in significant consequences despite being a minor structural alteration. Of the two types of alkylation, *O*-alkylation is generally more harmful and mutagenic than *N*-alkylation (Loveless, 1969). O^6-alkylguanine and O^4-alkylthymine tend to pair with non-canonical partners T and G, respectively, and result in a substitution of a G:C to an A:T pair and vice versa (Eadie et al., 1984; Preston et al., 1986). In contrast, N^3-methyladenine is less toxic as it only partially inhibits DNA synthesis, while the N^7-methylguanine residue is generally not harmful unless it undergoes a spontaneous cleavage to generate an AP site or opens the imidazole ring to form formamidopyrimidine (Larson et al., 1985; O'Connor et al., 1988; Tudek et al., 1992). Notably, in addition to causing DNA damage, controlled chromatin modification can involve the specific methylation of DNA nucleotides. An illustrative example is the methylation of CpG islands, which can induce changes in the chromatin architecture, leading to gene expression inactivation (Holliday & Ho, 1998).

Spontaneous base deamination

Deamination of nitrogenous bases is a prevalent hydrolytic damage to DNA, during which cytosine, adenine, and guanine nitrogenous bases lose their exocyclic amine and transfer to uracil, hypoxanthine, and xanthine, respectively (Lindahl, 1993). This chemical change takes place at a higher frequency in single-stranded DNA than in double-stranded DNA, and thus is exacerbated during active replication, transcription, and recombination (Barnes & Lindahl,

2004). Base deamination is a primary cause of spontaneous mutagenesis in human cells (Yonekura et al., 2009). For example, the conversion of cytosine to uracil results in a change from C:G base pairing to U:A base pairing. Subsequent replication leads to a CG to TA mutation (Yonekura et al., 2009). Likewise, when the deamination of adenine takes place, the resulting hypoxanthine prefers to pair with C instead of T and thus forms a mutagenic lesion (Lindahl, 1993). The deamination of guanine to xanthine is less mutagenic because xanthine pairs with C. However, the xanthine–deoxyribose bond is more susceptible to spontaneous hydrolysis, which can further generate an abasic site (De Bont & van Larebeke, 2004).

The deaminated bases may further undergo secondary assaults and pair with non-canonical partners. The 5-hydroxy uracil, for instance, is a secondary oxidative product of deaminated cytosine, which can pair with all four types of nucleotides (Thiviyanathan et al., 2008). Furthermore, the deamination of already modified bases can also lead to base conversions. For example, methylation of cytosine on the 5th position of the heterocyclic ring produces 5-methylcytosine, which can undergo spontaneous deamination to thymine (Holliday & Grigg, 1993). This base pairs with adenine in a canonical manner, replacing a C:G pair with a T:A pair during the next replication cycle. Cytosine and 5-methylcytosine are the most commonly deaminated bases, with 5-methylcytosine being deaminated three to four times more frequently than cytosine (Lindahl, 1979). As a result, the GC to AT transition at CpG sequences accounts for one-third of the single-site mutations responsible for hereditary diseases in humans (Cooper & Youssoufian, 1988; Yonekura et al., 2009).

Abasic sites

An AP site, also referred to as an abasic site, is a DNA or RNA location lacking a purine or pyrimidine base. These sites are generated continuously in DNA when the N-glycosyl bond hydrolyses spontaneously or is cleaved by DNA glycosylases (Tropp, 2012). It has been estimated that 10,000 apurinic and 500 apyrimidinic sites may be created in a mammalian cell daily under physiological conditions (Tropp, 2012). The generation of these sites is positively influenced by extreme pH conditions and high temperatures (Lindahl & Nyberg, 1972). Abasic sites are unstable and readily undergo a β-elimination reaction targeting the 3′ phosphodiester bond of the remaining deoxyribose, resulting in SSBs (Bailly & Verly, 1988). Besides, AP sites can cause replication fork stalling or mutations during semiconservative replication (Waters & Walker, 2006). In *E. coli*, mutations resulting from AP sites in DNA are predominantly single-base substitutions with a strong preference for adenine incorporation opposite the lesion,

known as the "A rule" (Sagher & Strauss, 1983). In higher eukaryotes, the nucleotide preference varies depending on the organism and environmental conditions (Chan et al., 2013).

Bulky adduct formation

Certain chemical compounds can react with biological molecules such as DNA and proteins, forming bulky adducts that branch off from the main molecule via covalent linkages. Bulky adducts in DNA can impede processes that involve DNA transcription and replication (Agapov et al., 2022; Minca & Kowalski, 2011). Bulky adducts inhibit transcription by impairing the translocation of the transcription elongation complex and reducing the fidelity of subsequent slow RNA extension (Agapov et al., 2022). Meanwhile, bulky adducts in the DNA stall replication in dividing cells and usually cause cell cycle arrest (Minca & Kowalski, 2011; Rocca et al., 2015). This allows the cells to assess the degree of the damage and recruit the repair machinery, or destine them to undergo cell death if the damage is irreparable (Roos & Kaina, 2013).

DNA crosslinking

DNA crosslinking is a process that occurs when exogenous or endogenous agents react with two nucleotides, resulting in a covalent linkage between them. This linkage can occur either within a single strand of DNA (intrastrand) or between opposite strands of double-stranded DNA (interstrand). The persistence of such adducts interferes with normal cellular metabolism, including DNA replication and transcription, ultimately leading to cell death (Huang & Li, 2013). One common cause of crosslinking is exposure to UV light, especially high-energy, short-wavelength UVB and UVC radiation, which can result in crosslinks between two pyrimidine residues, typically two thymine residues, that are located consecutively within a strand of DNA (Davies, 1995). Two types of UV-induced DNA adducts are cyclobutane pyrimidine dimers (CPDs) and 6–4 photoproducts (6-4 PPs), which occur at different frequencies depending on the wavelength and dose of the UV light (Kochetkov & Budovskii, 1972). CPDs are formed when a cyclobutane ring covalently links two adjacent pyrimidines, while 6–4 PPs involve covalent linkage between the C^6 and C^4 positions of two adjacent pyrimidines (Banaś et al., 2020; Mitchell & Nairn, 1989). During replication, these bulky adducts require the translesion synthesis (TLS) polymerases to proceed beyond them, thus contributing to mutagenesis. For instance, a great majority of pyrimidine dimers result in T to C transitions and characteristic tandem CC to TT mutations that are considered to be unique to UV-induced lesions (Dumaz et al., 1993; Gentil et al., 1996). While sunlight exposure can cause

up to 50-100 pyrimidine dimer reactions per second in a skin cell, these lesions are typically repaired within seconds by photolyase reactivation or nucleotide excision repair (Yokoyama & Mizutani, 2014). However, unrepaired pyrimidine dimer can cause a distortion both in naked and nucleosomal DNA helixes (Horikoshi et al., 2016). Such steric hindrance blocks the progression of DNA and RNA polymerases, disturbing replication/transcription and impairing cellular function (Chan et al., 1985; Mei Kwei et al., 2004).

Interstrand crosslink (ICL) is another type of DNA lesion where two complementary strands of DNA are covalently linked by crosslinking agents such as platinum compounds, nitrogen mustards, mitomycin C (MMC) and psoralens (Clauson et al., 2013). ICL is the major focus of our group and will be discussed in detail in section *1.3.DNA interstrand crosslink (ICL) and ICL repair.*

DNA strand breaks

DNA strand breaks occur due to the disruption of the continuity in the phosphodiester bonds within the sugar-phosphate backbone. Single-strand breaks (SSBs) are breaks in a single strand of DNA and are among the most common forms of DNA damage, whereas double-strand breaks (DSBs) that comprise breaks in both strands of DNA are less frequent yet considered the most severe type of damage in eukaryotic cells (Mckinnon & Caldecott, 2007). It has been estimated that ~55,000 SSBs and 10–50 DSBs are formed in each mammalian cell per day (Tice & Setlow, 1985; Vilenchik & Knudson, 2003).

Strand breaks in DNA occur frequently during cellular processes such as DNA replication and transcription, often due to the activity of topoisomerase enzymes. DNA topoisomerase 1 (TOP1), for example, relaxes DNA supercoiling by inducing transient nicks and enabling rotation of the broken strand around the TOP1-bound DNA strand (Carey et al., 2003). Once the DNA is relaxed, TOP1 re-ligates the broken strand by aligning the 5′-OH group of the DNA with the tyrosine-DNA phosphodiester bond (Stewart et al., 1998). However, the normally transient topoisomerase cleavage complexes can be converted into potential DNA lesions when the DNA is crosslinked, usually as a result of chemical crosslinkers (Pommier et al., 2006). Under this scenario, topoisomerase enzymes stalls in the transition state when the DNA backbone is cleaved and remains covalently linked to the DNA, leading to the formation of DNA strand breaks (Pourquier et al., 1997). Similar strand breaks caused by topoisomerase

stalling can be seen during DNA transcription, primarily due to transcription elongation blockage by the trapped Top1 cleavage complexes (Pommier et al., 2006).

Strand breaks can also be induced by ionising radiation, cosmic rays or medical procedures like X-rays in cancer treatment. IR induces strand breaks either directly or indirectly. The most direct path entails a collision between a high-energy particle or photon and a strand of DNA, breaking the phosphodiester backbone (Cannan & Pederson, 2016). More commonly, IR splits water molecules near DNA, creating hydrogen and hydroxyl free radicals (Yamaguchi et al., 2005). Through both routes, the IR is capable of inducing base lesions or cleaving the DNA backbone to form SSBs (Dianov & Parsons, 2007). IR-induced DSBs are usually formed when two SSBs occur on opposite DNA strands approximately 10–20 bp apart (Mahaney et al., 2009).

The formation of breaks in DNA represents a potent signal that triggers the recruitment of the DNA repair machinery to the site of damage. In healthy cells, DNA breaks are swiftly and accurately repaired unless there are defects in the mechanisms responsible for the recognition or processing of such damage, as is the case in some inherited diseases characterised by genomic instability (Caldecott, 2022; Mckinnon & Caldecott, 2007). The persistence of unrepaired DNA breaks, particularly DSBs, can have detrimental effects. DSBs produce reactive and unprotected DNA ends, which may initiate or participate in recombination with regions of partial homology in other parts of the genome, leading to various genome rearrangements, including deletions, translocations, fusions, breakage of chromosomes, and formation of minichromosomes (Lieber et al., 2007; Vilenchik & Knudson, 2003).

Replication errors

During DNA replication, high-fidelity replicative polymerases (pol δ and ε) ensure the insertion of a correct complementary deoxynucleotide opposite the template base and accurately copy approximately 3 x 10^9 DNA bases per cell per generation (Kunkel, 2004). Meanwhile, the mismatch repair (MMR) pathway contributes to replication fidelity by correcting rare errors that have escaped proofreading by replicative polymerases (Kunkel, 2009). However, base substitutions and single base insertion/deletion errors still occur at a frequency of 10^{-6} to 10^{-8} per cell per generation (Kunkel, 2009). One reason for this is that other DNA polymerases (pol α, β, σ, γ, λ, REV1, ζ, η, ι, κ, θ, ν, μ, Tdt and PrimPol) carry out lower fidelity DNA synthesis during DNA replication or repair (Kunkel, 2004). Another reason might be that replication

errors accumulate from strand slippage events at repetitive sequences, which cause insertions or deletions of nucleotides that can alter the reading frame (Viguera et al., 2001). Besides, replicative polymerases may incorrectly incorporate uracil in the DNA or have reduced fidelity due to changes in the relative and absolute concentrations of dNTPs and rNTPs in the cellular environment (Andersen et al., 2005; Kumar et al., 2011; Potenski & Klein, 2014; Vértessy & Tóth, 2009). These incorrectly paired or incorporated nucleotides that escape proofreading and MMR become mutations in the next round of replication and are a significant source of spontaneous mutagenesis (Kumar et al., 2011; Kunkel, 2011; Loeb & Monnat, 2008).

1.1.3 DNA Damage and Disease

The preservation of genome integrity is fundamental to ensuring the production of healthy and disease-free daughter cells, which in turn support diverse biological functions (Anand et al., 2020). While the DNA repair machinery can address most of the DNA damage, inadequately repaired or misrepaired genetic lesions may lead to genomic aberrations and mutations that result in the manifestation of human diseases (Jackson & Bartek, 2009). Conversely, the toxicity associated with DNA damage can be leveraged in the treatment of diseases, particularly cancer (Reuvers et al., 2020). This section explores the diseases caused by DNA damage, as well as the clinical application of DNA damage-inducing agents.

1.1.3.1 Diseases Associated with Defective DNA Repair

Maintaining functional DNA damage repair is essential for the preservation of human health. Defects in DDR factors can result in chromosomal instability, breakages, and various phenotypic consequences that may ultimately give rise to human diseases, including immune deficiency, neurological degeneration, premature ageing, and severe cancer susceptibility (Giglia-Mari et al., 2011). Below are diseases associated with impaired DDR mechanisms.

Fanconi anaemia (FA)

FA is caused by deleterious mutations in any of the 22 *FANC* genes, with a global carrier frequency estimated to be 1 in 180 (Niraj et al., 2019). The majority of these mutations, exceeding 80%, are observed in *FANCA, FANCG,* and *FANCC*, with no discernible differences in occurrence between the sexes (Rosenberg et al., 2011). *FANCE* and *FANCF* mutations account for roughly 8% of all *FANC* mutations, while *FANCD1* (*BRCA2*) mutations constitute

approximately 3%. FA arising from mutations in the remaining 16 *FANC* genes is rare, with only a handful of cases reported per mutation (Neveling et al., 2009). Such mutations impair the FA pathway, which is a vital mechanism that regulates the repair of ICLs (Ceccaldi et al., 2016). Further elucidation of FA and its relation to ICLs will be presented in section *1.3.2. Defective ICL repair and Fanconi Anaemia (FA).*

Ataxia-telangiectasia (A-T)

A-T is a hereditary disease caused by mutations in the *ATM* gene, which encodes the serine/threonine protein kinase ATM (ataxia-telangiectasia mutated) that mediates the activation of multiple signal transduction pathways following the induction of DNA DSBs (Stern et al., 2002). Loss of ATM function leads to a failure of DSBs detection and cell cycle checkpoints, resulting in cellular radiation sensitivity and a predisposition to cancer (Yang & Herrup, 2005). A-T predominantly affects maturing immune cells in the thymus and certain types of brain cells that experience high levels of oxidative stress, particularly in the cerebellum, resulting in the characteristic symptoms of immunodeficiency and ataxia (Barlow et al., 1999; Stern et al., 2002). The prevalence of A-T in the UK is estimated to be around 3 cases per million population, with similar figures expected in Germany, France, and Italy. In the USA, approximately 1,000 individuals out of a population of 325 million are thought to be affected by A-T. The condition affects both sexes and all ethnicities equally (Woods et al., 1990). In addition, A-T-like disorder arises from mutations in the *hMRE11* gene, which encodes the human MRE11 protein, a member of the MRE11/RAD50/NBS1 (MRN) protein complex that is involved in repairing DSBs. A-T-like disorder is a very rare condition, with only a few cases reported worldwide (Taylor et al., 2004).

Nijmegen breakage syndrome (NBS)

NBS arises from mutations in the *NBN* (*NBS1*) gene, which encodes another protein member NBS1 (Nibrin) in the MRN complex for the DSB repair (Waltes et al., 2009). The resulting phenotype is characterised by microcephaly, immunodeficiency, growth retardation, radiosensitivity, and cancer predisposition (Varon et al., 2000; Waltes et al., 2009). Most NBS patients originate from Slavic countries, particularly Poland and the Czech Republic, and carry a common founder mutation (*657del5* in exon 6 of *NBN*) (Varon et al., 2000). Nijmegen Breakage Syndrome-like disorder is an exceedingly rare condition, with only five cases reported in Europe. In one case, the disorder is caused by a mutation in the *RAD50* gene, which encodes the third member RAD50 of the MRN complex and is associated with increased

radiosensitivity (Waltes et al., 2009).

Bloom syndrome (BS)

BS is a rare autosomal recessive disorder resulting from mutations in the *BLM* gene. It encodes the protein BLM (RecQ like helicase), a DNA helicase of the highly conserved RecQ subfamily (German et al., 2007). The protein plays critical roles in several aspects of the homologous recombination (HR) pathways, including maintaining the stability of replication forks during both unperturbed and perturbed DNA replication, promoting DNA end resection, and facilitating the dissolution of double Holliday junctions (Taylor et al., 2019). The disease condition is characterised by severe pre- and post-natal growth deficiency, immunodeficiency, an increased risk for malignancies, craniofacial dysmorphisms, and "typical" erythematous sun-sensitive skin lesions of the face. Cancer is the leading cause of death in individuals with BS (Bouman et al., 2018). Additionally, closely related disorders have been reported, such as BS-like disorder, which is caused by mutations in *TOP3A* (encoding topoisomerase 3α), *RMI1*, and *RMI2* (encoding the RecQ-mediated genome instability proteins). This condition is characterised by small body size and dermal abnormalities (Taylor et al., 2019).

Diseases with deregulated DNA methylation

DNA methylation is an essential epigenetic modification of DNA (Cooper & Youssoufian, 1988). Aberrant methylation has been linked to several inherited human diseases, including Beckwith–Wiedemann, Prader–Willi, Angelman syndromes, Albright hereditary osteodystrophy, pseudohypoparathyroidism Ia/Ib, and transient neonatal diabetes (Cooper & Youssoufian, 1988; Watson et al., 2001). Besides, a defect in the machinery that reads methylation marks causes the Rett syndrome, a rare neurodevelopmental disorder that is caused by mutations in the gene encoding MECP2 (methyl-CpG binding protein 2), a protein that recognises methylated bases in DNA and selectively binds CpG dinucleotides in the mammalian genome to mediate transcriptional repression (Amir et al., 1999). Moreover, loss of genomic methylation is a frequent and early event in cancer and correlates with disease severity and metastatic potential in many tumour types (Widschwendter et al., 2004). DNA methylation patterns are globally disrupted in cancer, with genome-wide hypomethylation and gene-specific hypermethylation events occurring simultaneously in the same cell (Gopalakrishnan et al., 2008).

Cancer

Genomic instability is a widely recognised hallmark of cancer initiation and progression, as it generates an increased burden of mutations that can promote carcinogenesis, particularly when occurred in oncogenes and tumour-suppressor genes (Hanahan & Weinberg, 2011). Genomic instability leads to altered cellular behaviour, providing selective growth advantages and enabling the transformation of normal cells into malignant ones (Basu, 2018). In most cancers, genomic instability manifests as changes in chromosome number and structure, as well as alterations in DNA structure, such as nucleotide substitutions, insertions, and deletions (Y. Yao & Dai, 2014). Genetic alterations contributing to cancer onset are more frequently observed in actively dividing tissues (Bartek, 2011).

The dysregulation of DDR mechanisms is an essential event leading to the accumulation of genetic mutations in cancer cells, especially when the function of critical DNA repair factors is lost (Y. Yao & Dai, 2014). The frequency of mutational events is positively proportional to the extent of DNA damage and the attenuation of DNA repair machinery (Loeb & Loeb, 2000). For example, mutations in the gene encoding tumour suppressor protein p53 impair DNA damage repair and promote cancers (Halazonetis et al., 2008). Bulky adducts associated with benzopyrene metabolites have been implicated in the mutagenesis of the *p53* gene in smoking-related lung cancers (Tretyakova et al., 2002). Besides, nearly 15% of breast cancer cases have been linked to inactivating mutations in the genes encoding the BRCA1/2 (Breast cancer type 1/2 susceptibility) proteins, and the Lynch syndrome with increased cancer disposition has been linked to mutations in the DNA repair proteins MutS and MutL (Leach et al., 1993; Nik-Zainal et al., 2016).

1.1.3.2 DNA Damage and Cancer Therapies

Despite the association of disrupted DDR pathways and the onset/progression of cancers, the inherent genome instability of rapidly proliferating tumour cells presents opportunities for therapeutic targeting of DDR mechanisms. This can be achieved by inducing additional replication stress, exogenous DNA damage, and/or inhibition of remaining DDR pathways (Bartek, 2011). Phil Lawley, a leading researcher in the field of DNA damage and carcinogenesis, first demonstrated that certain alkylating agents, such as butadiene dioxide, can interact with DNA, resulting in the formation of harmful adducts that kill the cancer cells (Brookes & Lawley, 1961; Lawley & Brookes, 1967). Since then, several medications that induce catastrophic DNA damage have been developed for cancer treatments.

Traditional cancer treatments mostly consist of chemotherapy drugs and radiation (Bartek, 2011). Chemotherapeutic agents induce DNA damage, leading to cancer cell death through apoptosis, cell senescence, mitotic catastrophe, or autophagy (Vacchelli et al., 2012). Radiotherapy, on the other hand, is typically an immune-stimulatory process that triggers immunogenic cell death, inflammatory reactions, and the recruitment of T cells and dendritic cells to the tumour microenvironment to stimulate an anti-tumour response (Meng et al., 2012). Some examples of classic cancer treatments include radiotherapies such as X-rays, antimetabolites such as 5-fluorouracil, crosslinking agents including cisplatin, oxaliplatin and mitomycin C, alkylating agents such as methyl methanesulphonate and temozolomide, and agents that cause SSBs or DSBs by trapping topoisomerase I or II enzymes on DNA such as camptothecin and etoposide (Tannock, 1998).

Conventional cancer treatments are effective but often have limitations due to their non-specific toxicity, causing damage to normal cells and resulting in undesirable side effects (Tannock, 1998). Chemotherapy, for instance, can cause various short-term and long-term toxicities, including ovarian failure, bone loss, weight gain, neurotoxicity, neurocognitive changes, cardiac toxicity, and even secondary malignancies (Mayer, 2013; Vacchelli et al., 2012). These adverse effects can significantly impact patients' quality of life and overall health. Furthermore, these treatments may have undesirable impacts on cancer genomes. Persistent DNA damage and misrepair introduced by cancer therapies can result in additional genomic instability and clonal evolution, leading to more aggressive features in some cases (Barcellos-Hoff et al., 2005; Landau et al., 2017). Therefore, minimising chemotherapy-related toxicities and optimising cancer cell targeting is an essential area of research in oncology.

Medication resistance is another major challenge in cancer treatment. With a better knowledge of DDR pathways, synthetic lethality has emerged as a viable strategy to combat drug resistance. Synthetic lethality is based on DDR pathway alterations that occur in certain cancers, where genetic vulnerabilities of those cancer cells result in high reliance on alternative repair mechanisms. Thus, synthetic lethality can kill cancer cells more effectively by targeting specific alternative repair routes (Lord & Ashworth, 2012). For instance, conventional chemotherapy of tumours deficient in the BRCA1/2 HR factors leads to resistance due to the cancer cells' remanent ability to repair drug-induced SSBs. However, combining therapy with the Poly (ADP-ribose) polymerase (PARP) inhibitor, which blocks PARP's vital role in SSB repair, can increase the number of unrepaired SSBs, which ultimately leads to the accumulation

of DSBs that cannot be fixed by the HR-deficient cells, resulting in their death (Livraghi & Garber, 2015). Importantly, PARP inhibitors exhibit relatively low toxicity to normal cells, making them an attractive option for selectively targeting HR-deficient tumours.

It has subsequently been discovered that some tumours without HR deficiency can also exhibit hypersensitivity to PARP inhibitors via mechanisms independent of HR inactivation (Fugger et al., 2021). Except for PARP inhibitors, other potential DDR targets have been identified in recent years, such as anthracyclines targeting the topoisomerases (Helleday et al., 2008). The promotion of apoptosis is another potential application for DDR inhibitors, aimed at augmenting growth inhibition by DNA-damaging drugs. For example, the efficacy of DNA-damaging agents has been enhanced by using checkpoint kinase 1 (CHK1) inhibitors, particularly in p53-deficient cells (Chen et al., 2006). Synthetic lethality interactions are employed to design personalised medicine, which is based on a patient's unique genetic background, disease progression and specific cancer features, thus representing a paradigm shift towards precision medicine (Beggs & Yang, 2019).

1.2 DNA Damage Response (DDR)

As described above, our genomes are continuously exposed to damage from both internal and external sources. To maintain genome stability, cells have evolved a complex defence system known as DDR. This system includes multiple mechanisms, including DNA repair pathways, damage tolerance processes, cell cycle checkpoints and programmed cell death (Ciccia & Elledge, 2010; Harper & Elledge, 2007). The DDR is normally initiated by DNA damage recognition. Based on the type and severity of the damage incurred, the cellular responses may involve the modification of chromatin structure, activating transient cell cycle checkpoints and (or) modulating gene expression at the transcriptional or translational level. Meanwhile, the DNA repair pathway specific to the recognised lesion is activated to resolve the damage (Huang & Zhou, 2021; Pilié et al., 2019). If lesions are not repaired promptly, persistent DDR signalling can affect cell fate by promoting differentiation, senescence, permanent cell cycle arrest, or programmed cell death (Sherman et al., 2011). Through these mechanisms, the DDR plays a critical role in maintaining genome stability, which ensures the integrity and faithful transmission of genetic material to subsequent generations.

1.2.1 DDR Proteins

The cellular response to DNA damage is a complex process that involves a network of DDR proteins. These proteins can be broadly categorised into three functional groups: DDR sensors, DDR signal transducers, and DDR effectors (McGowan & Russell, 2004). Among these factors, the DDR is primarily mediated by members of the PARP family, as well as the members of the PIKK (phosphatidylinositol 3-kinase-like protein kinase) family — ATM, ATR (ATM RAD3-related), and DNA-PKcs (DNA-dependent protein kinase catalytic subunit) (Ciccia & Elledge, 2010).

As transducers of DNA damage signals, ATM and ATR detect DNA damage signals and initiate downstream phosphorylation events that orchestrate cellular responses including DNA repair, checkpoint activation and apoptosis (Blackford & Jackson, 2017). For example, the cell-cycle checkpoint kinases CHK1 and CHK2 are major substrates for ATR and ATM, respectively. In response to DNA damage, these cell-cycle checkpoint kinases are activated by ATR/ATM and downregulate cyclin-dependent kinases (CDKs) to halt cell cycle progression (Kastan & Bartek, 2004). This helps to prevent DNA replication or mitosis until the damaged DNA has been repaired. In addition, ATM and ATR promote DNA repair by enhancing the expression or post-

translational modification of DNA repair proteins (Huen & Chen, 2008). In fact, proteomics studies have revealed more than 900 ATM/ATR-mediated phosphorylation sites on over 700 proteins highly associated with the DDR system (Matsuoka et al., 2007). The importance of ATR/ATM in cells is undoubted, and their deficiency can result in chromosomal fragmentation, severe developmental defects, or even embryonic lethality (Brown & Baltimore, 2000).

Another member of the PIKK family is the DNA-PKcs. It is the catalytic subunit of the DSB repair enzyme DNA-PK, which contains another targeting subunit, the KU70–KU80 heterodimer (Smith & Jackson, 1999). DNA-PK is characterised by its DNA-activated serine/threonine-directed protein kinase activity, and its major role is to act as a DSBs sensor and promote the rejoining of DSBs by non-homologous end joining (NHEJ) (Jette & Lees-Miller, 2015). Thus, cells and animals deficient in DNA-PK are defective in DSB repair and in V(D)J recombination, a process by which antibody and T-cell receptor diversity is generated, and are consequently radiosensitive and immunodeficient (Smith & Jackson, 1999). Besides, DNA-PK may be involved in signalling DNA damage to the apoptosis machinery (S. Wang et al., 1999).

The PARPs are a family of enzymes that share the ability to catalyse the transfer of ADP-ribose to target proteins (poly ADP-ribosylation) (Amé et al., 2004). There are at least 18 members of the PARP family, and among them, the PARP1/2 are the most prominent proteins that have been implicated in the DDR as molecular sensors of SSBs and DSBs (Morales et al., 2014; Schreiber et al., 2006). Activation of PARP1/2 and subsequent synthesis of poly (ADP-ribose) chains on target proteins allows repair factors to access the damaged DNA (Satoh & Lindahl, 1992). PARP-mediated histone PARylation also contributes to chromatin reorganisation and recruitment of DNA repair and chromatin-modifying complexes to the damage sites (Chou et al., 2010). Besides, PARP1 is involved in both base excision repair (BER) and nucleotide excision repair (NER) in response to SSBs, and can compete with KU binding to DNA ends to promote HR during DSB repair (Caldecott et al., 1996; Hochegger et al., 2006). PARP1 is thought to mediate the initial accumulation of the MRN complex to DSBs, as well as the activation of the γH2AX cascade and stabilisation of DDR factors at damage sites (Haince et al., 2007; Haince et al., 2008). Also, part of PARP1's role in the DDR is achieved by facilitating the activation of ATM (Haince et al., 2007). Furthermore, when both of the two classical DSB repair pathways, NHEJ and HR, are not available, PARP1 acts to promote the alt-NHEJ, which functions as a backup mechanism for the DSB repair (Wang et al., 2006).

The tumour-suppressor protein p53 is another factor that the DDR system is heavily dependent on. Functional p53 protein is essential for maintaining a delicate balance between cell cycle arrest, DNA repair, and apoptosis when responding to DNA damage (Driessens et al., 2003). P53 is able to initiate cell cycle arrest, thus allowing the repair of damaged DNA prior to DNA synthesis or segregation of the genome (Lakin & Jackson, 1999). Specifically, p53 induces cell cycle arrest in response to DNA damage by stimulating transcription of the gene for the CDK inhibitory protein p21. The elevated level of p21 then inhibits CDKs, thus preventing these kinases from promoting cell cycle progression (Kastan & Bartek, 2004). Besides, mutations in the p53 gene can significantly impact DNA damage repair as well as the p53-induced apoptosis or senescence, leading to cancer onset (Halazonetis et al., 2008). Mice engineered to exhibit enhanced p53-dependent DDR are shown to be less tumour-prone than wild-type mice (García-Cao et al., 2002).

p53-binding protein 1 (53BP1) serves as an important molecule in the DDR system by acting as an intermediary or effector molecule that binds with p53 (Piccinno et al., 2019). It plays a crucial role in DSB repair by directly recognising the specific histone structure that arises from DSBs. Upon DSBs sensing, 53BP1 is rapidly recruited to DNA lesions, where it forms nuclear foci and transduces DNA repair processes (Hwang et al., 2020). Furthermore, 53BP1 is involved in promoting the terminal junction of DNA and in selecting the DSB repair pathway by facilitating the NHEJ pathway and inhibiting HR repair (Ghezraoui et al., 2018). Notably, the presence of 53BP1 amplifies the MRN complex-mediated activation of ATM at DSB sites, which is important for promoting ATM phosphorylation of substrates as well as for the repair of DNA DSBs in mammalian cells (Lee et al., 2010).

In addition to the core DDR machinery, there exist complementary mechanisms that are equally essential for maintaining genome integrity. Chromatin-remodelling proteins, for instance, play a crucial role in modifying chromatin structures, thus enabling the DNA repair machinery to access damaged DNA (Bell et al., 2011). Notably, research indicates that the activation of the ATM protein kinase induces chromatin relaxation at sites of DSBs (Ziv et al., 2006). Additionally, homologous recombination is dependent on the proximity of a sister chromatid and likely collaborates with the chromosome cohesion machinery to ensure effective DNA repair (Misteli & Soutoglou, 2009).

1.2.2 DNA Repair Pathways

DNA repair encompasses a set of intricate biological processes that detect and repair DNA damage, with the ultimate goal of restoring genomic integrity. This entails the detection of DNA damage through various sensing and signalling mechanisms and subsequent recruitment of specialised repair machinery proteins to the sites of damage. Physical repair of the lesion then occurs, followed by the release of the repair factors when the repair is completed. It is noteworthy that specific DNA lesions are repaired by distinct DNA repair mechanisms, as outlined below.

1.2.2.1 Direct Reversal

As previously described, DNA damage is usually induced by oxidative stress, alkylating agents, UV radiation, and cross-linking agents. Direct reversal of the base lesion is a cost-effective and straightforward mechanism for repairing such damage, which is error-free and does not require base excision or incisions of the sugar-phosphate backbone (Morita et al., 2010). The classical direct reversal mechanisms include the repair of *O*-alkylated DNA damage by the DNA alkyltransferases, the reverse of *N*-alkylated base adducts by the *E. coli* Alkylation B **(**AlkB) family dioxygenases, as well as the repair of photolesions caused by UV radiation via spore photoproduct lyases and photolyases (Eker et al., 2009; Yi & He, 2013).

Alkyltransferases play a key role in the direct removal of DNA base alkylation. Specifically, they are responsible for the removal of mutagenic alkyl adducts located on the O^6 position of guanine and the O^4 position of thymidine (Denisov et al., 2017). For instance, O^6-methyl guanine is mutagenic and carcinogenic as a result of its ability to cause G:C to A:T transitions during DNA replication (Yi & He, 2013). The O^6-methylguanine-DNA methyltransferase (MGMT) is capable of repairing such damage by transferring the methyl group from O^6-methyl guanine to a cysteine side chain, thereby restoring the normal base pairing (Christmann & Kaina, 2012; Pegg, 2011). Additionally, MGMT can repair other guanine products with additional groups on the O^6-position, such as O^6-[4-oxo-4-(3-pyridyl) butyl] guanine and O^6-chloroethyl guanine (Fahrer & Kaina, 2017).

Photolyases are light-driven enzymes that display remarkable specificity for reversing DNA damage induced by UV radiation, specifically pyrimidine dimers including CPDs and 6-4 PPs (Essen & Klar, 2006; Vechtomova et al., 2020). The mechanism involves the injection of an

electron at the site of the lesion, which leads to the photolyase-mediated cleavage of the pyrimidine dimers within the duplex DNA (Essen & Klar, 2006; Zhong, 2015). The energy required to power this reversal reaction is obtained from chromophores that are excited through photon absorption (Zhang et al., 2017).

In 2002, a third direct reversal mechanism involving the reversal of *N*-alkylated base adducts by the AlkB family was discovered (Falnes et al., 2002). In *E. coli*, AlkB uses molecular oxygen to oxidise the alkyl groups on alkylation-damaged nucleic acid bases, such as 1-methyladenine, 3-methylcytosine, and 1, N^6-ethenoadenine; the oxidised alkyl groups are subsequently released as aldehydes, regenerating the undamaged bases (Trewick et al., 2002). To date, nine human homologs of *E. coli* AlkB have been identified, designated as Alkylation Repair Homologs 1-8 (ALKBH1-8) and Fat Mass and Obesity associated (FTO) (Kurowski et al., 2003; Sanchez-Pulido & Andrade-Navarro, 2007; Yi & He, 2013). Among the nine homologs, only ALKBH2 and ALKBH3 have been recognised as *bona fide* nuclear DNA repair enzymes that can complement the function of *E. coli* AlkB (Aas et al., 2003; Duncan et al., 2002; Fu & Samson, 2012). ALKBH2 and ALKBH3 proteins have DNA repair activities similar to AlkB and remove both 1-methyladenine and 3-methylcytosine from single- and double-stranded DNA (Duncan et al., 2002).

1.2.2.2 Base Excision Repair (BER)

The BER process is a fundamental pathway for correcting subtle, non-helix-distorting base lesions, such as DNA base oxidation, alkylation, and deamination (Jackson & Bartek, 2009; Kavli et al., 2007). BER comprises two pathways, the short patch and the long patch, that repair a single nucleotide or longer stretches of DNA (normally containing two to ten nucleotides), respectively (Frosina et al., 1996). Four types of crucial proteins are involved in BER, including DNA glycosylase, AP endonuclease, DNA polymerase, and DNA ligase (Robertson et al., 2009). These proteins work in concert to remove and replace the damaged DNA base with an undamaged one, thereby restoring the integrity of the DNA strand.

BER employs DNA glycosylases as the primary enzyme to recognise base lesions and initiate the removal of the damaged bases. Upon binding to a damaged base, the DNA glycosylase triggers the abnormal base to flip out of the DNA double helix and enter the enzyme's binding site, leading to the formation of an enzyme-substrate complex. The glycosylase then catalyses the cleavage of the N-glycosidic bond between the substrate base and the 2'-deoxyribose,

efficiently removing the damaged base and generating an AP site (Jacobs & Schär, 2012). The resulting AP site is then incised by AP endonuclease or AP lyase, and the 5′ or 3′ phosphodiesterase removes the remaining sugar-phosphate at the DNA termini (Dalhus et al., 2009). Last, DNA polymerase (Pol) fills the DNA gap with correct nucleotides, followed by the DNA ligase seals the nicks (Kim & Wilson III, 2011). A good example of BER is the repair of the most prevalent form of oxidative DNA damage - the 8-oxo-dG resulting from the oxidation of deoxyguanosine, which is primarily accomplished by 8-oxo-guanine glycosylase 1 (OGG1), AP endonuclease 1 (APE1), PARP1, and the DNA ligase 1 (LIG 1) (Kim & Wilson III, 2011).

1.2.2.3 Nucleotide Excision Repair (NER)

In contrast to base lesions, which can be corrected by BER, bulky DNA adducts or cross-linking lesions that distort the DNA helix structure are normally processed by NER. These types of DNA damage typically arise from exposure to alkylating or cross-linking agents, such as IR/UV radiation, electrophilic chemical mutagens, cancer drugs, or endogenous metabolites (Dalhus et al., 2009). NER deficiency is associated with various human diseases presenting neurological abnormalities and premature ageing symptoms, such as Xeroderma pigmentosum and Cockayne syndrome (Kajitani et al., 2021). NER employs two mechanisms to identify and repair DNA damage: global genomic NER (GG-NER) and transcription-coupled NER (TC-NER). GG-NER constantly scans the genome for disruptions in base pairing or distortions in the DNA helix, whereas TC-NER recognises DNA lesions by elongating RNA polymerase getting blocked at damaged sites during transcription (Hanawalt & Spivak, 2008; Petruseva et al., 2014). Therefore, the TC-NER sub-pathway preferentially repairs DNA damage in actively transcribed genes, while the efficiency of GG-NER is mainly decided by the distinct conformational characteristics of the DNA damage in the genome (Cai et al., 2020; Kajitani et al., 2021).

The two NER mechanisms, GG-NER and TC-NER, differ primarily in the initial damage recognition step (Kobaisi et al., 2019). In TC-NER, RNA polymerase II stalling at damaged sites recruits Cockayne syndrome proteins B (CSB), which then recruits the CSA complex. CSA is required for the accumulation of XPA-binding protein-2 (XAB2), the nucleosome remodelling factor high-mobility group nucleosome-binding domain-containing protein-1 (HMGN1) and Transcription elongation factor IIS (TFIIS) to sites of arrested RNAPII (Hanawalt & Spivak, 2008; Spivak, 2015). In contrast, GG-NER recognises DNA helix

distortion through the Xeroderma pigmentosum group C (XPC) and its partners Rad 23 homolog B (RAD23B) and centrin 2 (CETN2), leading to recruitment of helicase TFIIH to form an XPC-RAD23B-TFIIH complex that unwinds the DNA helix (Missura et al., 2001). Once damage is detected, the two NER sub-pathways repair damage in a similar manner: endonucleases XPG and XPF-ERCC excision repair 1 (ERCC1) heterodimer are recruited to cut the strand at the 3′ and 5′ flanks of the damage site, respectively, and remove the damage-containing nucleotides (Hanawalt & Spivak, 2008; Kajitani et al., 2021; Petruseva et al., 2014). The NER pathway is completed by the synthesis of repair patches through the action of Pol δ or ε, replication factor C (RFC), proliferating cell nuclear antigen (PCNA), and LIG I or X-ray repair cross complementing 1 (XRCC1)-LIG III (Hanawalt & Spivak, 2008; Kajitani et al., 2021; Kobaisi et al., 2019; Missura et al., 2001; Petruseva et al., 2014; Spivak, 2015).

1.2.2.4 Mismatch Repair (MMR)

Mismatch repair (MMR) mainly corrects errors formed during DNA replication and recombination, such as base insertions, deletions, and misincorporations, which cause base 'mismatches' that distort the DNA helix (Huang & Zhou, 2021; Huang & Li, 2020). MMR is the principle mechanism that minimises replication errors to prevent the accumulation of mutations that could lead to tumorigenesis in the long term (Guillotin & Martin, 2014; G. M. Li, 2007). In fact, the inactivation of MMR is associated with most human cancers, either hereditary or non-hereditary (Ijsselsteijn et al., 2020; Kunkel & Erie, 2005). Besides, studies have uncovered non-canonical roles of MMR in repairing oxidative DNA lesions, helix-distorting nucleotide lesions, environmental toxicants induced damage, as well as regulating cell cycle arrest and apoptosis (Kunkel & Erie, 2005; Liu et al., 2008; Motegi et al., 2019). These findings highlight the broad-spectrum role of MMR in the DDR system (Jiricny, 2006).

Initiation of the MMR pathway is triggered by the recognition of mismatched bases and insertion/deletion loops by the MutS homologues (MSH) in mammalian cells (Jiricny, 2006). The most abundant mismatch-binding factor, MutSα, is composed of MSH2 and MSH6 and initiates the repair of base mismatches of one or two extrahelical nucleotides, whereas the repair of larger insertion/deletion loops is initiated by MutSβ, which is a heterodimer of MSH2 and MSH3 (Acharya et al., 1996; Gradia et al., 1997; Jiricny, 2006). Upon binding to DNA, MSH complexes undergo a transition, exchanging their bound ADP for ATP and adopting a clamp-like conformation. This altered state allows them to slide along the DNA until they reach the site of a lesion (Owen et al., 2009). This sliding action facilitates the recruitment of the MutL

homologue (MLH) complex, which acts as an intermediary, connecting the initial mismatch recognition by MutS to downstream repair activities (Manhart & Alani, 2016). Eukaryotic MutL activities come in three distinct forms, and similar to eukaryotic MutS activities, they function as heterodimeric complexes, with MLH1 being a common subunit (E. Kondo et al., 2001). MutLα, a heterodimer composed of MLH1 and PMS2, serves as the primary MutL activity in human mitotic cells and supports repair initiated by either MutSα or MutSβ (G. M. Li, 2007; G. M. Li & Modrich, 1995). In conjunction with MutLα, other key repair factors such as PCNA, replication factor C (RFC), and exonuclease 1 (EXO1) are recruited to the lesion site (Keijzers et al., 2019). The assembly of these repair factors initiates the endonuclease activity of PMS2, which makes an SSB near the mismatch. This, in turn, opens up the entry site for exonuclease 1 (EXO1) (Van Oers et al., 2010). The removal of mismatched nucleotides is then carried out by EXO1 in the 5′->3′ direction in a MutSα-dependent manner (Orans et al., 2011; Vallur & Maizels, 2010). Simultaneously, replication protein A (RPA) binds to the single-strand DNA produced by EXO1 to avoid DNA degradation (Bowena & Kolodnera, 2017; Jiricny, 2006). Next, MutLα physically interacts with DNA polymerase delta (Pol δ), mediating the synthesis of replacement nucleotides, and LIG1 seals the remaining nick (Guillotin & Martin, 2014; Huang & Li, 2020; Jiricny, 2006; Kunkel & Erie, 2005; Li, 2007).

1.2.2.5 Double Strand Break Repair

In human cells, two primary mechanisms are employed to repair DSBs: NHEJ and HR (Jackson & Bartek, 2009; McKinnon, 2009; Schipler & Iliakis, 2013). One key distinction between HR and NHEJ is that HR is selectively activated during the S and G2 cell cycle phases, whereas NHEJ operates throughout the cell cycle but is actively repressed at replication forks by the HR components (Moynahan & Jasin, 2010; Schipler & Iliakis, 2013; Shrivastav et al., 2007). Furthermore, HR is typically considered error-free as it employs a homologous template to restore the original DNA sequence (Moynahan & Jasin, 2010; Shrivastav et al., 2007). In contrast, NHEJ directly ligates the two ends of a DSB together, making it an error-prone repair mechanism (Kumar et al., 2016; Shrivastav et al., 2007). This error-prone nature of NHEJ has been exploited in the Clustered regularly interspaced palindromic repeats (CRISPR)-based genome editing system (Nambiar et al., 2022). However, in normal cells, NHEJ is highly efficient and repairs DSB accurately most of the time, and thus is the preferred mechanism except during DNA replication (Blackford & Jackson, 2017).

Non-homologous end joining (NHEJ)

NHEJ employs a complex of proteins to recognise, excise, polymerise, and ligate the broken ends of DSBs. The key proteins involved include the KU70/KU80 complex (XRCC6/XRCC5), DNA-PKcs, DNA end processing enzymes, XRCC4, and LIG4 (Lieber, 2010). The NHEJ pathway is initiated by the KU70/KU80 heterodimer, which recognises and binds the broken DNA ends via its central domain (KU core) (Walker et al., 2001). Ku primarily acts as a landing platform to recruit the downstream repair factor DNA-PKcs, while simultaneously protecting DNA ends from unwinding and degradation by cellular helicases and nucleases, respectively (Hosoya & Miyagawa, 2014). The initial binding of KU and DNA-PKcs forms a long-range synaptic complex that tethers the two DSB ends (Graham et al., 2016). Once DNA-PKcs is auto-phosphorylated, it dissociates from DNA and transitions to a short-range synaptic complex in which the DSB ends are closely aligned, allowing for efficient end processing and ligation (Blackford & Jackson, 2017; Graham et al., 2016; Hosoya & Miyagawa, 2014).

Subsequently, DNA-PKcs recruits end-processing enzymes, including Artemis, polynucleotide kinase/phosphatase (PNKP), APE1, and tyrosyl DNA phosphatase 1 (TDP1) (Jackson & Bartek, 2009; Schipler & Iliakis, 2013; Shrivastav et al., 2007). Phosphorylation of DNA-PKcs by itself or the MRN-activated ATM may promote Artemis recruitment and activation (Blackford & Jackson, 2017; Goodarzi et al., 2006; Jiang et al., 2015). After the DNA ends are processed by Artemis and other end-processing molecules, DNA-end ligation is performed by the LIG 4, with its binding partners XRCC4 (Critchlow et al., 1997; Gomes et al., 2010; Liu et al., 2008). In addition, the XRCC4-like factor (XLF) and the Paralogue of XRCC4 and XLF (PAXX) facilitate the completion of the ligation step. These two partially redundant NHEJ core factors participate in the recruitment and stabilisation of LIG4, XRCC4, and DNA-PKcs at the DSB site (Ahnesorg et al., 2006; Balmus et al., 2016; Ochi et al., 2015).

Homologous recombination (HR)

HR is a limited yet particularly critical part of DSB repair, as it allows accurate and efficient repair of collapsed replication forks, single-ended DSBs, and semi-processed ICLs (Li & Heyer, 2008; Saleh-Gohari et al., 2023). HR begins with nucleases digesting the broken DNA ends, producing ssDNA overhangs through a process known as “DNA-end resection” (Cejka & Symington, 2021). The initial ssDNA overhang is produced by the CtBP-interacting protein (CtIP) and the MRN complex (Reginato & Cejka, 2020). CtIP is recruited to DSB sites via its DNA-binding motif within the C-terminal Sae2-like domain (Mozaffari et al., 2021). When the

threonine 847 site of CtIP is phosphorylated by CDK, CtIP activates the nuclease activity of MRN, leading to the removal of a small stretch of DNA from the 5' end of the DSB and generating a 3' ssDNA overhang (Reginato & Cejka, 2020; Soria-Bretones et al., 2017). Next, two distinct but potentially redundant pathways further extend the 3' overhang, with the first dependent on the nuclease EXO1 and the second requiring the DNA replication helicase/nuclease 2 (DNA2) and the helicase BLM (Gravel et al., 2008; Zhu et al., 2008). The phosphorylation of CtIP required for end resection ensures that the HR is tightly regulated by CDKs, occurring only during S and G2 phases when sister chromatids allow faithful repair (Huertas & Jackson, 2009; Sartori et al., 2007). However, resection and HR can occur in G1-phase cells at repetitive genomic regions, such as ribosomal or centromeric DNA (van Sluis & McStay, 2015; Yilmaz et al., 2021).

Upon end resection, KU is removed from the DNA ends, and the resulting ssDNA is rapidly coated by RPA, which protects ssDNA from degradation, annealing with complementary strands, or forming secondary structures that may impede repair (Chen et al., 2013). The recombinase RAD51 then replaces RPA in the presence of BRCA1 and BRCA2 (Cejka & Symington, 2021; Tarsounas & Sung, 2020). Specifically, BRCA1 promotes BRCA2 recruitment to DSB sites through its interaction with the Partner and Localizer of BRCA2 (PALB2), where BRCA2 loads RAD51 directly onto the ssDNA ends (Bell et al., 2023; Tarsounas & Sung, 2020). Subsequently, with the aid of RAD51-associated protein 1 (RAD51AP1) and PALB2, RAD51 forms nucleoprotein filaments on ssDNA, initiating pairing and strand exchange with a homologous donor sequence to form a displacement loop (D-loop) (Kumar et al., 2016; Li & Heyer, 2008; Pires et al., 2021; Tarsounas & Sung, 2020; Yao et al., 2020). After ssDNA associates with the homologous template, RAD51 dissociates from the leading strand, allowing the invading 3' end to be extended across the break site by DNA polymerases (Cejka & Symington, 2021; Kumar et al., 2016; Li & Heyer, 2008; Shrivastav et al., 2007).

The final stage of HR encompasses two potential scenarios contingent upon the stability of the D-loop structure. If the D-loop undergoes collapse, an event that the helicase RTEL1 can actively initiate, the elongated DNA strand reanneals with the second end on the opposite side of the DNA break (Uringa et al., 2011). The remaining ssDNA gaps are then filled in by DNA polymerase and subsequently sealed by DNA ligase. This particular process is referred to as synthesis-dependent strand annealing (SDSA) (Morrical, 2015). Alternatively, in cases where

the D-loop maintains sufficient stability and the capture of the second end occurs, a double Holliday junction (dHJ) is formed. This dHJ can be resolved into two intact dsDNA molecules through three distinct pathways: BLM-TOP3A-RMI1-RIM2 (BTR)-mediated dissolution and decatenation, SLX1-SLX4-MUS81-EME1 (SLX-MUS)-mediated nucleolytic resolution, and GEN1-dependent cleavage (West et al., 2015). The BTR-mediated dHJ dissolution is considered the primary pathway for resolving dHJs generated during HR repair (Krejci et al., 2012). In the course of dHJ dissolution, the two Holliday junction branches migrate towards one another until they form a hemi-catenated intermediate (Vindigni & Hickson, 2009). This intermediate can then be decatenated by the topoisomerase III (Bachrati & Hickson, 2009). It is worth noting that HJ dissolution exclusively results in non-crossover products. Alternatively, dHJs can be resolved by specific structure-specific nucleases, known as resolvases, such as MUS81/EME1, SLX1/SLX4, and GEN1. Depending on the orientation of the cleavages, which can be either asymmetric or symmetric, this process can generate both crossover and non-crossover products (Castor et al., 2013).

Alternative nonhomologous end-joining (alt-NHEJ)

The alt-NHEJ is considered a backup mechanism for DSB repair when the more accurate repair pathways, NHEJ and HR, are compromised (McVey & Lee, 2008; Scully et al., 2019). The most well-studied alt-NHEJ sub-pathway is the microhomology-mediated end joining (MMEJ), which repairs DSBs independently of classical NHEJ factors such as KU proteins, DNA-PKcs, and LIG 4 (Ahrabi et al., 2016; Truong et al., 2013). Instead, MMEJ is mediated via CtIP, MRN complex, PARP1, Pol θ and LIG 3, and the repair depends on short regions of microhomology (2–6 bp) on either side of the break site (Ahrabi et al., 2016; Ghezraoui et al., 2014; Jones et al., 2014).

In mammalian cells, PARP1 initiates MMEJ by competing with KU heterodimer for binding to DNA ends, which in turn promotes the initiation of resection by MRN complex and CtIP (Ghezraoui et al., 2014; Haince et al., 2008; Wang et al., 2006). Subsequently, the low fidelity Pol θ is recruited to DSB ends by PARP1, where it facilitates end joining and microhomology annealing (Chan et al., 2010; Malaby et al., 2017; Mateos-Gomez et al., 2015). The repair is completed by the LIG 3-mediated ends ligation (Simsek et al., 2011; Wang et al., 2005). MMEJ generates deletions and translocations at the break sites and thus is highly mutagenic (McVey & Lee, 2008). Except for MMEJ, there are other types of alt-NHEJ events that do not rely on

such microhomologies. The ligation step in these pathways is facilitated through LIG1 (Decottignies, 2013).

Single-strand annealing (SSA)

An additional pathway to back up the classical NHEJ and HR repair is termed single-strand annealing (SSA) (Scully et al., 2019). This pathway is DNA end resection dependent and typically arises when sequence repeats are present on both sides of the DSB (Rothenberg et al., 2008). SSA involves the annealing of two complementary single strands generated at the repeats at the cost of deletion of intervening sequences (Ceccaldi, Rondinelli, et al., 2016; Pâques & Haber, 1999). Consequently, SSA is obligatorily error-prone, leading to the large deletions of sequences and the generation of chromosomal translocations (Mendez-Dorantes et al., 2018).

The repair by SSA necessitates extensive DNA end resection and RPA displacement to expose relatively long tract (more than 50 bp) homologous complementary sequences (Ceccaldi et al., 2016; Ramsden et al., 2021; Symington, 2016). Unlike HR, which relies on RAD51-mediated invasion, SSA requires the strand accessory protein RAD52 to aid in RPA displacement and facilitate homology searching between repeated regions (Ceccaldi et al., 2016; Rothenberg et al., 2008). Other proteins involved in promoting SSA include ERCC1 and RAD1/RAD10 (flap endonuclease) (Ivanov & Haber, 1995; Stark et al., 2004). SSA, like HR, requires end resection and thus is cell cycle-dependent, with the highest activity during the S/G2 phase (Iliakis et al., 2019).

DSB repair pathway selection

The selection of pathways for DSB repair, including NHEJ, HR, alt-NHEJ, and SSA, is influenced by several factors (Ceccaldi et al., 2016). One of the most critical factors is the DNA end resection (Symington & Gautier, 2011). When end resection is inhibited, NHEJ becomes the solely available pathway for repair, whereas end resection promotes a model where HR, alt-NHEJ, and SSA compete for lesion repair (Averbeck et al., 2014; Zhao et al., 2020). The initial phase of end resection, termed “end clipping,” involves the nuclease MRE11 and CtIP, which process a small number of base pairs (typically 20 bp in mammals) and render the DNA ends accessible for alt-NHEJ (Huertas & Jackson, 2009; Truong et al., 2013). The subsequent “extensive resection” phase involves helicases and exonucleases such as DNA2, BLM, CtIP,

EXO1 and WRN, which generate long stretches of ssDNA, committing cells to HR or SSA (Bennardo et al., 2008; Symington & Gautier, 2011).

The cell cycle stage is another key determinant of DSB repair route selection. While cell cycle-dependent phosphorylation events facilitate end resection and HR during S and G2 phases, the NHEJ remains the predominant DSB repair pathway throughout interphase (Beucher et al., 2009; Karanam et al., 2012). This is partly due to the chromatin-level regulation of DSB repair by the BRCA1- BARD1 (BRCA1 associated RING domain 1) complex and 53BP1, which compete in promoting or antagonising end resection, respectively (Daley & Sung, 2014). Two histone modifications are highly associated with this regulation – the H2A Lys15 ubiquitylation (H2AK15ub) and dimethylated H4 Lys20 (H4K20me2) (Sekiguchi & Matsushita, 2022). H2AK15ub is a DNA damage-induced histone marker deposited by Ring finger protein 168 (RNF168), whereas H4K20me2 is the marker of mature chromatin that is diluted during the S phase as new, unmodified histones are deposited onto nascent DNA (Paquin & Howlett, 2018; Sekiguchi & Matsushita, 2022). BRCA1-BARD1 and 53BP1 both read the modification status of H2AK15 and H4K20, which in turn influence the pathway selection for DSB repair (Daley & Sung, 2014; Fradet-Turcotte et al., 2013; Sekiguchi & Matsushita, 2022).

When 53BP1 recognises and binds nucleosomes containing H2AK15ub and H4K20me2, it recruits downstream effector proteins, including the Replication timing regulatory factor 1 (RIF1) and the Shieldin complex (SHLD1–SHLD2–SHLD3) (Daley & Sung, 2014; Noordermeer et al., 2018). This counteracts DNA end resection by modulating 3D chromatin structure, protecting DSB ends, and/or recruiting Pol α to fill in ssDNA gaps generated during resection (Feng et al., 2022; Mirman et al., 2018, 2022; Ochs et al., 2019). Additionally, 53BP1 ensures that RAD51 filaments of sufficient length cannot be assembled by inhibiting the production of ssDNA, thereby suppressing HR (Tripathi et al., 2007). Since mature chromatin becomes progressively methylated on H4K20 after replication, this process ensures that HR is suppressed in favour of NHEJ at DSBs occurring in mature chromatin during interphase (Pellegrino et al., 2017; Simonetta et al., 2018). Through a similar mechanism, the resection of DSB ends is greatly reduced in noncycling cells, thereby favouring NHEJ over resection-dependent repair pathways (HR, alt-NHEJ, and SSA) (Symington & Gautier, 2011).

Despite its importance in repairing DSBs during interphase, the NHEJ pathway becomes deleterious when collapsed replication forks produce one-ended DSBs during the S phase.

Ligating two such ends from different chromosomes results in chromosomal translocations, necessitating HR repair of replication-associated DSBs rather than NHEJ (Balmus et al., 2019; Dasika et al., 2000). This is achieved by the BRCA1-BARD1 complex, which specifically inhibits 53BP1 binding through dual recognition of H2AK15ub and H4K20me0 rather than H4K20me2 (Becker et al., 2021; Hu et al., 2021; Sekiguchi & Matsushita, 2022). Because nascent chromatin in the vicinity of a replication fork is enriched in unmethylated H4K20, BRCA1 is recruited to chromatin proximal to DSBs and promotes the repair by HR during replication (Nakamura et al., 2019). However, 53BP1 still binds to more distal chromatin sites at DSBs during the S phase to prevent excessive long-range resection, contributing to the maintenance of HR accuracy (Ochs et al., 2016). In contrast, the absence of adequately resected DNA ends results in short stretches of homology that favour the repair by alt-NHEJ (Ramsden et al., 2021).

Numerous other factors contribute to the selection of repair pathways for DSBs. First, post-translational modifications of repair factors are known to extensively mediate the pathway choice. CDKs, for example, phosphorylate CtIP as well as the long-range resection nuclease EXO1 during the S to G2 phases, thereby promoting the DNA end resection and HR (Tomimatsu et al., 2014). In contrast, ubiquitin conjugating enzyme E2 M (UBE2M)/RNF111-mediated neddylation inhibits end resection by CtIP via modulating the length of ssDNA (Jimeno et al., 2015). Second, the presence of repair pathway-specific proteins influences the choice of repair pathway (Wang et al., 2013). For instance, the MRN complex serves as an essential factor for end resection in HR (Reginato & Cejka, 2020). Mutations in genes encoding the components of the MRN complex lead to Ataxia-telangiectasia (A-T)-like disorder, Nijmegen breakage syndrome (NBS), and the NBS-like disorder (Taylor et al., 2004; Waltes et al., 2009). The loss or impaired function of the MRN complex in these patients redirects the repair of DSBs toward the NHEJ pathway, which does not require end resection. Similarly, the presence of Polθ is essential for the alt-NHEJ pathway to compete with HR, as its interaction with RAD51 inhibits HR activity (Ceccaldi et al., 2015). Conversely, some HR factors, such as FA proteins, can promote the alt-NHEJ activity, suggesting that these factors tend to shift the repair towards the resection-dependent pathways (Howard et al., 2015; Unno et al., 2014). In other cases, a repair factor functions in multiple pathways under diverse regulatory mechanisms, further increasing the intricacy of DSB repair pathway selection (Ceccaldi et al., 2016). In conclusion, multiple connections, either competitive or cooperative, exist between different repair pathways, ensuring prompt and accurate repair of DSBs.

1.2.3 DNA Damage Tolerance

Translesion synthesis (TLS) and template switching (TS) are key mechanisms that enable DNA replication to proceed despite the presence of DNA lesions that could otherwise impede the process (Lord & Ashworth, 2012). These mechanisms are therefore regarded as damage tolerance pathways within the DDR.

Translesion DNA synthesis (TLS)

In TLS, error-prone "translesion" DNA polymerases temporarily replace high-fidelity polymerases to synthesise DNA across a lesion site, utilising the undamaged template strand as a guide. Once the replication fork has passed the lesion, the translesion polymerases are often replaced back by high-fidelity polymerases to resume normal DNA synthesis (Waters et al., 2009). Eukaryotic TLS encompasses Y-family polymerases such as REV1, Pol η, Pol ι, and Pol κ, as well as the B-family polymerase Pol ζ (Gan et al., 2007; Sale et al., 2012). These polymerases lack 3' to 5' nucleotide proofreading activity and exhibit decreased selectivity for incoming nucleotides compared to high-fidelity replicative polymerases (Waters et al., 2009).

Although the reduced fidelity of TLS polymerases allows DNA lesion tolerance during replication, it also results in a significantly higher mutation rate. The error rates of TLS polymerases can be as high as 1 in every 10 nucleotides inserted, compared to 1 in every 10^{10} bases for replicative polymerases Pol ε and Pol δ (McCulloch & Kunkel, 2008; Sale, 2013). Mutagenic events caused by TLS polymerases have been implicated in tumorigenesis and may impact the response of cancer cells to DNA-damaging chemotherapies (Yamanaka et al., 2017; Yang et al., 2018). The recruitment of TLS polymerases to damage sites is mediated by the monoubiquitination of the DNA processivity factor PCNA at lysine 164 by the E3 ligase enzyme RAD18 (Watanabe et al., 2004). Loss of RAD18 contributes to genomic instability and increases sensitivity to DNA-damaging agents in non-malignant mammalian cells (Tateishi et al., 2023; Yoon et al., 2012). Nevertheless, RAD18-dependent PCNA ubiquitination also drives mutagenic TLS, which can sometimes promote tumorigenesis (Lou et al., 2021).

Template switching (TS)

While monoubiquitylated PCNA recruits TLS polymerases for the lesion bypass, the K63-linked polyubiquitylation of PCNA, following its initial monoubiquitination by the RAD18, activates an alternative error-free pathway relying on template switching (Chiu et al., 2006;

Lovett, 2017; Motegi et al., 2008; Ulrich, 2011). In TS, the stalled nascent strand switches from the damaged template to the undamaged newly synthesised sister strand for an extension past the lesion (Bi, 2015; Ulrich, 2011). Thus, the error-free TS is a complex but preferable process for bypassing DNA lesions (Bi, 2015). However, TS may promote genomic instability through genomic rearrangements, sister chromatid exchange, and gene amplifications when bypassing genomic regions with high numbers of repetitive sequences, such as telomeres, tRNA genes, and triplet repeats (Hasty & Montagna, 2014; Tanaka & Watanabe, 2020).

1.2.4 DNA Replication Stress

DNA replication is the fundamental process of duplicating and conveying genetic information from one generation to the next in living organisms. The initiation of DNA replication entails the formation of a pre-replicative complex comprising the origin-recognition complex (ORC), CDC6, CDT1, and a hexameric ring of MCM proteins (MCM2–7) assembled at specific DNA sequences known as replication origins (Bleichert et al., 2017). Subsequently, DNA synthesis initiates through the "origin firing" process, which is orchestrated by cyclin-dependent kinases (Nguyen et al., 2001). In eukaryotes, the unwinding of the parental DNA duplex is facilitated by the CDC45/MCM2–7/GINS (CMG) helicase complex and DNA is replicated by the leading and lagging strand polymerases, Pol ε and Pol δ, respectively (Ilves et al., 2010). The polymerases function in collaboration with the CMG helicase complex and other associated factors, collectively forming the replisome (N. Y. Yao & O'Donnell, 2010).

In eukaryotic linear chromosomes, DNA replication forks engage in a bidirectional movement, initiating from specified replication origins (Aria & Yeeles, 2019). Replication stress occurs when these forks confront diverse obstacles, spanning from DNA lesions and protein-DNA complexes (PDCs) to atypical DNA structures and concurrent RNA transcription (Berti & Vindigni, 2016; Zeman & Cimprich, 2013). The consequences of replication stress are contingent upon the particular impediment encountered. Relatively minor DNA lesions may navigate through the CMG helicase while inhibiting the advancement of DNA polymerases, leading to the physical uncoupling of the helicase from the polymerases (Byun et al., 2005). In contrast, larger DNA lesions such as PDCs, ICLs, or bulky DNA adducts impede the entire replisome, extensively blocking the unwinding of parental DNA strands (Calzada et al., 2005). When faced with fork stalling, a multifaceted array of cellular responses is set into motion to ensure the preservation of the fork's integrity. These responses encompass initiating precise

cell cycle checkpoints and resuming DNA synthesis through fork repair and restart (Lambert & Carr, 2005; Sidorova, 2017). Numerous essential participants coordinate these intricate processes, including ATP-dependent DNA translocases, fork remodelling enzymes, DNA binding proteins, DNA nucleases, and helicases (Ait Saada et al., 2018; Quinet et al., 2017).

Ensuring the stability of replication forks in stressful conditions safeguards against detrimental nucleolytic resection and promotes the restart of stalled forks (Liao et al., 2018). Importantly, proteins associated with the FA pathway, in addition to their established role in repairing ICLs, play a central role in protecting stressed replication forks (Howlett et al., 2005). Activation of the FA pathway is notably swift, as indicated by the monoubiquitination of FANCD2 upon the stalling of replication forks, even in the absence of ICLs at the stalling site (Lachaud et al., 2016). Both FANCD2 and FANCD1 (BRCA2) assume pivotal roles in shielding stalled replication forks from excessive resection mediated by MRE11, achieved through the stabilisation of the Rad51 nucleofilament (Schlacher et al., 2011, 2012). Furthermore, factors operating upstream of FANCD2 within the FA pathway protect stalled forks. For example, the FA core complex protein FANCB has been demonstrated to collaborate with the RECQL5 helicase to prevent the degradation of nascent DNA strands under hydroxyurea (HU) treatment, a drug that induces fork stalling through the deoxynucleotide triphosphates (dNTPs) depletion (T. M. Kim et al., 2015).

Upon the occurrence of replication stress, ssDNA is generated at the stalled fork due to several factors, including the dissociation of replicative polymerases, the decoupling of helicase and polymerase activities, or the nucleolytic degradation of newly synthesised DNA at gapped or reversed forks (Liao et al., 2018). The ssDNA accumulating at arrested forks becomes coated with RPA, which, in turn, facilitates the recruitment of the DNA replication checkpoint kinases, ATR, through its interaction with ATRIP (Byun et al., 2005; Nam & Cortez, 2011; Zou & Elledge, 2003). Following activation, ATR, working in conjunction with its effector kinase CHK1, orchestrates a temporary cell cycle arrest to allow the resolution of factors causing the stalling (Paulsen & Cimprich, 2007). Concurrently, ATR and CHK1 phosphorylate numerous proteins during the replication checkpoint process to prevent the collapse of the fork. This includes mechanisms like the suppression of excessive origin firing to prevent depletion of RPA, stabilising the replisome, and the regulation of fork repair enzymes (Cortez, 2015). In addition to ATR, the RPA-coated ssDNA is a platform for loading the RAD9/RAD1/HUS1 (9-1-1) complex (Kanoh et al., 2006). The 9-1-1 complex functions similarly to the replication

factor PCNA but is specialised for damage response and actively promotes the downstream checkpoint responses (Kemp & Sancar, 2009; S. Yan & Michael, 2009).

Stalled replication forks have the potential to be rescued by alternative replication origins referred to as “dormant origins” that are activated selectively in response to replication stress. Activation of dormant origins in proximity to stalled forks allows for the completion of DNA synthesis by another incoming replication fork (Ge & Blow, 2010). When fork stalling occurs within regions lacking dormant origins, several mechanisms associated with the replication stress response (RSR) are initiated to restart or repair the fork. These recovery mechanisms generally encompass damage bypass through fork traversal, translesion synthesis (TLS), or template switching (TS); fork reversal involving fork remodelling proteins; and fork breakage leading to one-ended DSBs (Yeeles et al., 2013).

Damage bypass is one of the strategies cells employ when replication forks encounter a DNA lesion. Three distinct methods are available to bypass various forms of DNA damage: fork traverse facilitated by a DNA translocase, translesion synthesis employing specialised TLS polymerases, and template switching utilising the newly synthesised sister DNA strand (Marians, 2018). Fork traverse is the process by which the replication machinery traverses through the lesion with the assistance of the FANCM translocase and MHF1/2 proteins, enabling replication to resume directly on the other side of the lesion (J. Huang et al., 2013). In this context, the replication fork bypasses damage by repriming DNA synthesis downstream of the lesion via the primase PRIMPOL (Mourón et al., 2013). TLS represents a highly adaptable mechanism for managing fork stalling at DNA lesions, although it may introduce mutations (Sale, 2013). Within TLS, the conventional replicative DNA polymerase is substituted by specialised TLS polymerases, including Pol ζ, Pol η, Pol ι, Pol κ, and REV1, to enable replication through a damaged template (Sale et al., 2012). Except for TLS, another mechanism for DNA damage tolerance, TS, involves the direct bypass of the lesion on the original parental DNA strand by utilising the newly synthesised sister DNA strand as the replication template (Branzei & Foiani, 2007). K63 poly-ubiquitination on PCNA at stalled replication forks signals the damage bypass to transition from TLS to TS (Kanao & Masutani, 2017). It is worth noting that these damage bypass mechanisms leave unreplicated ssDNA gaps behind the damaged forks, necessitating subsequent repair after replication (Ghosal & Chen, 2013).

Another common RSR mechanism involves reversing the course of the replication fork to avert potential fork collisions with DNA damage (Zellweger et al., 2015). Like TS, fork reversal incorporates correct nucleotides using the newly synthesised sister strand instead of the lesion-containing strand as a replicative template (Atkinson & McGlynn, 2009). Reversal of stalled replication forks necessitates the disassembly of the replisome. However, this process also provides protective mechanisms against fork breakage (Qiu et al., 2021). For instance, PARP1 binds to SSBs at the stalled fork, prompting fork reversal while preventing the formation of DSBs (Ray Chaudhuri et al., 2012). Also, the reversal process shields the fork from cleavage by structure-selective nucleases like MUS81, which exhibits higher enzymatic activity on three-way replication fork structures than on four-way junctions (S. Mukherjee et al., 2014). Fork reversal can be divided into two stages. First, the reversed fork is formed through the coordinated annealing of the two newly synthesised strands. Several factors play pivotal roles in mammalian cells to promote the reversed fork formation, including the recombinase factor RAD51 and several DNA translocases like RAD54, SMARCAL1**,** FANCM, ZRANB3 and the Rad5 homolog HLTF (Bugreev et al., 2011; Ciccia et al., 2012; Gari, Décaillet, Delannoy, et al., 2008; Kile et al., 2015; Zellweger et al., 2015). Subsequently, the reversed fork is reinitiated by relocating it back into the three-way junction with the assistance of the RECQ1 helicase (Berti et al., 2013).

The last mechanism to recover stalled replication forks involves fork breakage, whereby one of the fork arms is detached, leaving a one-ended DSB (Hanada et al., 2007). Fork breaks arise when the replication fork encounters an ssDNA gap or when it is cleaved by a structure-specific endonuclease (Pepe & West, 2014). Stalled replication forks that have been broken can be mended by HR-mediated break-induced DNA replication (BIR) (Yeeles et al., 2013). In this process, cleavage of the stalled replication fork by MUS81 leads to the creation of an ssDNA overhang that invades a nearby homologous sequence, forming a D-loop. This, in turn, drives DNA polymerase δ-dependent DNA synthesis to fix the broken forks (Sakofsky & Malkova, 2017). RAD51 has been implicated in restoring broken replication forks through HR-mediated fork recovery (Hashimoto et al., 2011; Lambert et al., 2010). Besides, RAD52 ensures cell survival when replication checkpoints are absent by stimulating DSB formation at stalled forks (Murfuni et al., 2013).

As introduced above, cells possess several strategies to address barriers encountered during replication. Selecting a specific recovery mechanism at stalled forks involves intricate interplay,

primarily guided by three interrelated yet non-exclusive factors. Firstly, the structural configuration of the stalled replication fork and the lesion location play a pivotal role. Lesions occurring on the lagging strand of DNA are typically well accommodated due to the inherently discontinuous nature of Okazaki-fragment synthesis and maturation. In contrast, lesions on the leading strand substantially hinder continuous DNA synthesis, requiring the initiation of recovery processes. Secondly, the proteins' composition at the stalled fork and their post-translational modification status in response to a stalled replication event influence the decision-making process. For example, monoubiquitination on PCNA at stalled forks initiates TLS, whereas PCNA polyubiquitination signals the TS. Thirdly, the timing within the cell cycle when a stalled fork arises and persists is a critical determinant. Notably, many types of lesions can be bypassed throughout multiple cell division cycles, with each cycle employing a distinct mechanism to overcome the hindrances.

1.3 DNA Interstrand Crosslink (ICL) and ICL Repair

ICLs covalently join the two strands of the double helix DNA and are highly toxic to cells. They impede the separation of DNA strands, resulting in significant blockades to DNA replication and transcription (Constantinou, 2012). ICLs can occur between adjacent functional groups within the major or minor grooves of DNA. Some ICLs can cause pronounced unwinding of DNA, helical bends, and even eversion of adjacent bases, while others cause only minor distortions (Legerski, 2010). Although the sites of crosslink formation vary depending on the genotoxic agent, purine nucleotides (dG and dA) tend to be more reactive than pyrimidine nucleotides (dT and dC). Specifically, deoxyguanines are the most common targets of physiologically and therapeutically relevant ICLs (Gates, 2009). Defective ICL repair is highly associated with the occurrence of Fanconi anaemia (FA), a bone marrow failure and cancer predisposition syndrome, while accelerated ICL repair can cause drug resistance in chemotherapies (Deans & West, 2011; Wang & Gautier, 2010). The repair of ICLs involves multiple mechanisms and can occur either through replication-dependent or -independent pathways (Deans & West, 2011). This section provides an overview of the origins of ICLs, Fanconi anaemia syndrome, and ICL repair mechanisms.

1.3.1 Sources of ICL

A variety of factors can lead to ICL formation, including both endogenous and exogenous sources such as metabolic byproducts, environmental carcinogens, and certain therapeutic agents (Clauson et al., 2013; Deans & West, 2011; Langevin et al., 2011). The chemical structure of ICLs varies depending on the specific crosslinking agent and the manner in which it reacts with the functional groups present in DNA nucleobases (Lopez-Martinez et al., 2016). Several well-studied crosslinkers are described below.

1.3.1.1 Endogenous Sources of ICL

Reactive aldehydes

Reactive aldehydes are one of the main endogenous sources of ICLs, with examples including acetaldehyde, formaldehyde, malondialdehyde, acrolein, and 4-hydroxynonenal (Clauson et al., 2013). These aldehydes can be generated via biological processes such as lipid peroxidation and dietary metabolism of biomolecules (Clauson et al., 2013; O'Brien et al., 2008; Stonez et al., 2008). Electrophilic aldehydes typically react with the exocyclic amines of purine nucleotides, specifically the N^2 position of dG and the N^6 position of dA. For instance,

formaldehyde can form a hydroxymethyl monoadduct through nucleophilic attack by an exocyclic amine, which can further react to form an ICL with a second exocyclic amine (Huang & Hopkins, 1993). Similarly, other reactive aldehydes like acrolein, crotonaldehyde, and 4-hydroxynonenal can interact with guanine bases to form exocyclic 1, N^2-dG adducts, which may subsequently be reopened and converted into ICLs (Huang et al., 2010; Stonez et al., 2008).

Abasic crosslinks

Loss of nucleobases, either by spontaneous depurination or through glycosylase-mediated hydrolytic cleavage, results in AP sites - the most frequent type of DNA lesions (Nakamura et al., 1998; Nakamura & Swenberg, 1999). ICL formation from AP sites occurs only in specific sequence contexts, such as dA-AP ICL located in a 5'CXT/5'AAG sequence (X=AP) (Housh et al., 2021). Nonetheless, given their high abundance, nonnegligible amounts of AP sites become ICLs *in vivo*. AP sites exist in a state of equilibrium between ring-closed hemiacetal (99%) and ring-opened aldehyde (1%) (Dutta et al., 2007). When AP sites are in the ring-opened form, reactions of the AP aldehyde with adenine or guanine residues on the opposing DNA strand generate ICLs (Housh et al., 2021). Other ICLs can form from C^4-oxidised abasic sites generated by DNA-damaging agents such as bleomycin, ionising radiation, and certain antitumour agents that cause oxidative DNA damage (Sczepanski et al., 2008). Similar to the repair of psoralen-induced ICLs, *N*-glycosyl cleavage by NEIL3 represents the primary unhooking pathway for AP-ICLs, whereas incisions represent backup mechanisms (Semlow et al., 2016).

1.3.1.2 Exogenous Sources of ICL

The sources of DNA ICLs that are more extensively studied are of exogenous origin. These ICL-inducing agents include a diverse range of chemotherapeutic compounds that hinder DNA replication and are particularly lethal to rapidly dividing cancer cells. Although the principles of ICL formation are generally similar, these ICL-inducing compounds exhibit distinct sequence preferences, topologically constrain DNA in different ways, and require specific processing within the cell to form active ICL-inducing species (Guainazzi & Schärer, 2010). Some of the most common exogenous crosslinking agents and their clinical benefits are discussed below.

Mitomycin C (MMC)

MMC is a widely used chemotherapeutic agent that was originally isolated from *Streptomyces caespitosus*. The natural MMC is not an inherent crosslinker and requires two reduction steps to activate its bifunctional alkylating activity (Tomasz, 1995). Same as most ICL-inducing agents, ICLs represent a relatively small proportion of damage caused by MMC, typically comprising between 5-13% of total lesions (Dronkert & Kanaar, 2001). Moreover, MMC exhibits sequence specificity, requiring the dinucleotide 5'-CG-3' to generate ICLs between the N^2 positions of two guanines, causing minor DNA distortions (Dronkert & Kanaar, 2001; Tomasz, 1995). Since only 5% of guanines in mammalian genomes exist in the 5'-CG-3' sequence context, together with only ~10% of total produced lesions being ICLs, the potential efficacy of MMC as a chemotherapeutic is limited (Tomasz, 1995). However, the hypoxic environments characteristic of solid tumours enhance the ICL-inducing capability of MMC, while the presence of oxygen in normal tissues mitigates its toxicity (Tomasz, 1995). Thus, MMC has been successfully employed in the treatment of bladder and oesophagal cancers (Tolley et al., 1988; Wolf et al., 2010).

Nitrogen mustards

The discovery and use of nitrogen mustard have a complex history. Despite being developed originally as a deadly weapon in World War II, mustard gas soon paved the way for nitrogen mustard and its derivatives in cancer treatments (Deans & West, 2011). This class of chemotherapeutic agents, such as Cyclophosphamide, Melphalan, Chlorambucil, and Ifosfamide, are used to treat various types of cancers, including malignant melanomas, lymphomas, ovarian cancer, chronic lymphocytic leukaemia (CLL), and non-small cell lung carcinoma (NSCLC) (Boone et al., 2018; Deans & West, 2011; Singh et al., 2018; Vitolo et al., 2017). Nitrogen mustards react with the N^7 position of guanine residues in a 5'-GNC-3' sequence context through the reactive *N*, *N*-bis-(2-chloroethyl)amine functional group in a two-step process (Guainazzi & Schärer, 2010; Singh et al., 2018). First, bis-(2-chloroethyl) amine undergoes intramolecular cyclisation to form an unstable and highly reactive aziridinium cation. In the second step, the strained aziridinium cation undergoes nucleophilic addition by DNA nucleophiles to form a monoalkylation adduct. These reactions can then be repeated to give a crosslink between two complementary strands of DNA (Singh et al., 2018). ICLs induced by nitrogen mustards create approximately 15° of DNA bending, which account for ~5% of the total lesions created by the compounds (Dronkert & Kanaar, 2001; Guainazzi & Schärer, 2010).

Platinum compounds

Platinum-based compounds are widely used as chemotherapeutics for treating various types of cancer, including testicular, ovarian, colorectal, prostate, breast and non-small-cell lung cancers (Deans & West, 2011). Cisplatin, Carboplatin, Oxaliplatin, Satraplatin, and Picoplatin are commonly employed platinum compounds in clinical practice (Clauson et al., 2013; Deans & West, 2011). While the exact ICL formation propensity differs among these crosslinkers, guanine residues in the 5'-GC-3' sequence context are mostly crosslinked (Dasari & Bernard Tchounwou, 2014; Lopez-Martinez et al., 2016). For example, cisplatin generates highly distorting ICLs resulting from the reaction at the N^7 position of two guanines in the 5'-GC-3' sequence (Dronkert & Kanaar, 2001; H. Huang et al., 1995). Upon the formation of a cisplatin-induced ICL, the DNA duplex undergoes a 110° unwinding and a 47° bend in the DNA backbone, with the cytosine bases opposite to the crosslinked guanines becoming extrahelical (Dronkert & Kanaar, 2001; Malinge et al., 1999). Despite its ability to form ~5–8% ICLs, cisplatin predominantly generates intrastrand crosslinks, including 65% d(GpG) intrastrand crosslinks and 25% d(ApG) intrastrand crosslinks (Dronkert & Kanaar, 2001).

Psoralens

Psoralens are a group of natural compounds derived from plants that, when activated by UVA, can induce covalent bonds between thymines in 5'-TA-3' sequences (Dronkert & Kanaar, 2001). Compared to other crosslinkers, psoralens have a much higher propensity to form ICLs, with a rate of approximately 40% (Dronkert & Kanaar, 2001). A derivative of psoralen, trimethylpsoralen (TMP), can even form ICLs that account for 90% of total lesions (Lopez-Martinez et al., 2016). The DNA distortion caused by psoralen adducts results in a relatively minor 25° local unwinding of DNA around the lesion (Dronkert & Kanaar, 2001; Spielmann et al., 1995). The combination of psoralen and UVA radiation has been used to treat various chronic skin diseases, including psoriasis and vitiligo (Guainazzi & Schärer, 2010; McEvoy & Stern, 1987). Importantly, the requirement for UV activation of psoralens allows for localised targeting in cancer therapies and thus reduces damage to normal tissues. Vitiligo patients, in particular, benefit from such localised treatment in which only diseased skin areas are exposed to radiation (Melough & Chun, 2018; Vieyra-Garcia & Wolf, 2021).

Diepoxybutane (DEB)

DEB is a metabolite of the carcinogen 1, 3-butadiene, a chemical compound commonly used in the production of synthetic plastics and rubbers (Bond & Medinsky, 2001). Unlike the crosslinkers mentioned above, DEB is not currently used as an anti-cancer agent, and thus, its cytotoxicity has not been as extensively studied. However, DEB, MMC and platinum compounds are normally employed in the clinical laboratory diagnosis of FA (Cirkovic et al., 2011). DEB-derived ICLs share the 5'-GNC-3' trinucleotide preference, as observed with nitrogen mustards, and induce a 34° bend in the DNA helix (Millard et al., 2012; Millard & White, 1993). DEB is cost-effective, stable, and requires no additional activation, making it particularly useful in cell biology research (Rogers, Lee, et al., 2020).

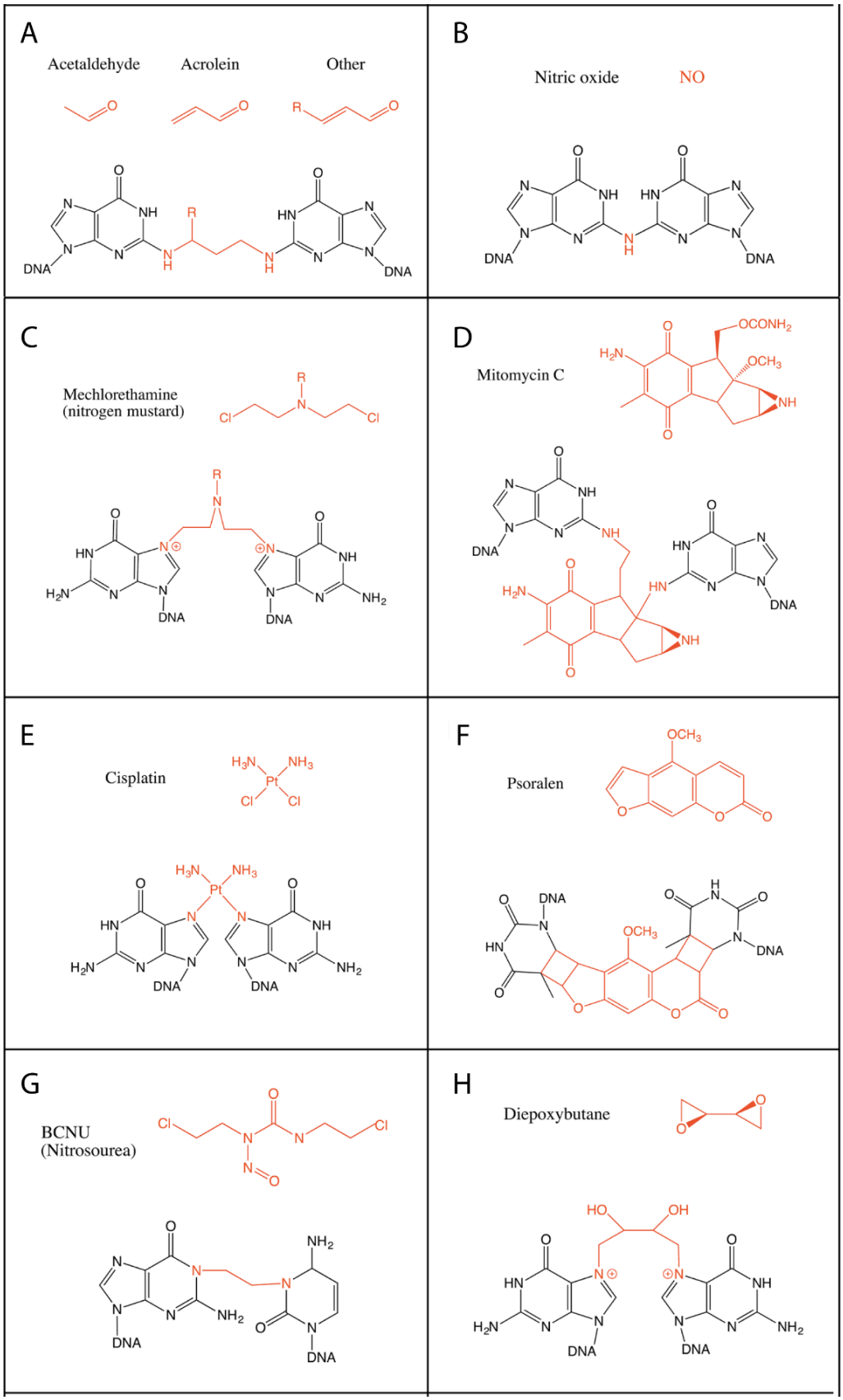


Figure 1-1 The chemical structures of diverse crosslinking agents and the resultant ICLs.
A) Reactive aldehydes. B) Nitric oxide. C) Mechlorethamine (nitrogen mustard). D). Mitomycin C. E) Cisplatin. F) Psoralen (when exposed to UVA). G) BCNU (nitrosourea). H) Diepoxybutane. Adapted from *Lopez-Martinez et al., 2016.*

1.3.2 Defective ICL Repair and Fanconi Anaemia (FA)

In 1927, Swiss paediatrician Guido Fanconi first identified and diagnosed patients with a rare genetic disorder showing congenital abnormalities and severe anaemia (Auerbach, 2009). Later, it was discovered that FA patient-derived cells show a high level of chromosomal aberrations upon exposure to bifunctional cross-linking agents, indicating a defect in DNA repair (Duxin & Walter, 2015). FA has since been established as a genetic instability syndrome characterised by congenital abnormalities, bone marrow failure, and cancer predisposition (Auerbach, 2009). To date, mutations in 22 different *FANC* genes have been implicated in the disease, with the majority exerting autosomal recessive inheritance patterns, except for *FANCB* and *FANCR (RAD51)* (Nalepa & Clapp, 2018; Niraj et al., 2019). *FANCB* is X-linked, with males carrying hemizygous genotypes, while *FANCR* mutations are autosomal dominant, leading to dominant-negative effects and FA-like symptoms (Ameziane et al., 2015; Meetei et al., 2004). The most common FA-causing mutations occur in *FANCA* and *FANCC* genes, which typically result in milder phenotypes than those in other FA genes (Alter & Rosenberg, 2013; Auerbach, 2009). FA is a rare genetic disorder that affects approximately 1 in every 100,000-160,000 individuals, with a slightly higher incidence in males due to the partially X-linked nature of the disease (Duxin & Walter, 2015; Meetei et al., 2004).

A hallmark of FA is hematologic manifestations resulting from a lack of functional bone marrow stem cells (Auerbach, 2009). In severe cases, FA patients develop acute myeloid leukaemia, a bone marrow cancer that produces abnormal myelocytes, negatively affecting the development of all types of blood cells (Auerbach & Allen, 1991; Meyer et al., 2005). Additionally, FA patients frequently exhibit congenital abnormalities, including vertebral abnormalities, anal atresia, cardiac defects, tracheoesophageal fistula, oesophageal atresia, renal and radial abnormalities, limb abnormalities, and hydrocephalus, which are collectively referred to as VACTERL-H (Alter & Rosenberg, 2013). Patients who exhibit VACTERL-H generally have a worse prognosis than those without such severe phenotypes, and mutations in less frequently mutated *FANC* genes, such as *FANCB, FANCI, FANCJ, FANCN*, and *FANCO*, are more likely to present with VACTERL-H association (Alter & Rosenberg, 2013). FA patients may also present growth retardations referred to as PHENOS, including skin pigmentation, small head and eyes, nervous system anomalies, otology, and short stature (Fiesco-Roa et al., 2019).

Diagnosis of FA is typically based on clinical presentation, including physical features, VACTERL-H and PHENOS, sometimes accompanied by bone marrow failure (Alter & Giri, 2016; Auerbach, 2009). Clinical suspicions of FA can be further confirmed by laboratory testing (Auerbach, 2009). The most commonly used tests are based on the hypersensitivity of FA cells to ICL agents such as MMC and DEB (Auerbach, 2003; Francies et al., 2018). Broad experience has confirmed the sensitivity, specificity and reproducibility of these tests (Auerbach, 2009). Aside from sensitivity analyses, the chromosome breakage test is widely employed in FA diagnosis. During this test, chromosome spreads are prepared from ICL agent-treated cells and evaluated for chromosomal aberrations, including radial chromosomes, chromatid gaps, and chromatid breaks (Auerbach, 2009). Laboratory tests have greatly improved FA diagnosis, allowing for earlier detection and treatment, thereby improving the survival and life expectancy of FA patients.

Hematopoietic stem cell transplantation (HSCT) is the current standard treatment for FA patients with bone marrow failure, as it effectively restores depleted stem cell populations (Bierings et al., 2018). HSCT is most successful when using donor cells from human leukocyte antigen (HLA)-matched siblings, with a 3-year survival rate of approximately 80% (Benajiba et al., 2015; Dufour, 2017). However, when performed with HLA-matched unrelated donors, the incidence of graft-versus-host disease can lower the 3-year survival rate to 52% (Dufour, 2017). While non-HSCT treatments such as anabolic steroids, including danazol, oxandrolone, and oxymetholone, are also employed in the clinic to temporarily increase blood counts, they are not curative options and are typically reserved for patients who lack access to HSCT (Dufour, 2017).

Improved diagnosis and hematopoietic treatments for FA have led to increased survival rates but have also introduced new challenges for patients, including reduced fertility and increased tumour incidence (Rosenberg et al., 2003; Vanni et al., 2022). Both male and female FA patients exhibit dramatically reduced fertility rates, which are thought to be caused by defects in primordial germ cell proliferation, likely due to the role of FA genes in meiosis and genomic integrity preservation (Vanni et al., 2022). Moreover, the risk for cancer development is 50-fold higher in FA patients compared to the general population (Alter, 2014). Among all types of cancer, head and neck squamous cell carcinomas (HNSCCs) pose the highest risk for FA patients, likely due to the increased replicative potential of these tissues (Alter et al., 2013; Lustig et al., 1995). According to the International FA Registry, approximately 3% of FA

patients develop HNSCCs, with the risk of which in FA patients being 500- to 700-fold higher than that in the general population (Kutler et al., 2003). Besides, the risk of acute myeloid leukaemia (AML) in FA patients is 700-fold higher, and the cumulative incidence is more than 20% by the age of 40 (Alter, 2014). Also, mutations in *FANCD1*, *FANCS*, *FANCJ*, *FANCM*, *FANCN* and *FANCO* have been linked to familial breast and ovarian cancer, and *FANCS/FANCD1* (*BRCA1/BRCA2*) mutations are found in familial and sporadic pancreatic cancers (Blair et al., 2018; del Valle et al., 2020).

The increased susceptibility to developing tumours in FA patients is partially attributed to underlying genetic predispositions but may also arise as an unintended consequence of hematopoietic treatments (Rosenberg et al., 2005). This duality of treatment benefits and potential cancer risk presents a significant challenge for FA management, underscoring the need for targeted therapies. In this regard, gene therapy using autologous hematopoietic stem cells (HSCs) has emerged as a promising therapeutic approach (Bueren et al., 2020; Malouf et al., 2022). Previous studies demonstrate that the correction of only a small number of HSCs can sufficiently rescue hematopoietic defects in mosaic FA patients (Bueren et al., 2020). Moreover, lentiviral transfection of the *FANCA* gene in CD34+ bone marrow cells isolated from FA patients restored cells' resistance to the MMC, indicating a promising gene therapy option based on viral transfection (Río et al., 2017). Gene engineering, such as CRISPR-Cas9 editing, has also been explored for treatment, considering that the NHEJ is still proficient in FA-deficient cells and may restore FA gene function through insertion or deletion in some cases (Richardson et al., 2018). In a previous study, a biallelic insertion mutation in *FANCA*, which causes FANCA protein deficiency in lymphoblastic cell lines via producing a premature stop codon, was successfully corrected through an NHEJ-editing approach (Román-Rodríguez et al., 2019). The same study also demonstrated the feasibility of NHEJ-editing for restoring the function of other *FANC* genes, such as *FANCB*, *FANCC, FANCD1*, and *FANCD2.* These advances in FA gene therapy have shown promising progress and may ultimately offer a more effective treatment option.

1.3.3 ICL Repair Pathways

1.3.3.1 Replication-Dependent ICL Repair

ICLs can severely inhibit DNA replication and have the potential to cause catastrophic damage. Thus, a stalled DNA replication fork is the primary event that triggers ICL repair. In the G1

phase, prereplication complexes composed of minichromosome maintenance 2–7 (MCM2–7) double hexamers are assembled along chromatin to prepare for replication initiation (Burgers & Kunkel, 2017). Following activation by CDK in the S phase, MCM2–7 associates with cell division cycle 45 (CDC45) and go-ichi-ni-san (GINS), forming the CDC45-MCM2–7-GINS (CMG) helicase complex. The CMG helicase then translocates along the leading strand template, unwinding DNA at the leading edge of the replisome (Burgers & Kunkel, 2017). Previous studies suggest that replication-coupled ICL repair is always initiated by the collision of CMG with the lesion, which triggers a complex network of DNA damage signalling and repair pathways to remove the crosslink and restore replication (Zhang et al., 2015).

1.3.3.1.1 Fanconi Anaemia (FA) Pathway

The canonical mechanism of replication-coupled ICL repair is referred to as the FA pathway, a multifaceted repair system responsible for the stepwise removal of ICLs (Kottemann & Smogorzewska, 2013). The efficacy of the FA pathway is contingent upon the concerted action of numerous FA factors that are subject to regulation through diverse mechanisms. This section introduces the mechanistic process and regulation of the FA pathway.

FA proteins

FA pathway involves 22 *FANC* gene products and their associated partners that can be divided into four functional groups: a damage-sensing module (group 1), an E3 ubiquitin ligase core complex (group 2), the repair effector FANCD2/FANCI complex (group 3), and a large group of DNA repair and damage tolerance factors (group 4) involved in the removal or bypass of the ICL lesion (Kottemann & Smogorzewska, 2013). Specifically, the first sensing module consists of the ATPase FANCM and its three interacting partners: Fanconi-associated protein 24 (FAAP24) and the histone-fold heterodimer MHF1 and MHF2 (Basbous & Constantinou, 2019). This module recognises stalled replication forks and recruits the group 2 proteins constituting the FA core complex. The core complex is an E3 ubiquitin ligase comprising FANCA, FANCB, FANCC, FANCE, FANCF, FANCG, FANCL, FAAP20 and FAAP100 (Swuec et al., 2017). The main role of the FA core is to recruit UBE2T, a ubiquitin-conjugating enzyme, to monoubiquitylate the group 3 proteins – the FANCD2/FANCI heterodimer (Smogorzewska et al., 2007). The ubiquitylation of FANCD2/FANCI dimer is essential for ICL repair, which recruits and activates the downstream group 4 factors for ICL removal, strand repair and lesion bypass (Taniguchi et al., 2002). The group 4 members include the Structure-specific endonuclease 4 (SLX4), a scaffolding protein that interacts with the structure-specific

endonuclease XPF-ERCC1 responsible for ICL unhooking; the HR factors BRCA1, BRCA2, PALB2, RAD51, RAD51C and XRCC2 for strand break repair; the E3 ubiquitin ligase FANCW that mediates RPA ubiquitination at stalled replication forks, and the REV7, which along with REV3, forms the TLS polymerase Pol ζ for lesion bypass (Elia et al., 2015; Kottemann & Smogorzewska, 2013).

ICL recognition

As demonstrated in the *Xenopus* egg extract that mimics the ICL repair of replicative plasmids, the initiation of repair requires the convergence of two replication forks on the ICL (Zhang et al., 2015). This fork convergence results in the ubiquitylation of the CMG helicase by the E3 ubiquitin ligase TRAIP, with MCM7 undergoing TRAIP-mediated ubiquitination and CMG being unloaded from the chromatin by the p97 ATPase (Fullbright et al., 2016; Wu et al., 2019). The converged fork at ICL is then recognised, at least in part, by FANCM, which harbours DNA translocase activity, associating with FAAP24, MHF1, and MHF2 to form the FANCM module (Ciccia et al., 2007; Singh et al., 2010). This complex has an affinity for fork-like structures and is constitutively associated with chromatin via MHF1 and MHF2 (Gari, Décaillet, Stasiak, et al., 2008; Z. Yan et al., 2010). The FANCM module subsequently recruits the FA core complex through an interaction with the core complex component FANCF (Deans & West, 2009). The FANCM-mediated core complex recruitment is facilitated by ATR-dependent checkpoint activation that phosphorylates the core complex components FANCA, FANCG and FANCE (Huang et al., 2010; Singh et al., 2013). Alternatively, it has been demonstrated that the Ubiquitin-like with PHD and RING finger domains 1 and 2 (UHRF1 and UHRF2) proteins fulfil the role of sensing ICLs. These two proteins amass at the sites of ICLs and play a crucial role in the recruitment of the FANCD2/FANCI dimer (Liang et al., 2015; Motnenko et al., 2018). Following CMG unloading, one of the converged replication forks probably undergoes reversal to generate a Y-shaped structure, yet whether the reversed fork represents a critical intermediate in ICL repair is yet to be established (Amunugama et al., 2018). Considering that fork reversal is frequently induced by replication challenges and purified XPF does not cleave X-shaped structures, the reversal may occur to convert X-shaped DNA into the suitable form for following XPF cleavage (Amunugama et al., 2018).

Ubiquitination of the FANCD2/FANCI heterodimer

The ubiquitination of the FANCD2/FANCI heterodimer is a critical step in the FA pathway that regulates the ICL removal and subsequent DNA repair processes. As an E3 ubiquitin ligase, the

FA core complex recruited by the FANCM module is responsible for mediating the FANCD2/FANCI ubiquitination (van Twest et al., 2017). The FA core complex comprises three subunits, namely FANCC-FANCE-FANCF (C-E-F), FANCA-FANCG-FAAP20 (A-G-20), and FANCB-FANCL-FAAP100 (B-L-100), with B-L-100 being the catalytic module (Huang et al., 2014). Specifically, FANCL within the B-L-100 subunit generates ubiquitinated-FANCD2/FANCI by transferring ubiquitin from the UBE2T to the dimer via its RING finger domain (Alpi et al., 2008; van Twest et al., 2017). Deletions of any B-L-100 component completely eliminate FANCD2 ubiquitylation in cells, whereas loss of C-E-F or A-G-20 factors reduces but does not abolish ubiquitination, suggesting their supporting roles (Huang et al., 2014; Rajendra, Oestergaard, et al., 2014). Indeed, the C-E-F complex has shown to be a molecular bridge between FANCD2/FANCI and the B-L-100 catalytic module, required to alter the FANCD2/FANCI dimer configuration, stabilising its dimerisation interface and thus greatly stimulate the FANCD2/FANCI ubiquitination (Swuec et al., 2017; van Twest et al., 2017).

Recent structural analyses of the FANCD2/FANCI dimer indicate that in the unmodified state, the FANCD2/FANCI assumes an open, trough-like configuration (Joo et al., 2011). When FANCD2/FANCI interacts with the core complex, the FANCL's RING domain inserts into the FANCD2/FANCI dimer interface near the FANCD2 K561 ubiquitination site and partly closes the trough (Wang et al., 2021). Upon binding to DNA, the FANCD2/FANCI trough fully closes, exposing K561in FANCD2 to allow its ubiquitination by the core complex (Alcón et al., 2020; Wang et al., 2020). The resulting FANCD2 ubiquitination, in turn, enables exposure and subsequent ubiquitination of K523 in FANCI (van Twest et al., 2017; Wang et al., 2021). The ubiquitination effectively locks the FANCD2/FANCI complex onto DNA and facilitates four major downstream mechanisms for ICL repair: ICL unhooking, lesion bypass via TLS, HR-mediated strand break repair and removal of remained adducts by BER or NER factors (Deans & West, 2011).

ICL unhooking

The unhooking cleaves one ssDNA on both sides of the lesion, causing the release of ICL from one of the DNA double helix (Klein Douwel et al., 2014). Several factors are believed to be involved in this process, including XPF-ERCC1, SLX3, SLX4, FANCD2 and FANCI associated nuclease 1 (FAN1), and SNM1A 5’ to 3’ exonuclease (Klein Douwel et al., 2014). First, the ubiquitinated FANCD2/FANCI dimer interacts with the SLX4 scaffolding protein to recruit the structure-specific endonuclease XPF-ERCC1 through SLX4’s MUS312/MEI9

interaction-like region (Kim et al., 2013; Klein Douwel et al., 2014). The XPF-ERCC1 complex then functions as a 3' flap endonuclease and cleaves one side of the ICL (Klein Douwel et al., 2014). The nuclease that incises the other side of the lesion is currently unclear (Zhang & Walter, 2014). Despite this, loss of XPF-ERCC1 appears to decrease the 5′ flap incision, suggesting that XPF-ERCC1 may cleave both sides or that the 5′ flap incision is dependent on or promoted by the 3′ incision (Zhang & Walter, 2014). MUS81-Essential meiotic structure-specific endonuclease 1 (EME1), SLX1-SLX4, and FAN1 are other nucleases that may contribute to the unhooking process, each with different structural preferences, indicating that the choice of nuclease employed depends on the characteristics of the crosslinked DNA (Zhang & Walter, 2014). Once the ICL is unhooked, SNM1A is recruited to the 5' end of the cleaved ICL, and its 5′-3′ exonuclease activity digested the incised DNA strand beyond the ICL (Wang et al., 2011). This leaves a single nucleotide crosslinked to one of the DNA strands, thus providing a better substrate for subsequent TLS (Wang et al., 2011). If fork reversal occurs during incisions, the leading strand must be restored to its original position before the following TLS can take place. However, proteins that may be involved in fork reversal or the leading strand restoration have not been identified.

Translesion synthesis (TLS)

Following unhooking, the cross-linked ICL remnant is bypassed by specialised TLS polymerases. As described in the previous section, the TLS polymerases, such as REV1, Pol ζ, Pol η, Pol κ, Pol ι and Pol ν, possess intrinsically disordered linker regions, allowing them to replicate DNA over lesions (Goodman & Woodgate, 2013). ICL bypass can be performed by multiple TLS polymerases based on the remnant structure as well as the extent of endo- or exonucleolytic processing of the ICL (Ho & Schärer, 2010; Roy & Schärer, 2016). The TLS is initiated when the high-fidelity replicative polymerases, Pol δ and Pol ε, encounter the ICL lesion, and their tight active sites halt the replication process. This results in the activation of the RAD6-RAD18 ubiquitin ligase complex, which monoubiquitinates PCNA at Lys164 to facilitate the recruitment of downstream TLS polymerases (Roy & Schärer, 2016). Following this, a yet-to-be-identified polymerase inserts a nucleotide across from the unhooked ICL, and a complex of the scaffold REV1 and Pol ζ extends the leading strand past the ICL remnant to ligate with the downstream Okazaki fragment of the converging fork (Budzowska et al., 2015). Except for PCNA monoubiquitination, the FA core complex is essential for the recruitment of TLS polymerases (Roy & Schärer, 2016). One of the core components, FAAP20, interacts with REV1 through its ubiquitin-binding zinc finger 4 domain to recruit REV1-associated

polymerases (Kim et al., 2012). This interaction enables FAAP20 to recruit multiple polymerases considering that REV1 associates with polymerases including Pol κ, Pol ζ, Pol ι, and Pol η (Guo et al., 2003; Wojtaszek et al., 2012). Additionally, studies using *Xenopus* egg extracts have shown that immunodepletion of FANCA, another FA core complex component, leads to the inhibition of chromatin-binding of REV1 and REV7 (a subunit of Pol ζ), suggesting FANCA's function in TLS polymerases recruitment (Budzowska et al., 2015).

Homologous recombination (HR)

The repair of DSB generated by ICL unhooking involves the RAD51-dependent HR (Long et al., 2011). This process requires the recruitment of end-resection factors, including BRCA1, BRCA2, RAD51, RAD51C, XRCC2, PALB2, and the initial 5′ end-resection is performed by CtIP and the MRN complex (Deans & West, 2011; Murina et al., 2014; Renaudin & Rosselli, 2020). Although the initial resected DSB ends can be repaired by Pol θ -mediated alt-NHEJ, they are normally further processed by nucleases, such as EXO1 and DNA2, to generate longer 3′ ssDNA overhangs for subsequent strand invasion, which guides the repair towards the HR mechanism (Ceccaldi et al., 2015; Karanja et al., 2012). The 3′ ssDNA ends are rapidly bound and protected by RPA to prevent their degradation and promote subsequent repair (Li & Heyer, 2008). The loading of RPA is facilitated by FANCJ, which physically interacts with RPA and simultaneously recruits CtIP to promote end resection (Gupta et al., 2007; Li & Heyer, 2008; Nath & Nagaraju, 2020). Other FA-associated proteins, including FANCM and FAAP24, are also involved in RPA loading (Huang et al., 2010). FANCM is additionally involved in CtIP recruitment to ICL sites, indicating its indispensable role in the end resection step for ICL repair (Duquette et al., 2012).

Following end resection, BRCA1 associates with PALB2 and BRCA2 to promote the assembly of RAD51 nucleofilaments (Al Abo et al., 2014). RAD51 then facilitates the first-end DNA synthesis via strand invasion at the D-loop. Pol δ is the primary DNA polymerase involved in this process, although TLS polymerases, such as Pol ζ and Pol η, can also participate (Li et al., 2013). For second-end DNA synthesis, which occurs after the second end of a DSB anneals to the displaced strand of the D-loop, Pol ε is assumed to be the major polymerase involved, but Pol δ and TLS polymerases may also play a role (McVey et al., 2016). Formation of a double Holliday junction might occur during HR-associated strand invasion and requires resolution for proper repair. In ICL repair, BTR-mediated decatenation appears to play a primary role in the double Holliday junction resolution (Semlow & Walter, 2021).

While the DSB resulting from the ICL unhooking is repaired by HR, the crosslinking adduct remanent on the other strand is bypassed by TLS and ultimately needs to be removed. It is suggested that this removal of the monoadduct can be mediated by BER and NER, and which pathway is used likely depends on the structure of the adduct (Muniandy et al., 2010).

ICL traverse

Initiation of ICL repair occurs through fork convergence in the *Xenopus* egg extract system (Zhang et al., 2015). However, in mammalian cells, the average inter-origin distance of approximately 100 kb suggests that replication fork convergence is not always guaranteed (Berezney et al., 2000). In fact, a DNA combing assay has shown that more ICLs are adjacent to a single replication fork than those sandwiched between converging forks (Huang et al., 2013). Importantly, unlike what is observed in egg extracts, in approximately 60% of cases, a single replication fork traverses through ICLs without unhooking, showing that mammalian cells' replication machinery can directly bypass the ICLs (Rohleder et al., 2016).

ICL traverse is the process in which the replication machinery proceeds through an ICL in a highly efficient manner without resolving the lesion (Rohleder et al., 2016). This mechanism is shown to be mediated by the FANCM-MHF1/2 complex and depends on FANCM's interaction with PCNA through its PIP-box motif (Huang et al., 2013; Rohleder et al., 2016). When the replication fork traverses an ICL, the GINS subunit is displaced from the CMG helicase, presumably allowing the CMG ring to open and bypass the lesion (Huang et al., 2019; Wasserman et al., 2019). The displacement of the GINS subunit is facilitated by ATR-mediated phosphorylation of FANCM and its interaction with the MCM2-7 complex, but independent of FANCM's ATPase activity (Huang et al., 2019). After traversing, the Primase and DNA directed polymerase (PRIMPOL) mediates the repriming of the leading strand beyond the lesion to allow the restoration of DNA synthesis on the other side (González-Acosta et al., 2021). Lesion traverse leaves behind an ICL that remains in the DNA structure, necessitating repair before cell entry into mitosis. NER factors are postulated to be central in resolving traversed ICLs, particularly those that induce significant distortion in DNA topology, such as cisplatin-ICLs (Smeaton et al., 2008). The structural configuration generated during the traverse resembles the X-shaped structure when two replication forks converge. The key distinguishing factor is that if DNA synthesis recommences just beyond the ICL, the 5' end of the newly synthesised leading strand following traverse is positioned closer to the lesion than

at a converged fork (Rogers, Simmons, et al., 2020). This spatial distinction influences the endonucleases responsible for unhooking the traversed ICL, and it is postulated that SLX1 or FAN1 is involved in cleaving on the 5' side of the traversed ICL, while MUS81-EME1 cuts on the 3' side of the lesion during traverse events (J. Zhang & Walter, 2014). Despite the majority of ICLs being traversed and FANCM's critical function in this process, cells with *FANCM* mutations are less sensitive to crosslinkers than those with an inactivated FA core. This indicates that the removal of ICLs via the FA pathway plays a more critical role in ensuring cell survival than the fork traverse mechanism (Datta & Brosh, 2019).

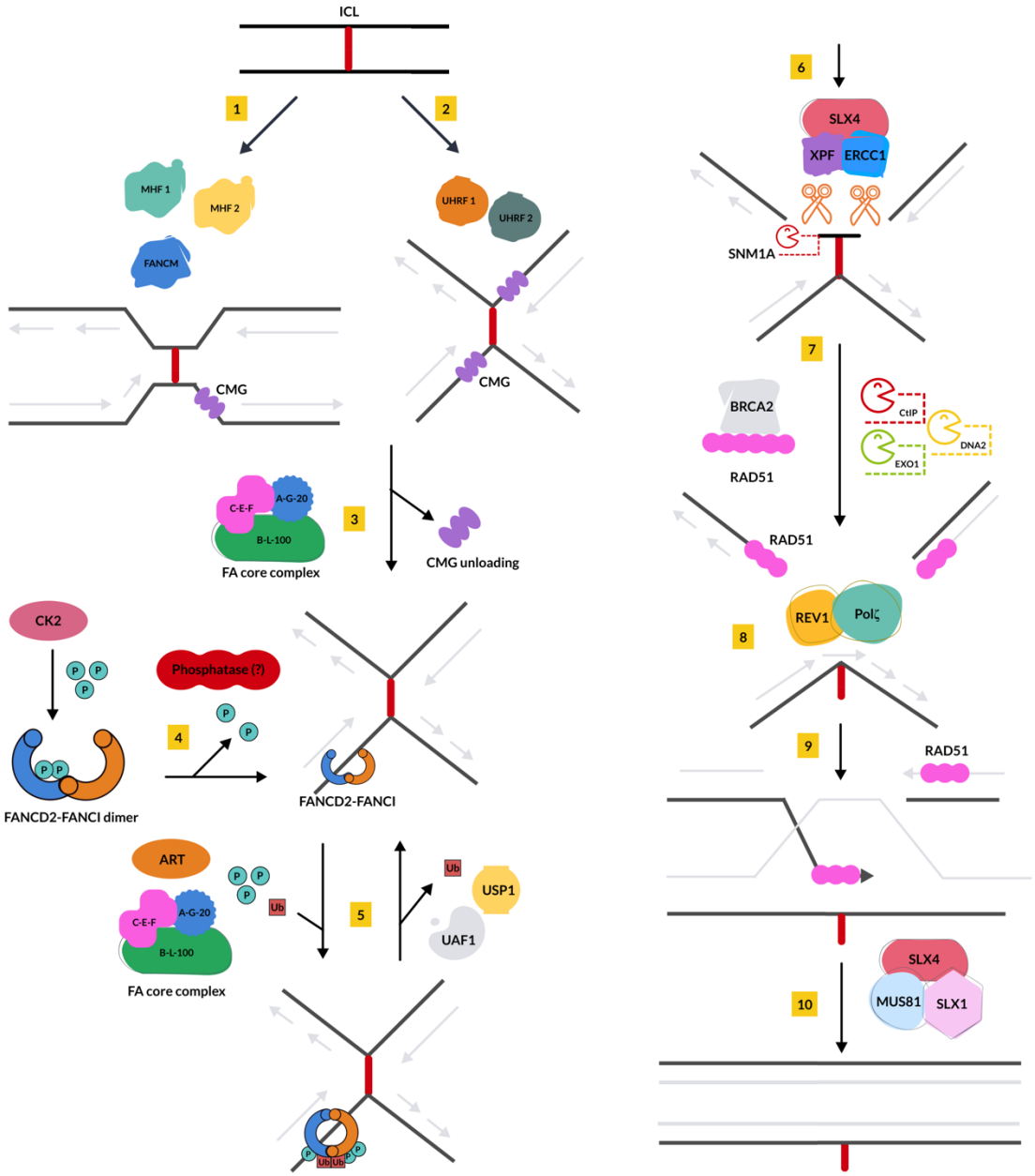


Figure 1-2 ICL repair by the FA pathway.
The ICL lesion is detected either through the FANCM/MHF complex, which initiates fork traverse (Step 1), or by specialised sensor proteins like UHRF1 and UHRF2 (Step 2). In both scenarios, fork convergence occurs at the ICL site, followed by the CMG helicase unloading and recruitment of the FA core complex through FANCM (Step 3). FANCD2 is constitutively phosphorylated by the kinase CK2. Removal of these phosphate groups from FANCD2, required prior to FANCD2/FANCI binding to DNA, is currently attributed to an unknown phosphatase (Step 4). Subsequently, ATR phosphorylates and the FA core complex monoubiquitinates the FANCD2/FANCI dimer. This monoubiquitination event locks the FANCD2/FANCI dimer onto DNA. The reverse deubiquitination reaction is catalysed by USP1/UAF1 (Step 5). Structure-specific nucleases, such as XPF/ERCC1 (complexed with scaffold protein SLX4), are recruited to the lesion. XPF/ERCC1 initiates incisions around the ICL and unhooks it, while SNM1A trims the unhooked nucleotide fragment past the crosslink (Step 6). Unhooking the ICL results in a double-strand break (DSB) on one sister chromatid and a lesion adduct on the other. The DSB ends are processed by CtIP, DNA2, or EXO1, generating overhangs that are primed for strand invasion, facilitated by BRCA2-dependent RAD51 deposition (Step 7). The TLS polymerases REV1/Pol ζ complex enables DNA synthesis past the unrepaired adduct (Step 8). RAD51 promotes strand invasion, followed by extension of the resected DSB ends (Step 9). Following DNA synthesis and strand ligation, a double Holliday junction is formed, which is resolved by SLX4/SLX1/MUS81 (Step 10). The residual crosslink adduct is ultimately eliminated through the nucleotide excision repair (NER) factors.

Regulation of the FA pathway

The sequential recruitment of FA proteins to chromatin is a highly coordinated process regulated by numerous factors. Among them, the most critical regulatory mechanism is associated with the ubiquitination of the FANCD2/FANCI dimer by the FA core complex, since the dysregulation of which disrupts both upstream and downstream activities (Kee & D'Andrea, 2012; Shimamura et al., 2002). The majority of FA mutations occur in genes that encode FA core complex subunits, and approximately 90% of FA patients have disrupted FANCD2/FANCI ubiquitination (Kee & D'Andrea, 2012).

Recognition of ICLs and the resulting FA core recruitment depends on the activity of FANCM. Upon encountering exposed ssDNA at the replication fork, FANCM undergoes phosphorylation by major checkpoint kinases ATM and ATR (Sobeck et al., 2009). During S-phase, FANCM undergoes moderate phosphorylation that leads to the association of the core complex with chromatin (Sobeck et al., 2009). However, FANCM becomes hyperphosphorylated through G2/M phases by the polo-like kinase 1 (PLK1), subjecting it to proteasomal degradation (Kee et al., 2009). Together, this regulation of FANCM's phosphorylation state limits the recruitment of core complex and FA pathway activity to S-phase (Kim et al., 2008). Chromosomal translocation occurs when the FANCM phosphorylation is deregulated, as MMC-induced radial chromosomes are observed in cells when non-degradable FANCM mutants permit a persistent association of the core complex to chromatin (Kee et al., 2009). Besides, FANCM's localisation to chromatin, as well as its phosphorylation, are partly dependent on the expression of FANCD2, which suggests a feedback loop in which activation of FANCD2 further enhances FANCM-mediated core complex recruitment (Sobeck et al., 2009).

FANCL is the enzymatic component of the FA core complex, acting as an E3 ubiquitin ligase for the FANCD2/FANCI monoubiquitination. Hence, the regulation of FANCL is critical for the execution and completion of the FA pathway. Studies suggest that the expression level of FANCL is tightly regulated by its autoubiquitination and the glycogen synthase kinase 3 beta (GSK3B)-dependent phosphorylation (Dao et al., 2013). While the GSK3B-mediated phosphorylation protects FANCL from proteasome-mediated degradation, the autoubiquitination makes it more vulnerable to proteasome inhibition (Dao et al., 2013). When responding to ICLs, damage-induced activation of the phosphoinositide-3-kinase (PI3K)-Protein kinase B (PKB, or Akt) pathway can promote the FANCL protein level by limiting the

FANCL polyubiquitination (Dao et al., 2013). Furthermore, RuvB like AAA ATPase 1 and 2 (RUVBL1 and RUVBL2) provide additional layers of regulation for the FA pathway, contributing to the steady-state level of the core complex in response to ICLs (Rajendra, Garaycoechea, et al., 2014). Depletion of RUVBL1 and RUVBL2 results in a co-depletion of the core complex and raises typical FA phenotypes, including cellular sensitivity to crosslinking agents and defects in hematopoietic stem cell maintenance (Rajendra, Garaycoechea, et al., 2014).

As a central signalling component of the FA pathway, the FANCD2/FANCI complex is subjected to tight regulation through kinases, including ATR, ATM, DNA-PKcs, CHK1 and casein kinase 2 (CK2) (Cheung et al., 2017; Shigechi et al., 2012). First, ATR-mediated phosphorylation of the S/TQ cluster in FANCI is essential for the monoubiquitination and chromatin localisation of the FANCD2/FANCI complex (Cheung et al., 2017; Ishiai et al., 2008; Tan et al., 2020). This phosphorylation event promotes the closure of the ID clamp onto DNA, thereby exposing FANCD2 K561 and FANCI K523 for subsequent ubiquitylation (Sijacki et al., 2022). Second, ATR/ATM and an S-phase checkpoint kinase CHK1 can phosphorylate FANCD2 at T691/S717 and S331, respectively, which are all required for FANCD2 monoubiquitination and cellular resistance to crosslinking agents (Ho et al., 2006; Zhi et al., 2009). Also, FANCD2 undergoes CDK regulatory S592 phosphorylation during the S phase to facilitate the FA pathway activation (Cantres-Velez et al., 2023). Last, the inhibitory phosphorylation event on FANCD2 can determine the on-off states of the FA pathway (Lopez-Martinez et al., 2019). CK2-mediated phosphorylation of FANCD2 between residues 882 and 898 (882-898 cluster) blocks FANCD2 monoubiquitination and its DNA binding capability, thus inhibiting the FA pathway in the absence of genotoxic stress. When ICLs are produced, dephosphorylation of the 882-898 cluster renders FANCD2 “facultatively active” and increases its affinity to DNA, allowing the onset of the FA pathway (Lopez-Martinez et al., 2019).

After completing its function, the monoubiquitinated FANCD2/FANCI complex is deubiquitinated by the Ubiquitin specific peptidase 1 (USP1)-USP1-associated factor 1 (UAF1) complex, which is a critical process for maintaining proper FA pathway function (Cohn et al., 2007; Nijman et al., 2005; Oestergaard et al., 2007). Deubiquitination of the dimer facilitates the rapid removal of the FANCD2/FANCI proteins from ongoing repair sites to recycle them for the next round of repair (Oestergaard et al., 2007). Studies have demonstrated that mice deficient in USP1 display FA-associated phenotypes, and USP1-deficient cells exhibit high

levels of FANCD2 ubiquitination and hypersensitivity to crosslinking agents (Kim et al., 2009; Oestergaard et al., 2007). FANCI contains a SUMO-like domain interacting motif that directly binds to the SUMO-like domain 2 on UAF1. Abrogation of this interaction prevents FANCD2/FANCI deubiquitination, leading to increased sensitivity to MMC and impaired HR-mediated DNA repair (Yang et al., 2011). Notably, it seems that the phosphorylation of validated ATR sites S559 and S565 in FANCI plays a role in preventing FANCD2/FANCI dimer from deubiquitination (Tan et al., 2020). Together with the aforementioned observation that ATR-mediated phosphorylation of the FANCI-S/TQ cluster can promote FANCD2/FANCI monoubiquitination, it is suggested that the ATR may act as a molecular switch for the FANCD2/FANCI ubiquitination and the overall FA pathway activity (Cheung et al., 2017; Ishiai et al., 2008).

1.3.3.1.2 DNA glycosylase 3 (NEIL3) Pathway

Investigation of the psoralen-ICL and AP-ICL repair in the *Xenopus* egg extract reveals that these lesions are not unhooked through an incision of the phosphodiester backbone as seen in the FA pathway. Rather, they are resolved by the DNA glycosylase NEIL3, which cleaves one of the two N-glycosyl bonds that form the crosslink (Semlow et al., 2016). In the case of psoralen-ICL repair, NEIL3 unhooking yields an AP site on one strand and a thymine-psoralen monoadduct on the other strand, both of which are bypassed in a Rev1-dependent manner. When it comes to the AP-ICL, NEIL3 directly reverses the crosslink, producing normal adenosine in one strand and an AP site in the other strand that can be bypassed by TLS (Semlow et al., 2016). Consistent with the relative complexities of the two mechanisms, the NEIL3 repair is more efficient than the FA pathway and does not generate dangerous intermediates such as the DSB (Semlow et al., 2016). However, the production of an AP site during the NEIL3-associated repair virtually guarantees the generation of a point mutation (Semlow et al., 2016). Inhibition of NEIL3 shifts repair towards the FA pathway, indicating that the repair of psoralen- and AP-ICLs prioritise the former but can be fixed by both (Li et al., 2020; Semlow et al., 2016). By contrast, cisplatin-ICLs cannot be processed by NEIL3, likely because their distorted DNA structure impedes the access of NEIL3 and necessitates the FA pathway to incise DNA adjacent to the lesion (Huang et al., 1995; Li et al., 2020).

The prioritisation of the NEIL3 pathway when repairing certain types of ICL is closely linked to CMG ubiquitylation and unloading (Wu et al., 2019). In the egg extract system, like the FA pathway, the initiation of the NEIL3 pathway requires the RING-Type E3 ubiquitin ligase

TRAIP (TRAF Interacting Protein)-mediated CMG ubiquitylation resulting from the replication fork convergence at ICL (Semlow et al., 2016; Wu et al., 2019). However, The recruitment of NEIL3 to the stalled CMGs is facilitated by short ubiquitin chains rather than longer chains that activate the p97 ATPase for CMG unloading (Wu et al., 2019). Thus, NEIL3 gains initial access to the stalled CMGs, but if it fails to cleave the ICL, the ubiquitin chains keep growing, leading to p97 recruitment, CMG unloading, and the activation of the FA pathway (Li et al., 2020; Wu et al., 2019).

Notably, the NEIL3 repair does not require replisome uncoupling, and in mammalian cells, the recruitment of NEIL3 to ICLs can be independent of fork convergence via a rapid, PARP-dependent mechanism (Li et al., 2020). This suggests that the NEIL3-mediated repair is the primary mechanism when handling the predominant traversed ICLs in mammalian cells (Huang et al., 2013; Rohleder et al., 2016). However, *NEIL3*$^{-/-}$ mice do not present FA manifestations, and a hypomorphic *NEIL3* allele has been linked to a human autoimmune disorder with no FA symptoms (Massaad et al., 2016; Sejersted et al., 2011). This absence of FA phenotypes may be due to residual glycosylase activity in the mutant NEIL3 protein or repair redundancy with the FA pathway. Taken together, while NEIL3 may prioritise over the FA pathway when dealing with the majority of certain lesions, the versatility of the FA pathway makes it capable of resolving any type of ICL and thus is more crucial for cell survival.

1.3.3.1.3 The Acetaldehyde Pathway

Alcohol metabolism can produce harmful acetaldehyde that crosslinks DNA. Acetaldehyde first reacts with guanine to generate an N^2-propanoguanine intermediate, which then interacts with the N^2-amine of the opposite guanine to form an ICL in a 5'-CpG sequence (Cho et al., 2006). In the egg extract system, fork convergence initiates two replication-coupled mechanisms to repair acetaldehyde-induced ICLs (AA-ICLs) - the canonical FA pathway and another mechanism without incisions (Hodskinson et al., 2020). This alternative repair route does not involve NEIL3 or generate AP sites. Instead, it regenerates an undamaged dG in one strand and a propanoguanine adduct in the other strand, from which the crosslink was initially formed. Following unhooking, the propanoguanine adduct is bypassed by REV1 and Pol ζ-dependent TLS, making the new route potentially error-prone (Hodskinson et al., 2020).

Although the new process suggests that the AA-ICL undergoes enzymatic reversal, the enzyme responsible has not been identified (Gallina & Duxin, 2020). Also, when the FA pathway is

impeded, the flow through the other AA-ICL unhooking pathway does not increase, indicating that a subset of lesions becomes irreversibly committed to the FA pathway after fork convergence. Alternatively, the novel AA-ICL repair pathway may not be capable of repairing all three AA-ICL isoforms produced during synthesis. Regardless of the underlying cause, the dependence on the FA pathway to process a certain amount of AA-ICLs further elucidates the reason why FA arises only when the FA pathway is compromised (Gallina & Duxin, 2020).

1.3.3.2 Replication-Independent ICL Repair

While replication-coupled ICL repair, particularly through the FA pathway, is crucial for protecting proliferating cells from ICL-induced cytotoxicity, it is also known that ICLs can be sensed and repaired independently of replication (Enoiu et al., 2012; Williams et al., 2012). The replication-independent repair (RIR) is especially important for maintaining genomic integrity and ensuring transcription in nondividing or slowly dividing cells, yet it can also help reduce the ICL burden in proliferating cells before they enter into the S phase (Williams et al., 2012). Hence, RIR is an important mode of ICL repair that complements the replication-coupled pathways.

In mammalian cells, RIR seems to be initiated when ICLs are detected by the NER protein XPC, which promotes at least one incision by XPF-ERCC1 on the 5' side of the ICL (Bessho et al., 1997). A proposed model suggests that the 5' gap provides an entry point for a 5' to 3' exonuclease that degrades DNA past the ICL for unhooking, and SNM1A and FAN1 are likely candidates for such a nuclease (Bessho et al., 1997). Following ICL unhooking, subsequent gap filling requires the TLS enzyme Pol ζ (Roy & Schärer, 2016). In *Xenopus* egg extracts, the recognition of lesions and at least one incision involve the MMR factors MutSα and MutLα, respectively, and TLS in this system has been shown to employ the Pol κ (Kato et al., 2017; Williams et al., 2012). Significantly enhanced activity of RIR occurs when ICLs induce distortions in the double helix, as these can be easier detected by XPC and/or MutSα independently of replication (Kato et al., 2017; Smeaton et al., 2008).

Nevertheless, ICL repair can also be triggered to resolve non-distorting lesions when the ICL collides with an RNA polymerase, as observed in another type of replication-independent mechanism - the transcription-coupled repair (TCR) (Enoiu et al., 2012). In situations where transcription stalling occurs, Senataxin, an RNA/DNA helicase, translocates to the damage site to prevent the build-up of R-loops. Senataxin then recruits SAN1 (Senataxin-associated

nuclease 1), which employs 5' to 3' ssDNA exonuclease activity in a yet unclear mechanism to process ICLs (Andrews et al., 2018). Alternatively, ICLs can be processed through the transcription-coupled NER pathway with the help of the NER-specific ATPase CSB (Enoiu et al., 2012).

1.3.3.3 ICL Repair Pathway Choice

To conclude, this section has described five distinct mechanisms for repairing ICLs, including three replication-coupled pathways and two replication-independent mechanisms. The replication-coupled pathways consist of the canonical FA pathway, the NEIL3 pathway, and a mechanism for repairing ICLs induced specifically by acetaldehyde. The replication-independent mechanisms include one for detecting and repairing highly distorting ICLs and another for transcription-coupled repair.

Given the range of ICL repair mechanisms, it is important to understand how cells balance between these various mechanisms. Three major factors influence the choice of ICL repair pathways. The first factor is the type of cross-link. Highly distorting ICLs can be recognised and repaired by the RIR pathway in a replication-independent manner during G1 or G2 phases. In contrast, ICLs that do not significantly distort the DNA structure may not be detected until they impede replication fork progression or RNA polymerase activity. In cases when replication fork convergence occurs, the structure of the ICL may further determine the specific replication-dependent pathway responsible for its repair. The second factor is timing. For example, while highly distorting ICLs are preferred to be resolved by RIR, they can also be processed by replication-coupled repair if they occur during the S phase. Finally, ICL's location affects its repair pathway choice. ICLs situated in highly transcribed regions are more likely to be repaired by transcription-coupled repair, especially when they are non-distorting. Also, specific chromatin structures may favour particular ICL repair pathways. Together, the competitive yet complementary nature of the ICL repair pathways contributes to highly efficient and accurate ICL resolution.

1.4 The Nucleolus and Nucleolar Stress

1.4.1 The Nucleolus and Its Function

The nucleolus is a membrane-less sub-nuclear organelle where ribosome biogenesis occurs (Hernandez-Verdun et al., 2010; Penzo et al., 2019). In mammalian cells, nucleoli form around specific chromosomal regions known as nucleolar organiser regions (NORs), which contain clusters of ribosomal DNA (rDNA) repeats (Aubert et al., 2018). Within the human genome, approximately 400 rDNA units are distributed among the short arms of chromosomes 13, 14, 15, 21, and 22 (Boulon et al., 2010; McStay, 2016; Stults et al., 2008). The number of rDNA loci varies across NORs, and only ~50%, are actively transcribed by RNA polymerase I (Pol I) to produce the precursor ribosomal RNA (pre-rRNA) 47S (McStay, 2016). The gene encoding 5S rRNA also exists in clusters containing thousands of repeats, with the major located on chromosome 1 (q42-q43) (Sirri et al., 2008; Sørensen & Frederiksen, 1991). The size, number, and organisation of nucleoli within cells are directly associated with nucleolar activity, specifically, the rate of Pol I transcription (Hernandez-Verdun et al., 2010). This activity is tightly regulated and influenced by various factors, including changes in cell proliferation, growth rates, and metabolic activities (Boulon et al., 2010).

Ribosome biogenesis is a complex and energy-intensive process that encompasses multiple steps, including the recruitment of transcriptional machinery, followed by RNA processing, maturation, and subsequent assembly and export of ribosome subunits (Suzuki et al., 2012). To ensure precise coordination of these steps, a functional nucleolus is organised into three distinct sub-compartments with well-defined boundaries (Feric et al., 2016). These sub-compartments include the fibrillar centre, housing the rDNA genes where Pol I transcription takes place; the dense fibrillar component, where initial pre-rRNA processing occurs; and the granular component, which is involved in the later stages of processing and ribosomal subunit assembly (Boisvert et al., 2007; Hernandez-Verdun et al., 2010; Rodrigo et al., 1992). Additionally, a recently identified fourth sub-compartment, known as the nucleolar rim, is proposed to contain proteins that tether the nucleolus to chromatin in the nucleolar periphery, although the precise biochemical role of the nucleolar rim remains to be fully understood (Stenström et al., 2020).

The process of rRNA transcription and processing involves the coordinated action of Pol I transcriptional machinery, consisting of Pol I core subunits and several essential transcriptional co-factors, including the transcription initiation factor-IA (TIF-IA), upstream binding factor

(UBF), and selective factor 1 (SL-1). The availability and activity of these factors play a crucial role in the regulation of rRNA transcription (Ni & Buszczak, 2023). Initiation of rRNA transcription occurs when the UBF/SL-1 preinitiation complex binds to the rDNA promoter (Hempel et al., 2023; Sanij & Hannan, 2009). This complex facilitates the assembly of the Pol I transcriptional machinery by recruiting Pol I, TIF-IA, and other co-factors such as sirtuin 7 (SIRT7) and CK2 (Ford et al., 2006; Goodfellow & Zomerdijk, 2013). The expression of rRNA plays a critical role in initiating the formation of nucleoli and the recruitment of nucleolar proteins. These proteins possess nucleolar localisation sequences that contain a significant proportion of positively charged amino acids, facilitating their binding to the negatively charged rRNA (Musinova et al., 2015). In the absence of rRNA, nucleolar proteins may form diverse protein aggregates that differ from the typical nucleolar architecture. This suggests that rRNA transcription is essential for proper nucleolar assembly (Falahati et al., 2016).

Transcription of the ribosomal DNA (rDNA) produces the precursor molecule 47S pre-rRNA. The transcribed 47S pre-rRNA then undergoes processing and chemical modifications to generate the mature 18S, 5.8S and 28S rRNAs with the assistance of multiple RNA processing proteins, including splicing factors, RNA helicases, and small nucleolar RNAs (snoRNAs) (Filipowicz et al., 1999; Yoshikawa et al., 2011). Additionally, the synthesis of 5S rRNA takes place in the nucleoplasm by RNA polymerase III (Pol III) and is then translocated into the nucleolus (Penzo et al., 2019). Subsequently, the 18S rRNA combines with 33 types of small ribosomal subunit proteins to form the Pre-40S ribosome particle, while the 5S, 28S, and 5.8S rRNAs assemble with 48 types of large ribosomal subunit proteins to form the Pre-60S ribosome particle (Couté et al., 2006). These pre-ribosomes exit the nucleolus and pass through the nuclear pore into the cytoplasm, where they combine to form the mature 80S ribosome that is capable of translating mRNA (Baßler & Hurt, 2019; Boisvert et al., 2007).

In addition to its established role in ribosome biogenesis, the nucleolus has emerged as a versatile organelle with diverse functions in regulating cellular homeostasis. Extensive analysis of the nucleolar proteome has revealed that more than 4,500 proteins localise in the nucleolus, of which only 30% are directly associated with ribosome biogenesis (Boisvert et al., 2007; Boulon et al., 2010). A comprehensive study examining 1318 nucleolar proteins finds that 87% of these proteins are also present in multiple other cellular compartments, including the nucleoplasm, cytosol, and mitochondria. This indicates the functional versatility and mobility of nucleolar proteins (Stenström et al., 2020). Furthermore, an analysis of the nucleolar

complex in HeLa cells identifies over 270 nucleolar proteins, among which about one-third of proteins have functions unrelated to ribosome biosynthesis (Andersen et al., 2002). It has been shown that these nucleolar proteins that are not involved in ribosome biogenesis may play crucial roles in cell cycle control, apoptosis, autophagy, viral infection, DNA replication and DNA repair (Andersen et al., 2002; Boulon et al., 2010; Jarboui et al., 2011). Therefore, the nucleolus serves as a central hub for coordinating multiple biological processes by sequestering or releasing various factors involved in these processes (Boisvert et al., 2007; Couté et al., 2006).

1.4.2 Nucleolar Stress

Ribosome assembly is the most energy-consuming process in a growing cell (Baßler & Hurt, 2019). This energetically demanding process is closely monitored, and any errors occurring during its various stages can trigger a condition known as “nucleolar stress” or “ribosomal stress”. A common reason for nucleolar stress is the inhibition of pre-rRNA transcription, which can be induced by factors such as nucleotide depletion, viral infection or sustained growth inhibition (Calkins et al., 2013; Huang et al., 2008; Poortinga et al., 2004; Westdorp et al., 2017). Numerous anticancer drugs that induce DNA damage also block pre-rRNA transcription (Burger et al., 2010). Pharmacological interventions using low concentrations of actinomycin D (Act D), for instance, can interfere with pre-rRNA transcription by inhibiting Pol I (Perry & Kelley, 1970). Nucleolar stress also arises from abnormalities in rRNA processing or modification, as well as disturbances in ribosome assembly (Hölzel et al., 2010). For example, imbalances in the expression levels of ribosomal proteins (RPs), including deficiencies in specific RPs, result in aberrant ribosome assembly, thereby inducing nucleolar stress (Luan et al., 2022). Furthermore, replication stress arising from replication fork arrest and collapse also triggers nucleolar stress (Lindström et al., 2022).

In response to nucleolar stress, the nucleolus undergoes significant morphological changes (Boulon et al., 2010). One well-documented structural modification is the formation of the nucleolar cap, which arises as a result of the stress-induced segregation of nucleolar components into a bipartite structure that resembles a cap-like appearance located at the periphery of the segregated nucleolus (Shav-Tal et al., 2005). The nucleolar cap typically comprises specific nucleolar proteins, endogenous nuclear body proteins, and several nucleoplasmic proteins (Shav-Tal et al., 2005). Furthermore, the membrane-less nature of the

nucleolus allows for dynamic behaviour, with nucleolar proteins constantly shuttling between the nucleolus and the nucleoplasm (Sirri et al., 2008). The initiation of nucleolar stress disrupts the conventional shuttling of nucleolar proteins, leading to their release from the nucleolus and the nucleolar sequestration of nucleoplasmic proteins (Boulon et al., 2010). Nucleolar stress has been recognised as a central sensing hub for various stress stimuli, including double-strand breaks, hypoxia, nutrient deprivation, oxidative stress, and thermal stress (Görner et al., 2002; Hayashi & Matsunaga, 2019; Korsholm et al., 2020; Sapio et al., 2021). These cellular stressors contribute to aberrations in nucleolar architecture and nucleolar protein shuttling, representing key events in the onset of nucleolar stress. Importantly, distinct spatial and temporal alterations in the nucleolar proteome have been observed in response to different stress insults, indicating that the nucleolus exhibits unique and specific responses to different stress stimuli (Moore et al., 2011).

Moreover, nucleolar stress assumes a critical role in stress response by initiating various stress-related signalling pathways. Among these pathways, three major signalling transductions stand out: Mouse double minute 2 homolog (MDM2)-p53, Nuclear factor-κB (NF-κB), and Hypoxia-inducible factor 1 alpha (HIF-1α) pathways (Fatyol & Szalay, 2001; Thoms & Stark, 2021; Yang et al., 2018). The MDM2-p53 signalling pathway, in particular, is extensively studied as a downstream response to nucleolar stress (Rubbi & Milner, 2003; Y. Zhang & Lu, 2009). In quiescent cells, p53 exhibits rapid turnover due to MDM2/MDM4-mediated ubiquitination and proteolysis (Shadfan et al., 2012). However, when ribosome biogenesis is disrupted, p53 is induced through a checkpoint mechanism termed the Impaired ribosome biogenesis checkpoint (IRBC) (Pelletier et al., 2017). The IRBC is activated upon the release of free RPs, specifically RPL11 and RPL5, into the nucleoplasm along with the 5S rRNA. This 5S RNP (5S rRNA/RPL5/RPL11) can sequester and inhibit MDM2, resulting in p53 stabilisation (Sloan et al., 2013; Zheng et al., 2015). Additionally, the release of ARF tumour suppressor ($p14^{ARF}$) from the nucleolus under nucleolar stress has been found to contribute to p53 activation (Llanos et al., 2001). Furthermore, under stress conditions, NPM can physically bind to the MDM2-p53 complex, leading to MDM2 inactivation and subsequent p53 accumulation (Kurki et al., 2004). The MDM2-p53 pathway is widely recognised for its pivotal role in transmitting nucleolar stress-mediated signalling and influencing cell-fate decisions such as apoptosis, senescence, and growth arrest (Hua et al., 2022). It has been proposed that disruption of nucleolar function and subsequent release of nucleolar components into the nucleoplasm are common features observed in most p53-inducing stresses (Rubbi & Milner, 2003).

The second pathway responding to nucleolar stress involves the NF-κB family, which comprises five distinct member proteins: p50 (NF-κB1), p52 (NF-κB2), p65 (RELA), RELB, and c-REL (Chen & Stark, 2018). These proteins play a central role in immune regulation, stress response, and maintaining cellular homeostasis (Verma, 2004). Studies have demonstrated that various pro-apoptotic stimuli, such as aspirin, serum withdrawal, and UVC radiation, lead to the sequestration of RELA within the nucleolus, resulting in impaired NF-κB transcriptional activity (Stark & Dunlop, 2023). Nucleolar sequestration of RELA can trigger its ubiquitination and contributes to the relocalisation of nucleophosmin (NPM) from the nucleolus to cytoplasm during cell apoptosis (Khandelwal et al., 2011; Thoms et al., 2010). Furthermore, both pharmacological and genetic induction of nucleolar stress, such as treatment with Act D or depletion of TIF-IA, can cause nuclear translocation and activation of NF-κB (Chen et al., 2018; Liu et al., 2016). Importantly, treatment with a more selective nucleolar stress inducer CX-5461, which inhibits the RNA Pol I-mediated rRNA transcription, activates p53 yet does not lead to NF-κB phosphorylation or activation, suggesting that NF-κB activation may occur independently of disruptions in the transcription of rDNA (Pan et al., 2022).

As a significant stress-responsive transcription factor, HIF-1α exhibits nucleolar translocation and is involved in the third pathway activated by nucleolar stress (Fatyol & Szalay, 2001). It has been reported that $p14^{ARF}$ can physically interact with HIF-1α, leading to the repression of its transcriptional activity through nucleolar sequestration independent of p53 (Fatyol & Szalay, 2001). Notably, von Hippel-Lindau tumor-suppressor protein (VHL), the primary E3 ligase responsible for catalysing HIF-1α ubiquitination and degradation, undergoes nucleolar sequestration and regulates HIF-1α stability under hypoxia or acidosis (Mekhail et al., 2004). Additionally, the nucleolar protein SUMO specific peptidase 3 (SENP3) may catalyse the de-SUMOylation of p300, enhancing the transcriptional activity of HIF-1α. This process occurs following the release of SENP3 from nucleoli into the nucleoplasm in response to ROS-induced stress (Huang et al., 2009). These findings indicate that the nucleolus may play a facilitating role in stress-induced activation of HIF-1α.

In conclusion, upon exposure to diverse stress stimuli, the nucleolus experiences nucleolar stress, characterised by perturbations in nucleolar morphology and function, due to disrupted ribosome biogenesis and altered nucleolar dynamics (Boulon et al., 2010). Consequently, nucleolar stress actively engages in multiple signalling cascades, such as the MDM2-p53, NF-κB, and HIF-1α pathways, and serves as a fundamental influencer in the cell fate decision and

disease progression (Weeks et al., 2019). Accumulating evidence has highlighted the pivotal involvement of nucleolar physiology in the pathogenesis of human diseases, including cancer, viral infection, cardiovascular and neurodegenerative diseases, as well as human ageing (Corman et al., 2023; Stochaj & Weber, 2020).

1.4.3 The Nucleolus and DNA Damage Response

As aforementioned, multiple investigations have provided evidence suggesting that the nucleolus functions as a sensor for monitoring the stability and integrity of genomic DNA (Weeks et al., 2019). Upon the occurrence of DNA damage, one of the initial cellular events is the stalling of rRNA synthesis, leading to the onset of nucleolar stress (Boulon et al., 2010; Weeks et al., 2019). This serves as a cellular strategy to halt the energy-consuming ribosomal biogenesis and redirect the energy towards DNA repair mechanisms (Boulon et al., 2010). Notably, the nucleolus exhibits distinct responses to various DNA-damaging stimuli. For instance, UV radiation and IR elicit notably differential reorganisation patterns of the nucleolar proteome. UV-induced stress causes sustained (lasting hours) fluctuations in nucleolar NHEJ proteins, while IR triggers more rapid (within minutes) but transient responses with limited magnitude (Moore et al., 2011).

The nucleolar cap formation is considered a characteristic feature of a transcriptional shutdown during the DNA damage response (Moore et al., 2011). This nucleolar segregation might be a passive process occurring as a consequence of transcriptional inhibition (van Sluis & McStay, 2015). Alternatively, it may facilitate the translocation of damaged rDNA to the nucleolar periphery to access repair factors normally excluded from nucleoli (Korsholm et al., 2020). During this process, DNA repair factors are recruited from the surrounding nucleoplasm and become enriched in the nucleolar cap (van Sluis & McStay, 2015). Meanwhile, DNA damage repair is promoted via the activation of ATM and its key substrate Treacle Ribosome Biogenesis Factor 1 (TCOF1, also known as Treacle) within the nucleolus (Blokhina & Buchwalter, 2020; Korsholm et al., 2019). Phosphorylation of TCOF1 by ATM facilitates the recruitment of the repair factor NBS1 to the nucleolar cap, enhancing the DNA repair process (Larsen et al., 2014). Furthermore, ATM-mediated TCOF1 phosphorylation promotes the nucleolar recruitment of DNA topoisomerase 2-binding protein 1 (TOPBP1), a cofactor involved in ATR signalling (Mooser et al., 2020). Notably, this mechanism of ATR activation within the nucleolus appears to be distinct compared to its nuclear activation, as it occurs

independently of end resection that serves as a canonical ATR activator (Mooser et al., 2020). Ultimately, the coordinated action of ATM and ATR contributes to the nucleolar DNA damage response and repair of rDNA.

Functional and proteomic investigations have revealed that various DNA repair proteins reside within the nucleolus, which upon DNA damage, undergo translocation to sites of damage (Ogawa & Baserga, 2017). This intricate mechanism underscores the nucleolus' role as a vital sensing centre for genome instability, orchestrating and coordinating cellular responses in the face of DNA damage. For instance, approximately 40% of PARP1 distributes within the nucleolus, which becomes activated and released into the nucleoplasm following DNA damage (Rancourt & Satoh, 2009). Similarly, DNA damage alters the localisation and interactome of Ku, an essential NHEJ factor interacting with rRNA and ribosomal proteins in the unperturbed nucleolus (Adelmant et al., 2012). Furthermore, several canonical nucleolar proteins such as $p14^{ARF}$, NPM and nucleolin (NCL) may also be released from nucleoli under genomic instability. Translocation of these nucleolar proteins to the nucleoplasm supports efficient DNA repair by inducing cell cycle arrest in both p53-dependent and independent manners (Colombo et al., 2011; Daniely et al., 2002; Gjerset & Bandyopadhyay, 2006; Lee et al., 2005). Besides their contribution to cell-cycle arrest, evidence suggests that NCL and NPM directly participate in the DNA damage response. NCL has been shown to modulate PCNA activity in the NER pathway, while NPM is implicated in the BER regulation (Poletto et al., 2014; Yang et al., 2002; Yang et al., 2009).

While numerous studies demonstrate nucleolus as a reservoir capable of releasing critical factors towards nucleoplasm, only a few proteins have been reported to translocate in the opposite direction, from nucleoplasm to nucleoli, during the stress response. Examples of such proteins are ING1 (Inhibitor of growth family member 1) and PML (Promyelocytic leukaemia protein), which translocate to nucleoli under genotoxicity and are thought to induce apoptosis and cell cycle arrest, respectively (Tembe & Henderson, 2007). Chaperones such as Heat shock cognate protein 70 (HSC70) are also targeted to the nucleolus following the stress response, potentially facilitating the restoration of nucleolar function during cellular recovery from stress (Kotoglou et al., 2009). Furthermore, RAD9B, a component of the RAD9-RAD1-HUS1 (9-1-1) DNA checkpoint clamp, relocates to the nucleolus following nucleolar stress and contributes to the delay of cell cycle progression after DNA damage (Pérez-Castro & Freire, 2012).

The DNA damage-induced changes in nucleolar protein localisation are presumably regulated by post-translational modifications (PTMs) (Boulon et al., 2010; Griffiths et al., 2009). For instance, acetylation regulates the DNA damage-triggered translocation of WRN from the nucleolus to nucleoplasmic foci as well as the nucleolar accumulation of APE1 (Blandert et al., 2002; Lirussi et al., 2012). SUMOylation is associated with the targeting of Ntg1, a *Saccharomyces cerevisiae N*-glycosylase/AP lyase, to nuclei containing oxidative DNA damage (Griffiths et al., 2009). Additionally, the structure-specific flap endonuclease 1 (FEN1) has been observed to migrate to the nucleoplasm in a phosphorylation-dependent manner upon UV irradiation (Guo et al., 2008). Remarkably, mutations that mimic or impair FEN1 phosphorylation result in UV sensitivity, supporting that protein shuttling between nucleolus and nucleoplasm triggered by DNA damage is crucial for an effective DNA damage response (Guo et al., 2008).

Chapter 2. Identification of Regulator of Chromatin Condensation 2 (RCC2) as a Novel Player in ICL Repair

2.1 Introduction

The Regulator of chromatin condensation 2 (RCC2) is initially known as Telophase Disk-60 (TD60). In 1991, Andreassen and colleagues revealed a novel mammalian mitotic organelle implicated in cytokinesis - the telophase disc by tracking the spread of a mitosis-specific 60-kD antigen using human autoimmune serum. This antigen, termed TD60, first appeared on centromeres and then relocated to the midzone of the mitotic spindle, similar to the behaviour observed for the chromosomal passenger complex (CPC) (Andreassen et al., 1991; Bellissent-Waydelich et al., 1999; Martineau-Thuillier et al., 1998). CPC is a crucial regulator of mitosis, which is named after its translocation from the inner centromeres in early mitosis to the spindle midzone during anaphase. This migration from the chromosomes to the spindle identifies the former position of the metaphase plate and signals the location of the cleavage furrow and cytokinesis plane (Adams et al., 2001; Cooke et al., 1987). Thus, the complex controls crucial components of mitosis, such as chromosomal congression, kinetochore-microtubule attachments, the spindle assembly checkpoint, and cytokinesis (Adams et al., 2000; Papini et al., 2015; Rosasco-Nitcher et al., 2008; Yang et al., 2007). Additional research demonstrates that TD-60 is essential for mitotic progression from prometaphase to metaphase and mitotic spindle activity (Hu et al., 2018; Mollinari et al., 2003). The absence of TD-60 substantially suppresses overall spindle assembly, blocks cells in prometaphase, and triggers the spindle assembly checkpoint (Mollinari et al., 2003; Yenjerla et al., 2013).

TD-60 highly interacts with CPC components despite not being a core member. When CPC proteins are suppressed in mammalian cells, TD-60 becomes mis-localised. Similarly, CPC's centromeric targeting during mitosis depends on the presence of TD-60 (Humphries et al., 2009; Mollinari et al., 2003; Papini et al., 2015). In addition, TD-60 binds microtubules to induce the activation of Aurora-B kinase, the catalytic subunit of the CPC, thus involving it in the regulation of cell cleavage (Mollinari et al., 2003; Papini et al., 2015; Rosasco-Nitcher et al., 2008). Aside from its involvement in mitosis, TD-60 is crucial in modulating signalling pathways that mediate interphase cell cycle progression. Upon TD-60 siRNA silencing, mammalian cells halt proliferation and arrest in either G1/S or G2 phase, depending on the cell cycle stage they are in when TD-60 expression is eliminated (Yenjerla et al., 2013).

Later, full-length TD-60 was isolated using JH antiserum from chromosomal fraction and identified using tandem mass spectrometry. The sequencing revealed that TD-60 has seven repeats that are homologous to the Regulator of chromatin condensation 1 (RCC1) family of guanine nucleotide exchange factors (GEFs) (Mollinari et al., 2003). This results in the protein being designated RCC2. GEFs are employed to activate the small GTPase superfamily, which uses GDP/GTP alternation to activate a number of functional switches essential for cell dynamics (Cherfils & Zeghouf, 2013). GDP-bound small GTPases are typically regarded as inactive, whereas GTP-bound forms activate downstream pathways through binding effectors. Because GDP is firmly bound, the activation of small GTPases requires the assistance of GEFs to allow GDP dissociation and the exchange of GDP for GTP (Bos et al., 2007).

RCC1, the family's original member, is a GEF for the small GTPase RAN/ARF1/RAB and governs bipolar spindle dynamics as well as nuclear envelope construction during the M-G1 transition (Hetzer et al., 2000; Kalab et al., 2002; Rosa et al., 1996). RCC2 is a highly conserved protein with sequence similarities to RCC1, notably between residues 100 and 500, which are nearly entirely composed of seven RCC1 motifs (Figure 2-1A, white boxes in the schematic represent RCC1 repeats) (Papini et al., 2015). Like RCC1, RCC2 has a propeller-like construction with seven blades (Figure 2-1B). Although buried residues of the seven-bladed propeller are retained across RCC1 and RCC2, the surface structural features are distinct. RCC2 lacks the β-wedge extension exerting GEF activity in RCC1. In place of this, RCC2 contains two switchback loops (loop 1/2) and an additional β-hairpin extension (Figure 2-1C, superimposition of human RCC1 and RCC2) (Song et al., 2018).

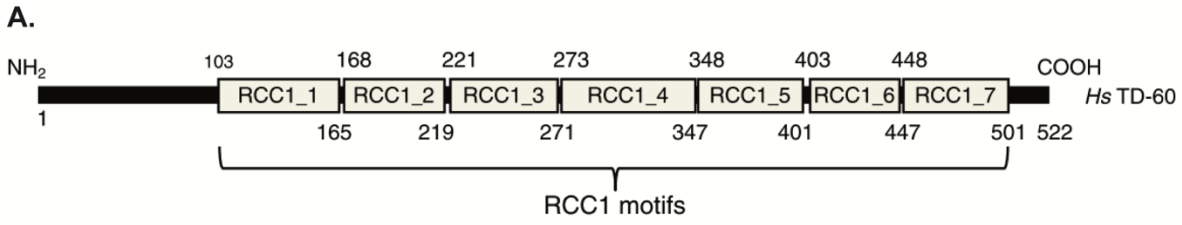


Figure 2-1 RCC2 is a conserved protein with sequence and structure similarities to RCC1.
A) Schematic of RCC2 protein. RCC2 comprises seven RCC1 motifs (shown as white boxes) between residues 100 and 500. The protein composition schematic is adapted from *Papini et al., 2015.*

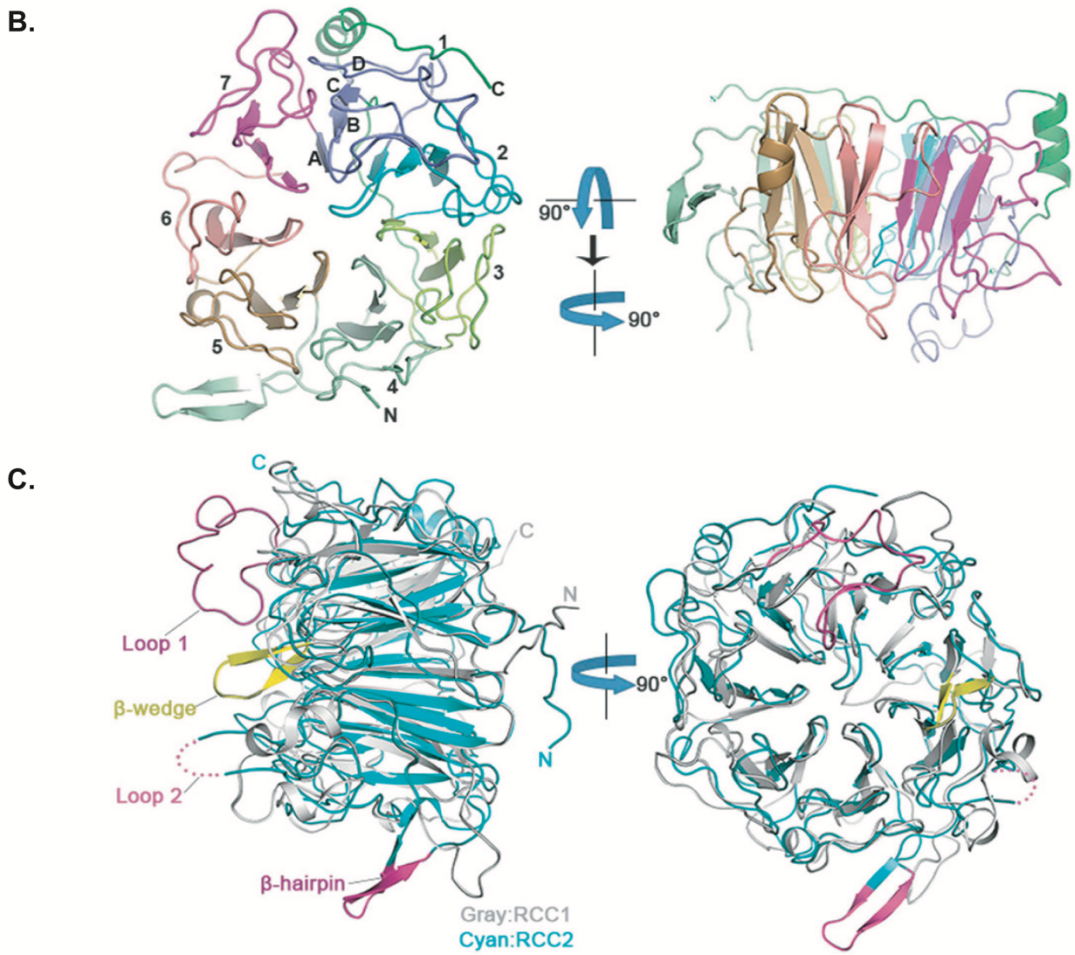


Figure 2-1 RCC2 is a conserved protein with sequence and structure similarities to RCC1. **B)** Ribbon diagram of the RCC2 propeller structure with seven blades. The blades are numbered (1–7) along the sequence. **C)** Superimposition of human RCC2 (cyan) and human RCC1 (grey). The extra structural elements in RCC2 (loop 1, loop 2 and β-hairpin) relative to RCC1 are shown in magenta. The extra β-wedge required for RCC1 GEF activity is shown in yellow. The ribbon diagram structures are adapted from *Song et al., 2018*.

Further investigations show that the distinctive β-hairpin domain of RCC2 supports its direct contact with the small GTPase RAC1 (Song et al., 2018). RCC2 selectively binds to the nucleotide-free form of RAC1 during mitosis and thus was initially thought to be a RAC1 GEF (Burke & Stukenberg, 2003; Mollinari et al., 2003). However, RNA interference (RNAi)-mediated knockdown of RCC2 stimulates RAC1 activation, indicating it has an inhibitory role as opposed to functioning as an activating GEF (Humphries et al., 2009). Later research utilising a GDP-release assay against a broad array of targets representing all human GTPase superfamilies demonstrated that RCC2 is indeed a GEF, albeit for RALA but not RAC1 GTPase. RCC2-RALA signalling modulates kinetochore-microtubule connections and CPC activity at centromeres during early mitosis (Papini et al., 2015).

In addition to its function in mitotic and interphase progression, RCC2 has been linked to cellular migration. RCC2 was detected in the α5β1 integrin-fibronectin signalling network that regulates directional cell migration at the junction of the Rac1 and Adenosine 5′-diphosphate ribosylation factor 6 (ARF6) subnetworks. These two small GTPases contribute to integrin-dependent membrane protrusion and membrane trafficking. As discussed previously, rather than being a GEF, RCC2 functions as a brake on RAC1 and ARF6 activation (Danen, 2009; Humphries et al., 2009; Williamson et al., 2014). Protrusive signals are required for sustained forward migration across a fibrillar extracellular matrix, and linear migration demands a decline in RAC1 activity at non-protrusive membrane regions and a shift in RAC1 to the leading edge (Bass et al., 2007). RCC2 blocks RAC1 activation by binding to its switch regions and competing with the GEFs that activate RAC1. This inhibition of RAC1 outside the protrusive tip facilitates directed cell migration by preventing off-axial protrusions (Williamson et al., 2014). Furthermore, the recognition of RCC2 as a *bona fide* GEF for RALA may further reveal RCC2's participation in cell migration, as RALA is implicated in membrane trafficking, cell shape modulation, and cell spreading (Papini et al., 2015; van Dam & Robinson, 2006).

It has been extensively documented in recent years that RCC2 is an oncogene engaged in cancer tumorigenesis and metastasis. According to the Kaplan-Meier analysis in the TCGA database, high RCC2 expression in many cancers is associated with malignant progression and poor prognoses (Gu et al., 2022). First, RCC2 promotes cell proliferation and invasion in several gastrointestinal malignancies, such as gastric carcinoma, oesophageal squamous cell carcinoma (ESCC), pancreatic, and colon cancer (Bruun et al., 2015; Matsuo et al., 2013; Wang et al., 2020; Wu et al., 2022; Yi et al., 2017). In gastric cancer, phosphorylated P21-activated kinase 4 (PAK4) stabilises the coronin-1C (CORO1C)/RCC2 complex at the migration leading edge, causing metastasis (Li et al., 2022). An oncogene in ESCC, Bromodomain containing protein 4 (BRD4), promotes tumour growth by enhancing RCC2 transcription (Wu et al., 2022). RCC2 modulates pancreatic cancer migration via regulating epithelial-mesenchymal transition (EMT) and is associated with DNA mismatch repair deficit in colon cancer (Bruun et al., 2015; M. Mukherjee & Goswami, 2021).

Moreover, two genome-wide SNP association analyses indicated that the SNP rs7538876, which mapped in the vicinity of RCC2, conferred a risk of melanoma and cutaneous basal cell carcinoma progression (Rendleman et al., 2013; Stacey et al., 2008). Also, RCC2 promotes EMT and extracellular matrix remodelling in lung cancer via MAPK-JNK signalling activation,

ultimately driving tumour aggressiveness (Fujii et al., 2018; Pang et al., 2017). In glioma, RCC2 has a dual oncogenic effect on cell cycle progression and metabolism, and higher RCC2 expression is linked with a worse clinical outcome (Liu et al., 2022; Yu et al., 2019). RCC2 exerts oncogenic activities also in breast cancer via activating the Wnt signalling pathway (Chen et al., 2019; Wang et al., 2020). Insulin-like growth factor 2 mRNA-binding protein 3 (IGF2BP3) is a protective gene that is overexpressed in AML. It promotes cell survival and overall survival rate by mediating the degradation of RCC2 mRNA by reading N^6-methyladenosine-modified regions (Zhang et al., 2022).

Non-coding RNAs such as microRNAs (miRNAs) and long non-coding RNAs (lncRNAs) are commonly dysregulated in human malignancies and can affect critical genes implicated in tumour onset and progression (Kent & Mendell, 2006; Ratti et al., 2020). Studies have shown miR-29c, miR-1247 and miR-331-3p directly target the 3′ untranslated region (3′ UTR) of RCC2 and negatively regulates RCC2 expression in gastric carcinoma, pancreatic cancer and ovarian cancer respectively, hence inhibiting cell growth and migration (Buranjiang et al., 2019; Matsuo et al., 2013; Yi et al., 2017). MiR-191 is induced by cisplatin treatment in HeLa cells, which increases cell mortality by lowering RCC2 mRNA and protein levels, thus causing G2/M arrest, cisplatin-induced DNA damage, and cell death (Xu et al., 2020). In contrast, lncRNAs such as lung cancer progression association transcript 1 (LCPAT1) upregulate RCC2, hence promoting cell proliferation, migration, and invasion in lung cancer (Feng et al., 2016; Lin et al., 2018).

RCC2 has also been demonstrated to induce tumour chemoresistance, one of the leading reasons for treatment failure and high mortality. RCC2 overexpression blocks drug-induced cell death by inhibiting the RAC1/JNK pathways, hence resulting in resistance to common chemotherapeutic drugs such as Taxol, Nocodazole, Daunorubicin, Cisplatin, and 5-Fluorouracil (Wu et al., 2018). Further evidence shows that RCC2 is upregulated in Cisplatin-resistant ovarian cancer cells as compared to sensitive cells. RCC2 enhances cell proliferation and migration in Cisplatin-resistant ovarian cancer cells by upregulating the small GTPase RALA and its downstream effector Ral binding protein-1 (RALBP1) (Gong et al., 2019). The AKT pathway, which is triggered by RCC2, promotes Cisplatin resistance in hepatocellular carcinoma, whereas Myeloma cell leukaemia-1 (MCL-1) knockdown restores paclitaxel sensitivity in chemotherapy-resistant ovarian cancer through regulating RCC2 (Chen et al., 2020; Nie et al., 2021).

To identify novel proteins implicated with ICL repair, a former lab member, Kelvin Yaprianto, utilised a purification strategy to isolate proteins that preferentially bound to crosslinked DNA probes over non-crosslinked counterparts (Figure 2-2). A list of potential protein candidates linked to the cellular response to ICLs is subsequently discerned via a tandem mass spectrometry analysis (the experiment was performed once). Tables 2-1 and 2-2 present partial lists of proteins identified through the mass spectrometry. These tables provide information about the number of peptides derived from various probe eluates for each protein. This count is subsequently normalised against the total peptides recovered from a specific eluate. Subsequently, a fold enrichment ratio is computed by dividing the normalised peptide count in the crosslinked eluate by the normalised count in the non-crosslinked eluate. This analysis is conducted separately for the linear double-stranded (Table 2-1) and replication fork mimic (Table 2-2) probes.

Proteins exhibiting a fold enrichment exceeding 3.0, for either the linear or fork probes, are identified as potential protein candidates associated with the cellular response to ICLs. Among these candidates, two proteins, RCC2 and ZNF638, are further investigated in this thesis (Table 2-1 and Table 2-2, highlighted in yellow). UHRF1 is a protein implicated in ICL repair in prior studies. UHRF1 functions upstream of FANCD2 in the FA pathway and contributes to the repair of ICLs induced by TMP, MMC, and cisplatin (Liang et al., 2015). Notably, in the purification scheme, UHRF1 demonstrates relatively high fold enrichments, particularly with a value of 4.17 for the linear probe (Table 2-1 and Table 2-2, highlighted in blue).

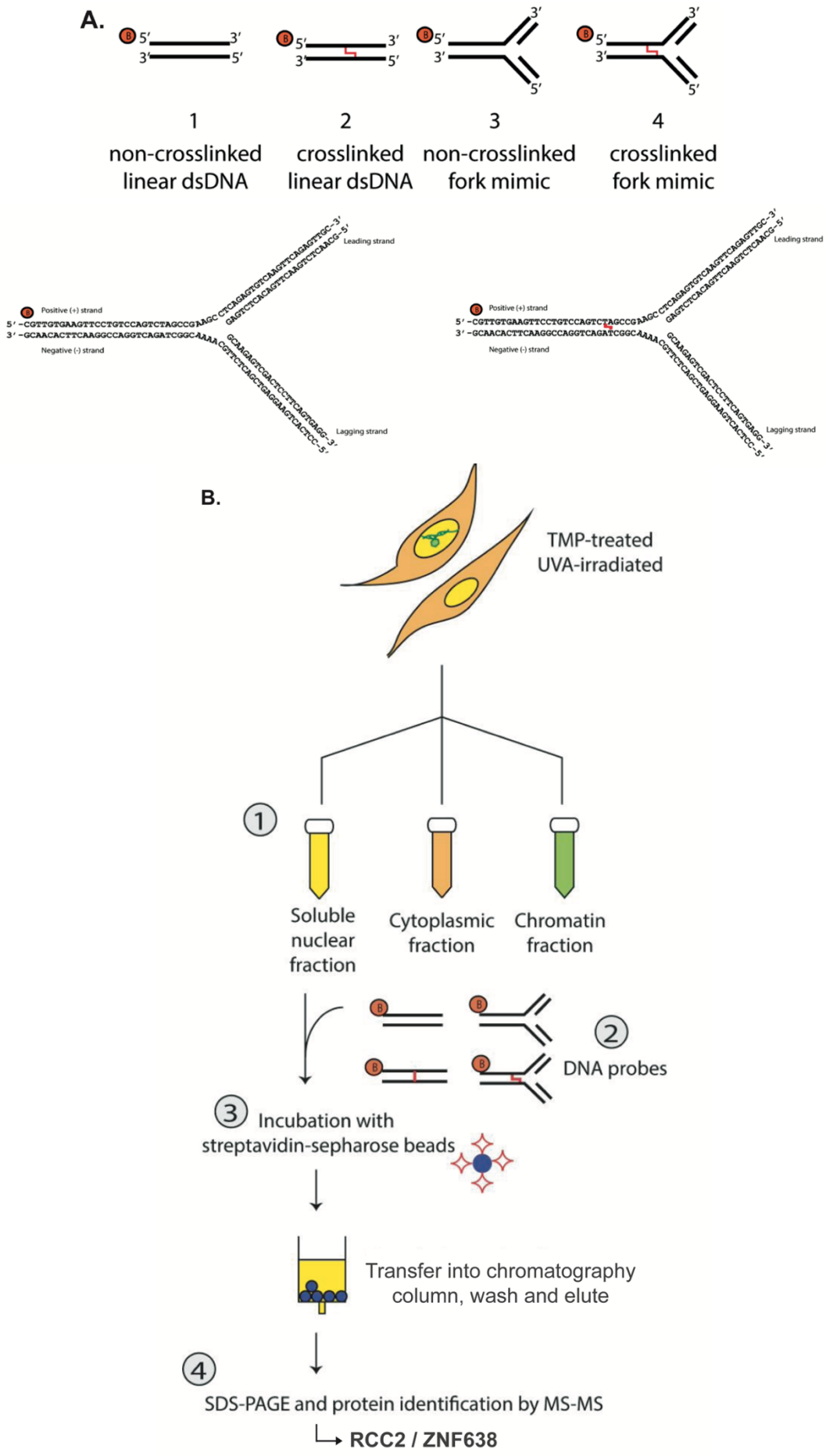

A.
1
non-crosslinked linear dsDNA
2
crosslinked linear dsDNA
3
non-crosslinked fork mimic
4
crosslinked fork mimic
Positive (+) strand
Negative (-) strand
Leading strand
Lagging strand
B.
TMP-treated UVA-irradiated
1
Soluble nuclear fraction
Cytoplasmic fraction
Chromatin fraction
2
DNA probes
3
Incubation with streptavidin-sepharose beads
Transfer into chromatography column, wash and elute
4
SDS-PAGE and protein identification by MS-MS
RCC2 / ZNF638

Figure 2-2 The identification of putative novel ICL repair proteins.
A) Schematic representation of the linear double-stranded and replication fork mimic probes employed in the purification process. The site of biotin attachment is marked, and the presence of a TMP-induced ICL is indicated in red. The complete sequences of the non-crosslinked and crosslinked replication fork mimic probes are displayed for reference.
B) Schematic of the purification scheme for identifying putative novel ICL repair proteins.
Step 1) Soluble nuclear proteins are obtained from TMP/UVA-treated HeLa S3 cells.
Step 2) The proteins are incubated with biotinylated DNA probes with either of the following structures: linear double-stranded oligonucleotide or replication fork mimic. The probes are either non-crosslinked or TMP/UVA-crosslinked.
Step 3) The biotinylated probes and any bound nuclear proteins are then captured using streptavidin-sepharose beads. The beads are transferred into a chromatography column and washed three times. DNA-bound proteins are subsequently eluted following probe digestion by Benzonase nuclease.
Step 4) The protein composition of the eluates is analysed by SDS-PAGE and tandem mass spectrometry (MS-MS). The schematic images are adapted from Kelvin Yaprianto.

RCC2 was enriched 3.52-fold by a linear crosslinked DNA probe relative to a non-crosslinked probe, and 1.39-fold when linear probes were replaced with fork-mimicking probes. Additional data from Kelvin revealed that RCC2 was rapidly recruited to DNA lesions produced by TMP/UVA in living cells (Figure 2-3). This observation demonstrates that RCC2 travels towards the psoralen-induced ICLs *in vivo* and thus likely plays a role in relation to ICL repair. Based on this information, this chapter describes efforts to examine the role of RCC2 as an ICL reactor and to investigate its underlying mechanism.

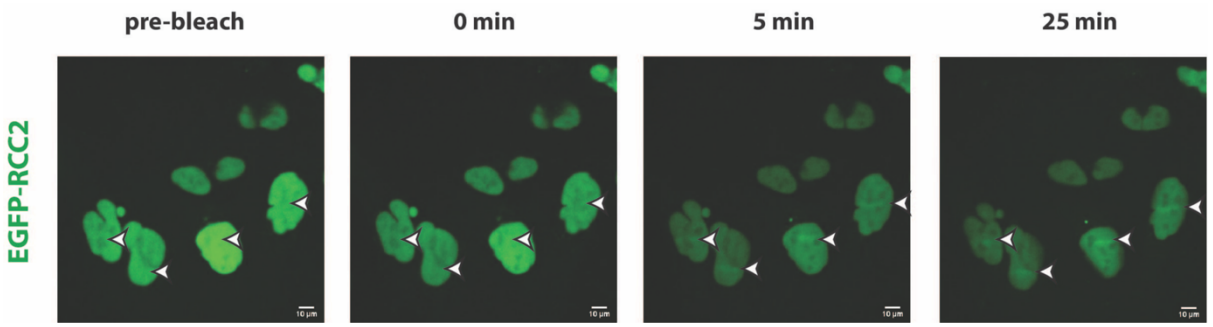


Figure 2-3. RCC2 is recruited to sites of damage upon TMP/UVA treatment.
ICL formation was induced via 30 mins of 20μg/ml TMP treatment followed by the micro-irradiation in a defined nuclear area of HeLa cells expressing EGFP-RCC2 proteins. The recruitment of RCC2 to the ICL sites, indicated by a bright stripe, was monitored for 30 minutes. White arrowheads show the irradiated areas (sites of damage). Scale bar = 10μm. The experiment was performed by Kelvin Yaprianto.

Table 2-1 Proteins identified via tandem mass spectrometry using linear DNA probes.
(The data was acquired by Kelvin Yaprianto)

Rank	Protein	No. of peptides (non-crosslinked linear)	Normalised No. of peptides (non-crosslinked linear/total x 10^4)	No. of peptides (crosslinked linear)	Normalised No. of peptides (crosslinked linear/total x 10^4)	Fold enrichment for linear probes (Normalised crosslinked linear/Normalised non-crosslinked linear)
1	ZNF638	1.00	4.56	15.00	45.05	9.89
2	DLD	1.00	4.56	15.00	45.05	9.89
3	HARS	1.00	4.56	14.00	42.04	9.23
4	HMGB3	1.00	4.56	11.00	33.03	7.25
5	CARS	2.00	9.11	21.00	63.06	6.92
6	ABCF1	2.00	9.11	19.00	57.06	6.26
7	BOD1L1	3.00	13.67	27.00	81.08	5.93
8	THYN1	1.00	4.56	7.00	21.02	4.61
9	CCDC124	1.00	4.56	7.00	21.02	4.61
10	DLAT	4.00	18.22	26.00	78.08	4.28
11	UHRF1	3.00	13.67	19.00	57.06	4.17
12	RCC2	3.00	13.67	16.00	48.05	3.52
13	EEF1B2	2.00	9.11	10.00	30.03	3.30
14	AHNAK	71.00	323.46	293.00	879.88	2.72
15	KIF2C	2.00	9.11	8.00	24.02	2.64
16	CACYBP	3.00	13.67	10.00	30.03	2.20
17	CAST	6.00	27.33	17.00	51.05	1.87
18	HSPA5	8.00	36.45	20.00	60.06	1.65
19	DDB1	11.00	50.11	23.00	69.07	1.38
20	DHX15	5.00	22.78	10.00	30.03	1.32
21	HNRNPA3	4.00	18.22	8.00	24.02	1.32
22	EZR	11.00	50.11	22.00	66.07	1.32
23	CHAF1A	6.00	27.33	11.00	33.03	1.21
24	HSPA9	12.00	54.67	22.00	66.07	1.21
25	APEX1	11.00	50.11	20.00	60.06	1.20
26	GTF2I	10.00	45.56	18.00	54.05	1.19
27	CHAF1B	6.00	27.33	10.00	30.03	1.10
28	EEF1G	10.00	45.56	16.00	48.05	1.05
29	EEF2	5.00	22.78	8.00	24.02	1.05
30	HSPA8	17.00	77.45	26.00	78.08	1.01
31	CCT8	9.00	41.00	13.00	39.04	0.95
32	HNRNPU	10.00	45.56	14.00	42.04	0.92
33	CPS1	23.00	104.78	32.00	96.10	0.92
34	EEF1A1	13.00	59.23	18.00	54.05	0.91
35	CCT2	6.00	27.33	8.00	24.02	0.88
36	CCT7	6.00	27.33	8.00	24.02	0.88
37	DNMT1	6.00	27.33	8.00	24.02	0.88
38	GATAD2B	6.00	27.33	8.00	24.02	0.88
39	ACTG2	9.00	41.00	12.00	36.04	0.88
40	EEF1D	9.00	41.00	12.00	36.04	0.88
41	CCT3	9.00	41.00	11.00	33.03	0.81
42	HNRNPA1	9.00	41.00	11.00	33.03	0.81
43	EEF1D	11.00	50.11	13.00	39.04	0.78
44	XRCC5	20.00	91.12	23.00	69.07	0.76
45	ACTB	15.00	68.34	17.00	51.05	0.75
46	DSG1	10.00	45.56	11.00	33.03	0.73
47	CHD4	17.00	77.45	18.00	54.05	0.70
48	DDX21	18.00	82.00	19.00	57.06	0.70
49	KRT2	34.00	154.90	35.00	105.11	0.68
50	HSPD1	14.00	63.78	14.00	42.04	0.66
51	CCT6A	8.00	36.45	8.00	24.02	0.66
52	DDX17	15.00	68.34	15.00	45.05	0.66
53	DDX46	9.00	41.00	9.00	27.03	0.66
54	EIF4A1	12.00	54.67	12.00	36.04	0.66
55	HNRNPA2B1	10.00	45.56	10.00	30.03	0.66
56	HNRNPK	10.00	45.56	10.00	30.03	0.66
57	GLUD1	20.00	91.12	19.00	57.06	0.63
58	HSP90AB1	19.00	86.56	18.00	54.05	0.62
59	EIF5B	28.00	127.56	26.00	78.08	0.61
60	XRCC6	27.00	123.01	25.00	75.08	0.61
61	DDX5	12.00	54.67	11.00	33.03	0.60
62	DHX9	23.00	104.78	21.00	63.06	0.60
63	GAPDH	20.00	91.12	17.00	51.05	0.56
64	HNRNPC	13.00	59.23	11.00	33.03	0.56
65	EIF4A3	11.00	50.11	9.00	27.03	0.54

Table 2-2. Proteins identified via tandem mass spectrometry using fork mimic DNA probes.
(The data was acquired by Kelvin Yaprianto

Rank	Protein	No. of peptides (non-crosslinked fork)	Normalised No. of peptides (non-crosslinked fork/total x 10^4)	No. of peptides (crosslinked fork)	Normalised No. of peptides (crosslinked fork/total x 10^4)	Fold enrichment for fork mimic probes (Normalised crosslinked fork /Normalised non-crosslinked fork)
1	KIF2C	2.00	7.46	8.00	28.55	3.83
2	THYN1	2.00	7.46	6.00	21.41	2.87
3	CCDC124	2.00	7.46	5.00	17.84	2.39
4	DSP	12.00	44.76	29.00	103.50	2.31
5	EEF2	5.00	18.65	12.00	42.83	2.30
6	UHRF1	6.00	22.38	13.00	46.40	2.07
7	DLAT	9.00	33.57	19.00	67.81	2.02
8	HNRNPA3	4.00	14.92	7.00	24.98	1.67
9	AHNAK	174.00	649.01	262.00	935.05	1.44
10	CAST	8.00	29.84	12.00	42.83	1.44
11	RCC2	11.00	41.03	16.00	57.10	1.39
12	CACYBP	12.00	44.76	15.00	53.53	1.20
13	HMGB3	9.00	33.57	11.00	39.26	1.17
14	APEX1	14.00	52.22	17.00	60.67	1.16
15	CARS	5.00	18.65	6.00	21.41	1.15
16	HSPD1	10.00	37.30	12.00	42.83	1.15
17	CCT7	6.00	22.38	7.00	24.98	1.12
18	GTF2I	31.00	115.63	36.00	128.48	1.11
19	HSPA5	19.00	70.87	22.00	78.52	1.11
20	DLD	7.00	26.11	8.00	28.55	1.09
21	DNMT1	8.00	29.84	9.00	32.12	1.08
22	HNRNPA1	8.00	29.84	9.00	32.12	1.08
23	KRT2	34.00	126.82	38.00	135.62	1.07
24	GLUD1	29.00	108.17	32.00	114.20	1.06
25	CCT3	10.00	37.30	11.00	39.26	1.05
26	HNRNPC	10.00	37.30	11.00	39.26	1.05
27	EEF1G	11.00	41.03	12.00	42.83	1.04
28	HSPA8	22.00	82.06	24.00	85.65	1.04
29	CPS1	28.00	104.44	30.00	107.07	1.03
30	EEF1A1	14.00	52.22	15.00	53.53	1.03
31	DDX21	16.00	59.68	17.00	60.67	1.02
32	HSPA9	16.00	59.68	17.00	60.67	1.02
33	BOD1L1	3.00	11.19	3.00	10.71	0.96
34	HNRNPK	6.00	22.38	6.00	21.41	0.96
35	HSP90AA1	6.00	22.38	6.00	21.41	0.96
36	ACTB	16.00	59.68	16.00	57.10	0.96
37	CCT2	7.00	26.11	7.00	24.98	0.96
38	DSG1	9.00	33.57	9.00	32.12	0.96
39	EZR	22.00	82.06	22.00	78.52	0.96
40	GAPDH	22.00	82.06	21.00	74.95	0.91
41	DDX17	15.00	55.95	14.00	49.96	0.89
42	HNRNPU	12.00	44.76	11.00	39.26	0.88
43	HSP90AB1	12.00	44.76	11.00	39.26	0.88
44	EIF4A1	11.00	41.03	10.00	35.69	0.87
45	ACTG2	10.00	37.30	9.00	32.12	0.86
46	EEF1D	10.00	37.30	9.00	32.12	0.86
47	EEF1D	9.00	33.57	8.00	28.55	0.85
48	EIF5B	16.00	59.68	14.00	49.96	0.84
49	ABCF1	24.00	89.52	20.00	71.38	0.80
50	CCT6A	6.00	22.38	5.00	17.84	0.80
51	CCT8	12.00	44.76	10.00	35.69	0.80
52	KPRP	6.00	22.38	5.00	17.84	0.80
53	DHX15	5.00	18.65	4.00	14.28	0.77
54	FLYWCH1	15.00	55.95	12.00	42.83	0.77
55	HNRNPA2B1	13.00	48.49	10.00	35.69	0.74
56	EIF4A3	8.00	29.84	6.00	21.41	0.72
57	XRCC5	15.00	55.95	11.00	39.26	0.70
58	DDX5	14.00	52.22	10.00	35.69	0.68
59	DDB1	20.00	74.60	14.00	49.96	0.67
60	DHX9	18.00	67.14	12.00	42.83	0.64
61	XRCC6	24.00	89.52	15.00	53.53	0.60
62	DDX46	13.00	48.49	8.00	28.55	0.59
63	ZNF638	7.00	26.11	4.00	14.28	0.55
64	GATAD2B	6.00	22.38	3.00	10.71	0.48
65	EEF1B2	4.00	14.92	2.00	7.14	0.48

2.2 Results

2.2.1 RCC2 knockout sensitises Hela cells to TMP/UVA and MMC treatments

Rapid RCC2 recruitment was found at TMP/UVA-induced ICLs, as indicated in Figure 2-3, which suggests that the protein translocates to the vicinity of the lesions and potentially serves as an ICL repair factor. To determine if the observed interaction between RCC2 and ICL is functionally meaningful, RCC2-depleted cells were generated through CRISPR-Cas9 deletion (Figure 2-4A) and then reconstituted with EGFP-tagged RCC2 (Figure 2-4B).

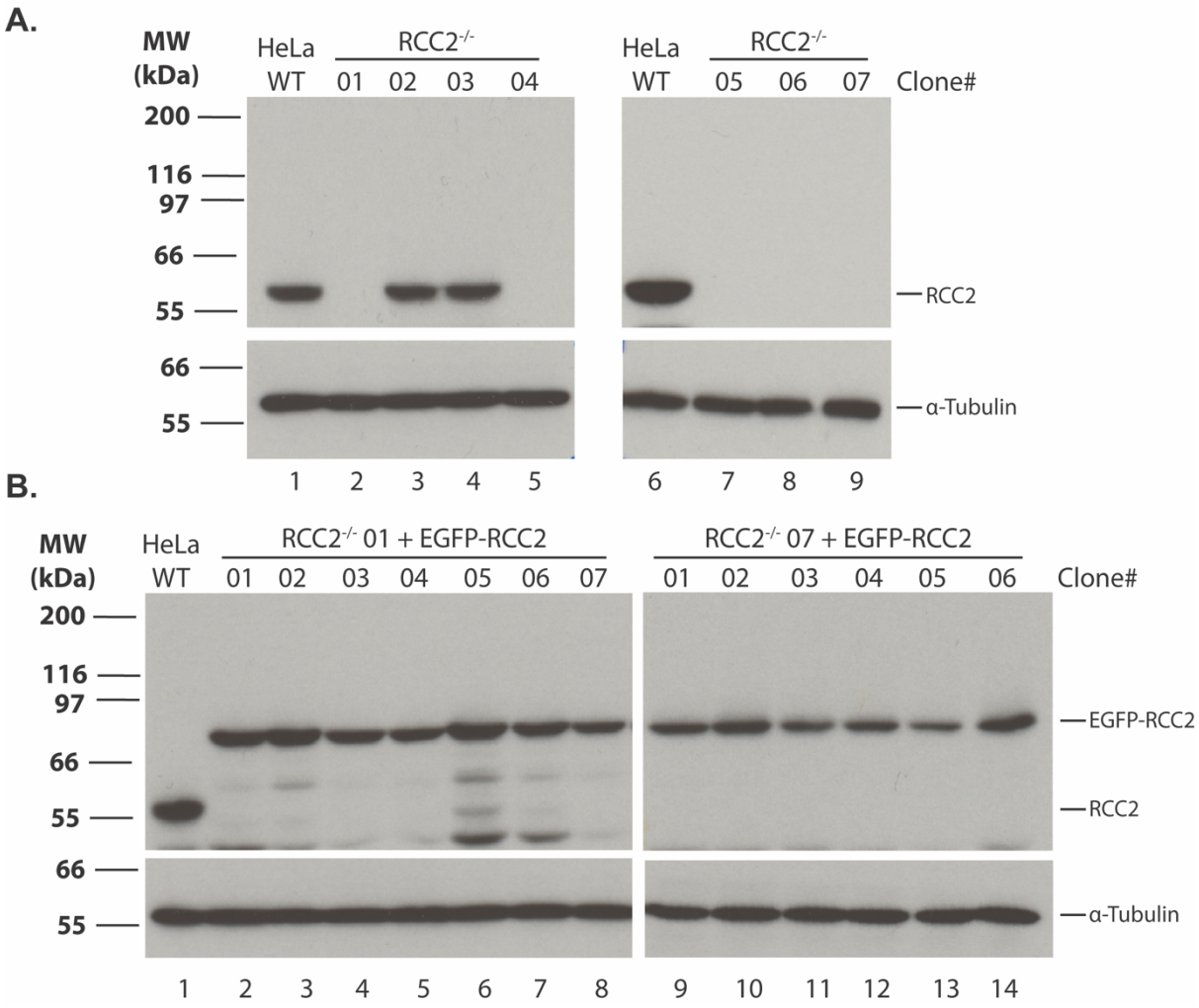


Figure 2-4. Production of RCC2 knockout and EGFP-RCC2 complemented cells.
Western blots using anti-RCC2 and anti-α-Tubulin antibodies showing that:
A) that RCC2 was knocked out from HeLa cells using the CRISPR-Cas9 system. Single clones 01 and 07 of RCC2 knockout (lanes 2 and 9) were used in the following clonogenic survival assay.
B) EGFP-RCC2 was re-expressed in the RCC2 knockout clones 01 and 07 via retroviral transfection.

Subsequently, to assess the impact of RCC2 deletion on cellular survival, two independent RCC2 knockout clones, along with four EGFP-RCC2 complemented clones (two for each knockout clone), and HeLa wild type (WT) controls were subjected to treatment with two crosslinkers: MMC and TMP/UVA. After 14 days following treatment, the cell survival rate

was measured. The results reveal that RCC2 deletion significantly compromises cellular survival in response to both MMC and TMP/UVA treatment, which can be reversed upon complementation with EGFP-RCC2. This indicates that RCC2 plays a protective role in shielding HeLa cells from the genotoxicity induced by MMC and TMP/UVA (Figure 2-5/2-6).

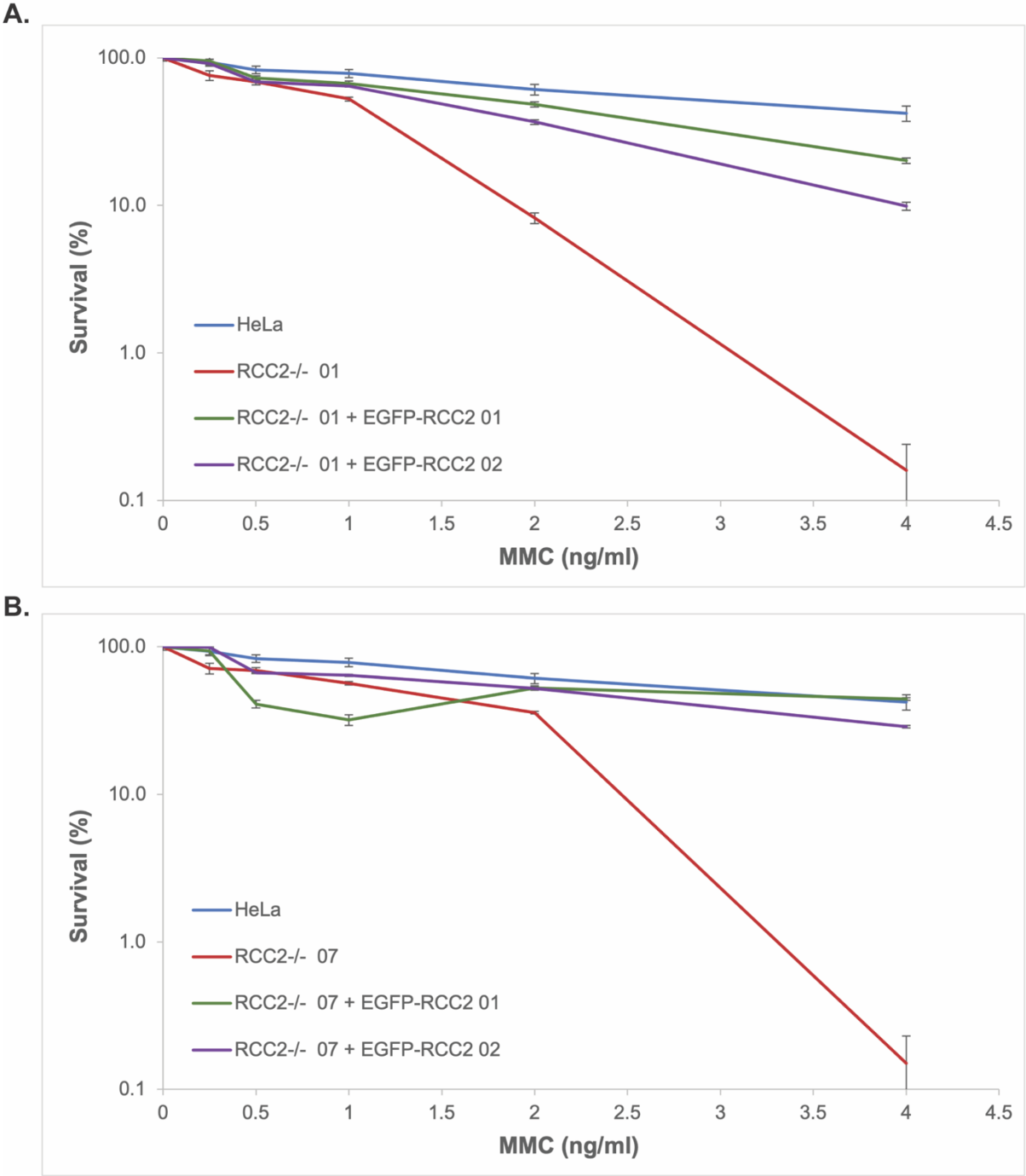


Figure 2-5. RCC2 knockout sensitises the HeLa cells towards MMC treatment, which is reverted by the EGFP-RCC2 complementation.
RCC2 knockout clones **A)** 01 and **B)** 07, together with two EGFP-RCC2 complemented clones for each knockout, were treated with 0, 0.25, 0.5, 1, 2, 4 ng/ml MMC for 14 days, and the colony formation was scored using 1% (w/v) crystal violet in methanol. Y values are shown in the logarithmic scale; thus, only positive values are presented (mean ± SEM, n = 3 technical replicates from a representative experiment, the experiments were performed twice).

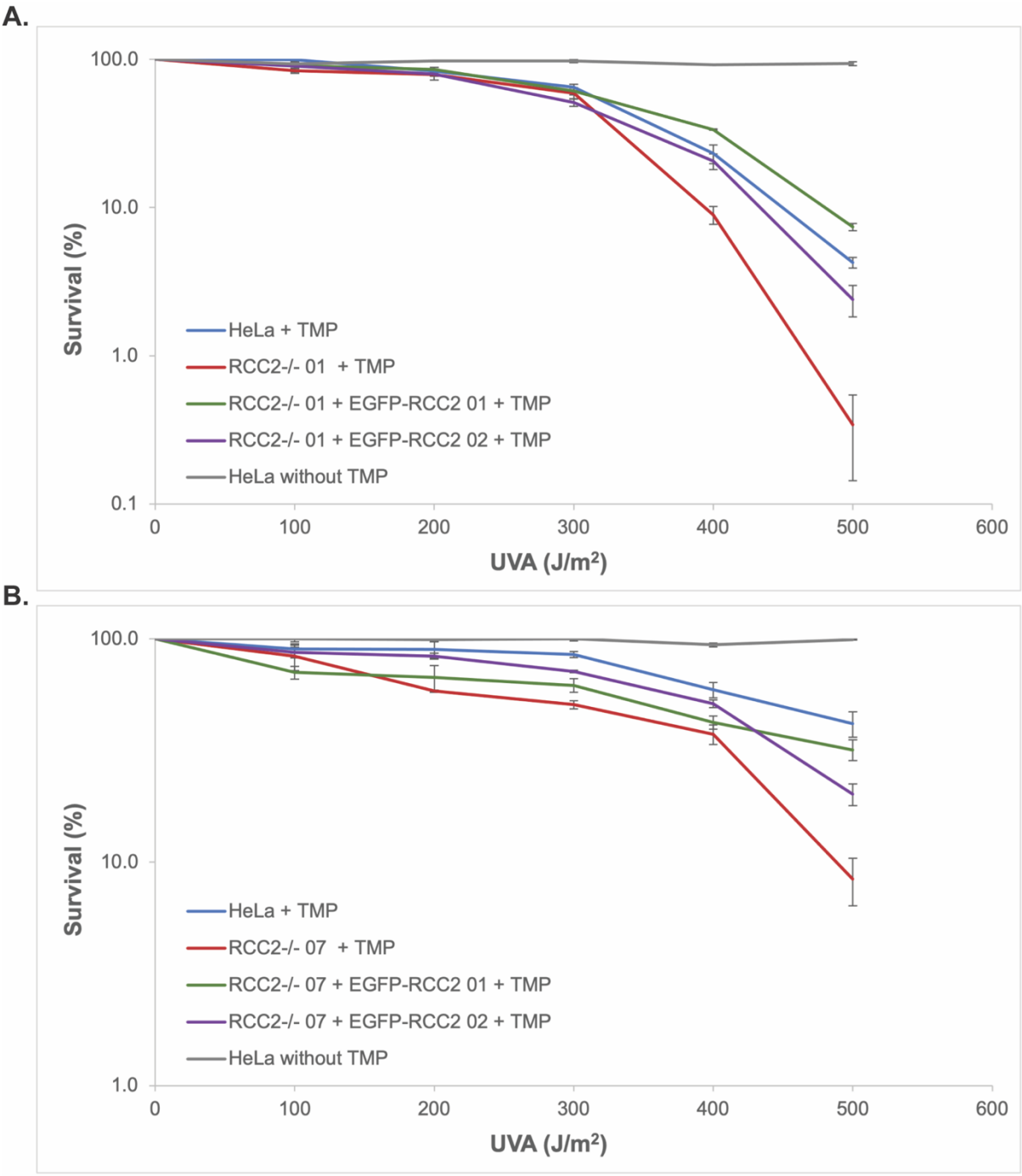
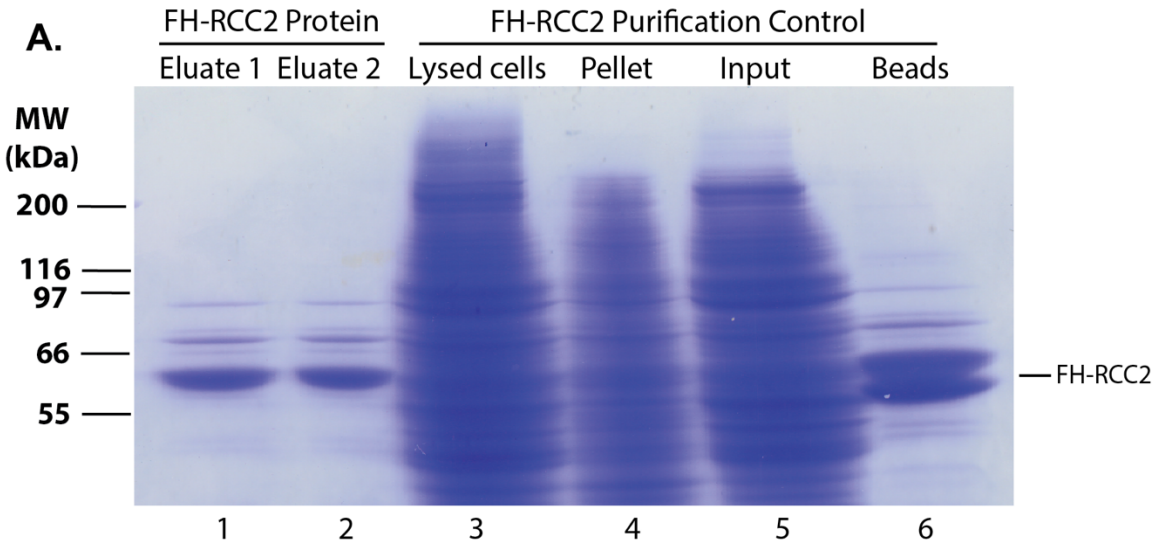


Figure 2-6. RCC2 knockout sensitises the HeLa cells towards TMP/UVA treatment, which is reverted by the EGFP-RCC2 complementation.
RCC2 knockout clones **A)** 01 and **B)** 07, together with two EGFP-RCC2 complemented clones for each knockout, were treated with 100ng/ml TMP for 1 hour and then radiated by 0, 100, 200, 300, 400, 500 J/m^2 365nm UVA. Treated cells were cultured for 14 days, and the colony formation was scored as previously. HeLa cells treated with UVA only were included as no TMP control. Y values are shown in the logarithmic scale; thus, only positive values are presented (mean ± SEM, n = 3 technical replicates from a representative experiment, the experiments were performed twice).

2.2.2 RCC2 does not physically interact with DNA probes *in vitro*

The clonogenic survival data have shown that RCC2 is functionally important for cell survival in the presence of crosslinking reagents. To further investigate whether the protein directly engages in ICL repair as a lesion recogniser, the protein's interaction with crosslinked DNA was tested. Recombinant RCC2 protein with a Flag-HA (FH) tag was purified from Sf9 insect cells via the baculovirus expression system. The purified FH-RCC2 protein in the final eluates (Figure 2-7A, lane 1 and 2), presented by the strongest bands between 55 and 66kDa, displayed a correct molecular weight of RCC2 (60kDa). However, a few faint bands above FH-RCC2 suggested the presence of low levels of contaminant proteins in the samples. With the purified FH-RCC2 protein, an Electrophoretic Mobility Shift Assay (EMSA) was performed to evaluate the binding capacity of recombinant RCC2 to crosslinked and non-crosslinked DNAs under different salt and pH conditions. Despite the notable interaction of the positive control UHRF1 protein with the DNA probe, RCC2 did not show any detectable physical binding with the four tested probes *in vitro* (Figure 2-7B and C). This result does not correspond to the initial screening strategy that identified RCC2 as a novel repair component. Throughout the previous screening, however, DNA probes were incubated with a complete nuclear extract rather than a single purified protein. Hence, if RCC2 is capable of interacting with nucleic acids, such binding likely requires the presence of functional protein partners or a unique biological milieu.



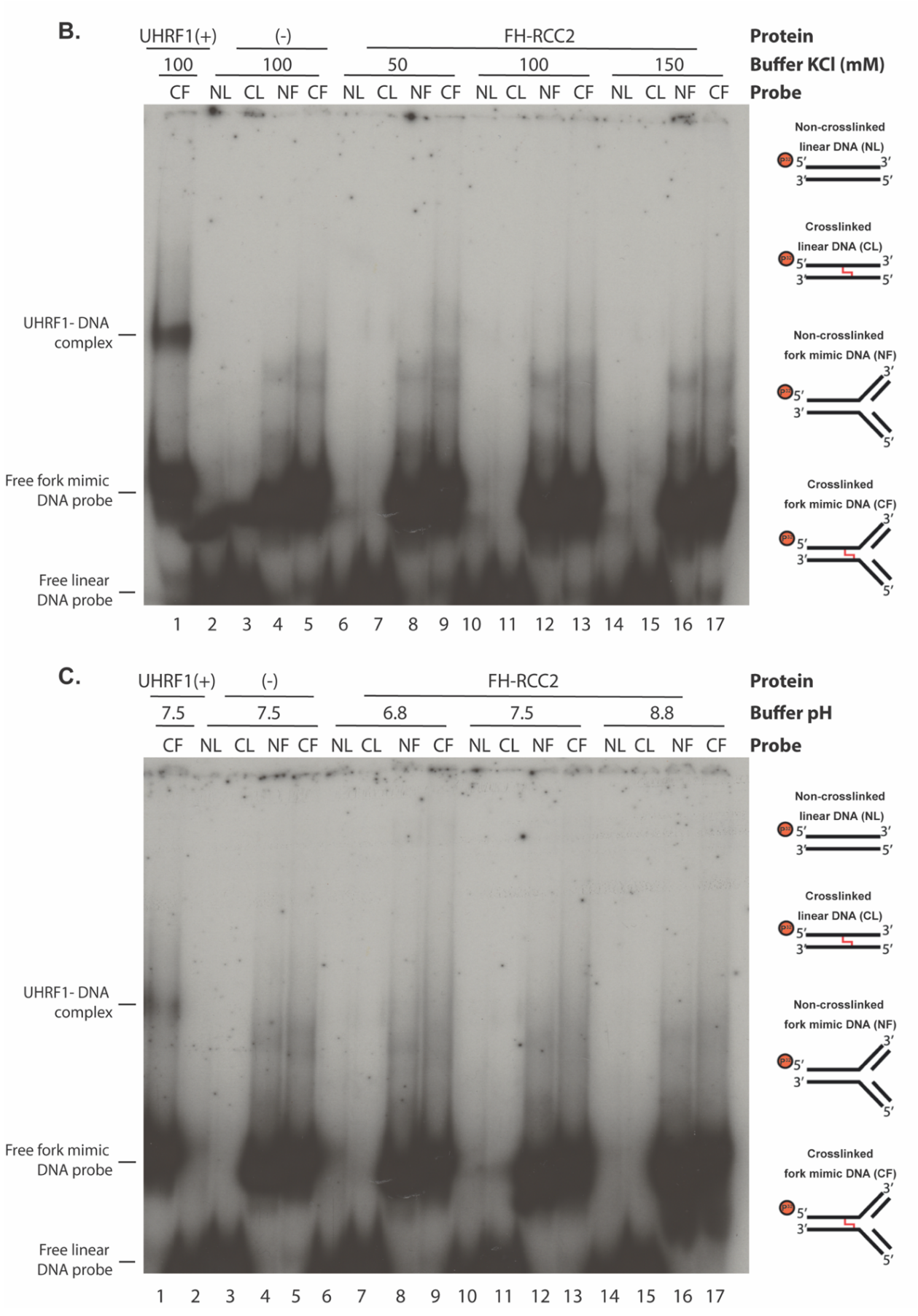
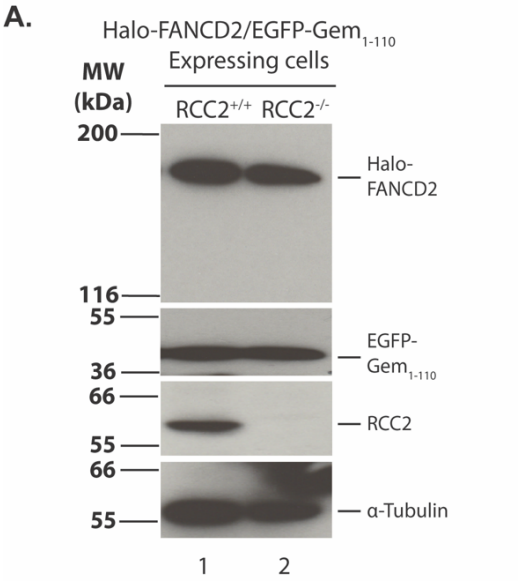

B.
UHRF1(+)
(-)
FH-RCC2
Protein
100
100
50
100
150
Buffer KCl (mM)
CF NL CL NF CF NL CL NF CF NL CL NF CF NL CL NF CF
Probe
UHRF1- DNA complex
Free fork mimic DNA probe
Free linear DNA probe
1 2 3 4 5 6 7 8 9 10 11 12 13 14 15 16 17
Non-crosslinked linear DNA (NL)
Crosslinked linear DNA (CL)
Non-crosslinked fork mimic DNA (NF)
Crosslinked fork mimic DNA (CF)
C.
UHRF1(+)
(-)
FH-RCC2
Protein
7.5
7.5
6.8
7.5
8.8
Buffer pH
CF NL CL NF CF NL CL NF CF NL CL NF CF NL CL NF CF
Probe
UHRF1- DNA complex
Free fork mimic DNA probe
Free linear DNA probe
1 2 3 4 5 6 7 8 9 10 11 12 13 14 15 16 17
Non-crosslinked linear DNA (NL)
Crosslinked linear DNA (CL)
Non-crosslinked fork mimic DNA (NF)
Crosslinked fork mimic DNA (CF)

Figure 2-7. RCC2 does not physically interact with DNA probes *in vitro*.
A) Coomassie blue gel showing the purified FH-RCC2 protein. Sf9 cells expressing FH-RCC2 were lysed in protein purification lysis buffer and centrifuged. The supernatant (input) was incubated with the M2 anti-FLAG agarose resin, centrifuged, and the protein was eluted from the Flag beads. Purified FH-RCC2 protein was in the two final eluates (lanes 1 and 2). **B)** EMSA data showing the binding capability of the FH-RCC2 protein to four DNA probes when using reaction buffer with different salt concentrations (50/100/150mM KCl) or **C)** different pH values (6.8/7.5/8.8). UHFR1 was previously proved to bind DNAs and thus included as a positive control. 200ng of UHFR1 protein or 300ng of RCC2 protein was used in each EMSA reaction. The negative controls are EMSA buffers containing indicated DNA probes (without protein). The schematic images demonstrate four ^{32}P radiolabelled DNA probes used in the experiment. The presence of a TMP/UVA-induced ICL in crosslinked probes is indicated in red.

2.2.3 RCC2 is not involved in the FA pathway for ICL repair

Based on the EMSA results, RCC2 does not appear to interact physically with crosslinked DNAs when responding to psoralen-induced ICLs. Therefore, to further investigate the association between RCC2 and the cellular response to ICLs, its connection to well-established ICL repair pathways was explored. As previously mentioned, the FA pathway is the most canonical mechanism for ICL repair, with FANCD2 playing a crucial role in this pathway. Hence, *in vivo* effects of RCC2 depletion on FANCD2 were investigated first. In Halo-FANCD2 knock-in cells, exogenous S/G2 marker EGFP-Geminin$_{1\text{-}110}$ was introduced, followed by a complete knockout of RCC2 from the co-expressing cells (Figure 2-8A). As the FA pathway is specifically activated during the S-phase, the recruitment of FANCD2 to ICLs in the S/G2 cells (positive for EGFP-Geminin$_{1\text{-}110}$) was observed in the presence or absence of RCC2. Following the induction of ICLs in a localised nuclear region of S/G2 cells, Halo-tagged FANCD2 progressively accumulated within the damaged regions, becoming pronounced at 15-30 minutes after TMP/UVA treatment. Depletion of RCC2 had no apparent impact on the recruitment of Halo-FANCD2 to the DNA damage induced by TMP/UVA when compared to cells with intact RCC2 functionality (Figure 2-8B and C).



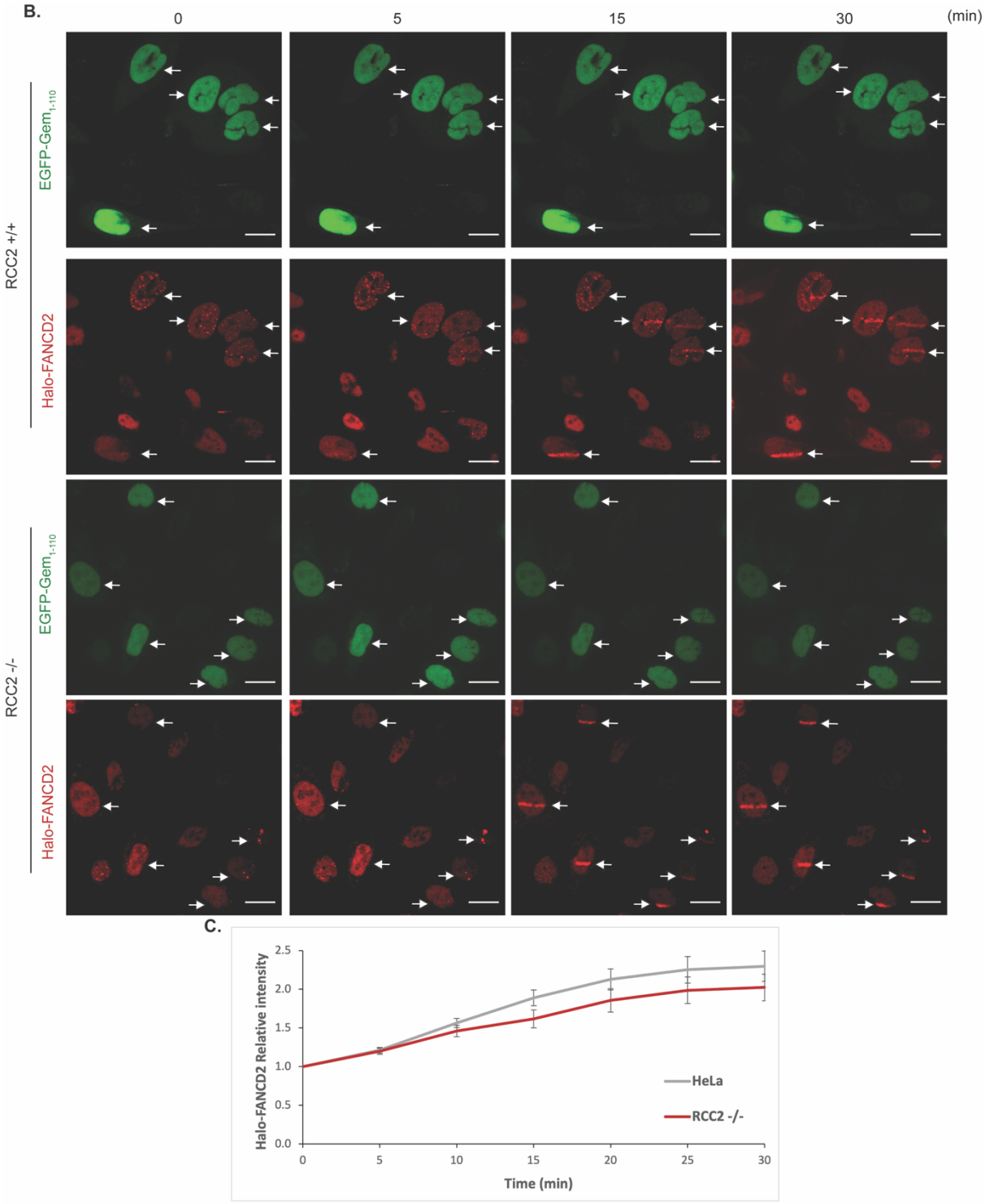


Figure 2-8. RCC2 deletion has no discernible impact on FANCD2 recruitment to ICLs.
A) Western blot showing the deletion of RCC2 from the Halo-FANCD2/EGFP-Geminin$_{1-110}$ co-expressing HeLa cells via CRISPR/Cas9 knockout using anti-FANCD2, anti-EGFP, anti-RCC2 and anti-α-Tubulin antibodies. **B)** Live-cell imaging was performed using Halo-FANCD2/EGFP-Geminin$_{1-110}$ co-expressing HeLa cells, either with or without RCC2 expression. 100nM JF549 was used to label the Halo-FANCD2. Cells were treated with 20μg/ml TMP for 30 minutes, then were micro-irradiated with 405 nm laser at specific areas indicated by the white arrows. The distribution of Halo-FANCD2 was monitored for 30 minutes post-irradiation. Scale bar = 10μm. **C)** Images were collected at the indicated time points, and the relative increase in fluorescence intensity representing the enrichment of Halo-FANCD2 in the irradiated regions was quantified as mean ± SEM (n=14 cells for RCC2$^{+/+}$ and n=13 cells for RCC2$^{-/-}$ cells from a representative experiment, the experiment was performed twice).

FANCD2's monoubiquitination is functionally necessary for its activity in the FA pathway for ICL repair. Therefore, the ubiquitination of FANCD2 following TMP/UVA treatment is examined with or without the presence of RCC2. Likewise, the level of ubiquitinated FANCD2 provoked by TMP/UVA-induced ICLs was not affected by RCC2 deletion (Figure 2-9).

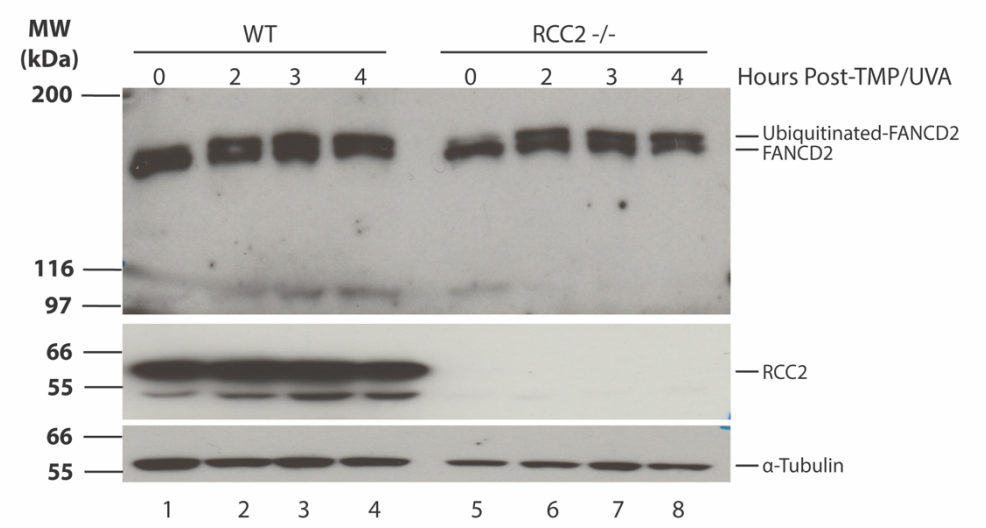


Figure 2-9. FANCD2 ubiquitination is not dependent on the presence of RCC2.
Western blot using anti-FANCD2, anti-RCC2 and anti-α-Tubulin antibodies shows the endogenous and ubiquitinated FANCD2 level of TMP/UVA-treated HeLa and RCC2$^{-/-}$ cells. Cells were treated with 2μg/ml TMP for 30 minutes and then irradiated with 1000 J/m^2 UVA. Whole-cell lysates were collected from cells 0, 2, 3, and 4 hours after irradiation. The level of ubiquitinated FANCD2 (the upper band) and unmodified FANCD2 (the lower band) was assessed using an anti-FANCD2 antibody.

While previous data (Figure 2-3 and Figure 2-8) have suggested that RCC2 is recruited to ICLs (~5min post-treatment) before FANCD2 (~15min post-treatment), the observations that neither FANCD2 recruitment nor ubiquitination requires RCC2 suggest that the protein may not operate within the FA pathway. To verify this hypothesis, RCC2 and FANCD2 were knocked out simultaneously from HeLa cells (Figure 2-10A), and their sensitivity to ICL-inducing drugs was compared to that of single knockout cells. If RCC2 operates in an alternative repair mechanism independent of the FA pathway, the double knockout, where both the FA repair pathway and the RCC2-associated repair are impaired, should exhibit greater sensitivity to crosslinkers compared to the single knockouts, in which only one mechanism is compromised. As anticipated, the RCC2 and FANCD2 double knockout cells displayed increased sensitivity to TMP/UVA and MMC compared to cells with single knockouts of FANCD2 or RCC2, providing further evidence that these two proteins function non-epistatically in ICL repair (Figure 2-10B and C).

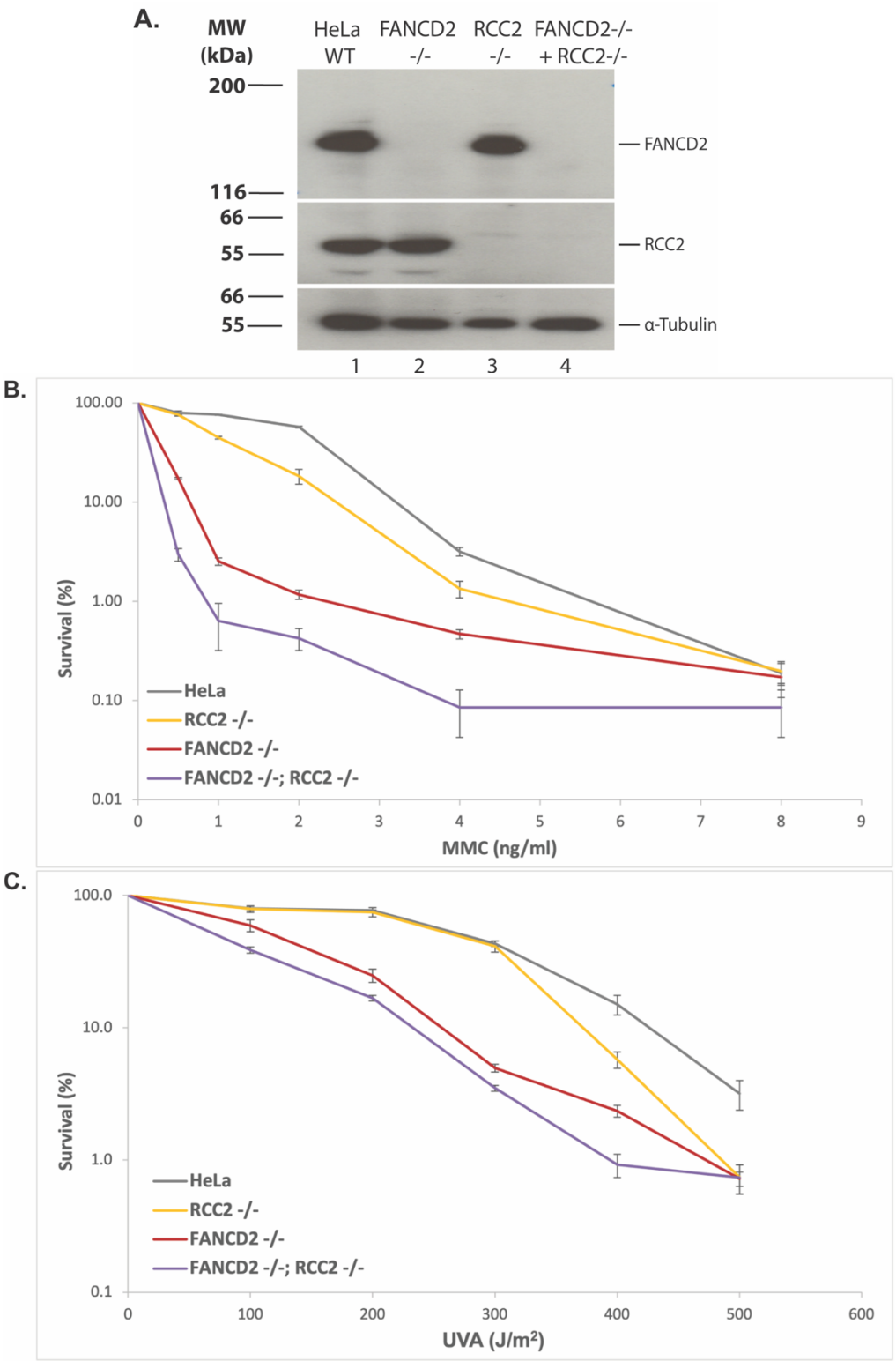


Figure 2-10. RCC2 does not function in the FA pathway.
A) Western Blot using anti-FANCD2, anti-RCC2 and anti-α-Tubulin antibodies showing the FANCD2 and RCC2 double or single knockout cells used in the clonogenic survival assays. The knockout was completed using the CRISPR-Cas9 system. **B)** Clonogenic survival assay was performed using the indicated cell lines. Cells were grown for two weeks in a culture medium containing 0, 0.5, 1, 2, 4 or 8 ng/ml MMC. The number of colonies formed was then counted. **C)** Cells were treated with 100 ng/ml TMP, incubated for 30 minutes, and subsequently irradiated with 0, 100, 200, 300, 400 or 500 J/m^2 UVA. The number of colonies formed was counted two weeks afterwards. Y values are shown in the logarithmic scale (mean ± SEM, n = 3 technical replicates from a representative experiment, the experiments were performed twice).

2.2.4 Exploring the connection between RCC2 and the NEIL3 repair pathway

The acquired data indicate that RCC2 is not associated with FANCD2 and the FA pathway to which FANCD2 belongs. Thus, experiments were performed to evaluate the relationship between RCC2 and another ICL repair mechanism, the NEIL3 pathway. Halo-FANCD2 knock-in cells expressing EGFP-tagged NEIL3 were constructed to evaluate the recruitment of NEIL3 to ICLs (Figure 2-11A). Surprisingly, exogenously expressed NEIL3-EGFP was not recruited to the TMP/UVA-induced ICLs, while the Halo-tagged FANCD2 (served as a positive control) relocated to ICL-containing regions (Figure 2-12). This finding contradicts a previous study by N. Li et al. (2020) which reports the aggregation of EGFP-tagged NEIL3 at psoralen-induced ICLs within one minute post-irradiation. This study examines NEIL3's behaviour in U2OS cells rather than in HeLa cells, suggesting the possibility that NEIL3's response to ICL formation is specific to cell types. To address this possibility, NEIL3-EGFP was expressed in U2OS cells (Figure 2-11B), and its response to TMP/UVA treatment was assessed. Still, there was no discernible change in the distribution of NEIL3-EGFP following ICL induction in the U2OS cells (Figure 2-13).

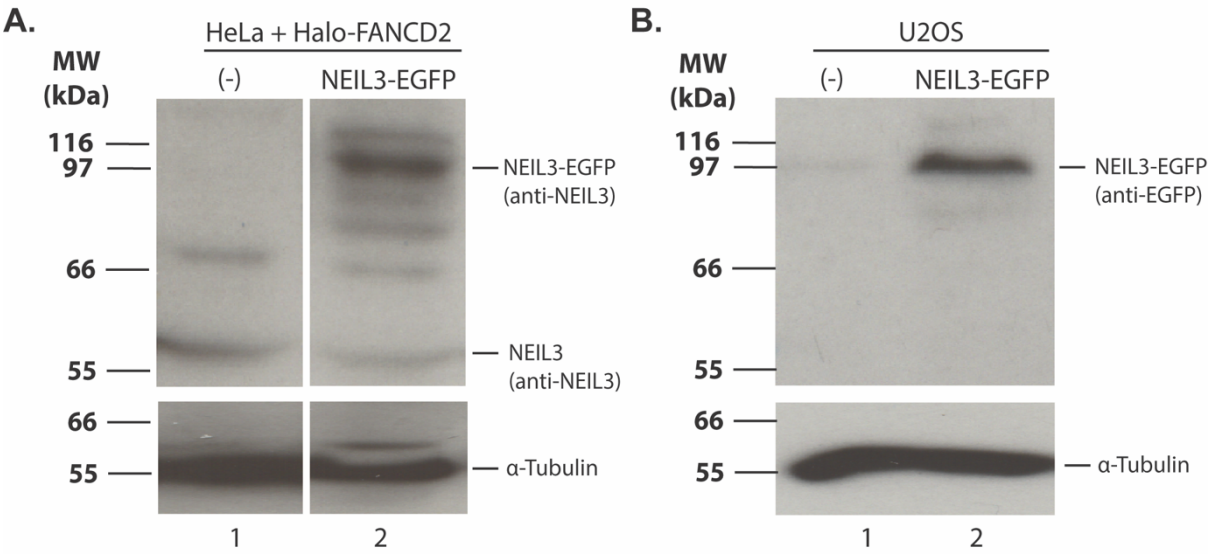


Figure 2-11. Generation of the NEIL3-EGFP expressing cells.
A) Western Blot showing that C-terminal EGFP tagged NEIL3 was exogenously expressed in Halo-FANCD2 knock-in HeLa cells by using the anti-NEIL3 and anti-α-Tubulin antibodies or **B)** U2OS cells via retroviral transfection. The anti-EGFP and anti-α-Tubulin antibodies were used.

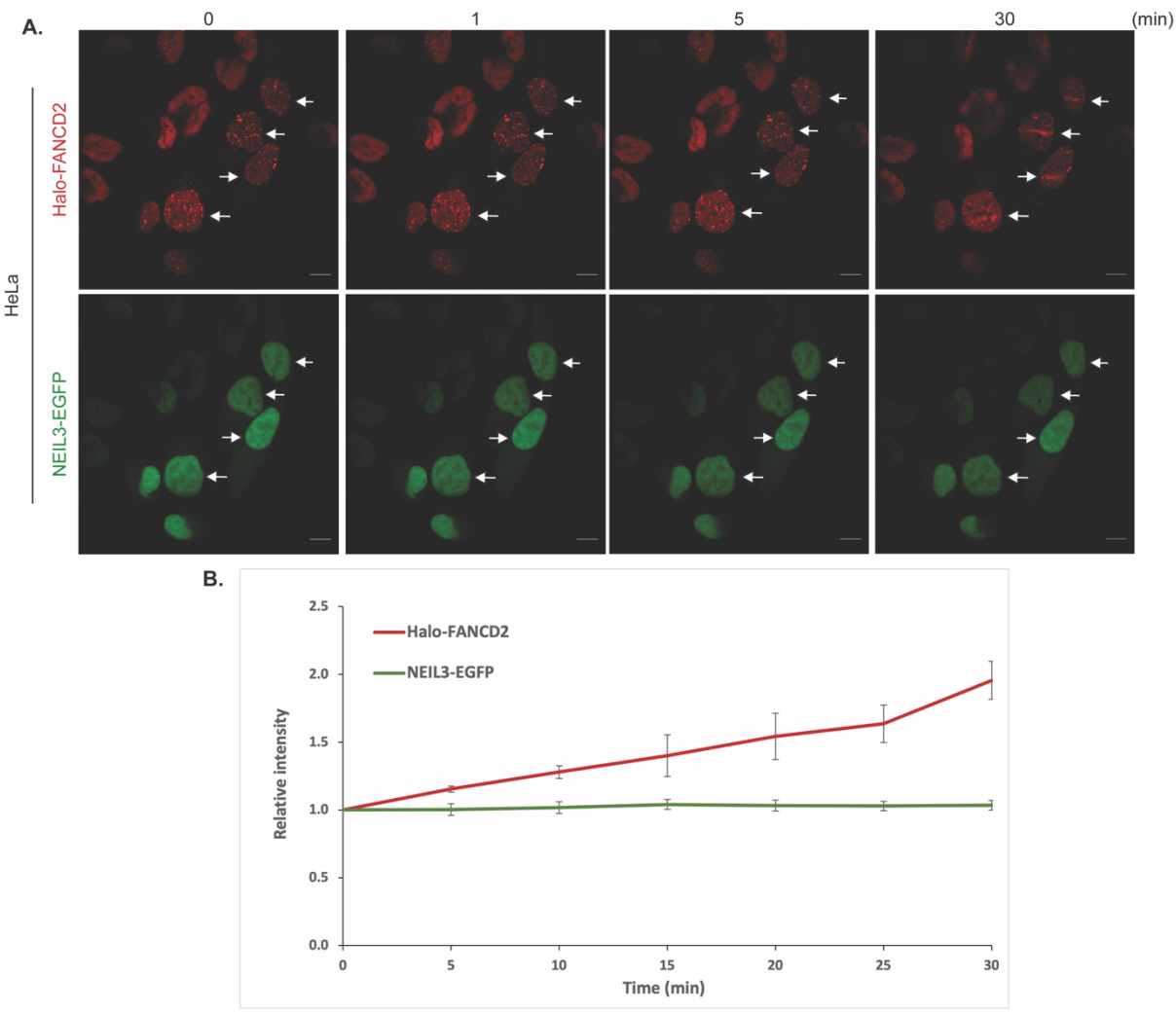


Figure 2-12. NEIL3 recruitment to TMP/UVA-induced ICLs is not observed in HeLa cells.
A) Live-cell imaging was performed using NEIL3-EGFP/Halo-FANCD2 co-expressing HeLa cells. 100nM JF549 was used to label the Halo-FANCD2. The cells were incubated with 20μg/ml TMP for 30 minutes, then micro-irradiated with 405 nm laser at specific areas indicated by the white arrows. The distribution of tagged proteins was monitored for 30 minutes post-irradiation. Halo-FANCD2 was used as a positive control to confirm ICL formation in the indicated regions. Scale bar = 10μm. **B)** Images were collected at the indicated time points, and the relative change in fluorescence intensities representing the accumulation of Halo-FANCD2 and NEIL3-EGFP in the irradiated regions was quantified as mean ± SEM (n=4 cells from a representative experiment, the experiment was performed twice).

In addition to cell type, the wavelength of UVA used in our live-cell imaging differs from that of the prior study. The aforementioned publication utilises UVA at 365 nm, while our live-cell imaging microscope is equipped with a laser at 405 nm that is potentially less effective in generating *in vivo* ICLs. To enhance the number of lesions in the irradiated areas, stronger doses of 405nm UVA were attempted to produce ICLs (the laser power was increased from 30% to 50% and 100% power). Despite testing with an extensive range of UVA intensities, NEIL3's ICL recruitment remained undetected (data not shown). Generating a greater number

of ICLs by increasing the UVA dosage is not optimal since laser power of more than 50% (estimated to be 1040 J/m^2) by itself (without TMP) recruits FANCD2 to the irradiated location, implying that the high level of UVA generates non-specific damage in addition to ICLs. To align the experimental setting, a UVA irradiator was employed to administer 365nm UVA exposure to the entire cells. Although NEIL3 foci were observed in a previous study following H_2O_2 treatment (Zhou et al., 2017), no NEIL3-EFGP foci formation was detected 5 minutes after ICL induction by TMP plus a pan-treatment of 365nm UVA (Figure 2-14). Nevertheless, the earliest time point at which the presence of NEIL3 foci could be examined was 5 minutes post-irradiation in this experiment, owing to the unavoidable delay of image capturing when transferring cells from the UVA irradiator to the imaging microscope. Since previous studies have shown that NEIL3 is rapidly recruited to ICLs within one minute, it is possible that the NEIL3 foci have disbanded by 5 minutes post-irradiation, rendering them undetectable. Thus, additional testing will necessitate the use of a microscope equipped with 365nm UVA to produce ICLs within specific nuclear regions in order to assess the recruitment of NEIL3 immediately after irradiation and further test how this recruitment may be affected by RCC2 depletion.

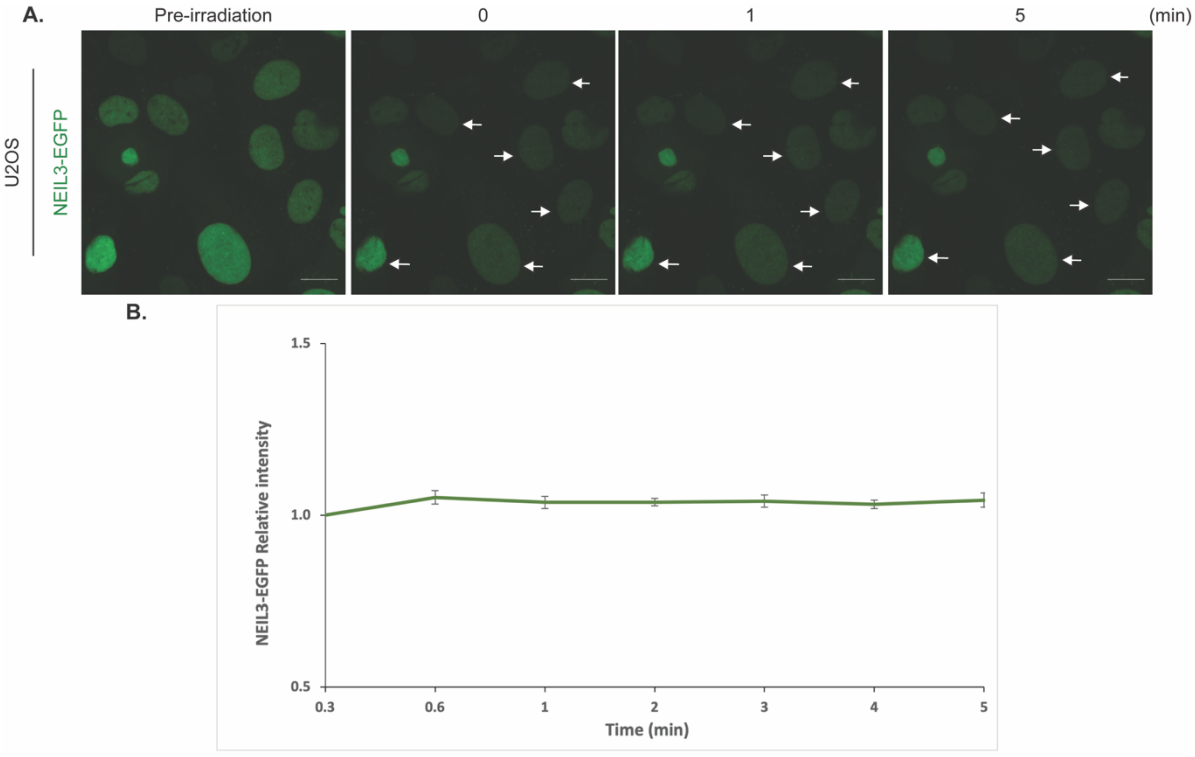


Figure 2-13. NEIL3 recruitment to TMP/UVA-induced ICLs is not observed in U2OS cells.
A) Live-cell imaging was performed using NEIL3-EGFP expressing U2OS cells. The cells were treated with TMP/UVA as previously. The distribution of NEIL3-EGFP was monitored for five minutes post-irradiation. Scale bar = 10μm. **B)** Images were collected at the indicated time points, and the relative change in fluorescence intensity representing the accumulation of NEIL3-EGFP in the irradiated regions was quantified as mean ± SEM (n=6 cells, the experiment was performed once).

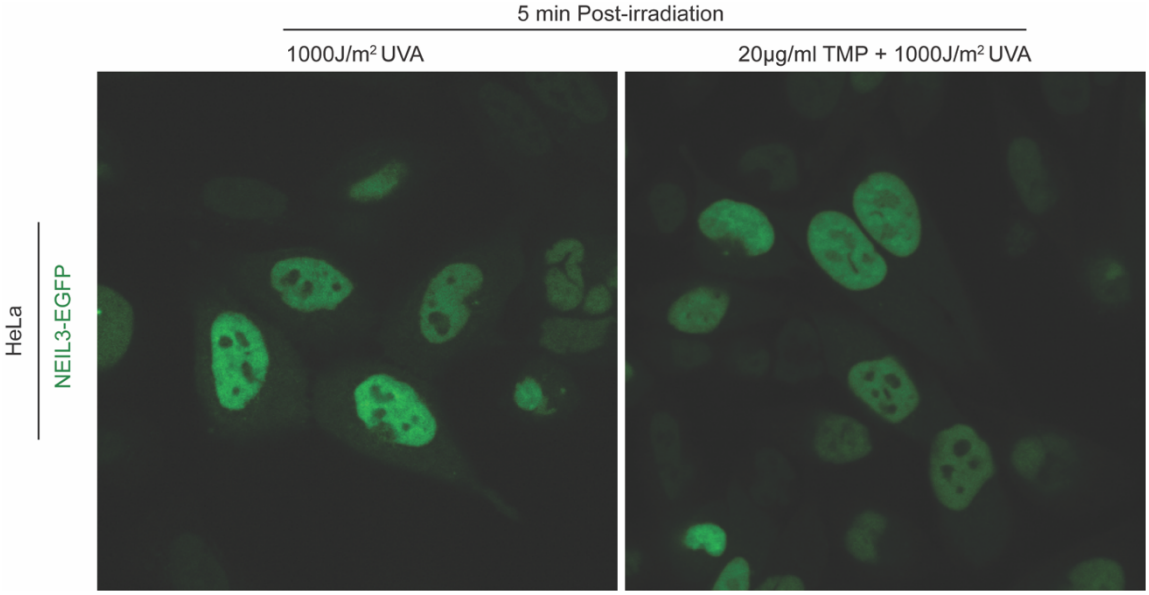
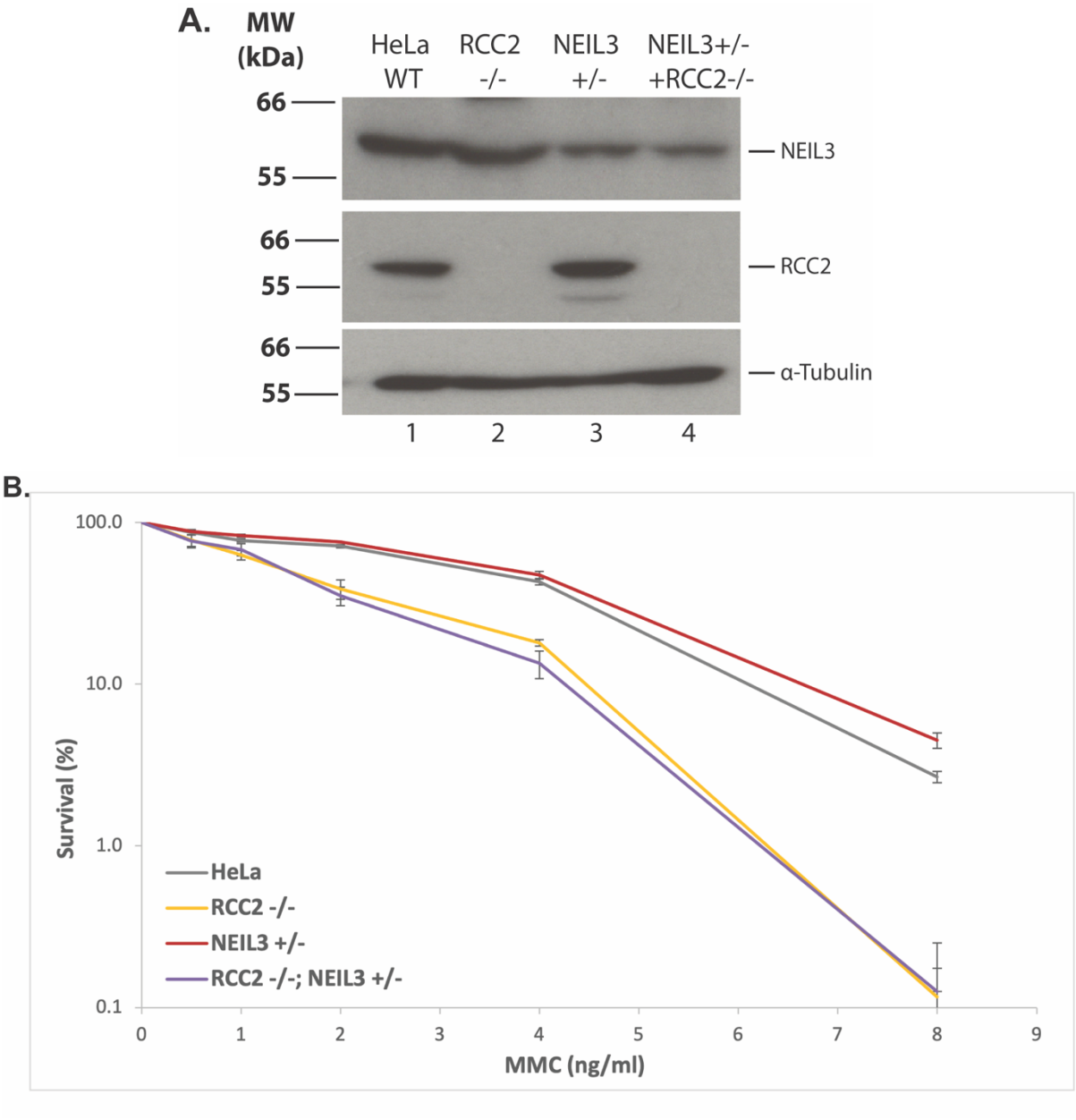


Figure 2-14. NEIL3 *in vivo* foci formation in response to TMP/UVA-induced ICLs is not observed in HeLa cells.
NEIL3-EGFP expressing HeLa cells were incubated with or without 20μg/ml TMP for 30 minutes, and then the entire cells were irradiated with 1000 J/m^2 365nm UVA using a UVA irradiator. Foci formation of NEIL3-EGFP was examined five minutes post-irradiation. Scale bar = 10μm.

2.2.5 Partial depletion of NEIL3 further sensitises RCC2-deficient cells to psoralen-induced ICLs

As the translocation of NEIL3 to TMP/UVA-induced ICLs was not observed in previous live-cell imaging, a double knockout of NEIL3 and RCC2 was attempted to investigate whether RCC2 is involved in the NEIL3 pathway. Although four unique guide RNAs were tested in the CRISPR-Cas9 procedure to deplete the NEIL3 protein, multiple attempts to create a full knockout clone were unsuccessful. Using two individual shRNAs also failed to fully deplete the NEIL3 protein (data not shown). As a result, heterozygous NEIL3 knockout (NEIL3$^{+/-}$) in HeLa WT and RCC2-deficient cells (Figure 2-15A) was subjected to clonogenic survival experiments. The survival of WT or RCC2 KO cells was not significantly affected by partial NEIL3 deletion when responding to MMC-induced ICLs (Figure 2-15B). However, while partial NEIL3 knockout did not sensitise WT cells to TMP/UVA-induced ICLs, a notable further reduction in cell survival was observed in RCC2-deficient cells (Figure 2-15C). Prior research (N. Li et al., 2020) has shown that NEIL3 is the preferred mechanism for repairing AA- and psoralen-induced ICLs; hence its limited function in the repair of MMC-induced ICLs is not surprising. Regarding TMP/UVA-induced ICLs, the clonogenic result suggests an assumption that such lesions can be repaired through either NEIL3 or an RCC2-associated mechanism, and the two pathways may function redundantly. When RCC2 functions

effectively, partial loss of NEIL3 is compensated by the RCC2-associated mechanism, and thus the NEIL3$^{+/-}$ cells exhibit a similar survival rate to WT cells. However, when RCC2 is deficient and its associated mechanism is eliminated, further NEIL3 knockdown notably decreases cell survival as the ICL repair now becomes more dependent on the alternative NEIL3 pathway. Notably, single RCC2 knockout sensitises cells to TMP/UVA-induced ICLs even when the NEIL3 is efficient, indicating that part of the psoralen-induced ICLs can only be fixed with the presence of the RCC2 involving mechanism. Overall, the clonogenic survival experiment suggests that RCC2 and NEIL3 are not epistatic when repairing psoralen-induced ICLs. Further experiments employing NEIL3 full knockout cells are needed to validate the data.



C.

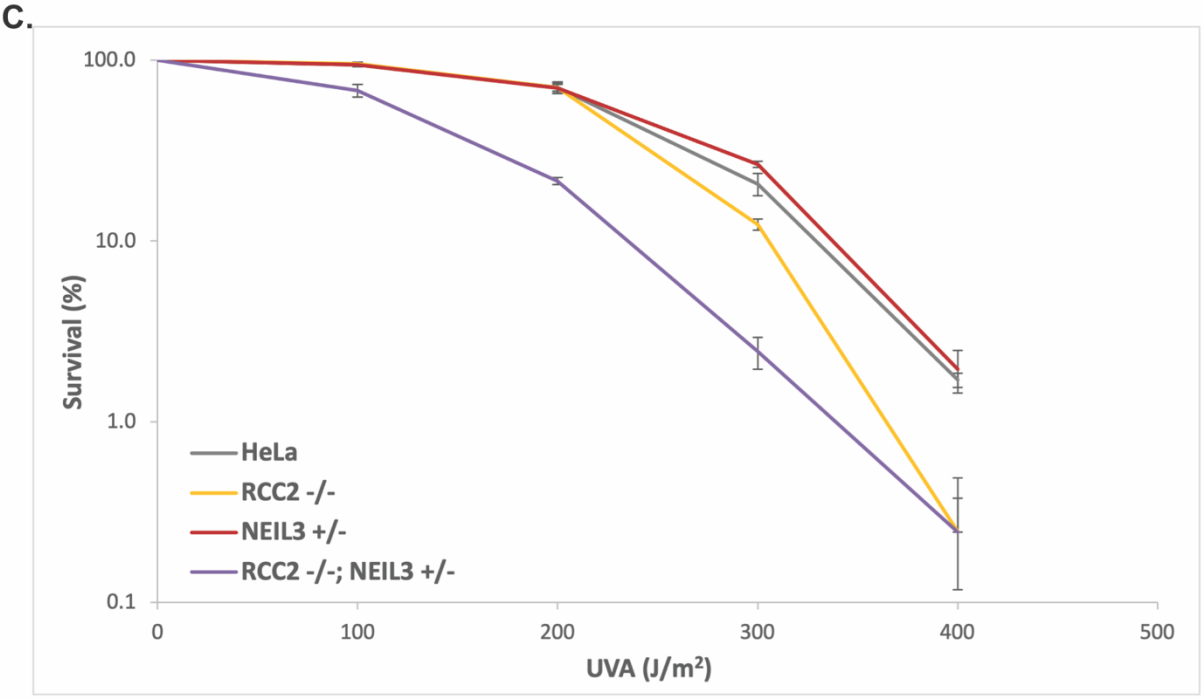


Figure 2-15. RCC2 is not associated with the NEIL3 pathway.
A) Western Blot showing the complete RCC2 knockout and (or) the partial NEIL3 knockout cells used in the clonogenic survival assay by using anti-NEIL3, anti-RCC2 and anti-α-Tubulin antibodies.
B) Clonogenic survival assay was performed using the indicated cell lines. Cells were grown for two weeks in the medium containing 0, 0.5, 1, 2, 4 or 8 ng/ml MMC. The number of colonies formed was then counted (mean ± SEM, n = 3 technical replicates, the experiment was performed once). **C)** Clonogenic survival assay was performed using the indicated cell lines. Cells were treated with 100ng/ml TMP, incubated for 30 minutes, and subsequently irradiated with 0, 100, 200, 300, 400 or 500 J/m^2 UVA. The number of colonies formed was counted two weeks afterwards (mean ± SEM, n = 3 technical replicates, the experiment was performed once). Y values are shown in the logarithmic scale.

2.3 Discussion

In dividing cells, ICLs are primarily repaired through three signalling pathways: the FA pathway, the NEIL3 pathway, and the newly identified mechanism for repairing acetaldehyde-induced ICLs (Semlow & Walter, 2021). The FA pathway is associated with 22 FA genes, and mutations in these genes lead to the genetic disorder Fanconi anaemia (Sakai & Sugasawa, 2019). Despite the reported FA genes, certain FA patients lack genetic mutations related to ICL repair pathways, indicating the presence of unidentified repair factors. Through a previous purification screening (Figure 2-2), RCC2 was identified as a potential novel participant in ICL repair, showing a preference for binding to crosslinked DNAs compared to non-crosslinked DNAs. Its rapid accumulation at TMP/UVA-induced ICLs within five minutes post-treatment in live cells further supports its role as an early responder in the resolution of such DNA damage (Figure 2-3).

Genetic deletion of RCC2 verifies its engagement in the cellular response to ICLs, as demonstrated by the decreased survival rate of RCC2 deficient cells treated with MMC and TMP/UVA. Restored cell viability by re-expressing EGFP-tagged RCC2 in knockout cells provides additional support for its function (Figure 2-5 and 2-6). Admittedly, the restoration of cell survival by exogenous EGFP-RCC2 did not reach the level observed in WT cells in some experiments (such as in Figure 2-5A and 2-6B). This is likely due to the potential adverse effect of the EGFP tag on the function of RCC2 protein or the irreversible damage to the cells' vitality during long-term culture at an exceptionally low cell concentration when producing single clones. Still, comparing the EGFP-RCC2 complemented cells to the knockout cells revealed an apparent increase in cell viability, confirming that the enhanced sensitivity to ICL-inducing drugs observed in RCC2-deficient cells was caused by the absence of RCC2 protein rather than off-target effects or variation between individual clones.

In the EMSA experiments, purified recombinant RCC2 from Sf9 insect cells did not bind to crosslinked or non-crosslinked DNA probes (Figure 2-7B and C). This result contradicts the earlier screening in which RCC2 bound preferentially to ICL-containing DNAs, possibly due to the following reasons:

1. The initial screening was conducted in HeLa S3 cells, while the protein used in the EMSA was derived from Sf9 insect cells. It is presumable that the post-translational modifications of the RCC2 protein vary between human and insect cells, potentially resulting in a

compromised DNA-binding capacity of the recombinant RCC2 from Sf9 cells in comparison to its human equivalent. Additionally, RCC2 may undergo transient PTMs or structural alterations in response to ICLs, facilitating its interaction with crosslinked DNA. In fact, the HeLa S3 cells employed in the purification screening were pre-treated with TMP/UVA prior to nuclear protein extraction, allowing potential ICL-induced modifications of RCC2 to occur. Nevertheless, the recombinant RCC2 used in the EMSA was obtained from unchallenged insect cells, which may have lacked any changes following ICL induction.

2. During the screening process, DNA probes were incubated with a soluble nuclear extract that contained a variety of nuclear proteins. It is possible that some of these proteins may function as partners that facilitate RCC2's DNA-binding abilities. In the EMSA, however, the DNA probes were incubated with pure recombinant RCC2 protein.
3. A Flag-HA tag was fused to the N-terminus of RCC2 to purify the recombinant protein for use in the EMSA. The presence of this fusion tag may have affected the protein's nucleic acid binding activity, potentially leading to differences compared to the endogenous protein that was pulled down by the biotin-labelled DNA probes during the screening process.

In conclusion, there are currently no indications of direct interaction between ICLs and RCC2 protein. However, because of the reasons listed, we cannot rule out the potential that RCC2 directly recognises and physically interacts with ICLs in human cells.

To discover the molecular mechanism behind RCC2's role in the cellular response to ICLs, the link between RCC2 and the two established ICL repair routes – the FA and NEIL3 pathways - was investigated. The finding that RCC2 deletion has no effect on FANCD2 recruitment or monoubiquitination suggests that RCC2 works either outside of the FA pathway or downstream of the ubiquitination of the FANCD2/FANCI dimer at ICLs (Figure 2-8 and 2-9). However, the recruitment of RCC2 to ICLs (within 5 minutes post-treatment, Figure 2-3) was faster than that of FANCD2 (around 15 minutes post-treatment, Figure 2-8), making the latter scenario less likely. A further clonogenic survival assay comparing cell survival between RCC2/FANCD2 double knockout with the two single knockouts supports the theory that RCC2 functions via a mechanism other than the FA pathway, as dual knockout results in a greater sensitivity to ICL-inducing drugs than single knockouts (Figure 2-10B and C).

Several methodological hurdles hindered research into RCC2's relationship to the NEIL3 pathway. First, exogenously expressed NEIL3-EGFP was not recruited to TMP/UVA-induced

ICLs in nuclear regions where Halo-tagged FANCD2 indicated effective induction of ICLs (Figure 2-12). This contradicts the previous study showing that EGFP-tagged NEIL3 accumulated at ICLs within one minute of TMP/UVA treatment (N. Li et al., 2020). The cell type specificity of NEIL3's response to ICLs was ruled out by expressing and visualising EGFP-tagged NEIL3 in U2OS cells (Figure 2-13). Similarly, no visible foci formation of NEIL3-EGFP was observed following TMP plus a pan-treatment of UVA at 365nm (Figure 2-14). It is currently uncertain whether the absence of NEIL3-EGFP's accumulation in ICL-containing areas was attributable to the wavelength of the laser (405nm) employed in our live-cell imaging. Additional testing using a microscope equipped with 365nm UVA is necessary for examining the recruitment of NEIL3. After successfully detecting NEIL3's translocation to ICLs, RCC2 may be depleted from NEIL3-EGFP expressing cells to determine whether NEIL3's distribution is reliant on the presence of RCC2.

Depleting the NEIL3 protein is another technical challenge when investigating the association between RCC2 and the NEIL3 pathway. CRISPR-Cas9 with four KO guide RNAs and protein knockdown using two shRNAs could not fully deplete NEIL3 from HeLa or U2OS cells. Partial NEIL3 knockout clones were therefore utilised in clonogenic survival assays to determine the difference between NEIL3/RCC2 double knockout and single knockouts. The inclusion of NEIL3 partial knockout cells introduces inherent challenges in the interpretation of the clonogenic data. Firstly, determining the functional activity of the remaining NEIL3 protein becomes challenging, as its presence can potentially mask the phenotypic consequences of protein loss. Secondly, there may be variations in the degree of NEIL3 depletion between NEIL3 partial knockout and RCC2/NEIL3 double knockout cells, leading to less precise comparisons. Nevertheless, when subjected to TMP/UVA-induced ICLs, a significant difference between RCC2/NEIL3 double knockout and single knockouts was detected. Reduced NEIL3 level has a detrimental effect on cell survival only in the absence of RCC2 (Figure 2-15C). This shows that the RCC2-associated mechanism and the NEIL3 pathway operate independently and that the two pathways might be redundant in response to psoralen-induced ICLs. However, further validation of this hypothesis necessitates the use of cells with complete NEIL3 knockout.

Based on the current data indicating that RCC2 functions independently of both the FA and NEIL3 pathways, it is plausible that RCC2 participates in a novel mechanism that is distinct from established ICL repair pathways. This mechanism may be involved in addressing both

MMC- and psoralen-induced ICLs. To further understand the underlying mechanism of RCC2, two potential approaches can be considered: Firstly, previous research has identified RCC2 as the guanine nucleotide exchange factor (GEF) for the small GTPase RALA, which has been implicated in DNA damage repair. It would be valuable to investigate the relationship between RALA and ICL repair, as well as to explore whether RALA's function in DDR is dependent on RCC2. Secondly, the identification of functional partners of RCC2 in the cellular response to ICLs can be achieved through the purification of putative RCC2 complex(es) from ICL-containing cells. The characterisation of these functional partners will provide valuable insights into the mechanism of RCC2.

Chapter 3. Exploring the Involvement of Zinc Finger Protein 638 (ZFN638) in DNA Damage Response

3.1 Introduction

ZNF638, also known as NP220, is a large nuclear protein with a molecular weight of 220 kDa that contains 1978 amino acids. ZNF638 has a DNA binding domain and binds to double-stranded DNA fragments by recognising clusters of cytidines. In close proximity to the DNA-binding domain are nine copies of the sequence LVTVDEVIEEEDL (acidic repeat), which contain numerous amino acids with metal-interacting oxygen atoms. In addition, ZNF638 possesses RNA recognition motifs (RRMs) and an arginine/serine-rich (RS) domain that are frequently observed in pre-mRNA splicing factors (Inagaki et al., 1996). The RS domains are prevalent in many spliceosome-involved non-snRNP proteins, while the RRMs of ZNF638 resemble hnRNPs I and L, the heterogeneous nuclear ribonucleoproteins (hnRNPs) that condense and package growing RNA transcripts (Ghetti et al., 1992; Krainer et al., 1991; Neugebauer et al., 1995; Zamore et al., 1992). ZNF638 also comprises C2H2 zinc finger (ZF) motifs, which are common in transcription factors (Figure 3-1 Domain structure of ZNF638) (Matsushima et al., 1996).

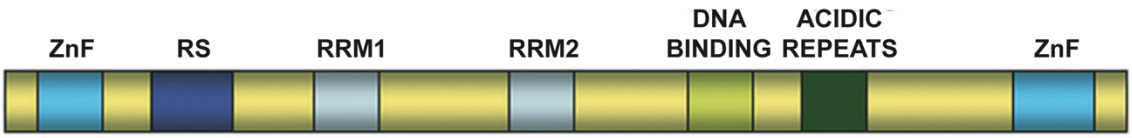


Figure 3-1. Domain organisation schema for the zinc finger protein ZNF638.
The ZNF638 protein is composed of two zinc finger domains (ZNF), a domain rich in arginine and serine (RS), two RNA recognition motifs (RRMs), a domain required for DNA binding, and a domain in which sequences with a consensus of LVTVDEVIEEEDL repeat nine times (Acidic repeats). The schematic is adapted from *Meruvu et al., 2011*.

Transcription factors are the primary regulators of gene transcription. The group of genes featuring C2H2 zinc fingers as DNA-binding motifs is the most prominent family of transcription factors in eukaryotes (Tupler et al., 2001). The C2H2 zinc finger motif consists of two cysteine and two histidine residues that form a four-coordinate bond with a single zinc ion. As a protein with C2H2 zinc finger domains, ZNF638 functions as a transcription cofactor for CCAAT/enhancer-binding proteins (C/EBPs) to regulate adipogenesis, the process of transforming undifferentiated mesenchymal cells into adipocytes capable of lipid storage and adipokine secretion. During early adipogenesis, ZNF638 physically interacts and transcriptionally cooperates with C/EBP β and C/EBP δ on the peroxisome proliferator-

activated receptor (PPAR) γ promoter. This interaction leads to the expression of PPAR γ, which is the key regulator of adipocyte differentiation (Meruvu et al., 2011).

Arginine/serine-rich (RS) proteins represent a substantial subclass of splicing regulators. The amino terminus of these proteins contains RRMs, whereas the carboxy terminus has RS repeats (Bourgeois et al., 2004). The presence of two RRMs and an RS domain in ZNF638 suggests a potential function in RNA processing. Indeed, biochemical purification of proteins that interact with ZNF638 in adipocytes and mass spectrometry found 172 unique ZNF638 interactors, from which 38% were known to be involved in constitutive or alternative splicing, present in interchromatin granule clusters or a part of early or late spliceosomal complexes (Du et al., 2014). Splicing factors are stored and modified in specialised structures called nuclear speckles (or splicing speckles). The same study reveals that ZNF638 localises in nuclear speckles via its RS and the C-terminal Zinc finger domain and regulates adipocyte differentiation (Du et al., 2014).

In addition to its function in adipogenesis, ZNF638 was discovered, through a genome-wide CRISPR-Cas9 screen, to be essential for the silencing of unintegrated murine leukemia virus (MLV) genomes in human cells (Zhu et al., 2018). As the major DNA-binding component, ZNF638 binds to cytidine clusters in unintegrated MLV DNA and recruits the human silencing hub (HUSH) complex, which consists of MPP8, PPHLN1, and TASOR. Histone-modifying enzymes, such as histone deacetylase (HDAC1/4) and histone methyltransferase (SETDB1), are subsequently recruited by the ZNF638-HUSH complex, resulting in the removal of acetyl marks and the insertion of repressive methyl marks, respectively. The expression of MLV DNA is eventually silenced by these histone modifications. Similarly, ZNF638 and the HUSH complex regulate the transcriptional silencing of single-stranded and self-complementary recombinant adeno-associated virus (rAAV) genomes (Das et al., 2022). In the absence of NP220-HUSH repressor complex components, the transcription of AAV genomes is increased due to the lack of H3K9 methylation, thus increasing transgene expression. Thus, ZNF638 functions in silencing both retroviruses that integrate into the host genome and recombinant AAV genomes that persist as episomes (Figure 3-2).

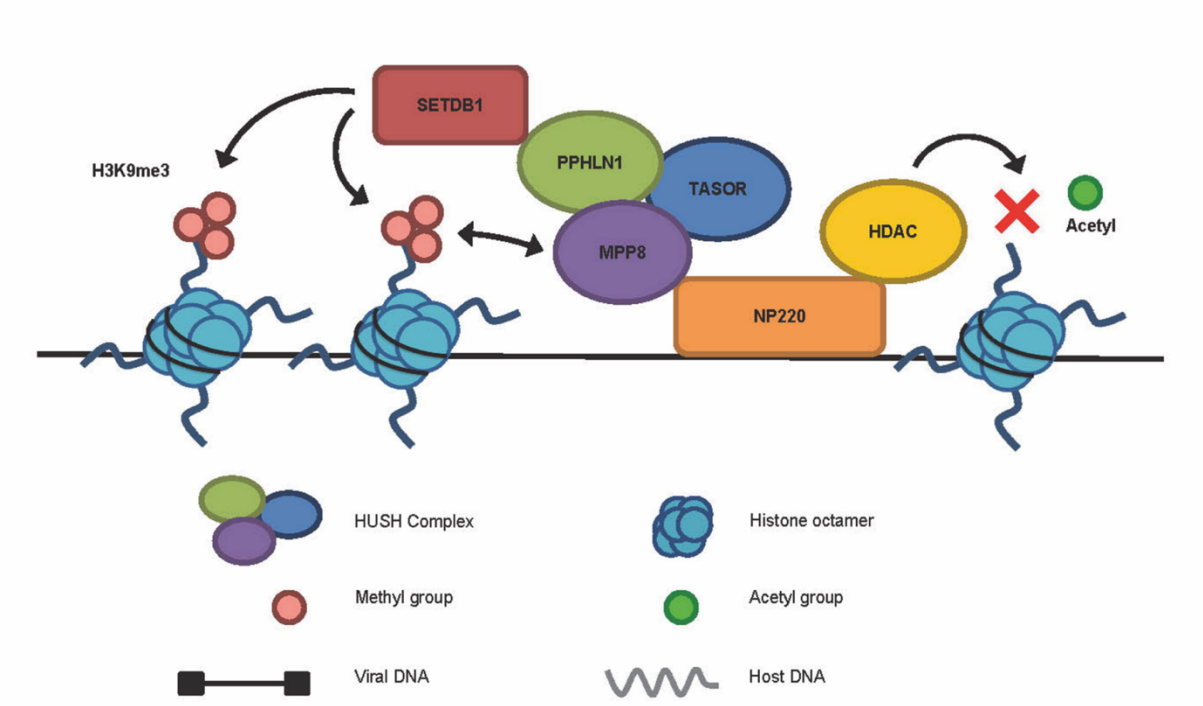


Figure 3-2. The transcriptional silencing of the unintegrated viral genome by ZNF638.
ZNF638 (NP220) attaches to the unintegrated viral DNA and draws in the HUSH complex (consisting of MPP8, TASOR and PPHLN1). The ZNF638-HUSH complex subsequently recruits the histone deacetylase HDAC and the histone methyltransferase SETDB1. HDAC removes the activation marks of histone acetylation, whereas SETDB1 inserts the repressive H3K9me3 marks, hence inhibiting viral gene expression. The schematic is adapted from *Zhu et al., 2018*.

Within its upstream regulatory region, the *ZNF638* gene has two putative cAMP response elements, which are activated by the transcription factor cAMP response element binding protein (CREB) (Ni et al., 2020; Perie et al., 2019). During cold exposure, CREB regulates the rise in ZNF638 mRNA levels in thermogenic adipocytes to induce heat production via binding to the cAMP response element regions of ZNF638 (Perie et al., 2019). Besides, USP7, a deubiquitinase, exerts regulating effect on ZNF638 in hepatic *de novo* lipogenesis (DNL) through CREB (Ni et al., 2020). In hepatocytes, USP7 deubiquitinates and stabilises ZNF638 at the protein level and simultaneously stimulates ZNF638 transcription by preserving its transcription factor CREB. The USP7 and ZNF638 proteins then increase the nuclear accumulation of cleaved-SREBP1C, allowing the activation of lipogenesis-associated enzymes.

More research shows that ZNF638 has a diverse set of physiological roles. Human height is a complicated genetic characteristic involving numerous loci, with heritability estimates of more than 80%, and ZNF638 has a strong relation with height (Hao et al., 2013; Lin et al., 2017).

Also, ZNF638 plays a potential role in heart muscle development and the maintenance of the heart phenotype by directly interacting with heart-specific FHL2 (four-and-a-half LIM-only protein 2) via its C-terminal regions (Ng et al., 2002). Moreover, ZNF638 may play a role in the pathophysiology of primary open-angle glaucoma, one of the leading causes of blindness globally (Gharahkhani et al., 2021). Last, ZNF638 aids in the identification and treatment of cancer. Autoantibodies to ZNF638 were found in 10-20% of colorectal cancer patients but only 0-5.7% of controls. Thus, ZNF638 is a possible capture antigen for the early diagnosis of colorectal cancer (O'Reilly et al., 2015; Roney et al., 2021). Ridaifen-G is a tamoxifen analogue with a potent growth inhibitory effect against a variety of cancer cell lines, and its growth inhibitory and cytotoxicity effect is achieved through regulating ZNF638 activities (Ikeda et al., 2015).

As described in Chapter 2, our team used a purification strategy to uncover new factors relating to ICL response, and ZNF638 is another protein candidate identified (Figure 2-2B). ZNF638 demonstrated 9.89 times more robust binding to linear crosslinked DNA probes than non-crosslinked counterparts in the screening. Although ZNF638 has a broad range of functions as described above, it has never been linked to DNA damage repair or response. This chapter discusses my research on ZNF638, which aimed to investigate the behaviour of the protein in response to DNA damage as well as its physiological functions in the process.

3.2 Results

3.2.1 ZNF638 re-localises to nucleoli upon ICL formation

As a zinc finger protein with a DNA-binding domain, ZNF638 is a feasible sensor that recognises and binds to ICL-containing DNAs. To analyse the behaviour of ZNF638 in response to ICLs, I began by affixing an N-terminal fluorescent tag to the ZNF638 protein to examine its distribution vis live-cell microscopy. Despite efforts to introduce exogenous EGFP-ZNF638 protein into HeLa cells using retroviral transduction, successful expression was not achieved. This failure could be attributed to the length of the inserted gene (14kb) exceeding the optimal integration size (typically 8-10kb), or ZNF638's function in silencing the unintegrated retroviral DNA as aforementioned (Zhu et al., 2018). Thus, via CRISPR-Cas9 knock-in, a Halo tag was instead added to the N-terminus of ZNF638 (Figure 3-3A). Meanwhile, exogenous EGFP-FANCD2 was co-expressed with Halo-ZNF638 as a positive control (Figure 3-3B) to demonstrate effective induction of ICLs in the following live-cell imaging.

Similar to our prior findings, thirty minutes after TMP-UVA treatment, FANCD2 evidently accumulated in areas bearing ICLs. ZNF638, however, did not migrate to the damaged regions as FANCD2 or RCC2 (as described in the preceding chapter). Instead, Halo-tagged ZNF638 moved away from the damaged area and re-localised to nucleoli. The nucleolar re-localisation of ZNF638 was initiated 30 minutes after treatment and accumulated over time to form ring-shaped structures at the periphery of nucleoli (Figure 3-4). This translocation of ZNF638 was triggered explicitly by ICL formation since UVA irradiation alone did not generate a discernible change in the ZNF638 nuclear localisation (Figure 3-5A). Also, Hela WT cells treated with TMP/UVA and then incubated with the JF549 Halo ligand exhibited a dim fluorescent background, confirming that the observed nucleolar accumulating pattern in the Halo-ZNF638 expressing cells represents the distribution of tagged ZNF638 rather than a non-specific accumulation of JF549 Halo-ligands upon ICL formation (Figure 3-5B). The observed nucleolar peripheral accumulation of ZNF638 (Figure 3-4C) closely resembles the nucleolar deposition pattern of the PTB-associated splicing factor (PSF), which has been shown to translocate to the nucleolar cap during transcriptional arrest (Shav-Tal et al., 2005). Thus, it is reasonable to infer that ZNF638 translocates and accumulates in the nucleolar cap in response to ICLs.

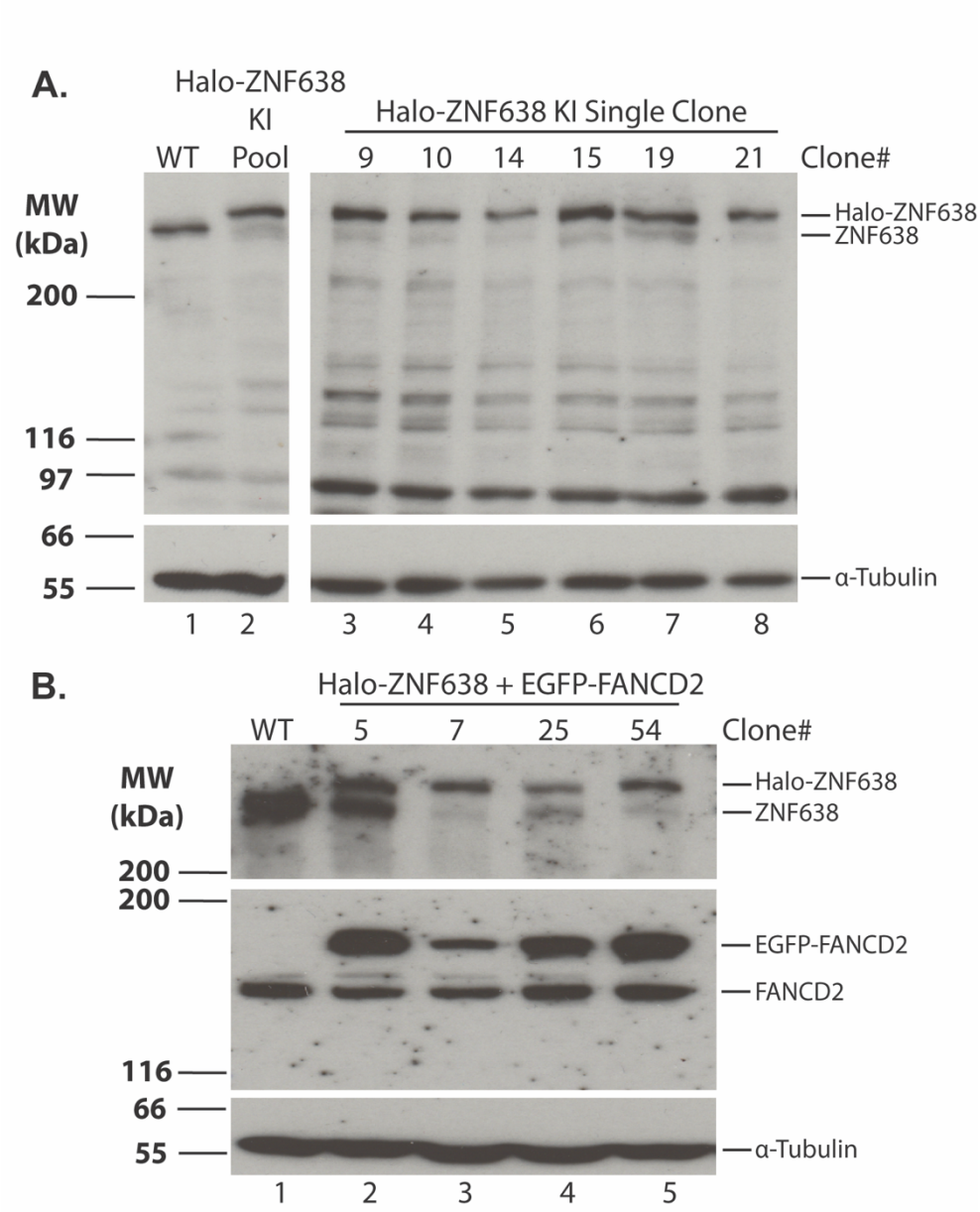


Figure 3-3. Generation of HeLa cells co-expressing Halo-ZNF638 and EGFP-FANCD2.
A) Western blot using anti-ZNF638 and anti-α-Tubulin antibodies that shows the establishment of the Halo-ZNF638 knock-in cell line. Halo Tag was knocked into the N-terminus of the ZNF638 protein using the CRISPR-Cas9 system.
B) Western blot using anti-ZNF638, anti-FANCD2 and anti-α-Tubulin antibodies showing that the EGFP-FANCD2 was co-expressed in the Halo-ZNF638 knock-in cells via retrovirus-mediated transfection. The single clone (C7, lane 3) exhibiting a high level of tagged/endogenous ZNF638 protein ratio was used in the subsequent live-cell imaging.

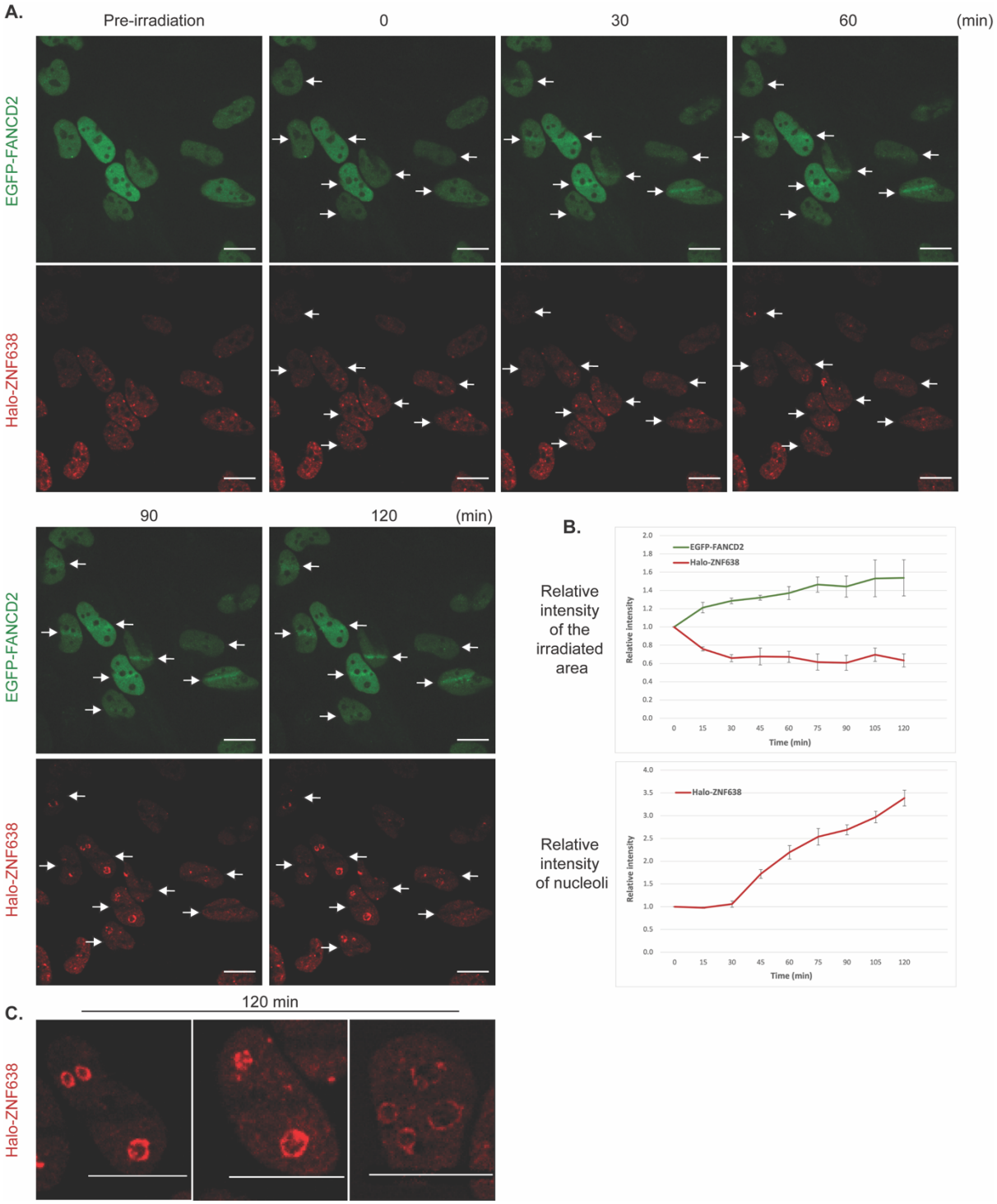


Figure 3-4. ZNF638 re-localises to nucleoli upon ICL formation.
A) Live-cell imaging performed with HeLa cells co-expressing EGFP-FANCD2 and Halo-ZNF638. 100nM JF549 HaloTag Ligand was used to label the Halo-ZNF638 protein. ICLs were then generated by 30 minutes of TMP treatment at 20µg/ml, followed by laser irradiation at 405nm in defined nuclear areas (indicated by the white arrows). EGFP-FANCD2 serves as a positive control to show ICL-containing regions. The distribution of Halo-ZNF638/EGFP-FANCD2 was monitored for 120 minutes post-treatment. **B)** The relative changes in fluorescence intensity in the irradiated and nucleolar areas were quantified as mean ± SEM at the specified time points (n=5 nuclei for the irradiated area and n=6 nucleoli for nucleolar areas from a representative experiment, the experiment was performed three times). **C)** Representative cells displaying Halo-ZNF638 nucleolar accumulation from the live-cell imaging (A) 120 minutes post-treatment. The localisation pattern of ZNF638 at the periphery of nucleoli was observed, suggesting its translocation to the nucleolar cap. Scale bar = 10µm.

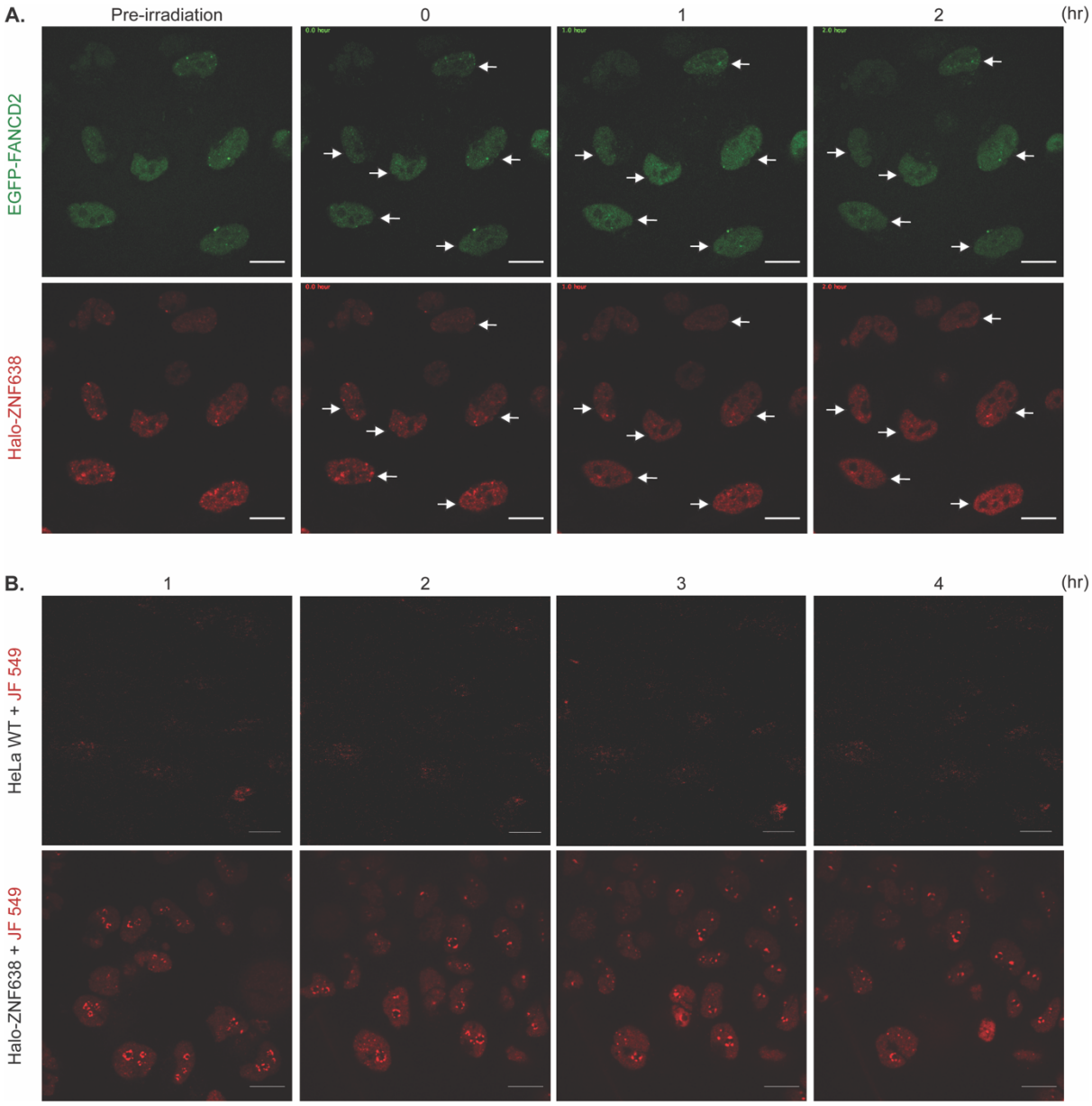


Figure 3-5. The translocation of ZNF638 is specifically triggered by ICLs.
A) Live-cell imaging performed with HeLa cells co-expressing EGFP-FANCD2 and Halo-ZNF638. Cells were incubated with 100nM JF549 for 20 minutes and then micro-irradiated with 405nm laser, without TMP treatment, at specific nuclear areas indicated by the white arrows. The distribution of Halo-ZNF638/EGFP-FANCD2 was monitored for two hours post-treatment.
B) Live cell imaging performed with HeLa WT and Halo-ZNF638 expressing cells. Cells were first incubated with 100nM JF549 for 20 minutes. ICLs were then generated by 30 minutes of TMP treatment at 20μg/ml, followed by a 1000J/m^2 365nm UVA pan-treatment. Cell images were collected for four hours post-treatment. Scale bar = 10μm.

3.2.2 The presence of ICL diminishes the interaction between ZNF638 and DNA *in vitro*

Recombinant Flag-HA tagged ZNF638 was expressed and purified from Sf9 insect cells (Figure 3-6A), and its binding capability to four types of DNA probe (non-crosslinked / crosslinked linear DNAs and non-crosslinked / crosslinked fork-mimic DNAs) was evaluated using EMSA. Since the ZNF638 protein contains a DNA-binding domain and two zinc finger domains, it is not surprising that it interacts physically with all four DNA probes. Intriguingly, the *in vitro* experiment reveals that ZNF638 prefers binding to non-crosslinked DNAs over crosslinked DNAs for both linear and fork-mimicking probes (Figure 3-6B and C). The EMSA results align with the previous live-cell imaging data (Figure 3-4), which shows that ZNF638 moves away from the TMP/UVA-induced ICLs (irradiated regions). This suggests that the presence of psoralen-induced ICLs between DNA double helices impedes the physical interaction between ZNF638 and crosslinked DNA.

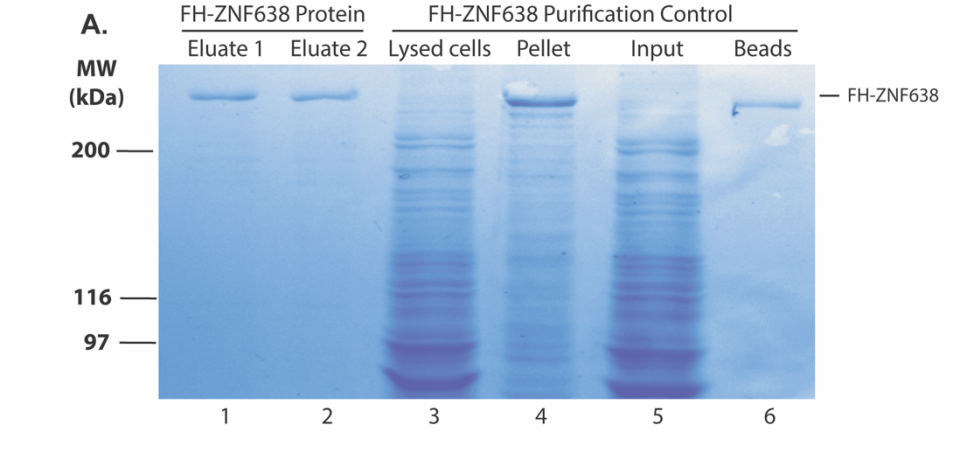


Figure 3-6. ZNF638 shows binding preference to the non-crosslinked DNA probes *in vitro*.
A) The purified FH-ZNF638 protein from Sf9 insect cells is shown on a Coomassie blue gel. The ZNF638 gene was cloned into a pFastBac vector with an N-terminal Flag-HA (FH) tag. Recombinant FH-ZNF638 protein was then expressed in the Sf9 cells and purified using the M2 anti-FLAG agarose resin. The FH-ZNF638 protein was enriched in the final Flag eluates (lanes 1 and 2).

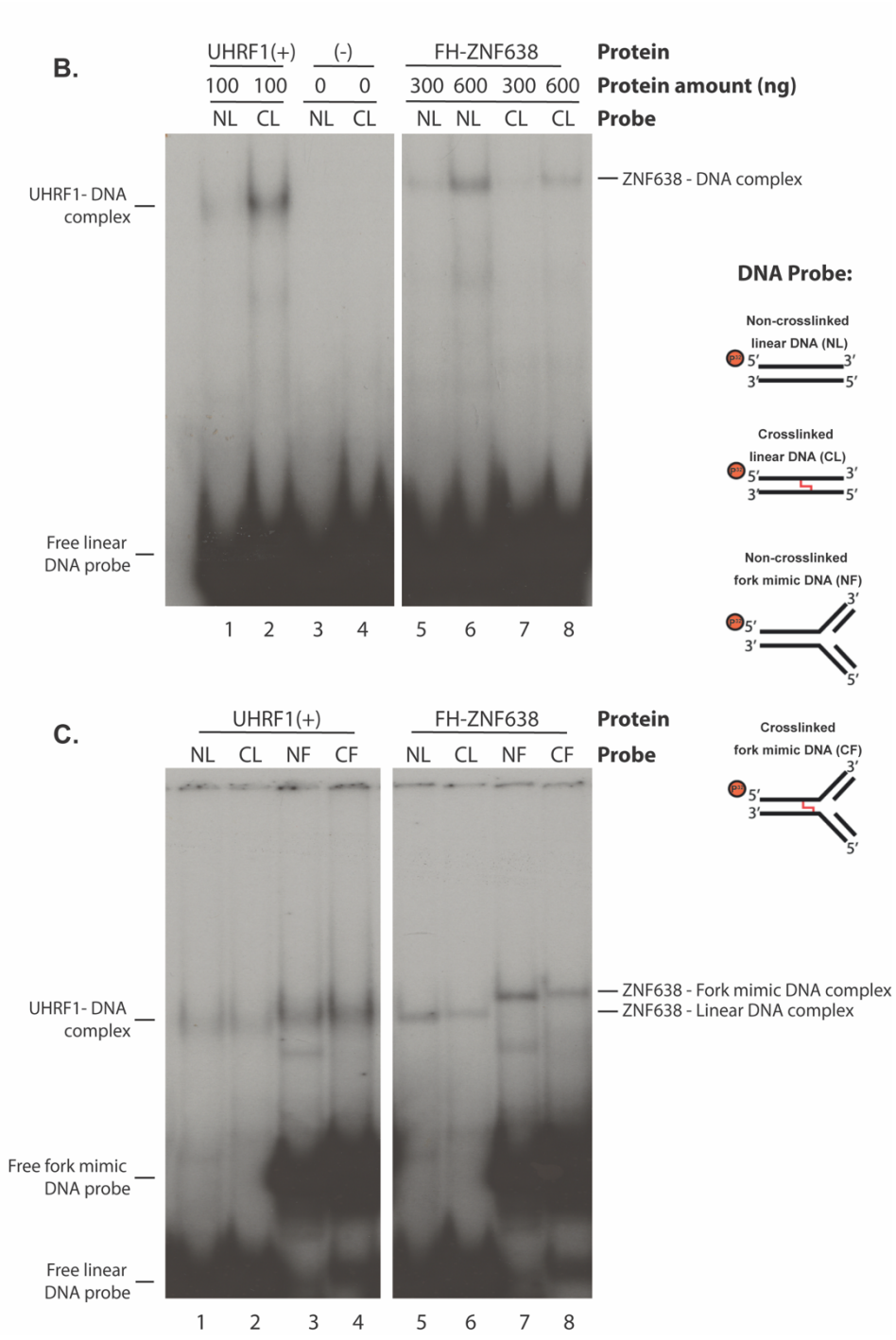


Figure 3-6. ZNF638 shows binding preference to the non-crosslinked DNA probes *in vitro*.
B) EMSA demonstrating the DNA binding affinity of FH-ZNF638 for radiolabelled non-crosslinked (lanes 5 and 6) and crosslinked (lanes 7 and 8) linear DNA probes. The UHFR1 protein is established to bind DNAs and thus is utilised as a positive control (lanes 1 and 2). The negative controls are samples containing DNA probes and reaction buffers but devoid of proteins (lanes 3 and 4).
C) EMSA showing the DNA binding affinity of FH-ZNF638 to both linear (lanes 5 and 6) and fork-mimic (lanes 7 and 8) probes. UHFR1 protein was included as a positive control (lanes 1-4). 100ng of UHFR1 protein or 500ng of ZNF638 protein was used in each EMSA reaction.
The schematic images demonstrate four ^{32}P radiolabelled DNA probes used in the EMSA. The presence of a TMP/UVA-induced ICL in crosslinked probes is indicated in red.

3.2.3 The nucleolar re-localisation of ZNF638 is a general response to genetic instabilities

Further tests reveal that, aside from TMP/UVA treatment, ZNF638's nucleolar accumulation occurs in response to MMC and cisplatin-induced ICLs in a dose-dependent manner (Figure 3-7). The observation that the redistribution of ZNF638 occurs only at a relatively high dose of treatment suggests that this response is activated when genomic damage surpasses a specific threshold. This threshold may signify the initiation of cell death or the maximum defensive capacity of redundant or alternative mechanisms.

Except for ICLs, evident ring-shaped nucleolar accumulation of Halo-ZNF638 was found in cells with single-strand breaks and secondary double-strand breaks caused by Camptothecin (CPT) and in cells with UVB-induced intrastrand crosslinks (Figure 3-8A, left and middle images). Generally, DNA damage can interfere with the transcription machinery, leading to a decrease or cessation of RNA synthesis. To determine whether the transcription inhibition invokes the ZNF638 response, Halo-tagged ZNF638 was monitored in live cells treated with a general transcription inhibitor - Actinomycin D (Act D). Indeed, Act D induces similar ZNF638 nucleolar re-localisation *in vivo* (Figure 3-8A, right image). Next, whether ZNF638 responds to cellular stresses other than genomic instabilities was examined. It turns out that the translocation of ZNF638 to nucleoli did not occur in response to nutrient deficiency, heat shock, or cold shock (Figure 3-8B). Hence, my experiments demonstrate that the nucleolar accumulation of ZNF638 appears to be a specific response to genotoxic instabilities across all tested cellular stressors.

During heat shock, ZNF638 demonstrates a distinct relocation to nuclear speckles, adopting a dotted accumulation pattern (Figure 3-8B middle image). Prior investigations have revealed that endogenous ZNF638 becomes localised within nuclear speckles in differentiating adipocytes, primarily through its RS domain (Meruvu et al., 2011). The pattern of nuclear speckle deposition observed in HeLa cells following heat shock aligns with these findings. As a putative transcription factor, ZNF638 may play a functional role in regulating the expression of specific heat shock genes, with its accumulation in speckles positioning it close to these gene loci for potential transcriptional regulation. Alternatively, ZNF638 may translocate to nuclear speckles to engage with chaperone proteins such as Hsp70 and Hsp90, contributing to its own stabilisation and refolding in response to heat-induced stress. However, it is essential to note

that the translocation of ZNF638 to nuclear speckles during heat shock differs from its re-localisation to nucleoli in response to genotoxic stress. As such, this particular aspect was not investigated further within the scope of this thesis.

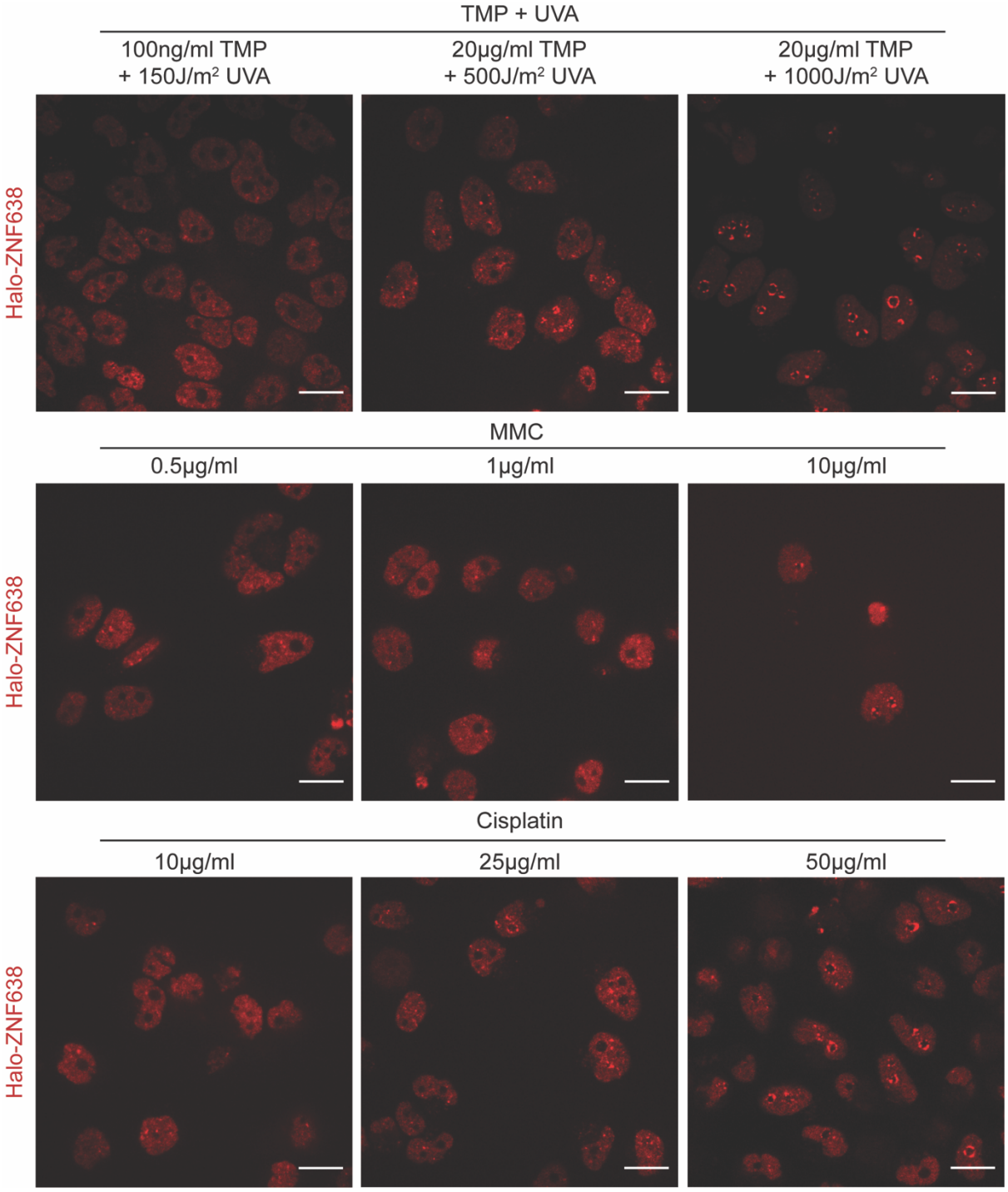


Figure 3-7. ZNF638 reacts to distinct types of ICL in a dose-dependent manner.
Live-cell imaging was performed using HeLa cells expressing Halo-ZNF638. Cells were incubated with 100nM JF549 for 20 minutes to label the Halo-ZNF638 protein. ICLs were induced by 0.5, 1, 10µg/ml MMC; 10, 25, 50µg/ml cisplatin or 0.1, 20µg/ml TMP, followed by 150, 500 or 1000J/m^2 of 365nm UVA pan-treatment. Distribution of Halo-ZNF638 was assessed 1-, 16- or 10-hour post-treatment for TMP/UVA, MMC and cisplatin, respectively. Scale bar = 10µm.

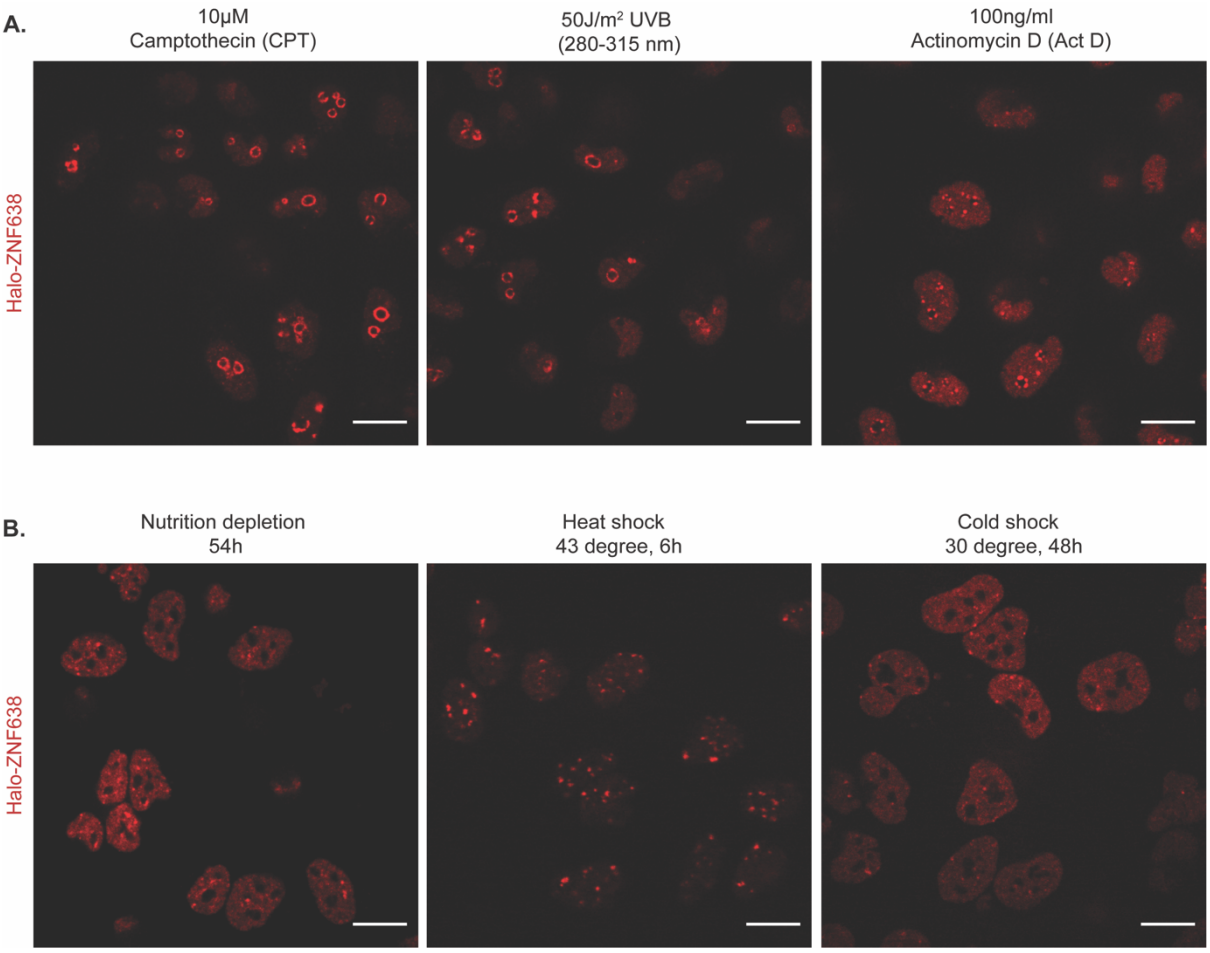


Figure 3-8. ZNF638 reacts to diverse genetic instabilities but not to other cellular stressors. Live-cell imaging was performed with Halo-ZNF638-expressing HeLa cells labelled with JF549. **A)** SSBs/DSBs, intra-strand crosslinks, and general transcription inhibition were produced by treating cells with 10μM CPT, 50J/m^2 UVB, and 100ng/ml Act D, respectively. Images were collected 4, 6, or 9 hours after CPT, UVB or Act D treatment, respectively. **B)** Cells were subjected to nutrient depletion (cultured in FBS-free media), heat shock at 43 Celsius degrees, or cold shock at 30 Celsius degrees for 54, 6 or 48 hours, respectively. Images were captured at the end of treatments. Scale bar = 10μm.

3.2.4 ZNF638 depletion increases HeLa cell sensitivity to DNA damage-inducing reagents

To determine if ZNF638 is physiologically functional when cells are under assaults of DNA damage, ZNF638 full knockout clone was generated (Figure 3-9A). The survival of ZNF638 knockout cells was evaluated in response to MMC, TMP/UVA, CPT, and UVB treatment. Loss of ZNF638 sensitised cells to all four DNA-damaging agents when compared to HeLa WT cells (Figure 3-9B), indicating that ZNF638 plays a functionally relevant role in maintaining cell viability under genomic stresses.

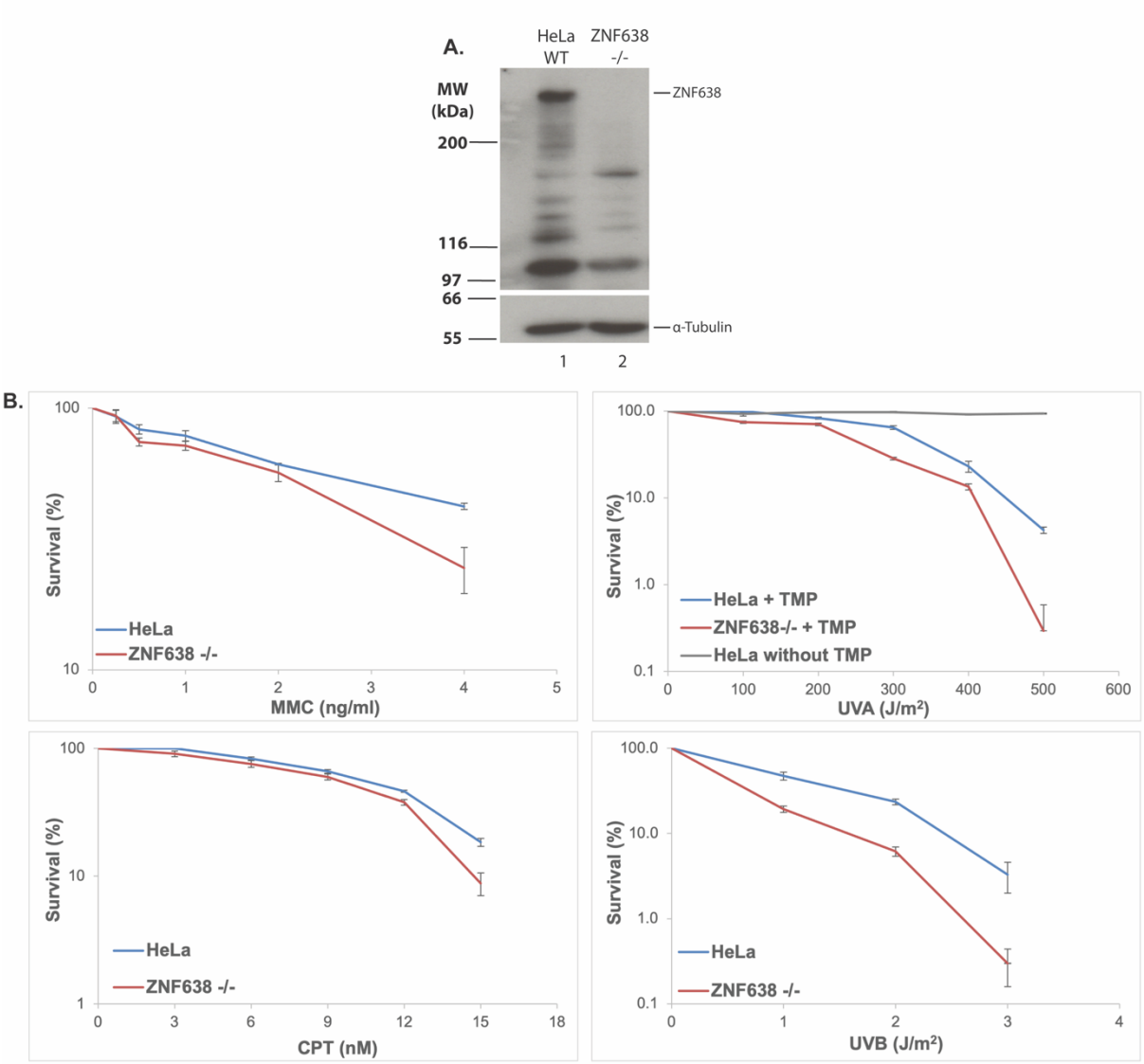


Figure 3-9. ZNF638 depletion increases cell sensitivity to DNA damage-inducing reagents.
A) Western blot using anti-ZNF638 and anti-α-Tubulin antibodies that shows the ZNF638 was knocked out from HeLa cells using the CRISPR-Cas9 system. **B)** ZNF638 knockout cells and HeLa WT controls were treated with indicated doses of MMC, TMP/UVA, CPT or UVB and the colony formation was scored using 1% (w/v) crystal violet in methanol 14 days later. Y values are shown in logarithmic scale, and thus only positive values are presented (mean ± SEM, n = 3 technical replicates from a representative experiment, the experiments were performed twice).

3.2.5 Exploration of factors affecting the ZNF638 nucleolar re-localisation

To explore how ZNF638 nucleolar translocation gets triggered, experiments were carried out to test factors that may affect the initiation of the response. To begin with, the exogenous cell phase marker EGFP-Geminin$_{1\text{-}110}$ was co-expressed in Halo-ZNF638 knock-in cells to evaluate whether the translocation is cell-cycle dependent (Figure 3-10A). One hour after TMP/UVA treatment, ZNF638 nucleolar redistribution was observed in both G1 (EGFP-Geminin$_{1\text{-}110}$ negative) and S/G2 (EGFP-Geminin$_{1\text{-}110}$ positive) phase cells. Nucleoli are interphase nuclear

organelles that disassemble during mitosis; hence no distinct distribution of Halo-ZNF638 was seen in mitotic cells (Figure 3-10B). In this experiment, the cell cycle distribution of 151 cells was analysed one hour after TMP/UVA treatment based on the EGFP-Geminin$_{1-110}$ marker. 50%, 45%, and 5% of the examined cells were in G1, S/G2, and M phases, respectively, indicating a typical cell cycle distribution of HeLa cells (Figure 3-10C). Next, 446 nucleoli from the abovementioned G1 and S/G2 cells were inspected to check if they had developed peripheral ZNF638 deposits. The result demonstrates that ZNF638 migrates to the majority of nucleoli independent of the cell cycle phase, 97% nucleoli in G1 cells and 93% nucleoli in S/G2 cells specifically, when responding to TMP/UVA-induced ICLs (Figure 3-10D). Together, the data indicate that the nucleolar re-localisation of ZNF638 is not cell-cycle dependent.

ZNF638 has been identified as a potential protein substrate of ATR and PARPs in previous proteomics research (Kliza et al., 2021; Matsuoka et al., 2007). These discoveries prompted experiments to test if post-translational modification of ZNF638 by ATR or PARPs is required for its nucleolar translocation in response to DNA damage. Halo-ZNF638 expressing cells were pre-treated for 3 hours with ATR or PARP1/2 inhibitor. Subsequently, the nuclear localisation of ZNF638 was monitored upon ICL formation in the presence of the inhibitor. The TMP/UVA treatment induced comparable nucleolar accumulation of ZNF638 in HeLa cells when ATR or PARP1/2 is inhibited (Figure 3-11A). Furthermore, an experiment was designed to check whether the activation of ZNF638 in the ICL cellular response requires FA pathway signalling. Live-cell imaging shows that the ZNF638 translocation persists following TMP/UVA treatment when the FA pathway is diminished through FANCD2 or FANCI knockdown (Figure 3-11B and C). In conclusion, the translocation of ZNF638 to nucleoli in response to DNA damage is independent of the cell cycle, FA pathway activation, or ZNF638 protein modifications catalysed by ATR/PARPs.

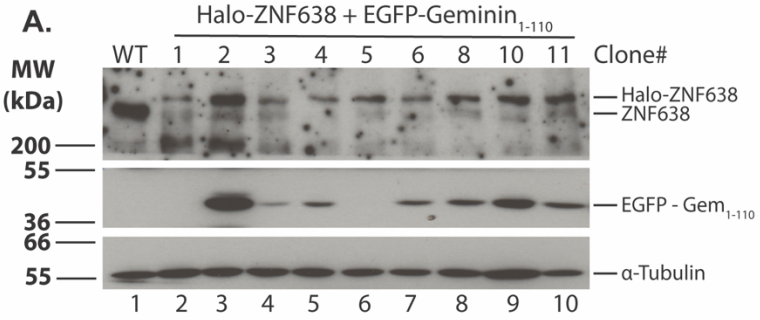


Figure 3-10. Nucleolar re-localisation of ZNF638 is not cell-cycle dependent.
A) Western blot using anti-ZNF638, anti-EGFP and anti-α-Tubulin antibodies showing that the cell phase marker EGFP-Geminin$_{1-110}$ was retrovirally transfected into Halo-ZNF638 knock-in HeLa cells. The single clone (C2, lane 3) expressing a high level of EGFP-Geminin$_{1-110}$, as well as the Halo-tagged ZNF638 closest to the WT level, was used in the following live-cell imaging.

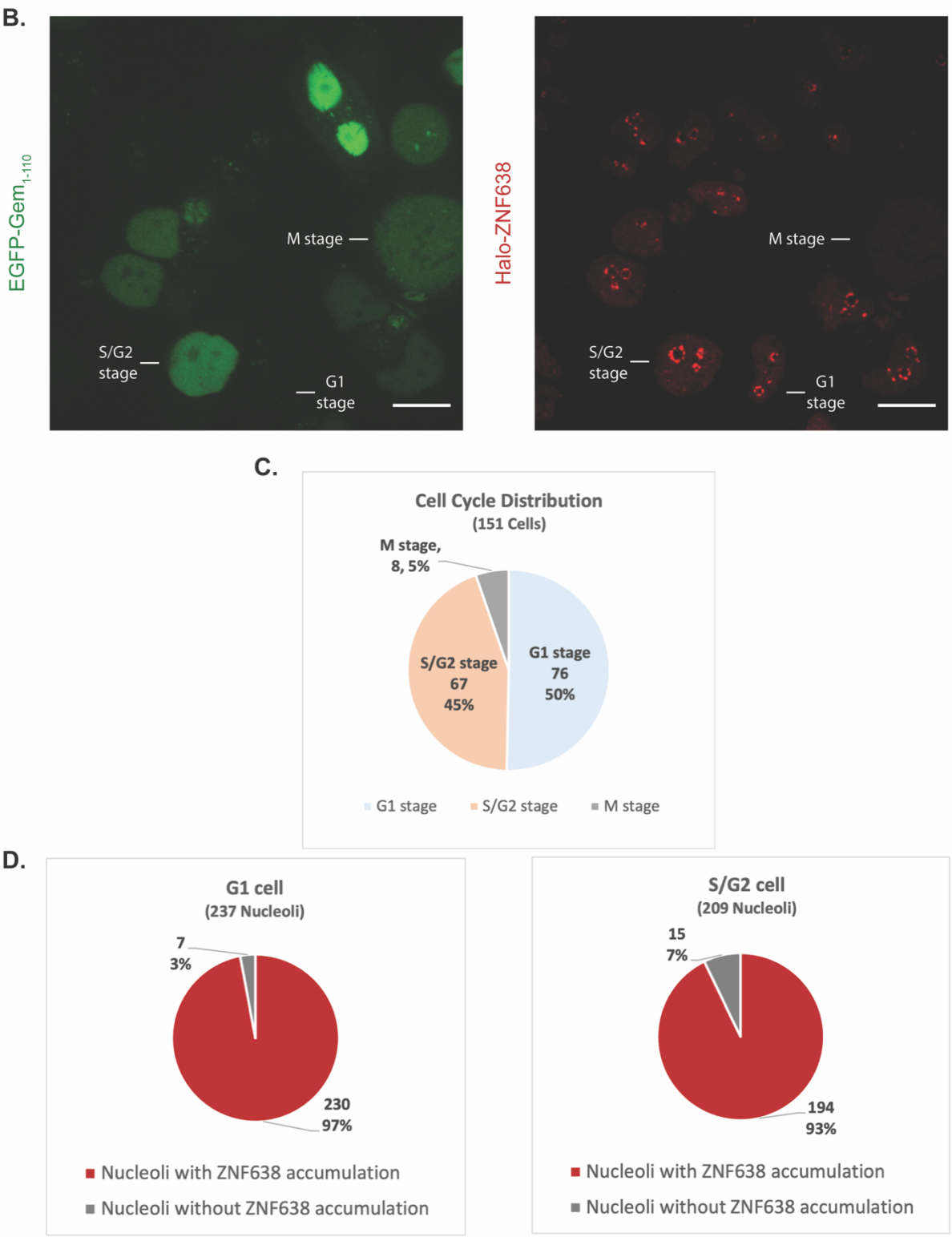


Figure 3-10. Nucleolar re-localisation of ZNF638 is not cell-cycle dependent.
B) Live-cell imaging was performed with HeLa cells co-expressing Halo-ZNF638 and EGFP-Geminin$_{1-110}$. Halo-ZNF638 was labelled for 20 minutes with 100nM JF549 HaloTag ligand. ICLs were then produced by incubating cells with 20µg/ml TMP for 30 minutes, followed by a 1000J/m^2 UVA pan-irradiation at 365nm. One hour after treatment, images of the treated cells were captured. Scale bar = 10µm. **C)** Pie chart showing the cell cycle distribution of 151 Halo-ZNF638/EGFP-Geminin$_{1-110}$ co-expressing HeLa cells assessed at one hour after treatment. **D)** Pie charts displaying the quantity and percentage of nucleoli with or without Halo-ZNF638 accumulation in G1 or S/G2 phase HeLa cells one hour after treatment.

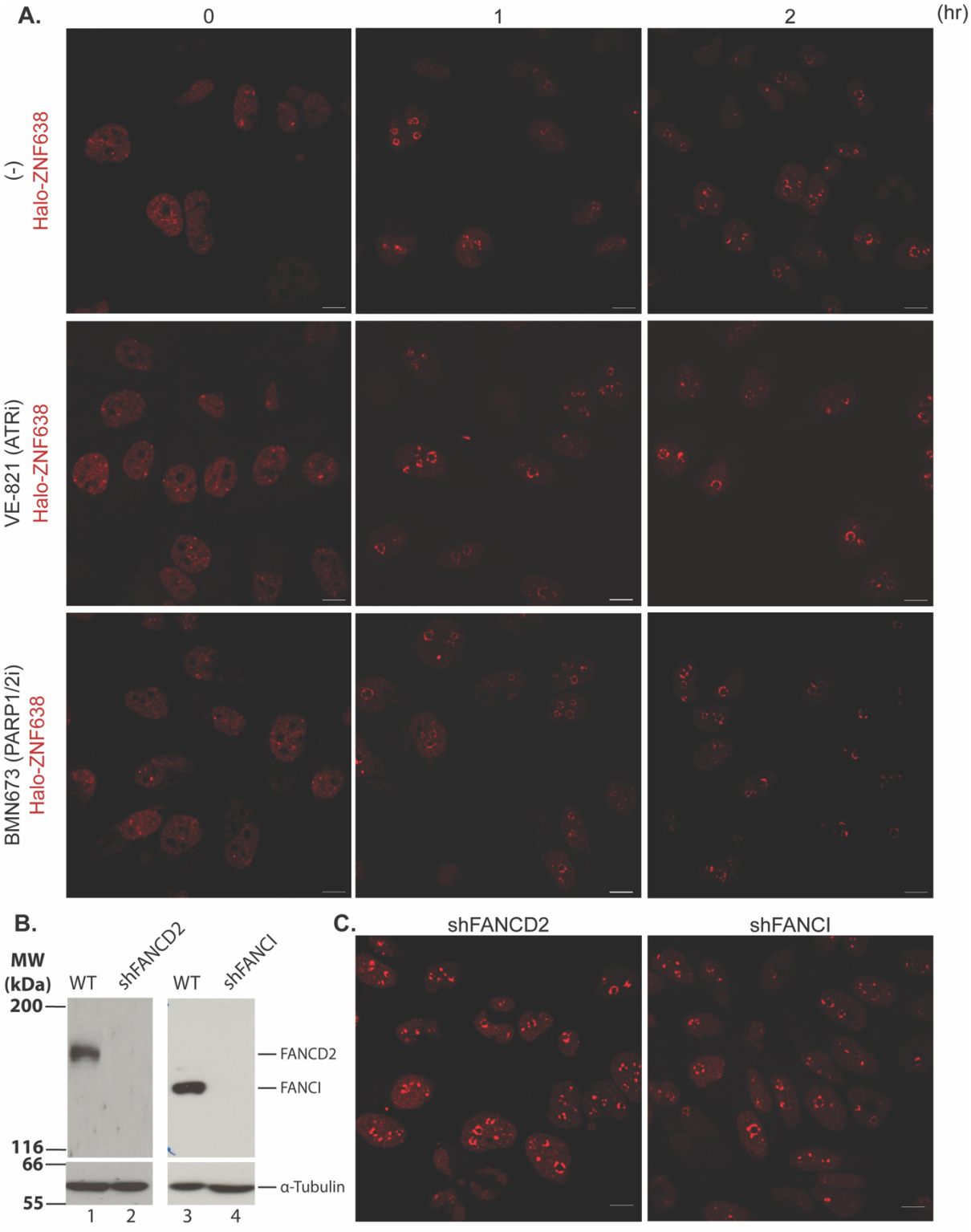
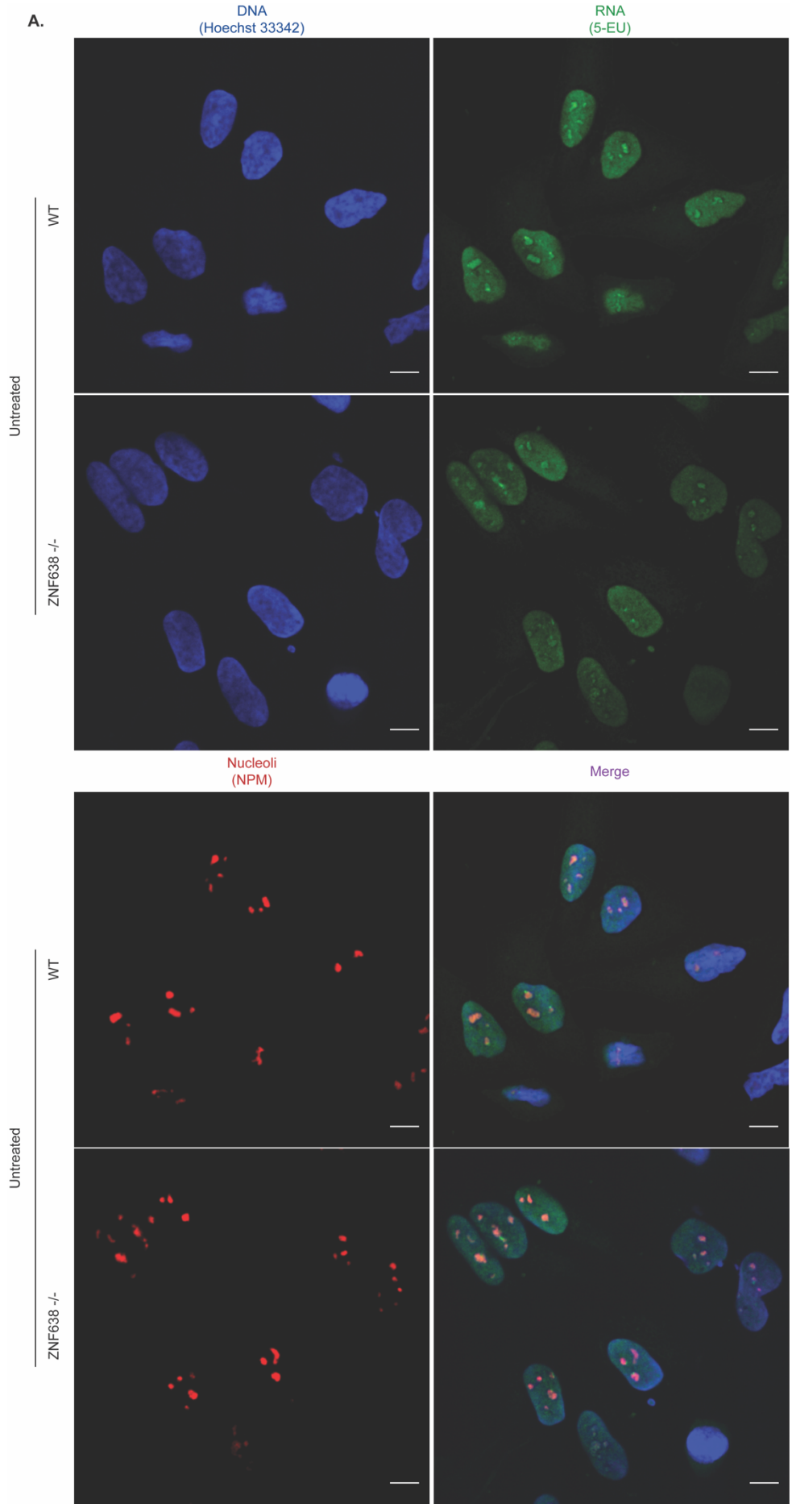


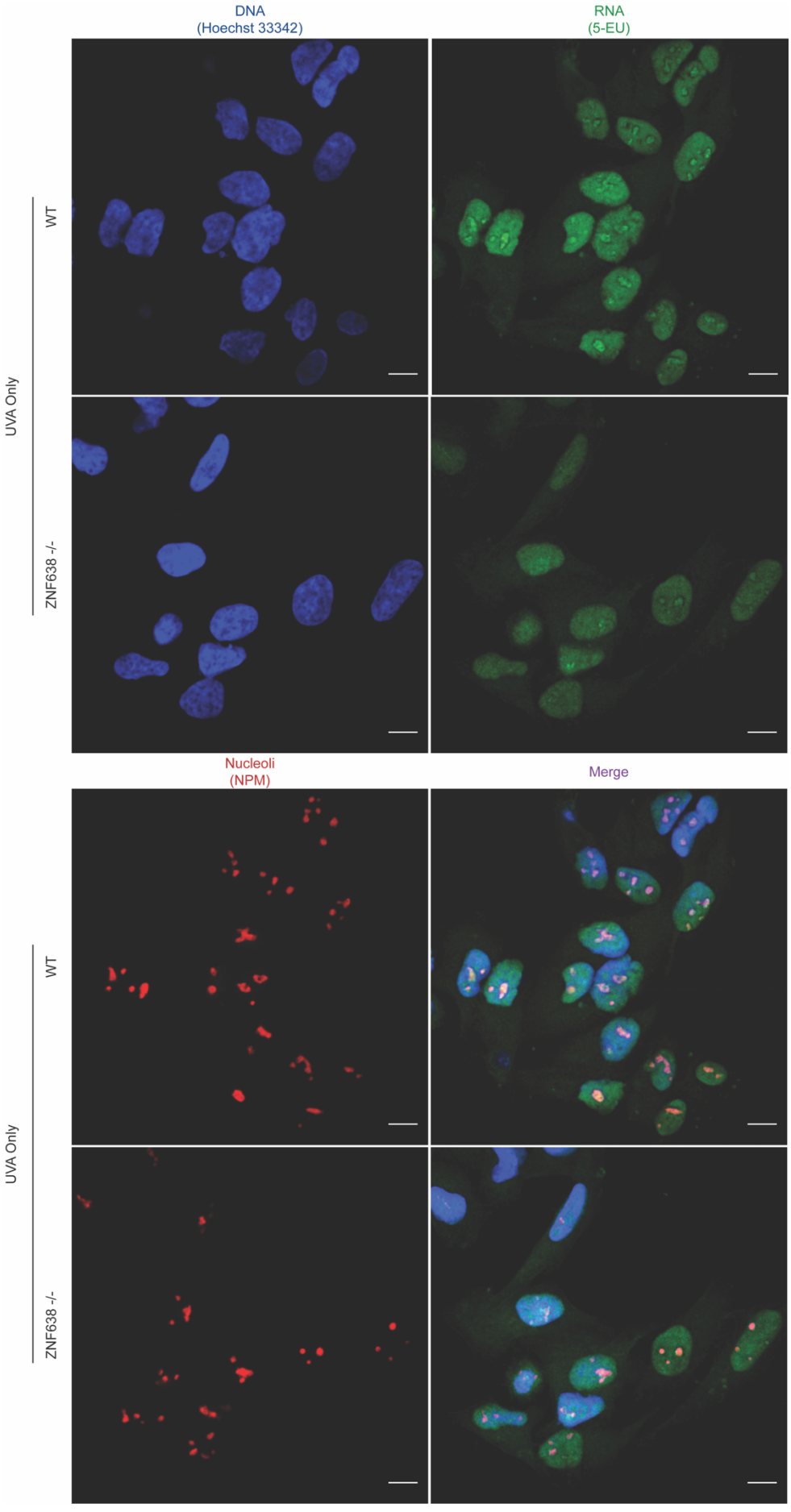
Figure 3-11. ZNF638 translocation to nucleoli is independent of ATR/PARPs or the FA pathway. **A)** Halo-ZNF638 expressing cells were pre-treated with 40 μM VE-821 (ATRi) or 10 μM BMN673 (PARP1/2i) for three hours. With the inhibitors, cells were incubated with JF549 to label Halo-ZNF638, followed by 20 μg/ml TMP and a 1000J/m^2 365 nm UVA pan-treatment. The distribution of Halo-ZNF638 protein was monitored for two hours after ICL induction. **B)** Western blot using anti-FANCD2, anti-FANCI and anti-α-Tubulin antibodies showing that FANCD2 or FANCI was depleted from Halo-ZNF638 expressing cells via shRNA knockdown. **C)** Live cell imaging was performed using the FANCD2 or FANCI-deficient cells. The cells were labelled with JF549, and ICLs were produced by 20 μg/ml TMP plus 1000J/m^2 UVA treatment. Images were captured two hours after irradiation. Scale bar = 10 μm.

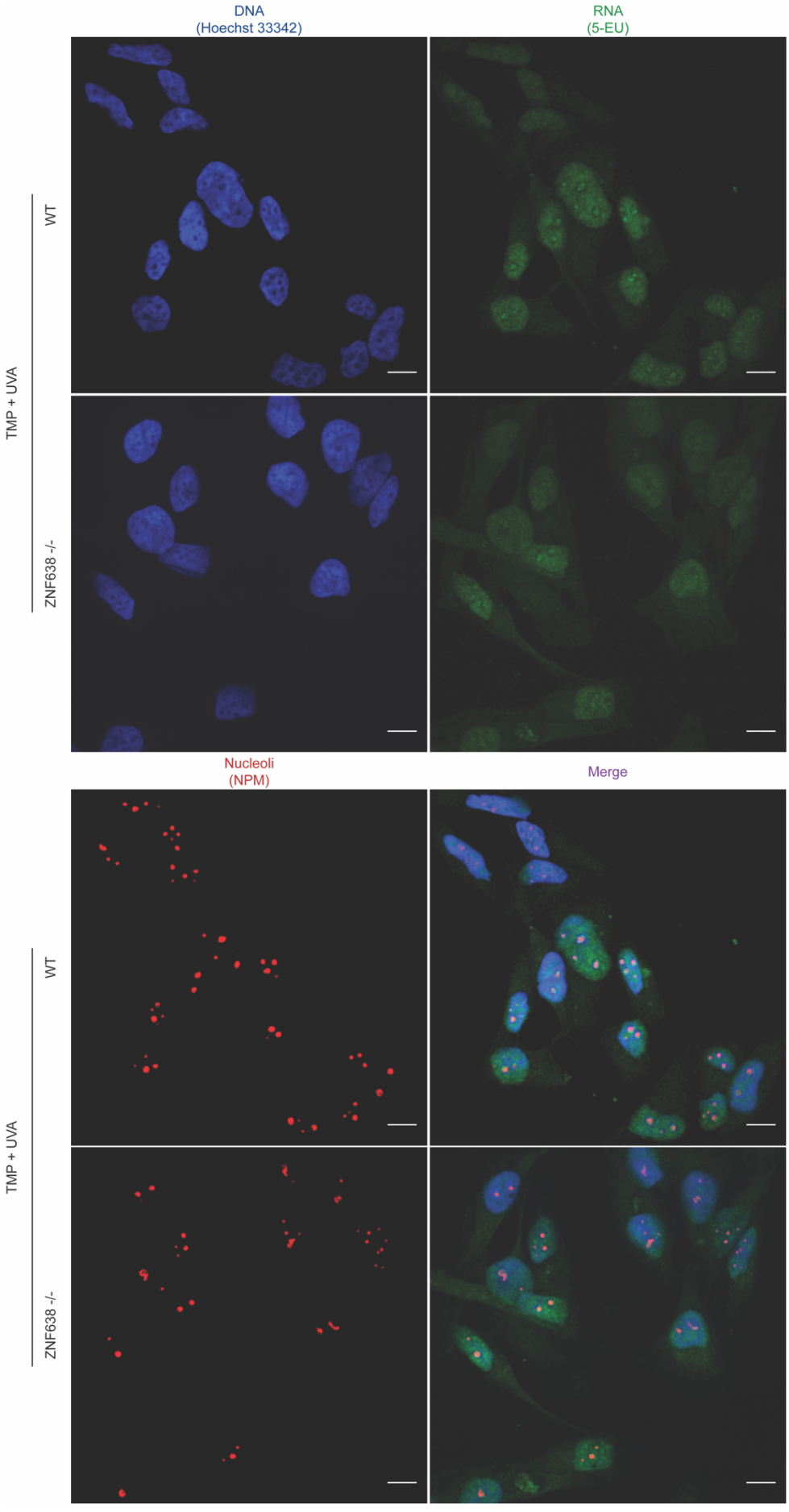
3.2.6 ZNF638 deficiency affects ribosomal RNA synthesis

The primary function of the nucleolus is the transcription and processing of ribosomal RNA. Given ZNF638's notable re-localisation to nucleoli under genomic stress, experiments were conducted to investigate its impact on rRNA production in response to DNA damage. The newly synthesised RNA in HeLa WT and ZNF638-deficient cells was labelled with 5-ethynyl uridine (5-EU) with or without ICL induction, and the rRNA level was measured using immunofluorescence. Newly synthesised RNA was visualised via Alexa Fluor 488 (AF488) coupled to the incorporated 5-EU, while the nucleolar marker NPM was used to identify nucleoli. After exposure to TMP/UVA treatment, a significant decrease in rRNA production was exhibited regardless of the presence of ZNF638. On the other hand, ZNF638-deficient cells, with or without ICLs, consistently displayed a lower level of rRNA synthesis (approximately one-third less than WT cells) (Figure 3-12). The data suggest that the absence of ZNF638 negatively impacts rRNA synthesis under both normal and genotoxic conditions.

The reduction in the rRNA synthesis observed in the ZNF638-deficient cells could be attributed to a decrease in the transcription of rDNA or impaired processing of the rRNA precursors. To investigate which stage of rRNA production is affected by ZNF638, a northern blot analysis was performed to measure the level of the primary transcript of rDNA - the 47S pre-rRNA. Consistent with the immunofluorescence data, ZNF638-null cells displayed decreased rRNA transcription levels compared to WT cells when untreated or treated only with UVA irradiation (Figure 3-13, compare lanes 1/2 and 4/5). Strikingly, TMP/UVA-induced ICLs completely halted rRNA transcription, resulting in the absence of detectable 47S pre-rRNA, regardless of the presence of ZNF638 (Figure 3-13, lanes 3 and 6). These findings indicate that the loss of ZNF638 leads to a diminished rRNA synthesis, potentially through inhibiting the transcription of rDNA, with or without the presence of ICLs.


A.
DNA
(Hoechst 33342)
RNA
(5-EU)
Nucleoli
(NPM)
Merge
Untreated
WT
ZNF638 -/-


DNA
(Hoechst 33342)
RNA
(5-EU)
UVA Only
WT
ZNF638 -/-
Nucleoli
(NPM)
Merge
UVA Only
WT
ZNF638 -/-


DNA
(Hoechst 33342)
RNA
(5-EU)
Nucleoli
(NPM)
Merge
TMP + UVA
WT
ZNF638 -/-
TMP + UVA
WT
ZNF638 -/-

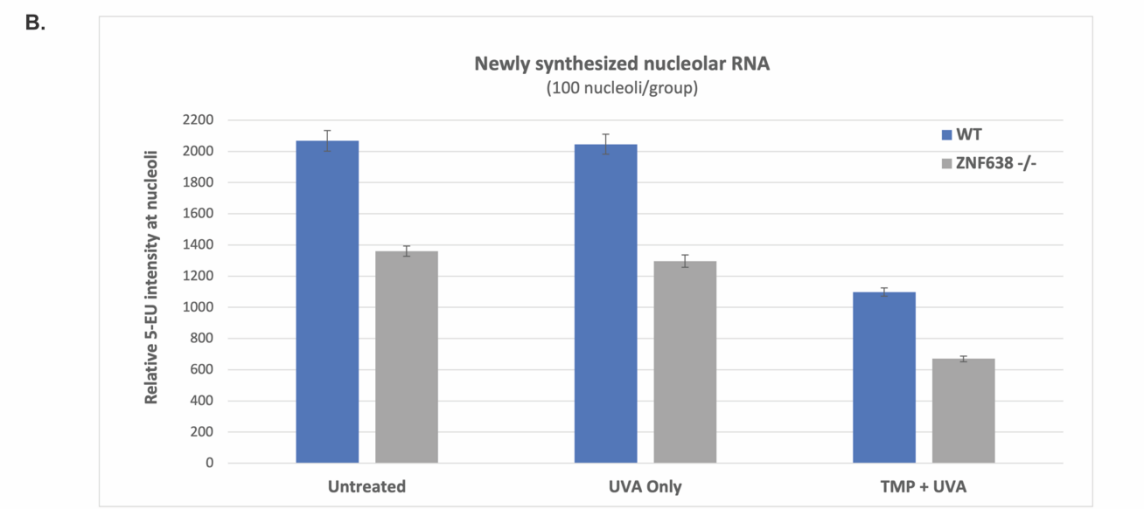


Figure 3-12. ZNF638 deficiency diminishes ribosomal RNA synthesis.
A) Immunofluorescence depicting the nuclei (Hoechst 33342), newly synthesised RNA (5-EU) and nucleoli (NPM) in WT and ZNF638-deficient cells. Three conditions were tested: untreated, 1000J/m^2 UVA, and 20µg/ml TMP plus 1000J/m^2 UVA. Cells were cultured in media containing 5-EU for one hour without or following TMP/UVA treatment and then fixed for immunofluorescence. Scale bar = 10µm.
B) Quantification of the relative fluorescence intensity of 5-EU within the nucleolar regions (masked by NPM staining) in WT and ZNF638-deficient cells under indicated conditions. The error bar represents the standard error (n=100 nucleoli per group, the experiment was performed once).

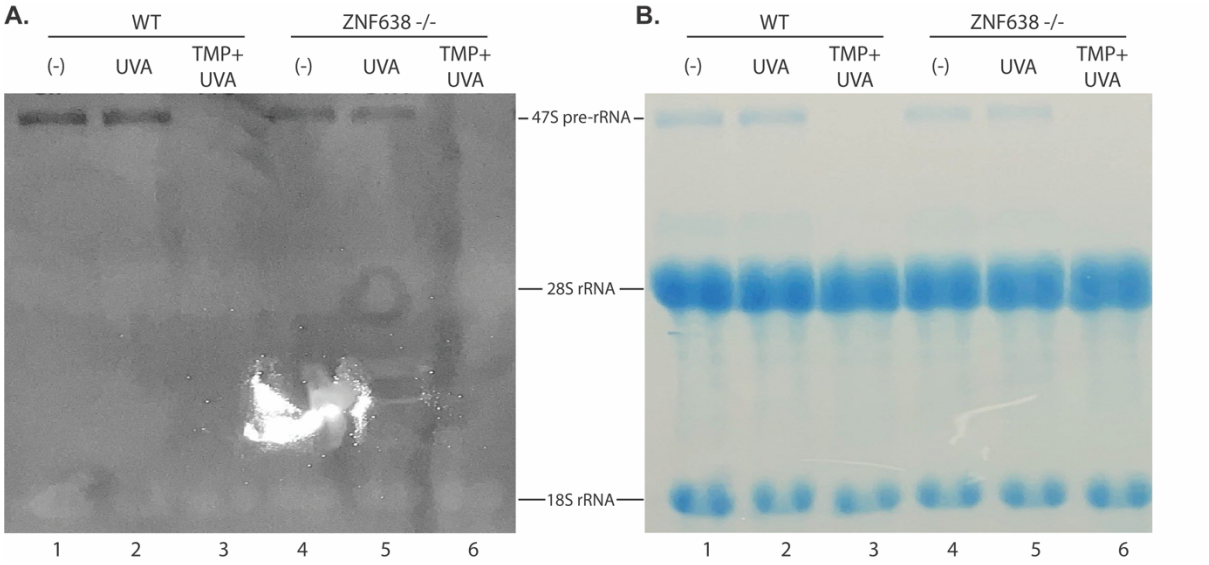


Figure 3-13. Transcription of ribosomal DNA is reduced by ZNF638 depletion.
HeLa WT and ZNF638 knockout cells were untreated, treated with 1000J/m^2 UVA, or with 20µg/ml TMP plus 1000J/m^2 UVA. One hour after treatment, total RNA was extracted and utilised for northern blotting. A DNA oligo probe that specifically targets the 5'-ETS in the 47S pre-rRNA was utilised to indicate the primary transcript in the northern blot. **A)** The 47S rRNA precursor was targeted by the biotin-labelled 5'-ETS probe and visualised via biotin chromogenic detection. **B)** The 47S pre-rRNA and the mature 18S/28S rRNA were stained with methylene blue. The 18S/28S rRNAs served as loading controls.

3.2.7 Rapid reduction in ZNF638 protein level has no effect on rRNA synthesis

ZNF638 knockout via CRISPR-Cas9 induces irreversible genomic alterations, which may result in cellular adaptability or secondary effects. To further test the protein's biological function, a dTAG ($FKBP12^{F36V}$ degron tag) was attached to the N-terminus of ZNF638 using CRISPR-Cas9 knock-in. This enables the rapid depletion of tagged ZNF638 protein upon treating cells with a small molecule - dTAG-13. The dTAG-13 compound comprises two distinct functional components. One component specifically recognises the $FKBP12^{F36V}$ tag present on ZNF638, while the other component interacts with the RING E3 ligase and facilitates the polyubiquitination of the tagged ZNF638, targeting it for subsequent proteasomal degradation. Despite several unsuccessful attempts to create complete dTAG knock-in cells, two partial knock-in clones were obtained in which more than half of the ZNF638 proteins were tagged. Within 6 hours, dTAG-13 induces the depletion of almost all tagged ZNF638 molecules in the two partial knock-in clones (Figure 3-14).

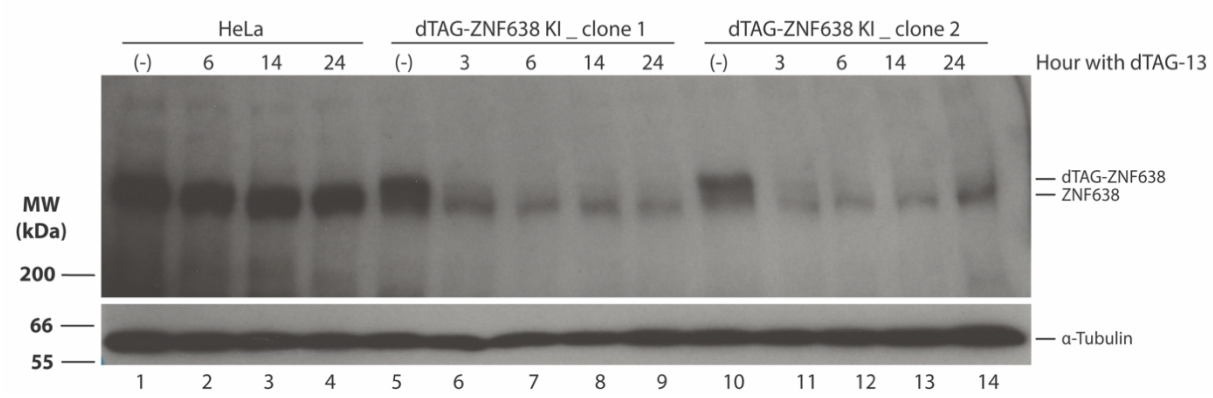
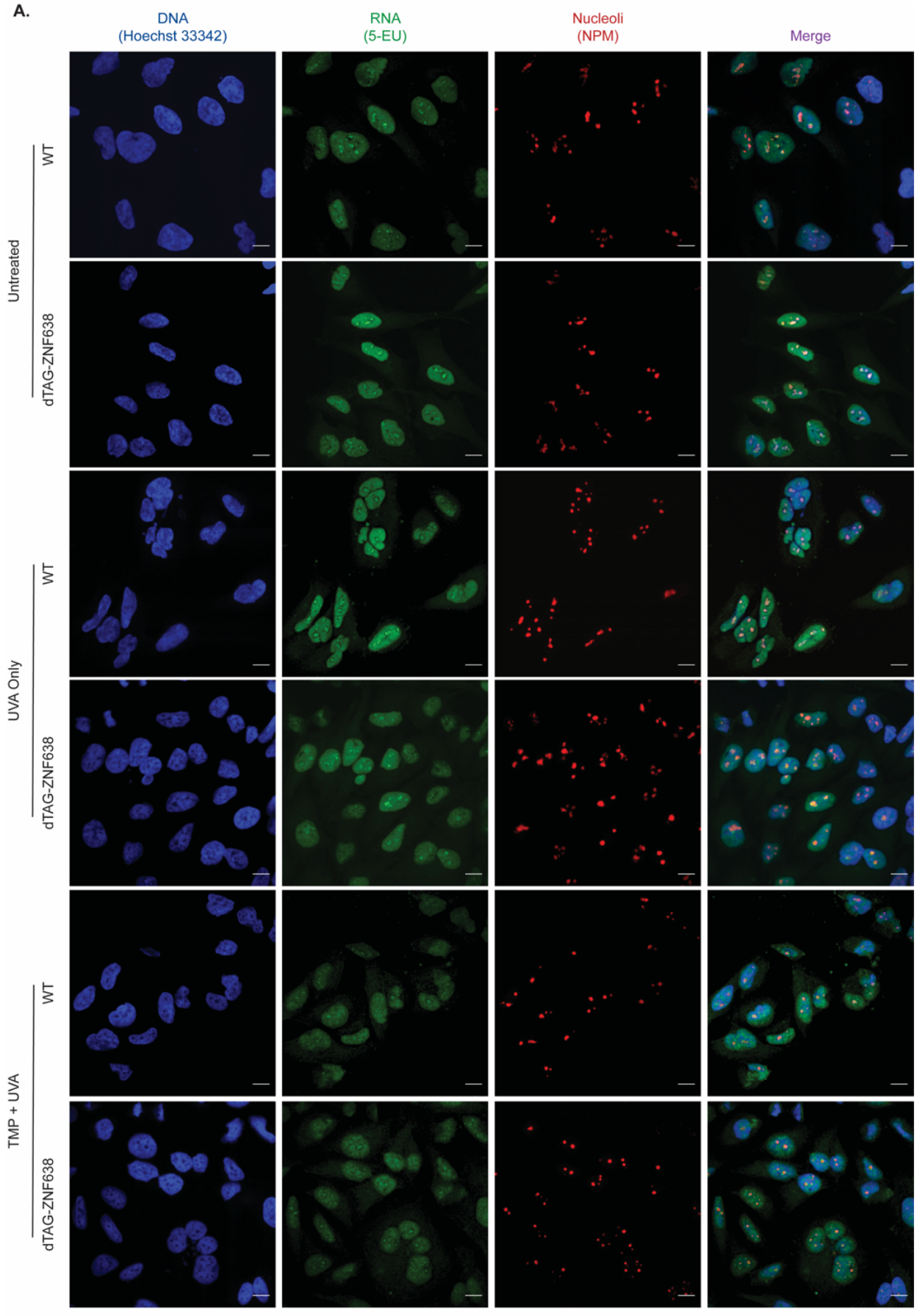


Figure 3-14 Generation of the dTAG-ZNF638 partial knock-in cells.
Western blot using anti-ZNF638 and anti-α-Tubulin antibodies showing that two single clones of partial dTAG-ZNF638 knock-in were acquired. The depletion of tagged ZNF638 protein was monitored for 24 hours after adding the degradation inducer dTAG-13. HeLa WT served as a negative control. Clone 2 was used in the following experiments. The production of dTAG-ZNF638 cells was conducted in cooperation with a Cohn lab part II student Charlotte Whittlesea.

Immunofluorescence and northern blot were then performed using dTAG-ZNF638 KI cells to investigate the impact of acute ZNF638 depletion on rRNA synthesis. The results indicate that there is no significant difference in rRNA synthesis (Figure 3-15) or rRNA transcription (Figure 3-16) between the WT cells and KI cells with more than 50% ZNF638 protein getting depleted rapidly. To validate previous data, full ZNF638 knockout was included in the northern blot, which yielded similar results as previous (Figure 3-16). Future research to verify the data will require the generation of a dTAG-ZNF638 full knock-in clone to ensure that the acute depletion of ZNF638 is comparable to the level achieved with CRISPR-Cas9 knockout, thereby avoiding any potential loss of phenotype due to the presence of non-tagged ZNF638 protein.


A.
DNA
(Hoechst 33342)
RNA
(5-EU)
Nucleoli
(NPM)
Merge
Untreated
WT
dTAG-ZNF638
UVA Only
WT
dTAG-ZNF638
TMP + UVA
WT
dTAG-ZNF638

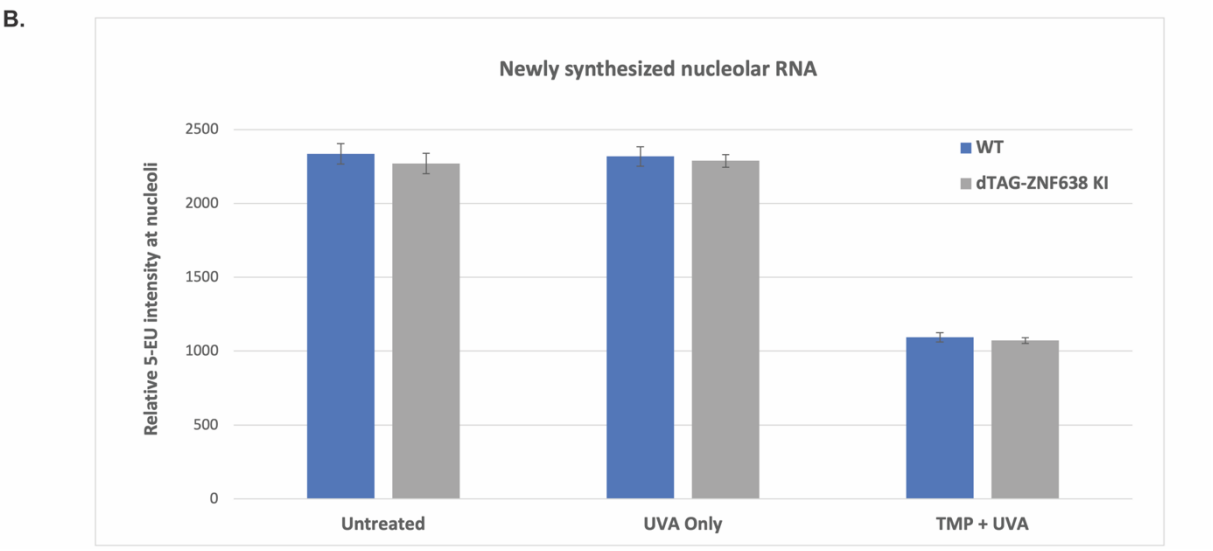


Figure 3-15 Rapid partial depletion of ZNF638 has no clear effect on rRNA synthesis.
A) Immunofluorescence was conducted using WT and dTAG-ZNF638 partial knock-in cells. Cells were pre-treated with dTAG-13 for 6 hours and then subjected to different treatments as indicated. Cells were then incubated with 5-EU for one hour and fixed for immunofluorescence. Scale bar = 10μm.
B) Quantification of the relative nucleolar fluorescence intensity of 5-EU in WT and dTAG-ZNF638 partial knock-in cells under indicated conditions. The error bar represents the standard error (n=80 nucleoli per group, the experiment was performed once).

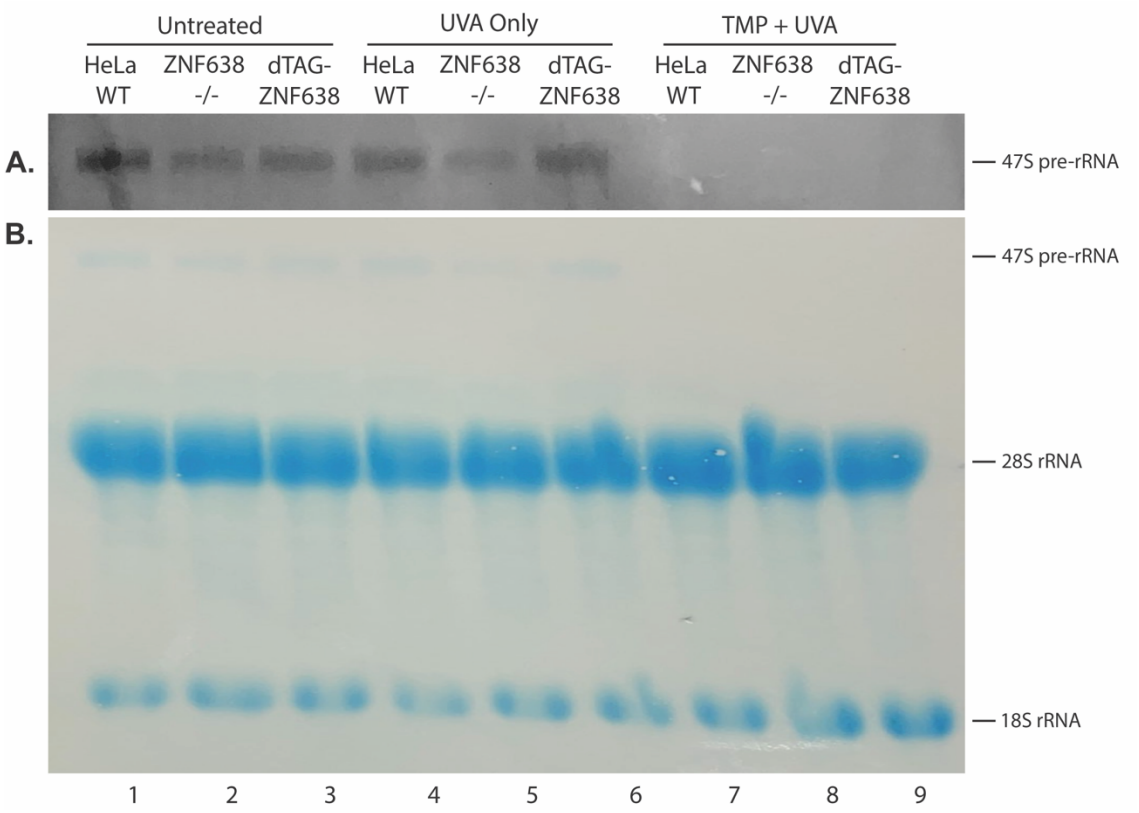


Figure 3-16. Rapid partial depletion of ZNF638 does not affect rDNA transcription.
HeLa WT, ZNF638 knockout, and dTAG-ZNF638 knock-in cells were pre-treated with dTAG-13 for 6 hours and then subjected to indicated treatments. After one hour of treatment, total RNA was extracted for subsequent northern blot analysis. **A)** The 47S rRNA precursor was specifically detected using a biotin-labelled 5'-ETS probe, followed by visualisation using biotin chromogenic detection. **B)** The 47S pre-rRNA and mature 18S/28S rRNA (loading controls) were visualised by staining with methylene blue.

3.2.8 Identification of ZNF638 binding partners

Given the absence of prior evidence linking ZNF638 to the DNA damage response, an alternative approach was pursued to elucidate its role following translocation to the nucleoli. The objective was to identify potential binding partners of ZNF638 in the context of genomic instability, with the aim of uncovering potential signalling pathways in which ZNF638 participates in response to DNA damage. To achieve this, co-immunoprecipitation (co-IP) was employed to purify ZNF638 and its potential binding partners. Using CRISPR-Cas9 knock-in, the Flag-HA tag was introduced at the N-terminus of ZNF638 in HeLa cells (Figure 3-17).

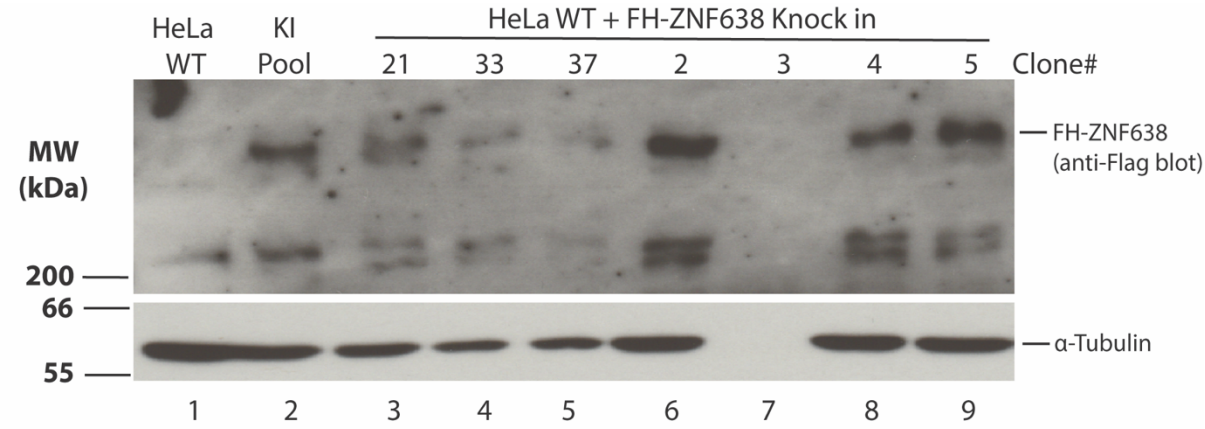


Figure 3-17 Generation of HeLa cells expressing Flag-HA tagged ZNF638.
Western blot using anti-Flag and anti-α-Tubulin antibodies showing that the Flag-HA Tag was attached to the N-terminus of the ZNF638 protein using CRISPR-Cas9 knock-in in HeLa cells. The Single clone (Clone 2, lane 6) with the highest expression level of FH-tagged ZNF638 protein was used in the following co-immunoprecipitation.

Flag IP of ZNF638 was first carried out from sonicated whole cell lysate, yet no ZNF638 protein was detected in the Flag eluate (Figure 3-18). Failure to pull down ZNF638 might be attributable to a low concentration of tagged protein in the starting material (the whole cell lysate) in this experiment. Therefore, Benzonase treatment and nuclear extraction were conducted prior to Flag-HA IP in order to concentrate ZNF638 and liberate the protein from its possible chromatin binding. Also, 4% PFA was utilised to crosslink proteins to avoid interruption of protein interactions during the purification process. Still, western blot detected ZNF638 in whole cell lysate and cytoplasmic fractions but not in nuclear extracts utilised for subsequent Flag-HA IP (Figure 3-19A). Additionally, silver staining did not display distinct protein bands in the final HA eluates when using both WT and FH-ZNF638 expressing cells (Figure 3-19B).

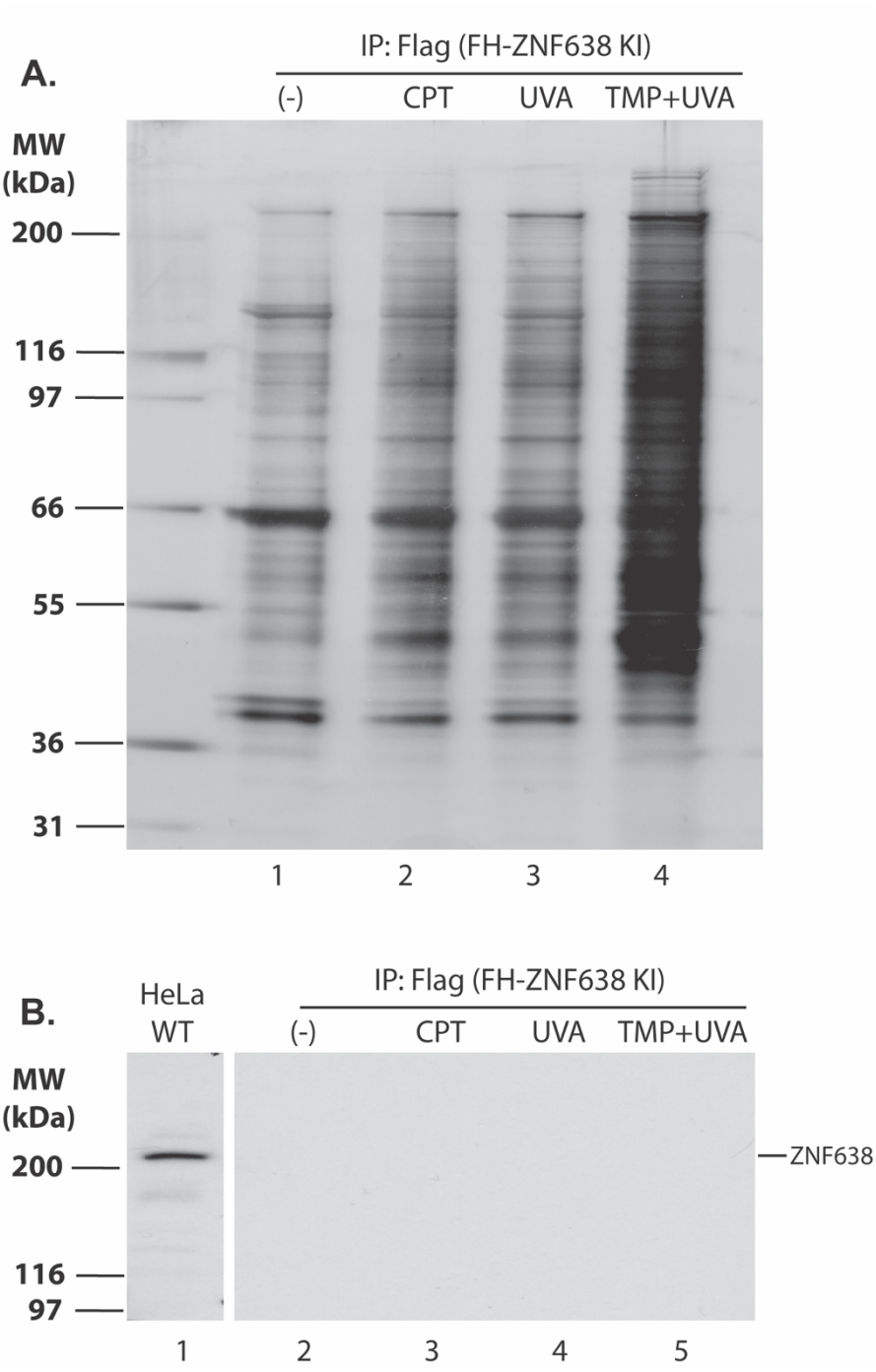


Figure 3-18 Flag-IP of FH-ZNF638 from whole cell lysate
HeLa cells expressing FH-ZNF638 were untreated, treated with 10μM CPT, with 1000J/m^2 of 365nm UVA alone, or with 20μg/ml TMP plus 1000J/m^2 of 365nm UVA. Four hours after CPT treatment and two hours after UVA exposure, cells were lysed and sonicated in the lysis buffer. The FH-ZNF638 was subsequently brought down using a Flag IP.
A) Silver staining displays the precipitated proteins in the Flag eluates.
B) Western Blot demonstrating the level of ZNF638 protein in Flag eluates by using the anti-ZNF638 antibody. A whole cell lysate of HeLa WT was included as a positive control for WB (lane 1).

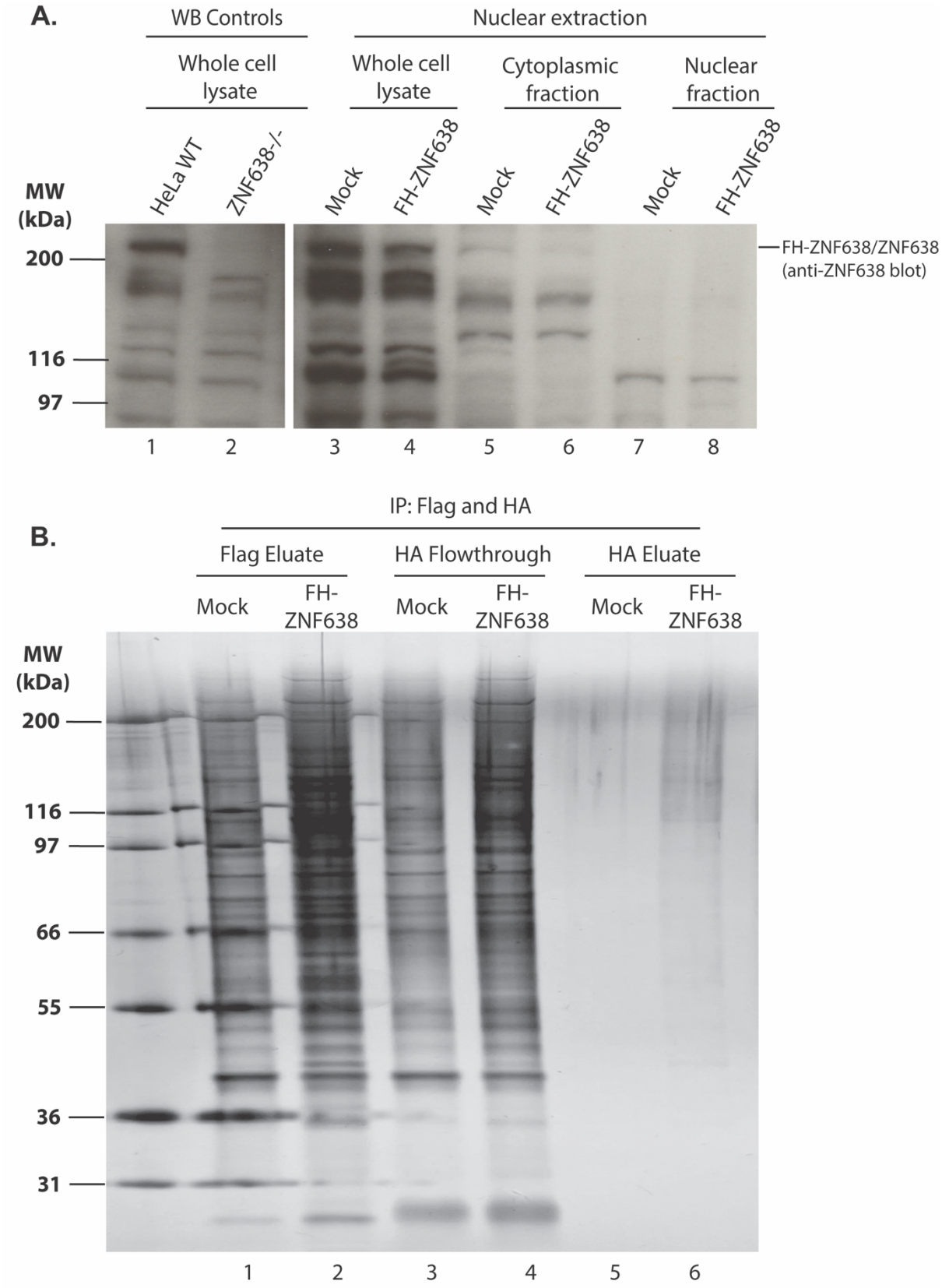


Figure 3-19 FH-ZNF638 purification with nuclear extraction, Benzonase and crosslinker. Untreated FH-ZNF638 KI and mock (WT) cells were homogenised, incubated with Benzonase, and crosslinked with 4% formaldehyde. The samples were then subjected to nuclear extraction and subsequent Flag-HA tandem IP. **A)** Western blot demonstrating the level of ZNF638/FH-ZNF638 in indicated samples from nuclear extraction by using the anti-ZNF638 antibody. **B)** Silver staining exhibiting the presence of proteins in indicated samples from Flag-HA IP.

Since the cytoplasmic fraction contained less ZNF638 protein than the whole cell lysate, yet there was no detectable ZNF638 in the soluble nuclear fraction, it is likely that ZNF638 formed large protein complexes (possibly due to the use of the crosslinker) and precipitated into the insoluble nuclear pellet. To avoid such potential ZNF638 precipitation, a crosslinker-free native nuclear purification method was attempted. In addition, to further enhance the amount of tagged ZNF638 protein in the starting material, the FH tag was knocked into ZNF638 in HeLa S3 cells, which can be cultivated in cell suspension and have a greater growth rate and cell density in the culture medium than adherent HeLa cells (Figure 3-20). With the use of HeLa S3 cells, the number of FH-ZNF638 expressing cells subjected to the co-IP was able to increase from approximately 3 x 10^8 to 3 x 10^9 cells.

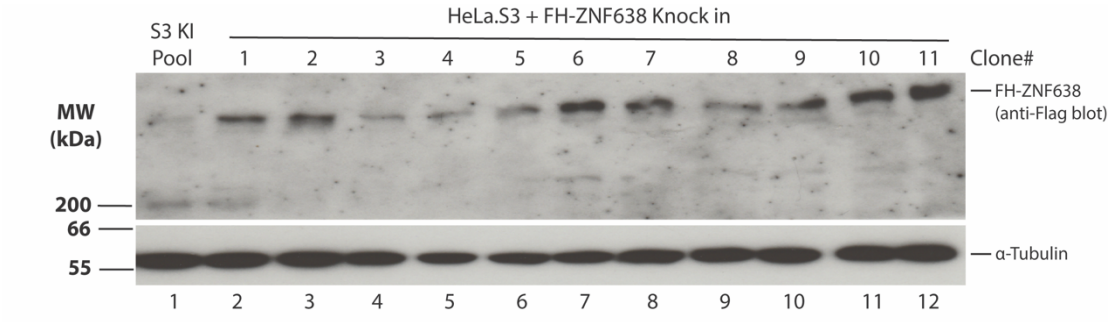


Figure 3-20 Expressing Flag-HA tagged ZNF638 protein in the HeLa.S3 cells.
Western blot using anti-Flag and anti-α-Tubulin antibodies showing that the Flag-HA tag was fused to the N-terminus of the ZNF638 protein in HeLa.S3 cells using CRISPR-Cas9 knock-in. In the subsequent co-immunoprecipitation, the single clone 11 (lane 12) with the highest expression level of FH-tagged ZNF638 was utilised.

Utilising the native nuclear purification approach with HeLa S3 cells, ZNF638 was successfully enriched in the nuclear extract (Figure 3-21A, lane 5). However, during the subsequent Flag IP, the protein exhibited poor binding affinity to the anti-Flag agarose beads, resulting in the majority of ZNF638 being washed off into the Flag flowthrough fraction (Figure 3-21A, lane 7). Increasing the volume of anti-Flag beads from 20 µl to 50 or 100 µl did not improve the elution of ZNF638 protein in the Flag IP (Figure 3-21B, lanes 7 and 8). These findings suggest that the binding issue is related to the accessibility of the anti-Flag beads to the FH tag on ZNF638 rather than the volume of beads used. One plausible explanation is that ZNF638 forms complexes with nucleic acids and/or proteins under normal cellular conditions, and the structural configuration of these complexes conceals the Flag tag, impeding its interaction with the anti-Flag beads.

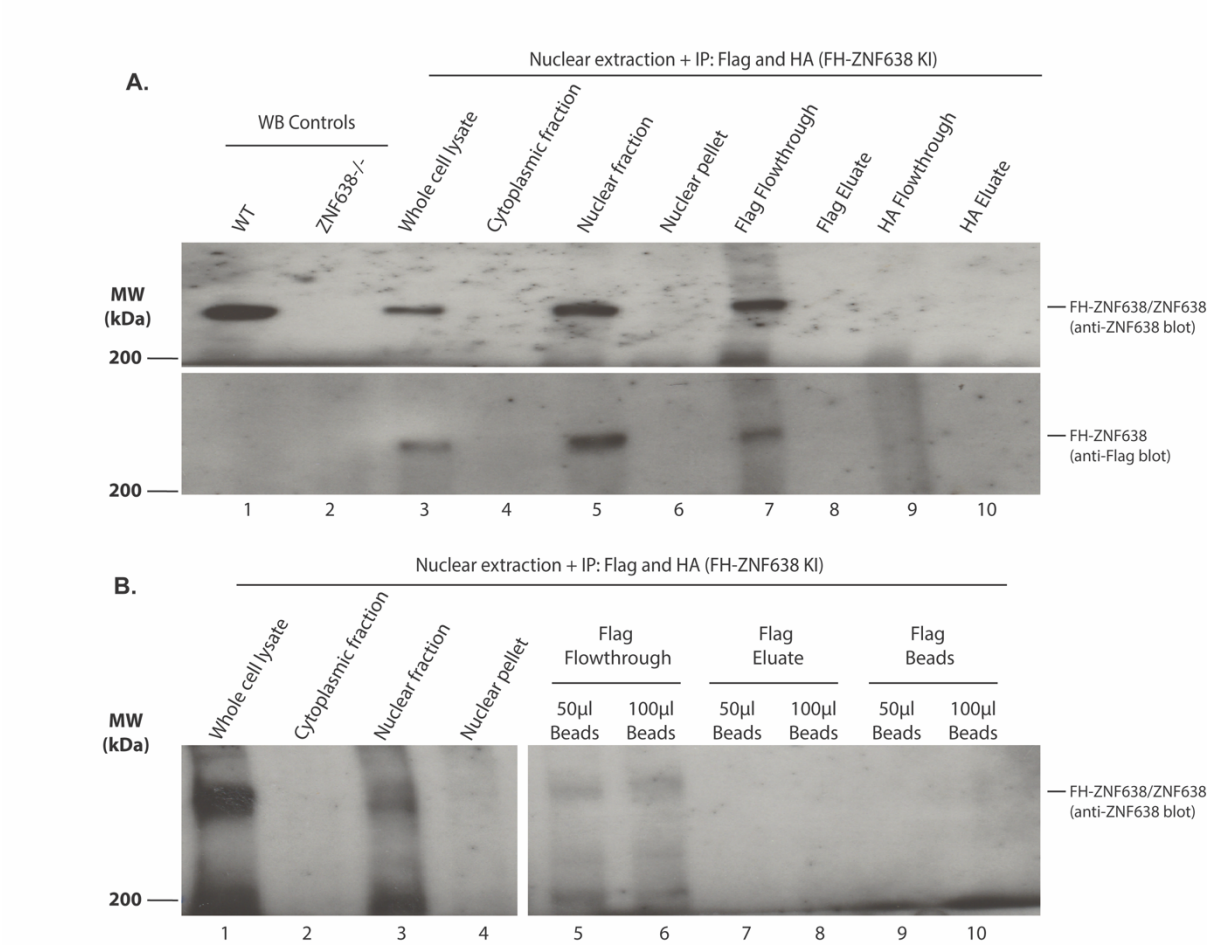


Figure 3-21 FH-ZNF638 exhibits poor binding affinity to the anti-Flag agarose beads.
FH-ZNF638 expressing HeLa S3 cells were untreated and homogenised in a hypotonic buffer. The nuclear proteins were then extracted using a high-salt buffer and subjected to the subsequent Flag-HA tandem IP. **A)** Western blot using anti-ZNF638 and anti-Flag antibodies showing the level of ZNF638/FH-ZNF638 in indicated samples when using 20 µl of anti-Flag agarose beads. **B)** Western blot using anti-ZNF638 antibody showing the level of ZNF638/FH-ZNF638 in indicated samples when increasing the volume of the anti-Flag beads to 50 µl and 100 µl.

To overcome the technical challenge, an alternative approach was employed to isolate the nucleolus specifically, rather than the entire nucleus, prior to IPs. This strategy was motivated by the assumption that the translocation of ZNF638 to nucleoli under genotoxicities may disassemble ZNF638 from its nucleoplasmic binding partners, thereby exposing its N-terminal Flag-HA tag. Also, nucleoli purification offers the advantage of enriching the ZNF638 protein in the extract intended for subsequent IPs. To this end, a nucleolus purification trial was first conducted using HeLa cells expressing Halo-ZNF638 to visualise the protein's localisation during purification. The substantial enrichment of the nucleolus marker NPM in the nucleolar fraction confirmed the effectiveness of nucleoli isolation, and the amount of ZNF638 protein was enriched in the nucleolar extract following TMP/UVA treatment, consistent with the *in vivo* imaging results previously obtained (Figure 3-22A). Notably, visualisation of Halo-

ZNF638 revealed its accumulation in nucleoli upon ICL formation, with the protein remaining at the periphery of each individual nucleolus during nucleoli extraction (Figure 3-22B).

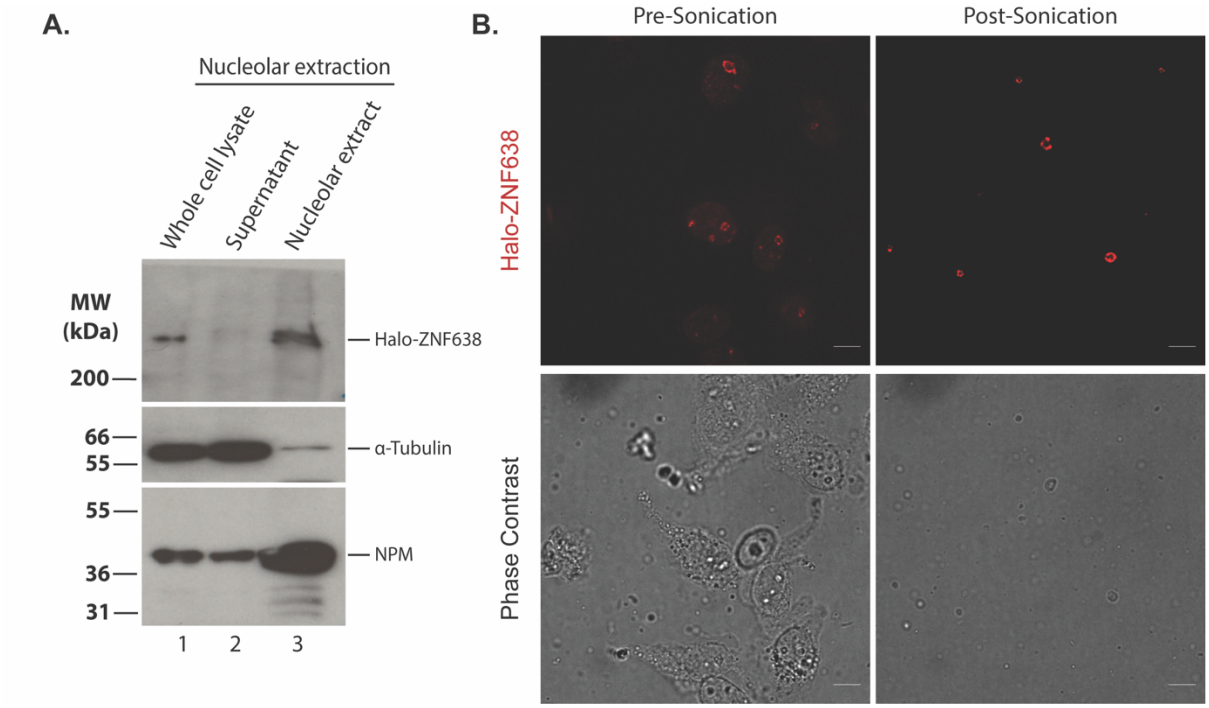


Figure 3-22. ZNF638 is enriched in the nucleolar extract.
Nucleoli isolation was performed using Halo-ZNF638 expressing cells. Cells were cultured with JF549 ligand and then treated with 20μg/ml TMP followed by 1000J/m^2 UVA pan-irradiation. One hour after treatment, cells were subjected to sonication and the nucleoli were isolated by centrifugation through a sucrose cushion twice. **A)** Western blot using anti-ZNF638, anti-α-Tubulin and anti-NPM antibodies that shows the level of Halo-ZNF638, α-tubulin and NPM (nucleolus marker) in the indicated samples. **B)** Fluorescent imaging showing the location of Halo-ZNF638 before and after sonication during nucleoli extraction. Scale bar = 10μm.

HeLa S3 cells expressing FH-ZNF638 were then subjected to nucleoli extraction and Flag-HA IPs. The nucleoli isolation successfully enhanced the interaction between the tagged protein and anti-Flag beads, resulting in the capture of over 50% of the ZNF638 protein in the Flag eluate (Figure 3-23, lane 5). A remaining challenge at the time was to elute ZNF638 protein (complex) from the anti-HA beads, as minimal protein was detected in both the HA flowthrough and the HA eluate fractions (Figure 3-23, lanes 6 and 7). Future research may use elution with a low pH Glycine solution (pH=2.5) to improve the recovery of FH-ZNF638 and its interaction partner(s) from anti-HA beads. After the FH-ZNF638 has been effectively eluted into the HA effluent samples, mass spectrometry will be used to determine the potential binding partners of FH-ZNF638 as well as the possible protein modifications of ZNF638 in response to genomic stress.

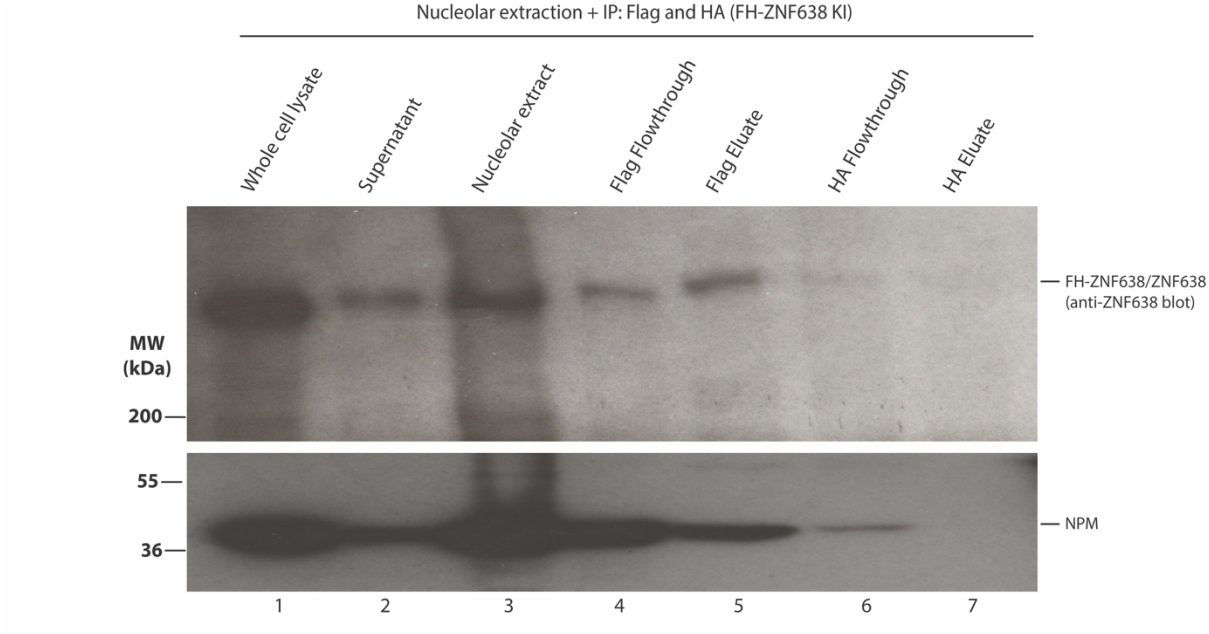


Figure 3-23. Co-IP of FH-ZNF638 and its binding partner(s) from the nucleolar extract.
Western blot using anti-ZNF638 and anti-NPM antibodies showing the level of ZNF638/FH-ZNF638 and NPM in indicated fractions from nucleoli extraction and Flag-HA IPs. ICLs were produced in FH-ZNF638 expressing HeLa S3 cells by incubating with 20μg/ml TMP for 30 minutes, followed by a 1000J/m^2 365nm UVA pan-treatment. One hour after irradiation, cells were sonicated, and the nucleoli isolation was performed using a sucrose cushion as previously. The extracted nucleoli were subjected to the subsequent Flag-HA tandem IP to isolate the FH-ZNF638 and its binding partner(s).

3.3 Discussion

ZNF638 is a large nuclear protein with DNA and RNA binding domains and zinc finger motifs (Figure 3-1). Prior research focused mostly on its role in adipogenesis as a transcription cofactor and its function in silencing non-integrated viral genomes by engaging the HUSH complex and subsequent histone modification enzymes (Meruvu et al., 2011; Y. Zhu et al., 2018). Although ZNF638 has been involved in other biological processes, such as heart muscle development and heat generation (Ng et al., 2002; Perie et al., 2019), it has never been associated with DNA damage repair or response. Previous research in our lab suggests that ZNF638 may be associated with the ICL response (a protein candidate identified in Figure 2-2 purification scheme); hence, a series of tests were conducted to determine whether the protein contributes to the DNA damage response and how it functions during the process.

Whether ZNF638 directly participates in the ICL repair was first analysed. Work in our laboratory has developed a live-cell imaging approach, combining UVA micro-irradiation with TMP treatment to induce ICLs in specific nuclear regions, enabling the evaluation of the dynamics of fluorescently tagged proteins of interest. Through this methodology, the recruitment of established ICL repair proteins, such as UHRF1 and FANCD2, to the ICL-containing sites has been observed. Interestingly, my imaging data reveal that instead of migrating towards the ICLs, ZNF638 redistributes to nucleoli and accumulates at their peripheries (Figure 3-4). This nucleolar accumulation of ZNF638 does not occur in WT cells or when cells are treated with UVA alone, demonstrating that the ring-shaped structure represents an authentic translocation of ZNF638 protein to the nucleoli, which reacts specifically to psoralen-induced ICLs (Figure 3-5). Additionally, EMSAs were performed to assess the binding capacity of purified ZNF638 to DNA probes *in vitro*, and the data suggest that the presence of ICL in probes diminishes the interaction between ZNF638 and the crosslinked DNA (Figure 3-6).

Data from the live-cell microscopy and EMSA lead to several hypotheses. First, ZNF638 may not directly engage in the repair mechanism since it does not approach the TMP/UVA-induced ICLs in live HeLa cells. On the contrary, the level of ZNF638 protein drops in the damaged area, indicating a release of the protein from the crosslinking (Figure 3-4). Besides, the accumulation of ZNF638 in the nucleoli appears later than that of FANCD2 in the irradiated regions. FANCD2, the key factor of the FA repair pathway, accumulated at ICLs within 30

minutes after irradiation, whereas the nucleolar deposition of ZNF638 became evident approximately 60 minutes post-treatment (Figure 3-4). This suggests that rather than resolving ICLs, the translocation of ZNF638 is more likely to associate with a secondary effect in response to genotoxic stress. Nevertheless, the possibility remains that ZNF638 indirectly contributes to the repair of ICLs by translocating to the nucleolus and triggering the release of repair-associated factors to the damaged site at a later stage of repair. This hypothesis is supported by previous studies showing that numerous DNA repair proteins sequester in the nucleolus until they are needed for DNA repair mechanisms (Ogawa & Baserga, 2017).

Second, in the live-cell imaging, the decline in Halo-ZNF638 level within the damaged area was most pronounced within the initial 30 minutes post-irradiation, a time frame during which Halo-ZNF638 had not yet begun to accumulate in the nucleoli (Figure 3-4). Thus, the cell may actively govern two distinct ICL response stages of ZNF638. In the first stage, which transpires within the initial 30 minutes post-treatment, ZNF638 is actively regulated to diminish its affinity for crosslinked DNA. This regulation may occur through signalling pathways or post-translational modifications induced by DNA damage. These mechanisms prompt the dissociation of ZNF638 from damaged sites, potentially enabling access for ICL repair factors. The second stage, occurring between 30 and 60 minutes after irradiation, involves the cell signalling ZNF638 from the entire nucleus, irrespective of the presence of ICLs, to re-locate to the nucleoli. This relocation is likely intended to induce nucleolar stress to facilitate damage repair or to engage in downstream pathways that ensure cell survival. This assumption is evidenced by the observation that the nucleolar accumulation of ZNF638 continued to increase beyond the 30-minute mark following irradiation, while the relative level of ZNF638 within the ICL-containing regions, normalised to the protein level outside the damaged zone (excluding nucleoli), evidently decreased only within the first 30 minutes and remained relatively unchanged afterwards (Figure 3-4B). These two ZNF638 response stages might be interconnected regarding the factors involved or represent distinct and independent response mechanisms.

It is worth mentioning that several potential explanations may account for the differential binding behaviour of ZNF638, initially showing a preference for crosslinked DNAs in the purification screen but binding less effectively to damaged DNAs in subsequent live-cell imaging and EMSA analyses:

1. The interactions observed between DNA probes and nuclear proteins, including ZNF638, during the initial purification screen occur in an *in vitro* reconstituted environment, which does not fully replicate the scenarios in live cells. In response to ICLs, live cells may actively regulate ZNF638, reducing its affinity for crosslinked DNA through signalling pathways or post-translational modifications. These regulatory processes can cause ZNF638 to disengage from damaged sites, allowing access to repair factors. However, such active regulation is absent in the *in vitro* conditions of the initial purification screen.
2. During the purification screen, nuclear proteins extracted from cells are subjected to changes in their native distribution and may exist at higher concentrations than *in vivo*. This alteration can result in proteins that do not typically interact *in vivo* or exist in lower abundance forming artificial complexes in the test tube. These artificial complexes may exhibit stronger binding to crosslinked DNAs and lead to the identification of false-positive candidates like ZNF638.
3. The non-crosslinked DNAs employed in the initial purification screen may untangle to form single-stranded DNAs. In contrast, the crosslinked DNA probes remain double-stranded due to the presence of ICLs. Given that ZNF638 demonstrates a binding preference for double-stranded DNAs (Inagaki et al., 1996), the transition of non-crosslinked DNAs into single-stranded forms could impair ZNF638's binding to the undamaged probes, concealing the protein's genuine binding preference.

Lastly, the accumulation of ZNF638 in the nucleolus is circumferential and creates a ring-like structure instead of aggregating throughout the nucleolus (Figure 3-4A and 3-5B). This is likely because ZNF638 accumulates in the "nucleolar cap," a structure that emerges under nucleolar stress by segregating nucleolar components. A collection of nucleoplasmic proteins, predominantly RNA-binding proteins, have been demonstrated to move from the nucleoplasm to the nucleolar cap under nucleolar stress (Boulon et al., 2010). For instance, the PTB-associated splicing factor (PSF), which is exclusively nucleoplasmic, localises to the nucleolar cap during transcriptional arrest (Shav-Tal et al., 2005), and its nucleolar deposition pattern closely resembles that of ZNF638. Therefore, it is assumable that ZNF638 translocates and accumulates in the nucleolar cap due to ICL-inducing nucleolar stress. Further microscopy of cells treated with varying concentrations of TMP/UVA, MMC, and cisplatin reveals that ZNF638 reacts to multiple forms of ICLs, but only when the ICL-inducing chemicals reach a relatively high dose (Figure 3-7). The dose-dependent behaviour of ZNF638 suggests that the

relocalisation of ZNF638 is driven by a secondary effect, potentially the nucleolar stress, that occurs under severe genomic stress.

When producing different types of ICL in the HeLa cells, a comparable redistribution of ZNF638 was observed, which motivated us to investigate further how specific the ZNF638 reaction is. Live-cell imaging of cells treated with CPT and UVB reveals that ZNF638 relocalisation is a rather general cellular response reacting to a variety of DNA damage types, including ICLs, single/double-strand breaks, and intra-strand crosslinks. Blocking the transcription machinery by a general transcription inhibitor, Act D, also induces the nucleolar relocalisation of ZNF638. Nevertheless, translocation of ZNF638 did not occur when cells were subjected to other physiological stressors such as nutrient deficiency, cold shock, and heat shock, suggesting that ZNF638 exclusively reacts to genomic instability (Figure 3-8). Taken together, the *in vivo* data suggest that when cells experience a high degree of genotoxic stress, the DNA damage and transcription arrest cause nucleolar stress and induce the accumulation of ZNF638 within the nucleolar cap.

The clonogenic survival assay provides evidence that the deletion of ZNF638 renders HeLa cells more vulnerable to various types of DNA damage (Figure 3-9). This validates the notion that ZNF638 has a meaningful biological function in responding to genotoxic stress beyond a mere change in its nuclear localisation. The subsequent investigation focuses on elucidating the underlying mechanism, such as how ZNF638 translocates to the nucleoli and what function it may serve in the nucleolar cap. The prerequisites for the nucleolar accumulation of ZNF638 were first investigated. It turns out that the ZNF638 relocalisation is not dependent on the cell cycle, the ATR/PARPs activities, or the activation of the FA pathway (Figure 3-10 and 3-11). These findings indicate that ZNF638 translocation does not require active DNA replication, the presence of cell-cycle-specific factors, or the ZNF638 phosphorylation/PARylation catalysed by ATR or PARPs. As we anticipate that the DNA lesions and transcription inhibition cause ZNF638 translocation, it is not surprising to see that ZNF638 migrates to nucleoli as long as the DNA damage is present, regardless of the availability of effective repair mechanisms such as the FA pathway.

The fundamental function of the nucleolus is the generation and processing of ribosomal RNAs. Early studies indicate that the nucleolus is a sensing hub for genomic instability (Weeks et al., 2019). In response to DNA damage, ribosome biogenesis within the nucleolus, the most energy-

consuming cellular process, is transiently halted to reinforce the DDR (Boulon et al., 2010). Meanwhile, this inhibition of rRNA synthesis produces nucleolar stress, leading to transient cell cycle arrest to further support the DNA damage repair (Y. Zhang & Lu, 2009). In this regard, an assumption is that ZNF638 translocates to the nucleolus and mediates the rRNA synthesis when ICLs are formed. By doing this, ZNF638 serves as a protein messenger to transfer the DNA damage signalling to the nucleolus, thus coordinating the cellular DDR and the nucleolar response. To test this hypothesis, the rRNA production level in ZNF638 deficient cells was evaluated with or without the presence of ICLs. Strikingly, the northern blot showed a complete shutdown of the rDNA transcription, indicated by the undetectable 47S pre-rRNA level, when ICLs were produced regardless of the presence of ZNF638 protein, making it difficult to compare the transcription level of rDNA between WT and ZNF638-deficient cells (Figure 3-13 and 3-16).

The immunofluorescence data suggest that ZNF638 depletion further inhibits *De novo* rRNA synthesis when ICLs are produced by TMP/UVA in HeLa cells. However, a similar reduction in rRNA levels (~1/3 less than WT) is observed in untreated ZNF638-deficient cells or cells treated with UVA alone (Figure 3-12B). This indicates a baseline decrease in rRNA production in the CRISPR-Cas9-generated knockout cells, possibly due to cellular adaptation or secondary effects caused by the permanent loss of ZNF638. Therefore, the decrease in nucleolar intensity of 5-EU observed in ZNF638 knockout cells when ICLs are present may be attributed to the background decrease in rRNA synthesis rather than the loss of ZNF638's function associated specifically with cellular DDR. Indeed, when depleted more than half of ZNF638 protein rapidly (for less than 10 hours) via a degron system, there was no detectable difference in rRNA synthesis, with or without ICL formation, between HeLa WT and the dTAG knock-in cells with a reduced ZNF638 level (Figure 3-15B). However, it cannot be ruled out that the loss of phenotype is attributed to the presence of the remaining endogenous ZNF638 protein, and a complete dTAG-ZNF638 knock-in clone, with which 100% rapid depletion of ZNF638 can be achieved, will be required for further validation. Besides, it will be worthwhile to explore a milder ICL-inducing condition in which both ZNF638 nucleolar translocation and 47S pre-rRNA level can be detected. Such a condition will allow us to compare the transcription level of rDNA between WT and ZNF638-deficient cells in response to ICLs.

In conclusion, the acquired data suggest that ZNF638 re-localises to the nucleolar cap in response to a relatively high degree of several types of DNA damage and transcription

inhibition. The release of ZNF638 from the ICL-containing regions is probably first due to its decreased interaction with crosslinked DNA, followed by an active migration to the nucleoli. The nucleolar migration of ZNF638 is shown to be not cell-cycle dependent nor reliant on ATR/PARPs-mediated modifications. It is unclear yet what function ZNF638 serves after relocating to the nucleoli. Since translocation occurs when ICLs are produced in restricted nuclear regions outside the nucleoli, one assumption is that the ZNF638 delivers the DNA damage signals to the nucleolus and mediates nucleolar stress to prioritise damage repair when the genotoxicity exceeds a specific threshold. Alternatively, as many DNA repair factors have been identified to reside within the nucleolus and released into the nucleoplasm during DDR, another assumption is that ZNF638 translocates into the nucleolus and signals the release of DDR factors under genomic stress. In addition, research conducted over the past decades has revealed that nucleolar stress plays a crucial role in the regulation of cell fate during stress reactions (Hua et al., 2022). Thus, ZNF638 may translocate to the nucleolar cap when cells experience severe genome instability and function within a signalling pathway downstream of nucleolar stress, potentially a mechanism associated with cell fate determination. Further investigations will be needed to test these hypotheses.

As there is currently no evidence indicating a precise mechanism behind the nucleolar deposition of ZNF638, an alternate method has been explored to advance the project: employing the co-immunoprecipitation to uncover putative ZNF638 functional partners. The results section displays significant advancements in the purification of ZNF638 and its associated binding partners through multiple rounds of optimisation in co-IP experiments (Figure 3-18 to 3-23). As soon as the ZNF638 protein is effectively enriched and recovered in the IP eluate, mass spectrometry will be utilised to identify the ZNF638 binding partners and protein modifications in response to DNA damage. This will help us to target the functional pathways involving ZNF638, as well as to determine if post-translational modifications are required for ZNF638's nucleolar translocation. Hopefully, this information can shed further light on the function of ZNF638 - a protein that appears to operate as a broad genomic instability reactor and coordinate the DDR with the nucleolar response.

Chapter 4. Discussion

ICLs are deleterious DNA lesions that obstruct DNA replication and transcription by inhibiting DNA strand separation (Constantinou, 2012). The formation and repair of ICLs have garnered significant attention in scientific research for two primary reasons. Firstly, the defective repair of ICLs is strongly associated with the inherited disease FA, which usually manifests in childhood and causes bone marrow failure, congenital abnormalities, and an increased risk of cancer (Auerbach, 2009). The only curative therapy for the bone marrow failure symptom of FA so far is bone marrow transplantation (Bierings et al., 2018); however, finding an HLA-matched sibling donor for transplantation is not always possible, and life-threatening complications may arise (Dufour, 2017). Therefore, further elucidation of the ICL repair mechanism is in need to identify new treatment targets. Secondly, ICL-inducing agents have a wide range of clinical applications in cancer therapy (Guainazzi & Schärer, 2010). ICLs are potent in blocking DNA replication and are particularly effective in killing rapidly dividing cancer cells. MMC, psoralen, nitrogen derivatives, and platinum compounds are among the most commonly used chemotherapeutic drugs in clinical practice. However, drug resistance may develop when using such agents, and a deeper understanding of ICL repair could aid in targeting alternative repair mechanisms, inhibiting the resolution of drug-induced lesions and thus promoting drug sensitivity.

Previous research has identified that ICLs can be repaired through both replication-dependent and -independent mechanisms (Semlow & Walter, 2021). Notably, significant progress has been made in the stepwise elucidation of ICL repair of replicative plasmids using a cell-free *Xenopus* egg extract system (Clauson et al., 2013). In this system, the repair of ICL is initiated when two replication forks converge, leading to the ubiquitination of the CMG helicase by the E3 ligase TRAIP (Wu et al., 2019). The NEIL3 glycosylase is first activated and recruited to the damage site by a short ubiquitin chain on CMG. If the NEIL3 pathway fails to correct the ICL, the ubiquitination of CMG by TRAIP continues, resulting in a longer ubiquitin chain that initiates the p97-mediated CMG unloading and activation of another replication-dependent repair mechanism - the canonical FA pathway. While the NEIL3 pathway is more efficient for repairing psoralen- and AP-induced ICLs, the FA pathway is required for repairing cisplatin-induced ICLs due to their highly distorting effects on the DNA helix that blocks NEIL3 accessibility (Huang et al., 1995; Li et al., 2020). Notably, a recent study suggests that the two mechanisms may not be entirely independent as NEIL3 appears to be involved in the repair of

MMC/cisplatin-induced ICLs via promoting the HR step in the FA pathway (Li et al., 2022). Additionally, acetaldehyde-induced ICLs require either the FA pathway or an incision-included, yet-to-be-explored AA-ICL-specific mechanism (Hodskinson et al., 2020). Notably, some AA-ICLs can only be repaired by the FA pathway, making it the most critical route for cell survival among the three replication-associated repair mechanisms (Gallina & Duxin, 2020). Indeed, mutations in genes encoding FA pathway factors have been found in FA patients, but the loss of proteins associated with the other two repair mechanisms has not been linked to diseases with FA phenotypes. Thus, the FA pathway seems to serve as a key safeguard for ensuring the repair of all types of ICLs and backing up other repair mechanisms. ICL repair mechanisms that do not rely on active DNA replication have also been identified as replication-independent mechanisms. These mechanisms include the repair of highly distorting ICLs and transcription-dependent repair (Williams et al., 2012).

The use of the *Xenopus* egg extract system has greatly promoted the elucidation of replication-associated repair of ICLs. Several findings from this system, such as TRAIP-mediated CMG ubiquitination and its role in pathway selection between NEIL3 and FA repair routes, have been verified in human cells (Li et al., 2020). Despite its great contribution to the exploration of ICL repair, the egg extract system cannot fully replicate the scenario in mammals. For instance, the replicative plasmids used in the system have a short origin firing distance, which facilitates a high frequency of replication fork convergence, an X-shaped structure that has been shown to initiate all repair mechanisms observed in the egg extract (Zhang et al., 2015). However, the inter-origin distance in mammals is much longer, and it has been discovered that more ICLs are located near a single replication fork than between two replication forks in mammalian cells (Huang et al., 2013). Thus, the egg extract system mainly enables the study of ICL repair at converged forks - a relatively infrequent scenario in mammalian cells, instead of the more frequent situation when one replication fork is hindered at the lesion. Furthermore, mammalian cells can directly bypass an ICL during replication, known as ICL traverse, and more than half of single replication forks directly traverse the ICL rather than initiating repair mechanisms (Rohleder et al., 2016). ICL traverse is likely the preferred option in mammalian cells as it is assumably the most efficient way to resume replication on the other side of the lesion. However, ICL traverse has not been observed in the egg extract system. Last, the proteome of the egg extract differs from that of human cells. Certain proteins involved in ICL repair in humans might not be expressed in the egg system or may have a different expression and (or) post-translational modification patterns.

Clinical observations have revealed that certain patients with FA syndromes lack mutations in the established genes associated with ICL repair, suggesting undiscovered repair factors. As aforementioned, the *Xenopus* egg extract system primarily investigates replication-dependent ICL repair involving fork convergence and does not comprehensively reflect the dynamics in mammals. To bridge the gap, our group devised a purification screen utilising a human cancer cell-based system to identify novel proteins involved in the cellular response to ICLs. Two types of biotin-labelled DNA probes were used in the screening, the linear DNA sequence and the fork mimic probe representing a Y-shaped structure that may occur when a single replication fork stalls at an ICL or after fork convergence undergoes reversal. These probes were then incubated with nuclear proteins extracted from HeLa cells, which were pre-treated with TMP/UVA to promote the expression and potential post-translational modifications of repair factors. Subsequent isolation of the biotin-tagged DNA probes using streptavidin-linked beads facilitated the retrieval of protein complexes that exhibited recognition and binding affinity towards the probed DNAs. The purified proteins were then subjected to mass spectrometry analysis to identify those demonstrating a preference for crosslinked DNAs over non-crosslinked DNAs. With this innovative system, novel ICL repair candidates were isolated directly from human cells using two distinct DNA probes that emulate structures complementary to the X-shaped fork convergence.

Nevertheless, several limitations must be acknowledged when evaluating the purification scheme. Firstly, the utilised short (~60 nt) linear or Y-shaped double-stranded DNA probes lack higher-order DNA structures and do not incorporate single-stranded DNA patches that account for unreplicated regions or Okazaki fragments. Secondly, the DNA lesions presented in the probes are TMP/UVA-induced ICLs, and the HeLa cells are pre-treated with TMP/UVA to facilitate the expression or modification of protein factors relevant to ICL repair. Therefore, this purification scheme primarily captures factors associated with the repair of one specific type of ICL (the psoralen-induced ICL). Thirdly, ICL repair likely follows a step-by-step process, such as the sequential repair of ICLs via the FA pathway, where access to the lesions of certain repair factors may necessitate the release of proteins from preceding steps. For example, the relative abundance of PCNA, Pol ε, MCM7, REV1, REV7, and FANCA in the vicinity of the ICL varies at different time points, reflecting their respective order in the repair process (Budzowska et al., 2015). Thus, this purification method may predominantly capture factors functioning at specific stages of repair while potentially missing factors released from previous steps or those yet to be recruited in subsequent steps. Lastly, interactions between

DNA probes and extracted nuclear proteins occur within a reconstituted environment (*in vitro*) rather than the natural cellular microenvironment. This discrepancy may impact the activity and recruitment of certain repair factors or disrupt essential protein complexes necessary for their function. Besides, the extracted proteins experience disturbance in their natural distribution within the nucleus. As a result, proteins that typically do not encounter *in vivo* may interact in the test tube, forming artificial complexes and leading to false-positive candidates. Hence, it is crucial to carefully validate the identified protein candidates before drawing conclusions regarding their involvement in genomic stability preservation. Through this purification screen, we identified approximately ten protein candidates exhibiting a binding preference for crosslinked DNAs. These proteins have not previously been implicated in DNA damage response or repair. Within this cohort, my work presented in this thesis focuses on two protein candidates, RCC2 and ZNF638. Given the stated limitations of the purification screen, my research aims to first verify the involvement of these two proteins in the cellular response to ICLs, and then elucidate their molecular mechanisms and functions in such response.

RCC2 is a protein candidate that exhibits rapid accumulation at TMP/UVA-induced ICLs. To ascertain its involvement in the ICL response, a complete RCC2 knockout in HeLa cells was generated and exposed to ICL-inducing agents including TMP/UVA and MMC. Remarkably, the loss of RCC2 rendered the cells more sensitive to both drugs, and the reintroduction of exogenous RCC2 protein restored the resistance. These findings strongly indicate that RCC2 plays a crucial role in promoting cell survival against ICLs. Furthermore, the live-cell imaging revealed that the recruitment of RCC2 to ICLs precedes the recruitment of FANCD2, the key factor in the FA repair pathway. This observation raises three possibilities: 1) RCC2 is involved in the FA pathway and functions upstream of the FANCD2/FANCI dimer; 2) RCC2 operates through an alternative repair mechanism preceding the FA pathway. This mechanism may not have been explored in previous research or could be the NEIL3 pathway that is known to be the preferred repair route for psoralen-induced ICLs; 3) RCC2 does not directly participate in the physical removal of ICLs but instead supports early-stage DDR processes that facilitate subsequent execution of ICL repair mechanisms.

Experiments were then designed to test the above assumptions. In order to explore the interplay between RCC2 and the FANCD2/FANCI dimer, the dependency of FANCD2 recruitment and monoubiquitination on RCC2 was first assessed. The results indicate that neither of these processes requires the presence of RCC2. To further investigate the potential connection

between RCC2 and the FA pathway, a double knockout HeLa cell line deficient of both FANCD2 and RCC2 was generated. Notably, the absence of RCC2 in FANCD2 knockout cells led to increased sensitivity to ICL-inducing agents compared to the FANCD2 single knockout. This suggests that RCC2 may be involved in an alternative, non-epistatic repair mechanism other than the FA pathway, or it may function at an early stage of the ICL response facilitating multiple repair mechanisms. However, it is important to note that in the former scenario, the potential alternative pathway involving RCC2 cannot fully substitute the role of the FA pathway in ensuring cell survival. This is supported by the observation that sensitivity induced by the sole absence of RCC2 is less pronounced than that observed in FANCD2 single-knockout cells.

Next, supposing that RCC2 is associated with an ICL repair mechanism, I attempted to explore whether it is the established NEIL3 pathway by generating a double knockout of NEIL3 and RCC2. Unfortunately, a complete knockout of NEIL3 from HeLa WT or RCC2-deficient HeLa cells was not achieved despite multiple attempts. As a result, partial NEIL3 knockout cells were utilised in the clonogenic survival assay. The results obtained from this assay suggest that RCC2 may function independently of the NEIL3 pathway as well, supporting its potential involvement in an undiscovered repair mechanism. Moreover, the attempt to evaluate RCC2's impact on the NEIL3 recruitment to ICLs failed as recruitment of EGFP-NEIL3 was not observed even when the RCC2 was present. This is likely attributed to the limitations of our live-cell imaging setup, where the UVA wavelength employed (405nm) may not be as efficient in ICL induction as the wavelength used in published studies (365nm). Therefore, further verification of the association between RCC2 and the NEIL3 pathway would be necessary once complete NEIL3 knockout cell lines become available. Nevertheless, the current findings provide intriguing insights. If RCC2 is directly involved in the physical removal of ICLs, it may be associated with a novel repair pathway that has not been identified in either the *Xenopus* egg extract system or mammalian cells.

In addition to the potential that RCC2 functions in ICL removal through a novel route, an alternative possibility is that RCC2 acts as an early effector in the DDR, promoting downstream repair processes and enhancing cell survival. This hypothesis is supported by early research showing that RCC2 functions as a guanine nucleotide exchange factor (GEF) for RALA, facilitating the exchange of GDP for GTP and thereby activating the small GTPase (Papini et al., 2015). Previous studies have demonstrated that RALA is involved in the Tumor necrosis

factor (TNF)-α signalling and regulates Stress-Activated map Kinase (SAPK) pathways, which are crucial for cell survival in tumorigenesis (Selimoglu et al., 2014). Notably, depletion of RALA has been shown to reduce cell survival and disrupt DSB repair by impairing the cells' ability to effectively repair the damage (Kidd et al., 2010). Based on these findings, it is plausible to propose that RCC2 promotes damage repair by activating RALA as its GEF. Indeed, a study investigating cisplatin-resistant ovarian cancer cells reveals that RCC2 plays a positive role in cell proliferation, apoptosis, and migration. This effect is mediated through its interaction with RALA and subsequent activation of RALA's downstream effector, RALBP1 (Gong et al., 2019). The study further demonstrates that the knockdown of RALA reverses the effects of RCC2, indicating the functional significance of the RCC2-RALA-RALBP1 axis. Besides, the expression levels of RCC2, RALA, and RALBP1 are found to be significantly elevated in tissues from cisplatin-resistant ovarian cancer compared to cisplatin-sensitive tissues. This suggests that the RCC2-RALA-RALBP1 axis is involved in promoting cancer cell survival and conferring resistance to DNA-damaging agents, potentially by upregulating DNA damage repair processes.

Furthermore, RCC2 possesses a p53 binding site within its promoter region, suggesting that it may be transcriptionally upregulated by the tumour suppressor protein p53 (Song et al., 2018). p53 plays a crucial role in maintaining genome stability and is often referred to as "the guardian of the genome." Extensive studies have demonstrated that p53 functions as a transcriptional activator, orchestrating the expression of genes involved in critical cellular processes such as growth arrest, DNA repair, and apoptosis (Abuetabh et al., 2022). Based on this knowledge, it is plausible to propose that p53 could transcriptionally enhance the expression of RCC2 in response to the formation of ICLs, thereby promoting RCC2's function in the DDR system. Nevertheless, it is important to note that this proposed mechanism for RCC2 remains speculative, and further exploration is required to determine whether RCC2 is transcriptionally upregulated by p53 in response to ICLs and whether it engages in DDR by activating RALA or other members of the Ras GTPase family. An alternative approach to explore RCC2's function without relying on prior knowledge is to perform co-IP experiments to identify its interacting partners. By elucidating the functional partners of RCC2 in the context of genomic stress, we can enhance our understanding of how RCC2 functions in maintaining genome stability.

The behaviour of ZNF638, another protein candidate identified in the screening, differs from that of RCC2 in its response to DNA lesions. Upon encountering DNA damage, ZNF638 relocates from the nucleoplasm to the peripheral nucleoli, exhibiting a distinct ring-shaped accumulation pattern. This pattern resembles a structure known as the nucleolar cap, which typically emerges in scenarios involving nucleolar stress. When nucleolar stress occurs, the standard nucleolar organisation consisting of the fibrillar centre, the dense fibrillar component, and the granular component disassembles, forming instead a peripheral nucleolar cap surrounding a segregated nucleolus (Hua et al., 2022). Notably, during nucleolar stress, specific nucleolar proteins tend to re-distribute to the nucleolar cap, whereas certain nucleoplasmic proteins relocate to the nucleoli. Consequently, the nucleolar cap comprises both relocalised nucleolar proteins and imported nucleoplasmic proteins (Shav-Tal et al., 2005). Therefore, it is reasonable to propose that ZNF638 belongs to the group of proteins that undergo relocalisation from the nucleoplasm to the nucleolar cap upon DNA damage.

Nucleolar stress can arise from impaired rRNA synthesis caused by direct rDNA lesions or DNA damage occurring outside the nucleoli. Direct lesions in the rDNA temporarily inhibit RNA polymerase I and suppress rDNA transcription through ATM, NBS1, and the Mediator of DNA-damage Checkpoint Protein 1 (MDC1). Activation of the ATM-NBS1-MDC1 signalling pathway following DNA damage disrupts the assembly of Pol I initiation complexes, leading to the progressive displacement of elongating Pol I holoenzymes from the rDNA (Kruhlak et al., 2007). As a result, rDNA transcription is halted and damaged rDNA becomes localised to the peripheral nucleolar cap, where DDR factors are recruited to facilitate rDNA repair (Xuan et al., 2021). Inhibition of Pol I transcription also occurs in response to DNA lesions present in chromatin outside the nucleoli. This response features ATM-dependent recruitment of NBS1 to the nucleolus in a manner that is partly dependent on PARP1 activity. Upon entering the nucleolus, NBS1 specifically accumulates in actively transcribed nucleolar regions, contributing to the inhibition of rDNA transcription (Larsen et al., 2014). Concurrently, nucleolar-sequestered PARP1 is activated and released into the nucleoplasm following DNA damage (Rancourt & Satoh, 2009). Throughout this process, PARP1 facilitates the translocation of other DNA repair factors, such as WRN and XRCC1, from the nucleolus to the nucleoplasm (Veith et al., 2019). Consequently, the release of PARP1, along with other repair factors, from the nucleolus may serve as a coordinated signalling response that links the global DDR with NBS1-mediated Pol I inhibition and nucleolar stress (Xuan et al., 2021).

Consistent with these studies, my data demonstrate the translocation of ZNF638 to the nucleolar cap when DNA lesions are produced either globally or outside the rDNA. When cells are exposed to a combination of TMP and UVA pan-treatment, ICLs form throughout the nucleus, including nucleolar regions. Considering that the rDNA is highly transcribed in eukaryotes and particularly susceptible to DNA damage, the nucleolar stress resulting from the pan-treatment is likely caused by a synthetic effect of both rDNA and global DNA damage, yet primarily triggered by direct lesions in the rDNA. In contrast, when the TMP treatment is followed by a micro-irradiation at specific nuclear areas, ICLs are generated exclusively in regions outside the nucleoli. Under this scenario, it is plausible that the nucleolar stress and the migration of ZNF638 to the nucleolar cap are associated with the interplay between global DDR and the nucleolar response. Furthermore, the onset of nucleolar stress is supported by the northern blot data, in which the primary transcript of rDNA - the 47S pre-rRNA becomes undetectable within one hour after treating HeLa cells with TMP/UVA, indicating an acute shutdown of the rRNA transcription in response to ICLs.

Scientific investigations have revealed that the nucleolus functions as a stress sensor and signalling centre in response to various stress conditions, such as glucose deprivation, thermal stress, and DNA damage (Görner et al., 2002; Hayashi & Matsunaga, 2019; Korsholm et al., 2020). Besides, it has been shown that nucleolar stress can be induced by several chemotherapeutic agents, including oxaliplatin, cisplatin, actinomycin D, 5-FU, and PARP inhibitors (Burger et al., 2010). In line with these findings, my data corroborate the occurrence of nucleolar stress and demonstrate the translocation of ZNF638 to the nucleolar cap in response to various DNA lesions, including SSBs, DSBs, intra-strand and inter-strand crosslinks, as well as general transcriptional inhibition. However, similar ZNF638 translocation is not observed under conditions of nutrient deprivation or thermal stress, such as cold and heat shock. These observations suggest that while diverse cellular stressors can trigger nucleolar stress, the specific signalling pathways and proteins being recruited to the stressed nucleolus may vary depending on the nature of the stressor. In this context, ZNF638 appears to be a protein relocating to the nucleolar cap when cells are responding specifically to genomic instability.

The role of ZNF638 following its relocation to the nucleoli remains unclear. Given that this translocation occurs when ICLs are generated in specific nuclear regions outside the nucleoli, the current hypothesis is that ZNF638 might serve as a messenger to transfer DNA damage

signals to the nucleoli, contributing to the induction of nucleolar stress to prioritise the damage repair. Previous research has revealed that ZNF638 can inhibit the transcription of non-integrated viral genomes by recruiting the HUSH complex and subsequent histone modification enzymes (Meruvu et al., 2011; Y. Zhu et al., 2018). Thus, it is conceivable that ZNF638 induces nucleolar stress by inhibiting rDNA transcription, likely by recruiting the silencing HUSH complex after translocating to the nucleoli. To test this hypothesis, changes in rDNA transcription in ZNF638-deficient cells in response to ICLs were examined. However, the results from northern blot analysis indicated a complete shutdown of rDNA transcription when ICLs were produced, regardless of the presence of ZNF638 protein. This made it challenging to compare the rDNA transcription levels between WT and ZNF638-deficient cells. Consequently, there is currently no evidence to support the notion that ZNF638 inhibits rRNA synthesis and initiates nucleolar stress under genotoxic conditions. Therefore, at this stage, it cannot be definitively concluded whether ZNF638 translocates to the nucleolar cap to participate in the onset of nucleolar stress or simply as a consequence of nucleolar stress and plays a role in downstream signalling pathways. Further investigations, such as exploring milder treatment conditions to compare rDNA transcription inhibition between WT and ZNF638-deficient cells, are needed to provide more insights into these hypotheses.

Efforts were made to develop a purification protocol aimed at isolating nucleolar-localised ZNF638 along with its potential binding partners following ICL formation. Successful nucleoli extraction and subsequent Flag-IP have been achieved, with the only remaining challenge being the final HA-IP step. Once this technical hurdle is overcome, the isolated ZNF638 protein (complex) will undergo mass spectrometry analysis to identify potential nucleolar binding partners and post-translational modifications of ZNF638 in response to genomic stressors. Another avenue for future investigation may involve exploring the relationship between ZNF638 and signalling pathways downstream of nucleolar stress. When nucleolar stress is produced in response to various cellular insults, it plays a pivotal role in the determination of cell fate, including apoptosis, senescence, autophagy and differentiation (Hua et al., 2022). As mentioned in the introduction chapter, the MDM2-p53, NF-κB, and HIF-1α pathways are known to be major signalling transductions triggered by nucleolar stress. Hence, it would be worthwhile to investigate whether ZNF638 participates in any of these three signalling pathways upon its relocation to the nucleolar cap.

In summary, this study investigates two novel proteins contributing to the cellular response to DNA damage. RCC2 appears to have a more specific role in response to ICLs, as it is recruited to the TMP/UVA-induced ICLs in HeLa cells. It is likely associated with an early-stage response that facilitates ICL repair mechanisms or potentially participates in an unreported novel ICL repair pathway. In contrast, ZNF638 exhibits a broader response to various types of DNA damage and transcriptional inhibition. Its translocation to the nucleoli suggests a potential role in mediating the nucleolar response and global DDR or contributing to cell fate determination. However, further investigations are needed to fully understand the functions of RCC2 and ZNF638, as well as the underlying molecular mechanisms involved in their actions.

Chapter 5. Materials and Methods

Cell lines and cell culture

HeLa, HeLa S3, U2OS and Phoenix A cells were grown in DMEM (D5796; Sigma-Aldrich) supplemented with 10% Fetal Bovine Serum (FBS) (F7524; Sigma-Aldrich) and passaged using Trypsin-EDTA (T4049; Sigma-Aldrich). All cells were kept in a 37°C incubator with a 5% CO2 supply. For nutrition depletion, cells were cultured in FBS-free DMEM media in a 37°C incubator with a 5% CO2 supply. For heat shock and cold shock, cells were cultured in 10% FBS supplemented DMEM with 5% CO2 in a 43°C incubator for 6 hours or a 30°C incubator for 48 hours, respectively.

Whole cell lysate preparation

Cells were harvested using cell scrapers and washed once with phosphate-buffered saline (PBS) at room temperature (RT). The resulting pellet was then suspended in an equal volume of Benzonase buffer, composed of 20 mM Tris-HCl (pH 8.0), 2 mM $MgCl_2$, 10% glycerol, and 1% Triton X-100, supplemented with 0.25 U/µl Benzonase (E1014; Sigma-Aldrich). The suspension was placed on ice for 5 minutes. Subsequently, an equal volume of 2% sodium dodecyl sulfate (SDS) was added to the sample. The sample was briefly vortexed and incubated for 5 minutes at 70°C using a heat block. The protein concentration in the sample was measured using Bradford reagent (500-0006; Bio-Rad).

Western blot (WB)

Cell lysates, nuclear extracts, or other protein samples were mixed with a pre-made SDS-PAGE loading buffer to prepare the final loading samples containing 10 µg proteins, 50 mM DTT (NP0009; Life Technologies), 62.5 mM Tris-HCl (pH 6.8), 2% SDS, 10% glycerol, and 0.01% bromophenol blue. The samples were boiled at 100°C for 5 minutes and then centrifuged at 15,000 rpm for 3 minutes to remove any precipitates from the supernatant. Subsequently, the samples were loaded onto a polyacrylamide gel with the desired percentage, alongside the unstained Mark12 protein ladder (100006637; Invitrogen). The separating gel was composed of 5-12% acrylamide/bis-acrylamide (A8887; Sigma-Aldrich), 400 mM Tris-HCl (pH 8.8), 0.1% SDS, 0.1% ammonium persulphate (APS), and 0.1% tetramethylethylenediamine (TEMED). The stacking gel contained 4% acrylamide/bis-acrylamide, 125 mM Tris-HCl (pH 6.8), 0.1% SDS, 0.1% APS, and 0.1% TEMED. The samples were electrophoresed in 1X Tris-Glycine-SDS running buffer (25 mM Tris, 192 mM Glycine, and 0.1% SDS) at a constant voltage of

80V for the stacking gel and later 100V for the separating gel. The electrophoresis was terminated when the dye front reached the end of the gel. Next, the proteins from the gel were transferred onto a nitrocellulose membrane at a constant current of 400 mA in the presence of transfer buffer (192 mM Glycine, 24 mM Tris, 0.0372% SDS, 20% methanol) in a 4°C cold room. The membrane containing the transferred proteins was then blocked with 5% milk (170-6404; Bio-Rad) for 1 hour at room temperature and subsequently incubated with the primary antibody overnight at 4°C. On the following day, the membrane was washed three times with TBS-T (10 mM Tris, 150 mM NaCl, 0.05% Tween-20). It was then incubated with the secondary antibody for 1 hour at RT, followed by two washes with TBS-T to remove any excess secondary antibody. After a final wash with TBS (10 mM Tris, 150 mM NaCl) to remove Tween-20, the membrane was developed using an ECL reagent (0RT2405 and 0RT2505; PerkinElmer) and exposed to films (28906837; GE Healthcare) in a dark room. Antibodies used in western blots are listed in Table 5-1 and 5-2.

Table 5-1. List of primary antibodies.

Antibody	**Species of Origin**	**Dilution**	**Manufacturer**
anti-FANCD2 (FI17)	Mouse	1:250	Santa Cruz Biotechnology (sc-20022)
anti-α-Tubulin (DM1A)	Mouse	1:2000	Millipore (05-829)
anti-NEIL3	Rabbit	1:500	abcam (ab110049)
anti-ZNF638	Rabbit	1:1000	GeneTex (GTX120667)
anti-RCC2	Rabbit	1:1000	Cell Signalling (D14F3)
anti-EGFP	Mouse	1:1000	abcam (ab184601)
anti-FANCI	Rabbit	1:1000	abcam (ab245219)
anti-Flag	Mouse	1:500	Sigma-Aldrich (F4042)
anti-NPM (B23)	Mouse	1:1000	Santa Cruz Biotechnology (3F291)

Table 5-2. List of secondary antibodies.

Antibody	**Species of Origin**	**Dilution**	**Manufacturer**
HRP-conjugated anti-mouse immunoglobulins	Rabbit	1:1000	Dako (P0260)
HRP-conjugated anti-rabbit immunoglobulins	Goat	1:1000	Dako (P0448)

CRISPR/Cas9-mediated gene editing (gene knockout and knock-in)

RCC2, ZNF638 and NEIL3 knockout were conducted using the pX459 plasmid, following the methodology outlined by *Ran et al. 2013*. The selection of gRNA target sequences was performed utilising the online CRISPR/Cas9 prediction tool CCTop (https://cctop.cos.uni-heidelberg.de:8043/). The specific target sequences and corresponding gRNA primers for RCC2, ZNF638 and NEIL3 knockout are listed in Table 5-3. The gRNA primers were annealed, phosphorylated, and ligated into BbsI-digested pX459 plasmids. The resulting plasmids were then electroporated into HeLa cells. To elaborate, HeLa cells were trypsinised, washed once with PBS, and resuspended in a suspension containing 2 x 10^6 cells/ml. A total of 400 µl of this cell suspension was mixed with 5 µg of pX459 plasmid and transferred into an electroporation cuvette (FBR-204; Scientific Laboratory Supplies), followed by a 10-minute incubation on ice. Electroporation was performed at 300 V and 500 µF. The cells were subsequently seeded onto culture dishes and allowed to recover overnight in the growth medium. After recovery, the cells were subjected to puromycin selection at a concentration of 2 µg/ml for 24 hours. Following the transient puromycin selection, the cells were grown in the regular growth medium. Subsequently, the cells were plated at low density to enable the formation of individual colonies. These colonies were then screened via Western blotting to confirm the loss of RCC2, ZNF638 or NEIL3 expression.

To introduce a Halo tag at the endogenous *ZNF638* locus in HeLa cells, a two-plasmid system was employed. The cutting plasmid, based on pX459, was designed along with a donor plasmid using a pBS-SK(+) backbone. The specific target sequence and gRNA primers for the cutting plasmid can be found in Table 5-3. The donor plasmid was assembled using Gibson's assembly reagent (M5510AA; New England Biolabs) following the provided instructions. The donor plasmid consists of four fragments: the pBS-SK(+) backbone, an 800bp ZNF638 upstream homology arm, a tag containing the sequence encoding the BSD-P2A-Halo, and an 800bp ZNF638 downstream homology arm. The design of the homology arms ensured complementarity to the genomic sequence surrounding the ZNF638 protein's start codon. Through homologous recombination, the BSD-P2A-Halo sequence was inserted right before the ZNF638 protein start codon. The BSD sequence conferred Blasticidin resistance to the cells, while the Halo sequence encoded the desired tag. The two sequences were separated by the self-cleaving P2A peptide sequence. Amplification of the pBS-SK(+) backbone, BSD-P2A-Halo fragments, and ZNF638 homology arms was achieved using primers listed in Table 5-4 for subsequent Gibson's assembly. Next, HeLa cells were electroporated with 5 µg of the

pX459 cutting plasmid and 15 µg of the donor plasmid. The cells were then seeded in a dish and allowed to recover for 72 hours. Blasticidin selection was applied at a concentration of 20 µg/ml BSD (SBR00032; Sigma-Aldrich) for 7 days. Subsequently, low-density plating was performed to enable the formation of individual colonies. These colonies were subjected to screening for Halo-ZNF638 expression using Western blot analysis.

The generation of FH-ZNF638 knock-in HeLa/HeLa S3 cells utilised for ZNF638 co-IP and dTAG-ZNF638 knock-in HeLa cells for rapid ZNF638 protein depletion followed the same CRISPR/Cas9 knock-in methodology as described above. The cutting plasmid employed was identical to the one listed in Table 5-3. Instead of the BSD-P2A-Halo fragment, the donor plasmids used for FH-ZNF638 and dTAG-ZNF638 knock-in contained the BSD-P2A-FH and BSD-P2A-FKBP12^{F36V} fragments, respectively. The amplification of the pBS-SK(+) backbone, BSD-P2A-FH segment, and ZNF638 homology arms for the Gibson's assembly of FH-ZNF638 knock-in donor was carried out using the primers specified in Table 5-4. The FANCD2 knockout cell line was generated by Dr. David Lopez-Martinez (Cohn lab), and the dTAG-ZNF638 knock-in donor plasmid was produced by Ms. Charlotte Whittlesea (Cohn lab).

Table 5-3. Target sequences and primers of RCC2/ZNF638/NEIL3 knockout (KO) and ZNF638 knock-in (KI) cutting plasmids.

KO/KI gRNA target	**Sequence (5' → 3')**
RCC2 gene knockout	GCAGTGCCGTTGCCCGAGCTCGG
NEIL3 gene knockout	CGCCGGTCACCGCCTGGCCCGGG
ZNF638 gene knockout	ATTAAACCTGGGTCTCGACATGG
ZNF638 gene knock-in	ATTAAACCTGGGTCTCGACATGG
KO/KI gRNA primers	**Sequence (5' → 3')**
RCC2 KO gRNA forward primer	CACCGCAGTGCCGTTGCCCGAGCT
RCC2 KO gRNA reverse primer	AAACAGCTCGGGCAACGGCACTGC
NEIL3 KO gRNA forward primer	CACCCGCCGGTCACCGCCTGGCCC
NEIL3 KO gRNA reverse primer	AAACGGGCCAGGCGGTGACCGGCG
ZNF638 KO gRNA forward primer	CACCATTAAACCTGGGTCTCGACA
ZNF638 KO gRNA reverse primer	AAACTGTCGAGACCCAGGTTTAAT
ZNF638 KI gRNA forward primer	CACCATTAAACCTGGGTCTCGACA
ZNF638 KI gRNA reverse primer	AAACTGTCGAGACCCAGGTTTAAT

Table 5-4. Primers for generating Halo/FH-ZNF638 knock-in donor plasmid.

ZNF638 homology arms (HA) cloning from the HeLa genome	**Sequence (5' → 3')**
Upstream HA forward	CATACTGTTTTCTTAGACTCTGTAGTC
Upstream HA reverse	GCCTATTTTCAAGAAAGCCTGATTTAATAAAG
Downstream HA forward	ATGTCGAGACCCAGGTTTAATCC
Downstream HA reverse	TCTTCAACAGGAAACATAGAATTACATATCAC
Gibson Assembly of the Halo-ZNF638 donor plasmid	**Sequence (5' → 3')**
pBS-SK (+) vector forward	CTGTTGAAGAGGTCGACGGTATCGATAAGC
pBS-SK (+) vector reverse	AAACAGTATGGGGGGGGCCC
BSD-P2A-Halo segment forward	GAAAATAGCCATGGCCAAGCCTTTG
BSD-P2A-Halo segment reverse	GTCTCGACATGCCGGAAATCTCG
ZNF638 upstream HA forward	GGGCCCCCCCCATACTGTTTTC
ZNF638 upstream HA reverse	GCTTGGCCATGGCTATTTTCAAGAAAGC
ZNF638 downstream HA forward	GATTTCCGGCATGTCGAGACCCAG
ZNF638 downstream HA reverse	ACCGTCGACCTCTTCAACAGGAAAC
Gibson Assembly of the FH-ZNF638 donor plasmid	**Sequence (5' → 3')**
pBS-SK (+) vector forward	CTGTTGAAGAGGTCGACGGTATCGATAAGC
pBS-SK (+) vector reverse	AAACAGTATGGGGGGGGCCC
BSD-P2A-FH segment forward	GAAAATAGCCATGGCCAAGCCTTTG
BSD-P2A-FH segment reverse	TGGGTCTCGACATCTCGAGTCCTC
ZNF638 upstream HA forward	GGGCCCCCCCCATACTGTTTTC
ZNF638 upstream HA reverse	GCTTGGCCATGGCTATTTTCAAGAAAGC
ZNF638 downstream HA forward	AGGACTCGAGATGTCGAGACCCAG
ZNF638 downstream HA reverse	ACCGTCGACCTCTTCAACAGGAAAC

Retroviral transfection of EGFP-tagged proteins

HeLa or U2OS cells were transduced with retroviral vectors harbouring EGFP-tagged RCC2, NEIL3, FANCD2, or Geminin$_{1\text{-}110}$ constructs. The gene of interest's cDNA sequence was reverse transcribed from a HeLa RNA pool and amplified to include XhoI and NotI restriction sites at the 5' and 3' ends, respectively. The amplified product was subsequently cloned into a modified version of the pOZ-N plasmid, which contained an EGFP sequence upstream of the cloning site in-frame. In the case of NEIL3, a pOZ-C plasmid was employed to fuse a C-terminal EGFP tag. The pOZ-N/C derivative, along with helper plasmids encoding retroviral Pol, Gag, and Env proteins, was transfected into Phoenix A cells using FuGENE6 (E2692; Promega) according to the manufacturer's guidelines. Typically, a transfection reagent volume ratio of 3:1 to a 1 μg/μl stock of purified (MIDIPrep) plasmid DNA was used. Three days after transfection, the culture supernatant from Phoenix A cells was harvested and filtered through a 0.45 μm filter unit. The resulting viral supernatant was diluted in fresh medium supplemented with 4 μg/ml polybrene. This medium, containing the virus, was used to transduce HeLa or U2OS cells for one day before replacing it with the standard growth medium. The EGFP construct facilitated the expression of an IL2Rα receptor sequence, allowing the selection of cells transduced with the plasmid based on their binding to anti-IL2Rα antibody-coated beads (anti-IL-2 receptor α: 05-170; Millipore, Dynabeads goat anti-mouse IgG: 11033; Invitrogen). The EGFP-Geminin$_{1\text{-}110}$ complemented FANCD2 knock-in cell line was generated by Dr. David Lopez-Martinez (Cohn lab) and Mr. Fengxiang Bai (Cohn lab). The EGFP-RCC2, EGFP-Geminin$_{1\text{-}110}$ and EGFP-FANCD2 plasmids were produced by Dr. Kelvin Yaprianto (Cohn lab), Dr. David Lopez-Martinez (Cohn lab) and Dr. Chih-Chao Liang (Cohn lab), respectively. The primers used for NEIL3-EGFP cloning are listed in Table 5-5.

Table 5-5. Primers for NEIL3-EGFP plasmid cloning.

NEIL3 cDNA reverse transcription	**Sequence (5' → 3')**
NEIL3 cDNA RT primer	GGACCAAACATTATACACAGTTTGAAG
NEIL3 cDNA amplification with restriction sites	**Sequence (5' → 3')**
NEIL3 cDNA forward primer	GTCACTCGAGATGGTGGAAGGACCAGGCTG
NEIL3 cDNA reverse primer	GTCAGCGGCCGCGCATCCAGGAATAATTTTTATTCCTGGCCC

shRNA-mediated knockdown

shRNA-mediated knockdown of the FANCD2, FANCI and NEIL3 genes was achieved by expressing the target sequences listed in Table 5-6 in the pSuper.retro vector (Clontech). The targeting sequences were searched in the RNAi Consortium shRNA Library from the Broad Institute. The pSuper FANCD2, FANCI or NEIL3 shRNA plasmid, along with helper plasmids encoding retroviral Pol, Gag, and Env proteins, was then transfected into Phoenix A cells using FuGENE6 as described above. Three days after transfection, the culture supernatant from Phoenix A cells was harvested and filtered through a 0.45 μm filter unit. The virus-containing medium was then used to transduce HeLa, U2OS or Halo-ZNF638 expressing HeLa cells for one day before replacing it with the standard growth medium. The cells were recovered in fresh medium overnight and then subjected to puromycin selection at a concentration of 10 μg/ml for 24 hours. Following the transient puromycin selection, the cells were grown in the regular growth medium, and the protein level of FANCD2, FANCI or NEIL3 was evaluated by Western blotting. The pSuper FANCD2/FANCI and pSuper NEIL3 shRNA plasmids were produced by Dr. Chih-Chao Liang (Cohn lab) and Dr. Kelvin Yaprianto (Cohn lab), respectively.

Table 5-6. Target sequences of FANCD2/FANCI/NEIL3 knockdown shRNA

Knockdown shRNA target	**Sequence (5' → 3')**
FANCD2 shRNA target	GAGCAAAGCCACTGAGGTA
FANCI shRNA target	GCAGTGTTCCTGCCTTCTT
NEIL3 shRNA target 01	GCTAATGGATCAGAACGTATT
NEIL3 shRNA target 02	AGAAGACAACAAACGATATAA

Live-cell imaging

HeLa or U2OS cell lines expressing proteins with fluorescent tags were seeded at approximately 50% density in 3.5 cm glass-bottom dishes (P35G-1.5-14-C; MatTek) one day prior to the experiment. For pan-treatments, the cells were exposed to 0.5, 1, 10 μg/ml MMC (ab120797; abcam); 10, 25, 50 μg/ml Cisplatin (P4394; Merck Life Science) or 0.1, 20 μg/ml TMP (T6137; Sigma-Aldrich), followed by 365nm UVA (BLE-1T151 365 nm tube, Spectro-UV) at the dose of 150, 500, or 1000 J/m^2 using a Spectrolinker XL-1500 UV Crosslinker. Live-cell imaging was performed at 1, 16, and 10 hours after TMP/UVA, MMC, and cisplatin treatments, respectively. Alternatively, cells were treated with 10μM Camptothecin (ab120115; abcam), 100 ng/ml Actinomycin D (ab141058; abcam) or 50 J/m^2 UVB (BLE-1T156 280-315

nm tube, Spectro-UV). Images were collected at 4-, 6-, and 9-hour following CPT, UVB, and Act D treatments, respectively. To investigate the effects of ATR or PARP1/2 inhibition, cells were pre-treated with 40μM ATR inhibitor VE-821 (SML1415; Sigma-Aldrich), or 10μM PARP1/2 inhibitor BMN673 (19782; Cambridge Bioscience) for 3 hours prior to TMP/UVA treatment. The inhibitors remained in the medium throughout subsequent ICL induction and live-cell imaging.

Before imaging, cells expressing Halo-ZNF638 were treated with 100 nM Janelia Fluor 549 HaloTag Ligand (GA1110; Promega) for 20 minutes, followed by three washes with 1 ml of colourless microscopy medium consisting of DMEM without phenol red (D1145; Sigma-Aldrich), 10% FBS, and 2 mM glutamine (G7513; Sigma-Aldrich), with each wash lasting 5 minutes. Subsequently, the cells were imaged using an Olympus IX81 microscope equipped with a PerkinElmer UltraView Vox spinning disk system. Imaging was performed at either 40X or 60X objective magnification. Live cells in a glass-bottom dish were placed inside an environmental chamber maintaining a stable temperature of 37°C and a continuous supply of 5% CO2 (Tokai hit). EGFP fluorescence was excited using a 488 nm laser, while Halo-JF549 fluorescence was excited using a 561 nm laser.

For micro-irradiation experiments, JF549 labelled cells were treated with 20 μg/ml TMP for 30-60 minutes. Micro-irradiation was then performed using a 30-40% powered 405 nm laser equipped in the Olympus IX81 microscope (the 100% powered 405 nm in the PE-SD1 corresponds to 1.112 mW ± 70 μW). Specific regions or stripes within the cell nucleus (40 x 3 pixels) were irradiated for a total of 60 cycles. Both image acquisition and micro-irradiation procedures were controlled using the FRAP preview mode of Volocity software. The Fiji software was utilised to assess the relative intensity of EGFP or JF549 within the irradiated areas or the nucleoli, which were normalised against the surrounding nuclear and extracellular background intensities. For the quantification of the nucleolar intensity of JF549, the nucleolar regions were outlined manually in Fiji based on the dark areas shown in the EGFP channel (indicating the nucleolar areas). The intensity of JF549 within the selected nucleolar regions was then measured in the JF549 channel. The relative intensity of the irradiated/nucleolar regions was calculated using the formula: (irradiated/nucleolar area intensity - background intensity) / (nuclear intensity - background intensity).

Clonogenic survival assay

Cells (200-2000) were plated in 6-well plates and allowed to incubate overnight. The following day, the medium was replaced by fresh medium supplemented with indicated concentrations of CPT or MMC. For TMP-UVA treatment, cells were cultured in 100 ng/ml TMP for 30 minutes, followed by indicated doses of 365nm UVA (0-500 J/m^2) using the Spectrolinker XL-1500 UV Crosslinker. When exposing cells to UVC irradiation, the culture medium was replaced with 200 µl of 1x PBS to optimise UV penetration and changed back to the normal growth medium after irradiation. The treated cells were then cultured for 14 days, fixed, and stained using a 1% (w/v) crystal violet solution in methanol. The number of colonies in each well was counted, and the survival rate for the corresponding treatment was calculated as the colony count divided by the number of initially seeded cells, then normalised to the untreated group.

Recombinant FH-RCC2 and FH-ZNF638 purification from Sf9 insect cells

RCC2 and ZNF638 were expressed in Sf9 insect cells using the pFastBac1 vector with an engineered N-terminal Flag-HA tag. The Bac-to-Bac Baculovirus Expression System (Life Technologies) was employed for protein expression according to the manufacturer's guidelines. FH-RCC2/FH-ZNF638 expressing Sf9 cells were washed once with 1x PBS and collected in cold (4°C) lysis buffer containing 20 mM Tris-HCl (pH 8.0), 100 mM KCl, 10% glycerol, 0.2% Tween-20, 2 mM β-mercaptoethanol, and 0.2 mM PMSF. The cell suspension was subjected to sonication using 4W power, with 1-second on/off pulses repeated for a total of 10 cycles. Subsequently, the lysate was clarified through centrifugation at 17,000g (4°C) for 20 minutes, and the resulting supernatant was collected. M2 anti-Flag agarose beads (A2220; Sigma-Aldrich) were incubated with the supernatant with constant rotation in a 4°C cold room for 2 hours. Afterwards, the sample was centrifuged at 2000 rpm (4°C) for 5 minutes, and the beads were resuspended in lysis buffer and transferred to a chromatography column (Bio-Rad). The beads were washed twice with lysis buffer containing 300 mM KCl. Finally, the bound protein was eluted by applying elution buffer (lysis buffer without Tween-20) supplemented with 0.5 mg/ml Flag peptide (Sigma-Aldrich).

Electrophoretic mobility shift assay (EMSA)

4 pmol of linear and fork-mimic crosslinked/non-crosslinked DNA probes (oligonucleotides used to construct the probes are listed in Table 5-7) were labelled with radioactive ^{32}P and resolved on a 12% polyacrylamide gel (TBE-PAA). Gel fragments containing the radiolabelled

probes were excised, and the DNA was purified and resuspended in water. The radioactivity of the ^{32}P labelled DNA was normalised to 500 counts per second per microliter (cps/µl) before use. 1 µl of the radiolabelled probe was then incubated with indicated amounts of recombinant FH-RCC2 or FH-ZNF638 for 1 hour at RT in EMSA binding buffer consisting of 5 mM Tris-HCl (pH 6.8/7.5/8.8), 50/100/150 mM KCl, 1 mM EDTA, 6% glycerol and 1 mM DTT. The samples were then supplemented with 0.05% bromophenol blue (BPB). A 4% PAA gel made with 0.4X TBE buffer was pre-electrophoresed at 150 V, 400 mA for 1 hour. Subsequently, the samples were loaded onto the gel and electrophoresed at 10 mA for 3 to 4 hours, with intermittent buffer exchange between the upper and lower chambers. The gel was then dried and exposed to X-ray films overnight for visualisation. The unlabelled DNA probes were produced by Dr. Kelvin Yaprianto (Cohn lab).

Table 5-7. List of oligonucleotides used to construct DNA probes for EMSA.

Oligonucleotides	**Sequence (5' → 3')**
Linear probe (+)	CGGTCACATTGTGAATTCGCCTCTCTGTCTAGTGAA AGACGCCGAATTCGTCTGATGGGC
Linear probe (-)	GCCCATCAGACGAATTCGGCGTCTTTCACTAGACAG AGAGGCGAATTCACAATGTGACCG
Fork-mimic probe (+)	CGTTGTGAAGTTCCTGTCCAGTCTAGCCGAAGCCTC AGAGTGTCAAGTTCAGAGTTGC
Fork-mimic probe (-)	CCTCACTGAAGGAGTCGACTCTTGCAAAACGGCTA GACTGGACAGGAACTTCACAACG
Fork-mimic probe (leading)	GCAACTCTGAACTTGACACTCTGAG
Fork-mimic probe (lagging)	GCAAGAGTCGACTCCTTCAGTGAGG

Immunofluorescence (IF)

The immunofluorescence was performed using the Click-iT RNA Alexa Fluor 488 Imaging Kit (C10329; Invitrogen) following the manufacturer's instructions. HeLa, ZNF638 knockout and dTAG-ZNF638 knock-in cells were plated on coverslips placed in 6-well plates at 40–50% confluency one day prior to the experiment. The following day, cells were untreated, treated with 20 µg/ml TMP for one hour and then exposed to 1000J/m^2 365nm UVA, or exposed to the same dose of UVA without TMP treatment. The cells were then incubated with 1 mM 5-ethynyl uridine (5-EU) for 1 hour to label the newly synthesised RNA. After incubation, the cells were

fixed by incubating with 3.7% formaldehyde in 1 x PBS for 15 minutes at RT. The fixative was removed, and the cells were washed once with 1 x PBS, and then permeabilised by incubating with 1 ml of 0.5% Triton X-100 in 1 x PBS for 15 minutes at RT. After removing the permeabilisation buffer, cells were washed once with 1 x PBS and incubated with 500 µl of Click-iT reaction cocktail containing the RNA reaction buffer, $CuSO_4$ and Alexa Fluor (AF) 488 azide for 30 minutes at RT (protected from light in following steps). Cells were then washed once with 1 ml of Click-iT reaction rinse buffer and twice with 1x PBS at RT.

For NPM labelling, cells were blocked in 10% normal goat serum (ab7481; abcam) for 1 hour at RT, and then washed with 1x PBS three times. The cells were then incubated with the 1:100 diluted NPM anti-mouse antibody (sc-70392; Santa Cruz) overnight at 4°C, and then washed with 1x PBS 3 times. The 1:500 diluted goat anti-mouse IgG H&L AF568 (ab175473; abcam) was then incubated with cells for 2 hours at RT and rinsed with 1x PBS three times. For DNA staining, 1:1,000 dilute Hoechst 33342 (Invitrogen) were incubated with cells for 15 minutes at RT. The staining solution was then removed, and cells were washed twice with 1x PBS, and proceeded to imaging. The cells were imaged using an Olympus IX81 microscope equipped with a PerkinElmer UltraView Vox spinning disk system at either 60X or 100X objective magnification. Image acquisition was controlled using Volocity software. Excitation of AF488 (labelling 5-EU) was achieved using a 488 nm laser, AF568 (labelling NPM) was excited using a 561 nm laser, and Hoechst 33342 (labelling nuclei) was excited with a 405nm laser. The newly synthesised nucleolar RNA level was subsequently measured using Fiji software. Specifically, the AF568 labelled NPM (the nucleolar marker) was used to mask the nucleolar regions. The intensities of AF488 (representing newly synthesised RNA) within the masked nucleolar regions were then measured and normalised against the extracellular background intensity.

Total RNA extraction for Northern blot

The total RNA extraction was performed using the Trizol Plus RNA Purification Kit (12183555; Invitrogen) following the manufacturer's instructions. HeLa WT, ZNF638 knockout and dTAG-ZNF638 knock-in cells were plated in 10cm culture dishes. Cells were untreated, treated with 20µg/ml TMP for one hour and then exposed to 1000J/m^2 365nm UVA (BLE-1T151 365 nm tube, Spectro-UV), or exposed to the same dose of UVA without TMP treatment. dTAG-ZNF638 knock-in cells were pre-treated with 500 nM dTAG-13 (6605; Tocris Bioscience) for 6 hours before TMP/UVA treatment and remained in the culture medium until the cells were

collected. One hour after UVA irradiation, 2 x10cm plates of cells (with ~80%-90% confluency) for each group were subjected to total RNA extraction. After removing the growth media, 4 ml of TRIzol reagent was added directly to each 10 cm culture dish to lyse the cells. The cell lysate was pipetted up and down several times to homogenise and transferred into 4 x 1.5 ml Eppendorf tubes and incubated for 5 minutes at RT. 0.2 ml of chloroform was then added into each tube and incubated for 2–3 minutes. Samples were centrifuged for 15 minutes at 12,000 × g at 4°C. The colourless, upper aqueous phase containing the RNA was then transferred to a new tube and mixed by vortexing with an equal volume of 70% ethanol. The mixture was transferred to a spin cartridge and centrifuged at 12,000 × g for 15 seconds. After discarding the flow-through, RNA on the spin cartridge membrane was washed with 700 µl of Wash Buffer I once and 500 µl of Wash Buffer II twice. During each wash, the wash buffer was added to the spin cartridge, centrifuged at 12,000 × g for 15 seconds, and the flow-through was discarded. After the final wash, the spin cartridge was centrifuged at 12,000 × g for 1 minute to dry the membrane. The RNA from each spin cartridge was eluted using 30 µl of RNase-free water by centrifuging at 16,000 × g for 2 minutes. The RNA concentration and 260/280 ratio for each sample were measured using NanoDrop 2000 Spectrophotometer (ThermoFisher Scientific). All RNA samples have a 260/280 ratio above 2.

Northern blot (NB)

20 µg of total RNA extracted as above for each group was used in the Northern blot. The total RNA was mixed with 3 volumes of NorthernMax Formaldehyde Load Dye (AM8552; Invitrogen) and incubated for 15 minutes in a 65°C heating block. The samples were briefly spined down in a microcentrifuge and chilled on ice. RNA samples were then loaded on a 1% formaldehyde gel (1% agarose, 37% formaldehyde in 1x MOPS buffer containing 20 mM MOPS pH 7.0, 8 mM NaAc and 2 mM EDTA) and ran at 120V for 7-8 hours in 1x MOPS buffer (until the Xylene Cyanol migrated to the ~3/4 of the gel). After electrophoresis, the gel was marked on the right lower edge, removed from the e/ph container and submersed in 10 mM NaOH for 20 min at RT with shaking. The gel was then washed quickly with MilliQ water and incubated with 20 x SSC buffer (3M NaCl, 0.3M sodium citrate, pH 7.0) for 5 minutes at RT, followed by the incubation with 10 x SSC buffer for 40 minutes at RT.

Next, samples were transferred from the gel to a BrightStar-Plus positively charged nylon membrane (AM10102; Invitrogen) in a tray filled with 10 x SSC buffer. Specifically, two Whatman 3MM filters (21 cm x 36 cm) were wetted with the 10 x SSC and laid over a glass

plate on the tray with both ends immersed in the buffer. Air bubbles between the plate and the filters were removed by rolling a sterile pipette on the filter. The gel was then put on the wet filters with the upper side down. Air bubbles between the gel and filters were removed carefully and the wet nylon membrane was put on the gel. Another 3 Whatman 3MM filters (10 cm x 14 cm) were wetted in 10 x SSC buffer and laid on the membrane and air bubbles were removed again. Then 3 dry Whatman 3MM filters were laid on top. A stack of paper towels (8-10 cm high) was then put on top of the dry Whatman 3MM filters, followed by a glass plate and a 500g weight on the top. The capillary transfer from the gel to the membrane was carried out overnight (18-24 hours). After transfer, the membrane was rinsed briefly in 2 x SSC, 0.1% SDS and then the RNA was immobilised on the membrane by 120 mJ UV-crosslinking using the UV Stratalinker 1800 (Stratagene). The membrane was then incubated with 3% HAc for 10 minutes at RT and stained for 1 minute with 0.04% methyleneblue/0.5M Na-acetate (pH 5.2-6.5). The membrane was de-stained with MilliQ water until the background was nearly white and images of the membrane with methyleneblue staining were captured.

The membrane was then hybridised with the 47S pre-rRNA 5'-ETS targeting oligo probe (5'CGGAGGCCCAACCTCTCCGACGACAGGTCGCCAGAGGACAGCGTGTCAGC3') using the ULTRAhyb–oligo buffer (AM8663; Invitrogen). 20 ml of ULTRAhyb–oligo buffer was pre-heated at 68ºC and then transferred to a glass roller bottle. The membrane was then curled and inserted into the roller bottle with RNA facing inside. For pre-hybridisation, the membrane was incubated with the ULTRAhyb–oligo buffer for 2 hours at 42°C under continuous rolling. Next, 1µg of the oligo probe was labelled with BIOTIN-11-dUTP using the Biotin DecaLabel DNA Labeling Kit (K0651; ThermoFisher Scientific), and the biotin-labelled 5'-ETS oligo probe was added directly into the pre-hybridisation buffer to make the final probe concentration 100 ng/ml. The membrane was then hybridised with the biotin-labelled 5'-ETS probe overnight (18-24 hours) at 42°C under continuous rolling. After hybridisation, the membrane was washed twice in 2 x SSC/0.5% SDS for 10 minutes at RT, then washed once with 0.1 x SSC/0.1% SDS for 20 minutes at RT with agitation. Following the washing steps, the biotin-labelled probes bound to the 47S pre-rRNA species on the membrane were detected using the Biotin Chromogenic Detection Kit (K0661; ThermoFisher Scientific).

FH-ZNF638 Flag-immunoprecipitation (IP)

Mock and FH-ZNF638 knock-in HeLa cells were seeded as a monolayer in 6 x 15 cm dishes. Cells were untreated, treated with 10µM CPT, with 1000 J/m^2 of 365nm UVA alone, or with

20 μg/ml TMP for one hour and then exposed to 1000 J/m^2 of 365nm UVA. Four hours after CPT treatment or two hours after UVA exposure, all cells were harvested and centrifuged at 1,800 x g (4°C) for 5 minutes. The pellet was washed once in cold PBS and then once in one pellet volume of cold lysis buffer (20mM HEPES pH 7.5, 100 mM NaCl, 0.01% CHAPS, 10% Glycerol, 0.2 mM PMSF and 2 mM β-mercaptoethanol). The pellet from each group was then resuspended in 20 ml of cold lysis buffer and sonicated for 10 minutes (4 seconds on/off intervals) at 4 W in an ice bath. The sonicated cells were then centrifuged at 15,000 rpm (4°C) for 30 minutes. Subsequently, the supernatant was collected and incubated with 250 μl of anti-Flag M2 agarose beads (A2220; Sigma-Aldrich) for 2 hours at 4°C on a rotator. The mixture was centrifuged at 1,000 x g (4°C) for 5 minutes. The beads were transferred into a chromatography column (Bio-Rad) and washed three times with cold lysis buffer (2 ml buffer for each wash). The protein was eluted for 2 hours in 300 μl lysis buffer supplemented with 1 mg/ml Flag peptide. The Flag eluates were used in following silver staining and Western blot to detect the purified FH-ZNF638 protein. For silver staining, the samples were prepared in the same manner as WB samples as described above. The samples were then loaded on a 4-12% NuPage Bis-Tris gradient gel (NP0323; Life Technologies) and visualised using the SilverQuest Silver Staining Kit (LC6070; Invitrogen) following the manufacturer's instructions.

FH-ZNF638 co-immunoprecipitation (with Benzonase and crosslinker)

Mock and FH-ZNF638 knock-in HeLa cells were seeded as a monolayer in 16 x 15 cm dishes. Untreated cells were harvested and centrifuged at 1,800 x g (4°C) for 5 minutes. The pellet was washed once in cold 1 x PBS and then once in one pellet volume of hypotonic buffer (10 mM HEPES-KOH pH 7.5, 10 mM KCl, 1.5 mM $MgCl_2$, 0.2 mM PMSF, 2 mM β-mercaptoethanol). The pellet was then resuspended in twice pellet volume of hypotonic buffer and left on ice for 10 minutes. The suspension was subjected to homogenisation in a Dounce homogeniser (pestle size “B”) for 20 strokes. The homogenised sample was centrifuged at 3,300 x g (4°C) for 15 minutes. The supernatant (cytoplasmic fraction) was collected for western blot and the pellet was resuspended in half its volume of low salt NE buffer (20 mM HEPES-KOH pH 7.5, 50 mM KCl, 1.5 mM $MgCl_2$, 20% glycerol, 0.2 mM PMSF, 2 mM β-mercaptoethanol) supplemented with 0.01% Triton X-100 and 0.75 U/μL Benzonase. The resuspended nuclear pellet was kept on ice for 30 minutes. The samples were then crosslinked using 4% formaldehyde for 4 minutes at RT. Subsequently, 0.05% of the total volume of 2.5 M glycine was added to quench the non-crosslinked formaldehyde. The mixture was centrifuged at 3,000

x g (4°C) for 10 minutes. The supernatant was discarded, and the crosslinked nuclei were washed three times with ten times the pellet volume of cold 1 x PBS. After the last wash, the nuclei were resuspended in equal volumes of high salt NE buffer (20 mM HEPES-KOH pH 7.5, 1 M NaCl, 1.5 mM $MgCl_2$, 1% Tween-20, 0.15% SDS, 25% glycerol, 0.2 mM PMSF, 2 mM β-mercaptoethanol), and then sonicated for 20 minutes (1 second on/off intervals) at 4 W in an ice bath. The sonicated lysate was diluted five-fold with low salt NE buffer supplemented with 125 mM NaCl and 1% Tween-20 and centrifuged at 17,000 x g (4°C) for 20 minutes. The supernatant was then collected as the soluble nuclear fraction.

Next, the nuclear extract was incubated with M2 anti-Flag beads (0.025% of total extract volume) for 2 hours at 4°C on a rotator. The mixture was centrifuged at 1,000 x g (4°C) for 5 minutes. The beads were then resuspended in 1 ml of Buffer A (20 mM Tris-HCl pH 8.0, 100 mM NaCl, 5 mM $MgCl_2$, 0.1% Tween-20, 10% glycerol, 0.2 mM PMSF, 2 mM β-mercaptoethanol) and transferred into a chromatography column (Bio-Rad) on ice. The beads were washed three times with Buffer A (2 ml buffer for each wash) on ice. The protein was then eluted for 1 hour in one bed volume of Buffer A supplemented with 0.5 mg/ml Flag peptide in a cold room (4°C). Subsequently, the Flag eluate was mixed with 0.2% eluate volume of anti-HA agarose (Protein A- sepharose; Sigma-Aldrich, 12CA5 serum; Babco) and incubated on a rotator for 2 hours in the cold room (4°C). The mixture was centrifuged at 1,000 x g (4°C) for 5 minutes and the supernatant was collected as HA flowthrough for silver staining. The HA beads were resuspended in 200 µl of buffer A and transferred into a chromatography column on ice. The HA beads were washed three times in the column with Buffer A (2 ml buffer for each wash) on ice. Last, the protein sample was eluted in one bed volume of Buffer A supplemented with 0.5 mg/ml HA peptide (I2149; Sigma- Aldrich) in the cold room (4°C). Western blot and silver staining were performed to detect the presence of FH-ZNF638/ZNF638 in the samples. The whole cell lysate, cytoplasmic fraction and soluble nuclear fraction were prepared as previously described and used in the Western blot. Flag eluates, HA flowthrough and HA eluates were subjected to silver staining and visualised using the SilverQuest Silver Staining Kit (LC6070; Invitrogen).

FH-ZNF638 co-immunoprecipitation (with native nuclear extraction)

FH-ZNF638-expressing HeLa.S3 cells were cultured in suspension in 1L culture medium. Untreated cells were harvested and centrifuged at 200 x g (4°C) for 5 minutes. The cells were washed once in cold 1 x PBS and once in cold hypotonic buffer (10 mM Tris-HCl pH 7.3, 10

mM KCl, 1.5 mM $MgCl_2$, 0.2 mM PMSF, 10 mM β-mercaptoethanol). The cell pellet was then resuspended in twice its volume of cold hypotonic buffer and left on ice for 10 minutes. The resuspended pellet was homogenised using a Dounce homogeniser (size "B" pestle) for 20 strokes and centrifuged at 3,000 x g (4°C) for 15 minutes. The supernatant (cytoplasmic fraction) was collected as control sample. The nuclear pellet was resuspended in half its volume of low salt buffer (20 mM Tris-HCl pH 7.3, 3 mM $MgCl_2$, 0.2 mM EDTA, 25% glycerol, 0.3% Tween-20, 0.2 mM PMSF, 10 mM β-mercaptoethanol). Subsequently, half nuclear pellet volume of high salt buffer (20 mM Tris-HCl pH 7.3, 1.5 mM $MgCl_2$, 0.2 mM EDTA, 25% glycerol, 1.6 M KCl, 0.2 mM PMSF, 10 mM β-mercaptoethanol) was added dropwise into the sample, under constant vortexing. The sample was incubated on a rotator for 30 minutes in the cold room and then centrifuged at 17,000 x g (4°C) for 30 minutes. The supernatant (soluble nuclear fraction) was collected and dialysed against BC-100 (20 mM Tris- HCl pH 7.3, 100 mM KCl, 0.2 mM EDTA, 20% glycerol, 0.2 mM PMSF, 10 mM β-mercaptoethanol) for 1 hour in the 4°C cold room. The dialysed sample was centrifuged again at 17,000 x g (4°C) for 20 minutes and the supernatant was collected as the soluble nuclear extract.

The extract was then incubated with M2 anti-FLAG agarose beads (20/50/100 µl) on a rotator for 2 hours in the 4°C cold room. After incubation, the mixture was centrifuged at 1,000 rpm (4°C) for 5 minutes and the beads were washed twice with Flag wash buffer (20 mM Tris-HCl pH 8.0, 100 mM KCl, 0.2 mM EDTA, 0.1% Tween-20, 5 mM $MgCl_2$, 10% glycerol, 0.2 mM PMSF, 2 mM β-mercaptoethanol). The beads were then resuspended in the same buffer, transferred into a chromatography column (Bio-Rad), and washed twice with Flag wash buffer. Bound proteins were eluted for 2 x 1 hour in one bed volume of Flag wash buffer supplemented with 0.5 mg/ml Flag peptide. The Flag eluate was mixed with anti-HA agarose (20% of eluate volume) and incubated on a rotator for 2 hours in the cold room. The mixture was then centrifuged at 1,000 rpm (4°C) for 5 minutes and the beads were washed twice in HA wash buffer (100 mM Tris-HCl pH 6.8, 0.2 mM EDTA, 100 mM KCl, 0.1% Tween-20, 10% glycerol, 0.2 mM PMSF, 2 mM β- mercaptoethanol). Next, the beads were transferred to a chromatography spin column (Bio-Rad) and washed again twice with HA wash buffer. Bound proteins were eluted for 2 x 1 hour in one bed volume of HA wash buffer supplemented with 0.5 mg/ml HA peptide. The presence of FH-ZNF638/ZNF638 in eluates and control samples was detected by Western blot.

Nucleoli extraction

Halo-ZNF638 knock-in HeLa cells were seeded as a monolayer in a 15 cm culture dish. Prior to treatment, the cells were labelled with 100nM Janelia Fluor 549 HaloTag Ligand (GA1110; Promega) for 20 minutes and then washed with 1 x PBS 3 times (5 minutes for each wash). Cells were then treated with 20 μg/ml TMP for 30 minutes and then exposed to 1000 J/m^2 365nm UVA (BLE-1T151 365 nm tube, Spectro-UV). One hour after UVA irradiation, cells were rinsed twice with 20 ml of cold solution I (0.5 M sucrose, 3 mM $MgCl_2$, 0.2 mM PMSF, 10 mM β-mercaptoethanol, pre-cooled to 4°C) and then scraped from the dish on ice. ~700 μl of acquired cell suspension was quickly transferred into a 1.5 ml Eppendorf tube. The cells were then sonicated on ice at 5W, 30s on and 30s off, for five cycles. Images of the cell suspension were captured before and after the sonication using the Olympus IX81 microscope. Subsequently, 0.98 ml of pre-cooled (4°C) solution II (1.0 M sucrose, 3 mM $MgCl_2$, 0.2 mM PMSF, 10 mM β-mercaptoethanol) was carefully added below the sonicated cell suspension and centrifuged at 1,800 ×g for 10 minutes at 4°C. The supernatant was collected as a control sample and the resulting pellet containing nucleoli was resuspended in 0.5 ml of cold (4°C) Solution I. 0.7 ml of pre-cooled (4°C) solution II was again carefully added below the resuspended nucleoli and the sucrose cushion was centrifuged at 1,800 × g for 5 minutes at 4°C. The resulting pellet containing isolated nucleoli was processed for Western blot to detect the protein level of Halo-ZNF638, NPM and α-tubulin.

FH-ZNF638 co-immunoprecipitation (following nucleoli extraction)

FH-ZNF638 knock-in HeLa.S3 cells were seeded in 20 x 15 cm culture dishes. Cells were treated with 20 μg/ml TMP for 30 minutes and then exposed to 1000 J/m^2 365nm UVA in a Spectrolinker™ XL-1500 UV Crosslinker. One hour after UVA irradiation, nucleoli were isolated as described above. The resulting pellet containing isolated nucleoli was resuspended in 1 ml of Buffer A (20 mM Tris-HCl pH 8.0, 100 mM KCl, 5 mM $MgCl_2$, 0.1% Tween-20, 10% glycerol, 0.2 mM PMSF, 2 mM β-mercaptoethanol) and incubated with 200 μl of M2 anti-Flag beads for 2 hours in cold room (4°C) under constant rotating. The mixture was centrifuged at 1,000 x g (4°C) for 5 minutes and the supernatant was collected as Flag flowthrough for Western blot. The Flag beads were then resuspended in 1 ml of Buffer A and transferred into a chromatography column (Bio-Rad) on ice. The beads were washed three times with Buffer A (2 ml buffer for each wash). The protein was then eluted for 1 hour in 200 μl of Buffer A supplemented with 1 mg/ml Flag peptide in a cold room (4°C). The Flag eluate was mixed with

100 µl of anti-HA agarose and incubated on a rotator for 2 hours in the cold room (4°C). The mixture was centrifuged at 1,000 x g (4°C) for 5 minutes and the supernatant was collected as HA flowthrough. The HA beads were resuspended in 100 ul of buffer A and transferred into a chromatography column on ice. The HA beads were washed three times in the column with Buffer A (2 ml buffer for each wash) on ice, and the protein was eluted in 50 µl of Buffer A supplemented with 1 mg/ml HA peptide in the cold room (4°C).

Chapter 6. References

Aas, P. A., Otterlei, M., Falnes, P., Vågbø, C. B., Skorpen, F., Akbari, M., Sundheim, O., Bjørås, M., Slupphaug, G., Seeberg, E., & Krokan, H. E. (2003). Human and bacterial oxidative demethylases repair alkylation damage in both RNA and DNA. *Nature 2003 421:6925*, *421*(6925), 859–863. https://doi.org/10.1038/nature01363

Abuetabh, Y., Wu, H. H., Chai, C., Al Yousef, H., Persad, S., Sergi, C. M., & Leng, R. (2022). DNA damage response revisited: the p53 family and its regulators provide endless cancer therapy opportunities. *Experimental & Molecular Medicine 2022 54:10*, *54*(10), 1658–1669. https://doi.org/10.1038/s12276-022-00863-4

Acharya, S., Wilson, T., Gradia, S., Kane, M. F., Guerrette, S., Marsischky, G. T., Kolodner, R., & Fishel, R. (1996). hMSH2 forms specific mispair-binding complexes with hMSH3 and hMSH6. *Proceedings of the National Academy of Sciences of the United States of America*, *93*(24), 13629. https://doi.org/10.1073/PNAS.93.24.13629

Adams, R. R., Carmena, M., & Earnshaw, W. C. (2001). Chromosomal passengers and the (aurora) ABCs of mitosis. *Trends in Cell Biology*, *11*(2), 49–54. https://doi.org/10.1016/S0962-8924(00)01880-8

Adams, R. R., Wheatleya, S. P., Gouldsworthy, A. M., Kandels-Lewis, S. E., Carmena, M., Smythe, C., Gerloff, D. L., & Earnshaw, W. C. (2000). INCENP binds the Aurora-related kinase AIRK2 and is required to target it to chromosomes, the central spindle and cleavage furrow. *Current Biology : CB*, *10*(17), 1075–1078. https://doi.org/10.1016/S0960-9822(00)00673-4

Adelmant, G., Calkins, A. S., Garg, B. K., Card, J. D., Askenazi, M., Miron, A., Sobhian, B., Zhang, Y., Nakatani, Y., Silver, P. A., Iglehart, J. D., Marto, J. A., & Lazaro, J. B. (2012). DNA Ends Alter the Molecular Composition and Localization of Ku Multicomponent Complexes. *Molecular & Cellular Proteomics : MCP*, *11*(8), 411. https://doi.org/10.1074/MCP.M111.013581

Agapov, A., Olina, A., & Kulbachinskiy, A. (2022). RNA polymerase pausing, stalling and bypass during transcription of damaged DNA: from molecular basis to functional consequences. *Nucleic Acids Research*, *50*(6), 3018. https://doi.org/10.1093/NAR/GKAC174

Ahnesorg, P., Smith, P., & Jackson, S. P. (2006). XLF interacts with the XRCC4-DNA Ligase IV complex to promote DNA nonhomologous end-joining. *Cell*, *124*(2), 301–313. http://www.cell.com/article/S0092867406000031/fulltext

Ahrabi, S., Sarkar, S., Pfister, S. X., Pirovano, G., Higgins, G. S., Porter, A. C. G., & Humphrey, T. C. (2016). A role for human homologous recombination factors in suppressing microhomology-mediated end joining. *Nucleic Acids Research*, *44*(12), 5743–5757. https://doi.org/10.1093/NAR/GKW326

Ait Saada, A., Lambert, S. A. E., & Carr, A. M. (2018). Preserving replication fork integrity and competence via the homologous recombination pathway. *DNA Repair*, *71*, 135. https://doi.org/10.1016/J.DNAREP.2018.08.017

Al Abo, M., Dejsuphong, D., Hirota, K., Yonetani, Y., Yamazoe, M., Kurumizaka, H., & Takeda, S. (2014). Compensatory functions and interdependency of the DNABinding domain of BRCA2 with the BRCA1-PALB2-BRCA2 complex. *Cancer Research*, *74*(3), 797–807. https://doi.org/10.1158/0008-5472.CAN-13-1443/651278/AM/COMPENSATORY-FUNCTIONS-AND-INTERDEPENDENCY-OF-THE

Alcón, P., Shakeel, S., Chen, Z. A., Rappsilber, J., Patel, K. J., & Passmore, L. A. (2020).

FANCD2–FANCI is a clamp stabilized on DNA by monoubiquitination of FANCD2 during DNA repair. *Nature Structural & Molecular Biology 2020 27:3*, *27*(3), 240–248. https://doi.org/10.1038/S41594-020-0380-1

Alhmoud, J. F., Woolley, J. F., Al Moustafa, A.-E., & Malki, M. I. (2020). DNA Damage/Repair Management in Cancers. *Cancers 2020, Vol. 12, Page 1050*, *12*(4), 1050. https://doi.org/10.3390/cancers12041050

Alpi, A. F., Pace, P. E., Babu, M. M., & Patel, K. J. (2008). Mechanistic Insight into Site-Restricted Monoubiquitination of FANCD2 by Ube2t, FANCL, and FANCI. *Molecular Cell*, *32*(6), 767–777. https://doi.org/10.1016/J.MOLCEL.2008.12.003

Alter, B. P. (2014). Fanconi anemia and the development of leukemia. *Best Practice & Research Clinical Haematology*, *27*(3–4), 214–221. https://doi.org/10.1016/J.BEHA.2014.10.002

Alter, B. P., & Giri, N. (2016). Thinking of VACTERL-H? Rule out Fanconi Anemia according to PHENOS. *American Journal of Medical Genetics Part A*, *170*(6), 1520–1524. https://doi.org/10.1002/AJMG.A.37637

Alter, B. P., Giri, N., Savage, S. A., Quint, W. G. V., De Koning, M. N. C., & Schiffman, M. (2013). Squamous cell carcinomas in patients with Fanconi anemia and dyskeratosis congenita: A search for human papillomavirus. *International Journal of Cancer*, *133*(6), 1513–1515. https://doi.org/10.1002/IJC.28157

Alter, B. P., & Rosenberg, P. S. (2013). VACTERL-H Association and Fanconi Anemia. *Molecular Syndromology*, *4*(1–2), 87–93. https://doi.org/10.1159/000346035

Amé, J. C., Spenlehauer, C., & De Murcia, G. (2004). The PARP superfamily. *BioEssays : News and Reviews in Molecular, Cellular and Developmental Biology*, *26*(8), 882–893. https://doi.org/10.1002/BIES.20085

Ameziane, N., May, P., Haitjema, A., Van De Vrugt, H. J., Van Rossum-Fikkert, S. E., Ristic, D., Williams, G. J., Balk, J., Rockx, D., Li, H., Rooimans, M. A., Oostra, A. B., Velleuer, E., Dietrich, R., Bleijerveld, O. B., Maarten Altelaar, A. F., Meijers-Heijboer, H., Joenje, H., Glusman, G., … Dorsman, J. C. (2015). A novel Fanconi anaemia subtype associated with a dominant-negative mutation in RAD51. *Nature Communications 2015 6:1*, *6*(1), 1–11. https://doi.org/10.1038/ncomms9829

Amir, R. E., Van Den Veyver, I. B., Wan, M., Tran, C. Q., Francke, U., & Zoghbi, H. Y. (1999). Rett syndrome is caused by mutations in X-linked MECP2, encoding methyl-CpG-binding protein 2. *Nature Genetics 1999 23:2*, *23*(2), 185–188. https://doi.org/10.1038/13810

Amunugama, R., Willcox, S., Wu, R. A., Abdullah, U. B., El-Sagheer, A. H., Brown, T., McHugh, P. J., Griffith, J. D., & Walter, J. C. (2018). Replication Fork Reversal during DNA Interstrand Crosslink Repair Requires CMG Unloading. *Cell Reports*, *23*(12), 3419–3428. https://doi.org/10.1016/j.celrep.2018.05.061

Anand, S. K., Sharma, A., Singh, N., & Kakkar, P. (2020). Entrenching role of cell cycle checkpoints and autophagy for maintenance of genomic integrity. *DNA Repair*, *86*, 102748. https://doi.org/10.1016/J.DNAREP.2019.102748

Andersen, J. S., Lyon, C. E., Fox, A. H., Leung, A. K. L., Lam, Y. W., Steen, H., Mann, M., & Lamond, A. I. (2002). Directed proteomic analysis of the human nucleolus. *Current Biology : CB*, *12*(1), 1–11. https://doi.org/10.1016/S0960-9822(01)00650-9

Andersen, S., Heine, T., Sneve, R., König, I., Krokan, H. E., Epe, B., & Nilsen, H. (2005). Incorporation of dUMP into DNA is a major source of spontaneous DNA damage, while excision of uracil is not required for cytotoxicity of fluoropyrimidines in mouse

embryonic fibroblasts. *Carcinogenesis*, *26*(3), 547–555. https://doi.org/10.1093/CARCIN/BGH347

Andreassen, P. R., Palmer, D. K., Wener, M. H., & Margolis, R. L. (1991). *Telophase disc: a new mammalian mitotic organelle that bisects telophase cells with a possible function in cytokinesis*.

Andrews, A. M., McCartney, H. J., Errington, T. M., D'Andrea, A. D., & Macara, I. G. (2018). A senataxin-associated exonuclease SAN1 is required for resistance to DNA interstrand cross-links. *Nature Communications*, *9*(1). https://doi.org/10.1038/S41467-018-05008-8

Aria, V., & Yeeles, J. T. P. (2019). Mechanism of Bidirectional Leading-Strand Synthesis Establishment at Eukaryotic DNA Replication Origins. *Molecular Cell*, *73*(2), 199. https://doi.org/10.1016/J.MOLCEL.2018.10.019

Arjunan, K. P., Sharma, V. K., & Ptasinska, S. (2015). Effects of atmospheric pressure plasmas on isolated and cellular DNA—a review. *International Journal of Molecular Sciences*, *16*(2), 2971–3016. https://doi.org/10.3390/IJMS16022971

Atkinson, J., & McGlynn, P. (2009). Replication fork reversal and the maintenance of genome stability. *Nucleic Acids Research*, *37*(11), 3475. https://doi.org/10.1093/NAR/GKP244

Aubert, M., O'donohue, M. F., Lebaron, S., & Gleizes, P. E. (2018). Pre-Ribosomal RNA Processing in Human Cells: From Mechanisms to Congenital Diseases. *Biomolecules*, *8*(4). https://doi.org/10.3390/BIOM8040123

Auerbach, A. D. (2003). Diagnosis of Fanconi Anemia by Diepoxybutane Analysis. *Current Protocols in Human Genetics*, *37*(1), 8.7.1-8.7.15. https://doi.org/10.1002/0471142905.HG0807S37

Auerbach, A. D. (2009). Fanconi Anemia and its Diagnosis. *Mutation Research*, *668*(1–2), 4. https://doi.org/10.1016/J.MRFMMM.2009.01.013

Auerbach, A. D., & Allen, R. G. (1991). Leukemia and preleukemia in Fanconi anemia patients. *Cancer Genetics and Cytogenetics*, *51*(1), 1–12. https://doi.org/10.1016/0165-4608(91)90002-c

Averbeck, N. B., Ringel, O., Herrlitz, M., Jakob, B., Durante, M., & Taucher-Scholz, G. (2014). DNA end resection is needed for the repair of complex lesions in G1-phase human cells. *Cell Cycle*, *13*(16), 2509–2516. https://doi.org/10.4161/15384101.2015.941743/SUPPL_FILE/KCCY_A_941743_SM1184.PDF

Bachrati, C. Z., & Hickson, I. D. (2009). Dissolution of double Holliday junctions by the concerted action of BLM and topoisomerase IIIalpha. *Methods in Molecular Biology (Clifton, N.J.)*, *582*, 91–102. https://doi.org/10.1007/978-1-60761-340-4_8

Bailly, V., & Verly, W. G. (1988). Possible roles of beta-elimination and delta-elimination reactions in the repair of DNA containing AP (apurinic/apyrimidinic) sites in mammalian cells. *Biochemical Journal*, *253*(2), 553. https://doi.org/10.1042/BJ2530553

Balmus, G., Barros, A. C., Wijnhoven, P. W. G., Lescale, C., Hasse, H. L., Boroviak, K., le Sage, C., Doe, B., Speak, A. O., Galli, A., Jacobsen, M., Deriano, L., Adams, D. J., Blackford, A. N., & Jackson, S. P. (2016). Synthetic lethality between PAXX and XLF in mammalian development. *Genes & Development*, *30*(19), 2152–2157. https://doi.org/10.1101/GAD.290510.116

Balmus, G., Pilger, D., Coates, J., Demir, M., Sczaniecka-Clift, M., Barros, A. C., Woods, M., Fu, B., Yang, F., Chen, E., Ostermaier, M., Stankovic, T., Ponstingl, H., Herzog, M., Yusa, K., Martinez, F. M., Durant, S. T., Galanty, Y., Beli, P., … Jackson, S. P. (2019). ATM

orchestrates the DNA-damage response to counter toxic non-homologous end-joining at broken replication forks. *Nature Communications 2019 10:1*, *10*(1), 1–18. https://doi.org/10.1038/s41467-018-07729-2

Banaś, A. K., Zgłobicki, P., Kowalska, E., Bażant, A., Dziga, D., & Strzałka, W. (2020). All You Need Is Light. Photorepair of UV-Induced Pyrimidine Dimers. *Genes*, *11*(11), 1–17. https://doi.org/10.3390/GENES11111304

Barbin, A., Wang, R., O'Connor, P. J., & Elder, R. H. (2003). Increased Formation and Persistence of 1,N6-Ethenoadenine in DNA Is Not Associated with Higher Susceptibility to Carcinogenesis in Alkylpurine-DNA-N-Glycosylase Knockout Mice Treated with Vinyl Carbamate. *Cancer Research*, *63*(22), 7699–7703. http://aacrjournals.org/cancerres/article-pdf/63/22/7699/2509392/zch02203007699.pdf

Barcellos-Hoff, M. H., Park, C., & Wright, E. G. (2005). Radiation and the microenvironment – tumorigenesis and therapy. *Nature Reviews Cancer 2005 5:11*, *5*(11), 867–875. https://doi.org/10.1038/nrc1735

Barlow, C., Dennery, P. A., Shigenaga, M. K., Smith, M. A., Morrow, J. D., Roberts, L. J., Wynshaw-Boris, A., & Levine, R. L. (1999). Loss of the ataxia–telangiectasia gene product causes oxidative damage in target organs. *Proceedings of the National Academy of Sciences of the United States of America*, *96*(17), 9915. https://doi.org/10.1073/PNAS.96.17.9915

Barnes, D. E., & Lindahl, T. (2004). Repair and Genetic Consequences of Endogenous DNA Base Damage in Mammalian Cells. *Https://Doi.Org/10.1146/Annurev.Genet.38.072902.092448*, *38*, 445–476. https://doi.org/10.1146/ANNUREV.GENET.38.072902.092448

Bartek, J. (2011). DNA damage response, genetic instability and cancer: From mechanistic insights to personalized treatment. *Molecular Oncology*, *5*(4), 303–307. https://doi.org/10.1016/J.MOLONC.2011.07.006

Basbous, J., & Constantinou, A. (2019). A tumor suppressive DNA translocase named FANCM. In *Critical Reviews in Biochemistry and Molecular Biology* (Vol. 54, Issue 1, pp. 27–40). Taylor and Francis Ltd. https://doi.org/10.1080/10409238.2019.1568963

Bass, M. D., Roach, K. A., Morgan, M. R., Mostafavi-Pour, Z., Schoen, T., Muramatsu, T., Mayer, U., Ballestrem, C., Spatz, J. P., & Humphries, M. J. (2007). Syndecan-4-dependent Rac1 regulation determines directional migration in response to the extracellular matrix. *Journal of Cell Biology*, *177*(3), 527–538. https://doi.org/10.1083/JCB.200610076/VIDEO-7

Baßler, J., & Hurt, E. (2019). Eukaryotic Ribosome Assembly. *Annual Review of Biochemistry*, *88*, 281–306. https://doi.org/10.1146/annurev-biochem-013118-110817

Basu, A. K. (2018). DNA damage, mutagenesis and cancer. *International Journal of Molecular Sciences*, *19*(4), 970. https://doi.org/10.3390/IJMS19040970

Becker, J. R., Clifford, G., Bonnet, C., Groth, A., Wilson, M. D., & Chapman, J. R. (2021). BARD1 reads H2A lysine 15 ubiquitination to direct homologous recombination. *Nature 2021 596:7872*, *596*(7872), 433–437. https://doi.org/10.1038/s41586-021-03776-w

Beggs, R., & Yang, E. S. (2019). Targeting DNA repair in precision medicine. *Advances in Protein Chemistry and Structural Biology*, *115*, 135–155. https://doi.org/10.1016/BS.APCSB.2018.10.005

Bell, J. C., Dombrowski, C. C., Plank, J. L., Jensen, R. B., & Kowalczykowski, S. C. (2023). BRCA2 chaperones RAD51 to single molecules of RPA-coated ssDNA. *Proceedings of the*

National Academy of Sciences of the United States of America, *120*(14), e2221971120. https://doi.org/10.1073/PNAS.2221971120/SUPPL_FILE/PNAS.2221971120.SM03.MOV

Bell, O., Tiwari, V. K., Thomä, N. H., & Schübeler, D. (2011). Determinants and dynamics of genome accessibility. *Nature Rev. Genet.*, *12*(8), 554–564. https://doi.org/10.1038/nrg3017

Bellissent-Waydelich, A., Vanier, M. T., Albigès-Rizo, C., & Simon-Assmann, P. (1999). Talin concentrates to the midbody region during mammalian cell cytokinesis. *The Journal of Histochemistry and Cytochemistry : Official Journal of the Histochemistry Society*, *47*(11), 1357–1367. https://doi.org/10.1177/002215549904701102

Benajiba, L., Salvado, C., Dalle, J. H., Jubert, C., Galambrun, C., Soulier, J., Socié, G., & De Latour, R. P. (2015). HLA-matched related-donor HSCT in Fanconi anemia patients conditioned with cyclophosphamide and fludarabine. *Blood*, *125*(2), 417–418. https://doi.org/10.1182/BLOOD-2014-10-605113

Bennardo, N., Cheng, A., Huang, N., & Stark, J. M. (2008). Alternative-NHEJ Is a Mechanistically Distinct Pathway of Mammalian Chromosome Break Repair. *PLoS Genetics*, *4*(6), 1000110. https://doi.org/10.1371/JOURNAL.PGEN.1000110

Berezney, R., Dubey, D. D., & Huberman, J. A. (2000). Heterogeneity of eukaryotic replicons, replicon clusters, and replication foci. *Chromosoma*, *108*(8), 471–484. https://doi.org/10.1007/S004120050399/METRICS

Berquist, B. R., & Wilson, D. M. (2012). Pathways for Repairing and Tolerating the Spectrum of Oxidative DNA Lesions. *Cancer Letters*, *327*(1–2), 61. https://doi.org/10.1016/J.CANLET.2012.02.001

Berti, M., Chaudhuri, A. R., Thangavel, S., Gomathinayagam, S., Kenig, S., Vujanovic, M., Odreman, F., Glatter, T., Graziano, S., Mendoza-Maldonado, R., Marino, F., Lucic, B., Biasin, V., Gstaiger, M., Aebersold, R., Sidorova, J. M., Monnat, R. J., Lopes, M., & Vindigni, A. (2013). Human RECQ1 promotes restart of replication forks reversed by DNA topoisomerase I inhibition. *Nature Structural & Molecular Biology 2013 20:3*, *20*(3), 347–354. https://doi.org/10.1038/nsmb.2501

Berti, M., & Vindigni, A. (2016). Replication stress: getting back on track. *Nature Structural & Molecular Biology 2016 23:2*, *23*(2), 103–109. https://doi.org/10.1038/nsmb.3163

Bessho, T., Mu, D., & Sancar, A. (1997). Initiation of DNA Interstrand Cross-Link Repair in Humans: the Nucleotide Excision Repair System Makes Dual Incisions 5′ to the Cross-linked Base and Removes a 22- to 28-Nucleotide-long Damage-Free Strand. *Https://Doi-Org.Ezproxy-Prd.Bodleian.Ox.Ac.Uk/10.1128/MCB.17.12.6822*, *17*(12), 6822–6830. https://doi.org/10.1128/MCB.17.12.6822

Beucher, A., Birraux, J., Tchouandong, L., Barton, O., Shibata, A., Conrad, S., Goodarzi, A. A., Krempler, A., Jeggo, P. A., & Löbrich, M. (2009). ATM and Artemis promote homologous recombination of radiation-induced DNA double-strand breaks in G2. *The EMBO Journal*, *28*(21), 3413–3427. https://doi.org/10.1038/EMBOJ.2009.276

Bi, X. (2015). Mechanism of DNA damage tolerance. *World Journal of Biological Chemistry*, *6*(3), 48. https://doi.org/10.4331/WJBC.V6.I3.48

Bierings, M., Bonfim, C., Peffault De Latour, R., Aljurf, M., Mehta, P. A., Knol, C., Boulad, F., Tbakhi, A., Esquirol, A., McQuaker, G., Sucak, G. A., Othman, T. B., Halkes, C. J. M., Carpenter, B., Niederwieser, D., Zecca, M., Kröger, N., Michallet, M., Risitano, A. M., … Fegueux, N. (2018). Transplant results in adults with Fanconi anaemia. *British Journal of Haematology*, *180*(1), 100–109. https://doi.org/10.1111/BJH.15006

Bjelland, S., & Seeberg, E. (2003). Mutagenicity, toxicity and repair of DNA base damage

induced by oxidation. *Mutation Research/Fundamental and Molecular Mechanisms of Mutagenesis*, *531*(1–2), 37–80. https://doi.org/10.1016/J.MRFMMM.2003.07.002

Blackford, A. N., & Jackson, S. P. (2017). ATM, ATR, and DNA-PK: the trinity at the heart of the DNA damage response. *Molecular Cell*, *66*(6), 801–817. https://doi.org/10.1016/J.MOLCEL.2017.05.015

Blair, A. B., Groot, V. P., Gemenetzis, G., Wei, J., Cameron, J. L., Weiss, M. J., Goggins, M., Wolfgang, C. L., Yu, J., & He, J. (2018). BRCA1/BRCA2 Germline Mutation Carriers and Sporadic Pancreatic Ductal Adenocarcinoma. *Journal of the American College of Surgeons*, *226*(4), 630-637.e1. https://doi.org/10.1016/J.JAMCOLLSURG.2017.12.021

Blandert, G., Zalle, N., Daniely, Y., Taplick, J., Gray, M. D., & Oren, M. (2002). DNA damage-induced translocation of the Werner helicase is regulated by acetylation. *The Journal of Biological Chemistry*, *277*(52), 50934–50940. https://doi.org/10.1074/JBC.M210479200

Bleichert, F., Botchan, M. R., & Berger, J. M. (2017). Mechanisms for initiating cellular DNA replication. *Science*, *355*(6327). https://doi.org/10.1126/SCIENCE.AAH6317/ASSET/D9D2B899-B012-46D1-8108-E71A5CA6208F/ASSETS/GRAPHIC/355_AAH6317_F5.JPEG

Blokhina, Y. P., & Buchwalter, A. (2020). *Moving fast and breaking things: Incidence and repair of DNA damage within ribosomal DNA repeats*. https://doi.org/10.1016/j.mrfmmm.2020.111715

Boisvert, F. M., Van Koningsbruggen, S., Navascués, J., & Lamond, A. I. (2007). The multifunctional nucleolus. *Nature Reviews Molecular Cell Biology 2007 8:7*, *8*(7), 574–585. https://doi.org/10.1038/nrm2184

Bolt, H. M. (2008). Vinyl Chloride—A Classical Industrial Toxicant of New Interest. *Http://Dx.Doi.Org/10.1080/10408440490915975*, *35*(4), 307–323. https://doi.org/10.1080/10408440490915975

Bond, J. A., & Medinsky, M. A. (2001). Insights into the toxicokinetics and toxicodynamics of 1,3-butadiene. *Chemico-Biological Interactions*, *135–136*(136), 599–614. https://doi.org/10.1016/S0009-2797(01)00199-5

Book, S., Plummer, A. ; L. N., Jones, B. F., Tresdell, A. H., Cunningham, U. S. ; M., Goldberg, M. C., & Weiner, E. R. (1988). Toxic DNA Damage by Hydrogen Peroxide Through the Fenton Reaction in Vivo and in Vitro. *Science*, *240*(4852), 640–642. https://doi.org/10.1126/SCIENCE.2834821

Boone, B. A., Perkins, S., Bandi, R., Santos, E., McCluskey, K., Bartlett, D. L., & Pingpank, J. F. (2018). Hepatic artery infusion of melphalan in patients with liver metastases from ocular melanoma. *Journal of Surgical Oncology*, *117*(5), 940. https://doi.org/10.1002/JSO.24984

Borek, C. (2004). Antioxidants and radiation therapy. *Journal of Nutrition*, *134*(11). https://doi.org/10.1093/JN/134.11.3207S

Bos, J. L., Rehmann, H., & Wittinghofer, A. (2007). GEFs and GAPs: Critical Elements in the Control of Small G Proteins. *Cell*, *129*(5), 865–877. https://doi.org/10.1016/j.cell.2007.05.018

Boulon, S., Westman, B. J., Hutten, S., Boisvert, F. M., & Lamond, A. I. (2010). The Nucleolus under Stress. *Molecular Cell*, *40*(2), 216. https://doi.org/10.1016/J.MOLCEL.2010.09.024

Bouman, A., van Koningsbruggen, S., Karakullukcu, M. B., Schreuder, W. H., & Lakeman, P. (2018). Bloom syndrome does not always present with sun-sensitive facial erythema. *European Journal of Medical Genetics*, *61*(2), 94–97.

https://doi.org/10.1016/J.EJMG.2017.10.010
Bourgeois, C. F., Lejeune, F., & Stévenin, J. (2004). Broad Specificity of SR (Serine/Arginine) Proteins in the Regulation of Alternative Splicing of Pre-Messenger RNA. *Progress in Nucleic Acid Research and Molecular Biology*, *78*, 37–88. https://doi.org/10.1016/S0079-6603(04)78002-2
Bowena, N., & Kolodnera, R. D. (2017). Reconstitution of Saccharomyces cerevisiae DNA polymerase e-dependent mismatch repair with purified proteins. *Proceedings of the National Academy of Sciences of the United States of America*, *114*(14), 3607–3612. https://doi.org/10.1073/PNAS.1701753114/ASSET/8BF67A80-1E5C-4D4C-8983-FC1A36672434/ASSETS/GRAPHIC/PNAS.1701753114FIG06.JPEG
Branzei, D., & Foiani, M. (2007). Template Switching: From Replication Fork Repair to Genome Rearrangements. *Cell*, *131*(7), 1228–1230. https://doi.org/10.1016/j.cell.2007.12.007
Breen, A. P., & Murphy, J. A. (1995). Reactions of oxyl radicals with DNA. *Free Radical Biology and Medicine*, *18*(6), 1033–1077. https://doi.org/10.1016/0891-5849(94)00209-3
Brookes, P., & Lawley, P. (1961). The reaction of mono- and di-functional alkylating agents with nucleic acids. *Biochemical Journal*, *80*(3), 496–503. https://doi.org/10.1042/bj0800496
Brown, E. J., & Baltimore, D. (2000). ATR disruption leads to chromosomal fragmentation and early embryonic lethality. *Genes & Development*, *14*(4), 397–402. https://doi.org/10.1101/GAD.14.4.397
Bruun, J., Kolberg, M., Ahlquist, T. C., Røyrvik, E. C., Nome, T., Leithe, E., Lind, G. E., Merok, M. A., Rognum, T. O., Bjørkøy, G., Johansen, T., Lindblom, A., Sun, X. F., Svindland, A., Liestøl, K., Nesbakken, A., Skotheim, R. I., & Lothe, R. A. (2015). Regulator of Chromosome Condensation 2 Identifies High-Risk Patients within Both Major Phenotypes of Colorectal Cancer. *Clinical Cancer Research : An Official Journal of the American Association for Cancer Research*, *21*(16), 3759–3770. https://doi.org/10.1158/1078-0432.CCR-14-3294
Budzowska, M., Graham, T. G., Sobeck, A., Waga, S., & Walter, J. C. (2015). Regulation of the Rev1–pol ζ complex during bypass of a DNA interstrand cross-link. *The EMBO Journal*, *34*(14), 1971–1985. https://doi.org/10.15252/EMBJ.201490878
Bueren, J. A., Quintana-Bustamante, O., Almarza, E., Navarro, S., Río, P., Segovia, J. C., & Guenechea, G. (2020). Advances in the gene therapy of monogenic blood cell diseases. *Clinical Genetics*, *97*(1), 89–102. https://doi.org/10.1111/CGE.13593/
Bugreev, D. V., Rossi, M. J., & Mazin, A. V. (2011). Cooperation of RAD51 and RAD54 in regression of a model replication fork. *Nucleic Acids Research*, *39*(6), 2153–2164. https://doi.org/10.1093/NAR/GKQ1139
Buranjiang, G., Kuerban, R., Abuduwanke, A., Li, X., & Kuerban, G. (2019). MicroRNA-331-3p inhibits proliferation and metastasis of ovarian cancer by targeting RCC2. *Archives of Medical Science : AMS*, *15*(6), 1520–1529. https://doi.org/10.5114/AOMS.2018.77858
Burger, K., Mühl, B., Harasim, T., Rohrmoser, M., Malamoussi, A., Orban, M., Kellner, M., Gruber-Eber, A., Kremmer, E., Hölzel, M., & Eick, D. (2010). Chemotherapeutic Drugs Inhibit Ribosome Biogenesis at Various Levels. *The Journal of Biological Chemistry*, *285*(16), 12416. https://doi.org/10.1074/JBC.M109.074211
Burgers, P. M. J., & Kunkel, T. A. (2017). Eukaryotic DNA Replication Fork. *Annual Review of Biochemistry*, *86*, 417. https://doi.org/10.1146/ANNUREV-BIOCHEM-061516-044709

Burke, D. J., & Stukenberg, P. T. (2003). The quest for the holy 'G' of chromosomal passengers. In *Developmental Cell* (Vol. 5, Issue 2, pp. 187–188). Dev Cell. https://doi.org/10.1016/S1534-5807(03)00230-2

Byun, T. S., Pacek, M., Yee, M. C., Walter, J. C., & Cimprich, K. A. (2005). Functional uncoupling of MCM helicase and DNA polymerase activities activates the ATR-dependent checkpoint. *Genes & Development*, *19*(9), 1040–1052. https://doi.org/10.1101/GAD.1301205

Cadet, J., Delatour, T., Douki, T., Gasparutto, D., Pouget, J. P., Ravanat, J. L., & Sauvaigo, S. (1999). Hydroxyl radicals and DNA base damage. *Mutation Research/Fundamental and Molecular Mechanisms of Mutagenesis*, *424*(1–2), 9–21. https://doi.org/10.1016/S0027-5107(99)00004-4

Cadet, J., Douki, T., & Ravanat, J. L. (2010). Oxidatively generated base damage to cellular DNA. *Free Radical Biology and Medicine*, *49*(1), 9–21. https://doi.org/10.1016/J.FREERADBIOMED.2010.03.025

Cadet, J., Douki, T., & Ravanat, J. L. (2011). Measurement of oxidatively generated base damage in cellular DNA. *Mutation Research/Fundamental and Molecular Mechanisms of Mutagenesis*, *711*(1–2), 3–12. https://doi.org/10.1016/J.MRFMMM.2011.02.004

Cadet, J., Ravanat, J. L., TavernaPorro, M., Menoni, H., & Angelov, D. (2012). Oxidatively generated complex DNA damage: Tandem and clustered lesions. *Cancer Letters*, *327*(1–2), 5–15. https://doi.org/10.1016/J.CANLET.2012.04.005

Cai, Y., Geacintov, N. E., & Broyde, S. (2020). Variable impact of conformationally distinct DNA lesions on nucleosome structure and dynamics: Implications for nucleotide excision repair. *DNA Repair*, *87*, 102768. https://doi.org/10.1016/J.DNAREP.2019.102768

Caldecott, K. W. (2022). DNA single-strand break repair and human genetic disease. *Trends in Cell Biology*, *32*(9), 733–745. https://doi.org/10.1016/J.TCB.2022.04.010

Caldecott, K. W., Aoufouchi, S., Johnson, P., & Shall, S. (1996). XRCC1 polypeptide interacts with DNA polymerase beta and possibly poly (ADP-ribose) polymerase, and DNA ligase III is a novel molecular 'nick-sensor' in vitro. *Nucleic Acids Research*, *24*(22), 4387. https://doi.org/10.1093/NAR/24.22.4387

Calkins, A. S., Iglehart, J. D., & Lazaro, J. B. (2013). DNA damage-induced inhibition of rRNA synthesis by DNA-PK and PARP-1. *Nucleic Acids Research*, *41*(15), 7378. https://doi.org/10.1093/NAR/GKT502

Calzada, A., Hodgson, B., Kanemaki, M., Bueno, A., & Labib, K. (2005). Molecular anatomy and regulation of a stable replisome at a paused eukaryotic DNA replication fork. *Genes & Development*, *19*(16), 1905–1919. https://doi.org/10.1101/GAD.337205

Cannan, W. J., & Pederson, D. S. (2016). Mechanisms and Consequences of Double-strand DNA Break Formation in Chromatin. *Journal of Cellular Physiology*, *231*(1), 3–14. https://doi.org/10.1002/JCP.25048

Cantres-Velez, J. A., Blaize, J. L., Vierra, D. A., Boisvert, R. A., Garzon, J. L., Piraino, B., Tan, W., Deans, A. J., & Howlett, N. G. (2023). Cyclin-Dependent Kinase-Mediated Phosphorylation of FANCD2 Promotes Mitotic Fidelity. *Https://Doi.Org/10.1128/MCB.00234-21*, *41*(8), 234–255. https://doi.org/10.1128/MCB.00234-21

Carey, J. F., Schultz, S. J., Sisson, L., Fazzio, T. G., & Champoux, J. J. (2003). DNA relaxation by human topoisomerase I occurs in the closed clamp conformation of the protein. *Proceedings of the National Academy of Sciences of the United States of America*,

100(10), 5640. https://doi.org/10.1073/PNAS.1031537100
Castor, D., Nair, N., Déclais, A. C., Lachaud, C., Toth, R., Macartney, T. J., Lilley, D. M. J., Arthur, J. S. C., & Rouse, J. (2013). Cooperative Control of Holliday Junction Resolution and DNA Repair by the SLX1 and MUS81-EME1 Nucleases. *Molecular Cell*, *52*(2), 221. https://doi.org/10.1016/J.MOLCEL.2013.08.036
Ceccaldi, R., Liu, J. C., Amunugama, R., Hajdu, I., Primack, B., Petalcorin, M. I. R., O'Connor, K. W., Konstantinopoulos, P. A., Elledge, S. J., Boulton, S. J., Yusufzai, T., & D'Andrea, A. D. (2015). Homologous-recombination-deficient tumours are dependent on Polθ -mediated repair. *Nature*, *518*(7538), 258–262. https://doi.org/10.1038/nature14184
Ceccaldi, R., Rondinelli, B., & D'Andrea, A. D. (2016). Repair Pathway Choices and Consequences at the Double-Strand Break. *Trends in Cell Biology*, *26*(1), 52. https://doi.org/10.1016/J.TCB.2015.07.009
Ceccaldi, R., Sarangi, P., & D'Andrea, A. D. (2016). The Fanconi anaemia pathway: New players and new functions. In *Nature Reviews Molecular Cell Biology* (Vol. 17, Issue 6, pp. 337–349). Nature Publishing Group. https://doi.org/10.1038/nrm.2016.48
Cejka, P., & Symington, L. S. (2021). DNA End Resection: Mechanism and Control. *Https://Doi.Org/10.1146/Annurev-Genet-071719-020312*, *55*, 285–307. https://doi.org/10.1146/ANNUREV-GENET-071719-020312
Chakarov, S., Petkova, R., Russev, G. C., & Zhelev, N. (2014). DNA damage and mutation. Types of DNA damage. *BioDiscovery 11: E8957*, *11*(11), e8957-. https://doi.org/10.7750/BIODISCOVERY.2014.11.1
Chan, G. L., Doetsch, P. W., & Haseltine, W. A. (1985). Cyclobutane Pyrimidine Dimers and (6-4) Photoproducts Block Polymerization by DNA Polymerase I†. *Biochemistry*, *24*(21), 5723–5728. https://doi.org/10.1021/BI00342A006/ASSET/BI00342A006.FP.PNG_V03
Chan, K., Resnick, M. A., & Gordenin, D. A. (2013). The choice of nucleotide inserted opposite abasic sites formed within chromosomal DNA reveals the polymerase activities participating in translesion DNA synthesis. *DNA Repair*, *12*(11), 878–889. https://doi.org/10.1016/J.DNAREP.2013.07.008
Chan, S. H., Yu, A. M., & McVey, M. (2010). Dual Roles for DNA Polymerase Theta in Alternative End-Joining Repair of Double-Strand Breaks in Drosophila. *PLOS Genetics*, *6*(7), e1001005. https://doi.org/10.1371/JOURNAL.PGEN.1001005
Chatterjee, N., & Walker, G. C. (2017). Mechanisms of DNA damage, repair, and mutagenesis. *Environmental and Molecular Mutagenesis*, *58*(5), 235–263. /pmc/articles/PMC5474181/
Chen, H., Lisby, M., & Symington, L. S. (2013). RPA coordinates DNA end resection and prevents formation of DNA hairpins. *Molecular Cell*, *50*(4), 589–600. https://doi.org/10.1016/J.MOLCEL.2013.04.032
Chen, J., Lobb, I. T., Morin, P., Novo, S. M., Simpson, J., Kennerknecht, K., Von Kriegsheim, A., Batchelor, E. E., Oakley, F., & Stark, L. A. (2018). Identification of a novel TIF-IA–NF-κB nucleolar stress response pathway. *Nucleic Acids Research*, *46*(12), 6188–6205. https://doi.org/10.1093/NAR/GKY455
Chen, Q., Jiang, P., Jia, B., Liu, Y., & Zhang, Z. (2020). RCC2 contributes to tumor invasion and chemoresistance to cisplatin in hepatocellular carcinoma. *Human Cell*, *33*(3), 709–720. https://doi.org/10.1007/S13577-020-00353-7
Chen, & Stark. (2018). Crosstalk between nf-κb and nucleoli in the regulation of cellular homeostasis. In *Cells* (Vol. 7, Issue 10, p. 157). Multidisciplinary Digital Publishing Institute. https://doi.org/10.3390/cells7100157

Chen, Z., Wu, W., Huang, Y., Xie, L., Li, Y., Chen, H., Li, W., Yin, D., & Hu, K. (2019). RCC2 promotes breast cancer progression through regulation of Wnt signaling and inducing EMT. *Journal of Cancer*, *10*(27), 6837–6847. https://doi.org/10.7150/JCA.36430

Chen, Z., Xiao, Z., Gu, W. Z., Xue, J., Bui, M. H., Kovar, P., Li, G., Wang, G., Tao, Z. F., Tong, Y., Lin, N. H., Sham, H. L., Wang, J. Y. J., Sowin, T. J., Rosenberg, S. H., & Zhang, H. (2006). Selective Chk1 inhibitors differentially sensitize p53-deficient cancer cells to cancer therapeutics. *International Journal of Cancer*, *119*(12), 2784–2794. https://doi.org/10.1002/IJC.22198

Cheng, K. C., Cahill, D. S., Kasai, H., Nishimura, S., & Loeb, L. A. (1992). 8-Hydroxyguanine, an abundant form of oxidative DNA damage, causes G → T and A → C substitutions. *Journal of Biological Chemistry*, *267*(1), 166–172. https://doi.org/10.1016/s0021-9258(18)48474-8

Cherfils, J., & Zeghouf, M. (2013). Regulation of small GTPases by GEFs, GAPs, and GDIs. *Physiological Reviews*, *93*(1), 269–309. https://doi.org/10.1152/PHYSREV.00003.2012/SUPPL_FILE/TABLES1.PDF

Chetsanga, C. J., Lozon, M., Makaroff, C., & Savage, L. (1981). Purification and characterization of Escherichia coli formamidopyrimidine-DNA glycosylase that excises damaged 7-methylguanine from deoxyribonucleic acid. *Biochemistry*, *20*(18), 5201–5207. https://doi.org/10.1021/BI00521A016

Cheung, R. S., Castella, M., Abeyta, A., Gafken, P. R., Tucker, N., & Taniguchi, T. (2017). Ubiquitination-Linked Phosphorylation of the FANCI S/TQ Cluster Contributes to Activation of the Fanconi Anemia I/D2 Complex. *Cell Reports*, *19*(12), 2432–2440. https://doi.org/10.1016/j.celrep.2017.05.081

Chiu, R. K., Brun, J., Ramaekers, C., Theys, J., Weng, L., Lambin, P., Gray, D. A., & Wouters, B. G. (2006). Lysine 63-Polyubiquitination Guards against Translesion Synthesis–Induced Mutations. *PLOS Genetics*, *2*(7), e116. https://doi.org/10.1371/JOURNAL.PGEN.0020116

Cho, Y. J., Wang, H., Kozekov, I. D., Kurtz, A. J., Jacob, J., Voehler, M., Smith, J., Harris, T. M., Lloyd, R. S., Rizzo, C. J., & Stone, M. P. (2006). Stereospecific formation of interstrand carbinolamine DNA cross-links by crotonaldehyde- and acetaldehyde-derived α-CH3-γ-OH-1, N2-propano-2′-deoxyguanosine adducts in the 5′-CpG-3′ sequence. *Chemical Research in Toxicology*, *19*(2), 195–208. https://doi.org/10.1021/TX050239Z/SUPPL_FILE/TX050239ZSI20051026_070335.PDF

Chou, D. M., Adamson, B., Dephoure, N. E., Tan, X., Nottke, A. C., Hurov, K. E., Gygi, S. P., Colaiácovo, M. P., & Elledge, S. J. (2010). A chromatin localization screen reveals poly (ADP ribose)-regulated recruitment of the repressive polycomb and NuRD complexes to sites of DNA damage. *Proceedings of the National Academy of Sciences of the United States of America*, *107*(43), 18475–18480. https://doi.org/10.1073/PNAS.1012946107/SUPPL_FILE/ST01.DOCX

Christmann, M., & Kaina, B. (2012). O 6-methylguanine-DNA methyltransferase (MGMT): Impact on cancer risk in response to tobacco smoke. *Mutation Research - Fundamental and Molecular Mechanisms of Mutagenesis*, *736*(1–2), 64–74. https://doi.org/10.1016/J.MRFMMM.2011.06.004

Ciccia, A., & Elledge, S. J. (2010). The DNA Damage Response: Making It Safe to Play with Knives. *Molecular Cell*, *40*(2), 179–204.

Ciccia, A., Ling, C., Coulthard, R., Yan, Z., Xue, Y., Meetei, A. R., Laghmani, E. H., Joenje, H., McDonald, N., de Winter, J. P., Wang, W., & West, S. C. (2007). Identification of

FAAP24, a Fanconi Anemia Core Complex Protein that Interacts with FANCM. *Molecular Cell*, *25*(3), 331–343. https://doi.org/10.1016/j.molcel.2007.01.003

Ciccia, A., Nimonkar, A. V., Hu, Y., Hajdu, I., Achar, Y. J., Izhar, L., Petit, S. A., Adamson, B., Yoon, J. C., Kowalczykowski, S. C., Livingston, D. M., Haracska, L., & Elledge, S. J. (2012). Polyubiquitinated PCNA Recruits the ZRANB3 Translocase to Maintain Genomic Integrity after Replication Stress. *Molecular Cell*, *47*(3), 396–409. https://doi.org/10.1016/j.molcel.2012.05.024

Cirkovic, S., Guc-Scekic, M., Vujic, D., Ilic, N., Micic, D., Skoric, D., & Jovanovic, A. (2011). Diagnosis of Fanconi's Anemia by Diepoxybutane Analysis in Children from Serbia. *Balkan Journal of Medical Genetics : BJMG*, *14*(2), 65. https://doi.org/10.2478/V10034-011-0048-6

Clauson, C., Schärer, O. D., & Niedernhofer, L. (2013). Advances in Understanding the Complex Mechanisms of DNA Interstrand Cross-Link Repair. *Cold Spring Harbor Perspectives in Biology*, *5*(10), a012732. https://doi.org/10.1101/CSHPERSPECT.A012732

Cohn, M. A., Kowal, P., Yang, K., Haas, W., Huang, T. T., Gygi, S. P., & D'Andrea, A. D. (2007). A UAF1-Containing Multisubunit Protein Complex Regulates the Fanconi Anemia Pathway. *Molecular Cell*, *28*(5), 786–797. https://doi.org/10.1016/j.molcel.2007.09.031

Colombo, E., Alcalay, M., & Pelicci, P. G. (2011). Nucleophosmin and its complex network: a possible therapeutic target in hematological diseases. *Oncogene 2011 30:23*, *30*(23), 2595–2609. https://doi.org/10.1038/onc.2010.646

Constantinou, A. (2012). Rescue of replication failure by Fanconi anaemia proteins. *Chromosoma*, *121*(1), 21–36. https://doi.org/10.1007/S00412-011-0349-2/FIGURES/4

Cooke, C. A., Heck, M. M. S., & Earnshaw, W. C. (1987). The inner centromere protein (INCENP) antigens: movement from inner centromere to midbody during mitosis. *The Journal of Cell Biology*, *105*(5), 2053. https://doi.org/10.1083/JCB.105.5.2053

Cooper, D. N., & Youssoufian, H. (1988). The CpG dinucleotide and human genetic disease. *Human Genetics*, *78*(2), 151–155. https://doi.org/10.1007/BF00278187

Corman, A., Sirozh, O., Lafarga, V., & Fernandez-Capetillo, O. (2023). Targeting the nucleolus as a therapeutic strategy in human disease. *Trends in Biochemical Sciences*, *48*(3), 274–287. https://doi.org/10.1016/J.TIBS.2022.09.006

Cortez, D. (2015). Preventing Replication Fork Collapse to Maintain Genome Integrity. *DNA Repair*, *32*, 149. https://doi.org/10.1016/J.DNAREP.2015.04.026

Couté, Y., Burgess, J. A., Diaz, J. J., Chichester, C., Lisacek, F., Greco, A., & Sanchez, J. C. (2006). Deciphering the human nucleolar proteome. *Mass Spectrometry Reviews*, *25*(2), 215–234. https://doi.org/10.1002/MAS.20067

Critchlow, S. E., Bowater, R. P., & Jackson, S. P. (1997). Mammalian DNA double-strand break repair protein XRCC4 interacts with DNA ligase IV. *Current Biology*, *7*(8), 588–598. https://doi.org/10.1016/S0960-9822(06)00258-2

Daley, J. M., & Sung, P. (2014). 53BP1, BRCA1, and the Choice between Recombination and End Joining at DNA Double-Strand Breaks. *Molecular and Cellular Biology*, *34*(8), 1380. https://doi.org/10.1128/MCB.01639-13

Dalhus, B., Laerdahl, J. K., Backe, P. H., & Bjørås, M. (2009). DNA base repair – recognition and initiation of catalysis. *FEMS Microbiology Reviews*, *33*(6), 1044–1078. https://doi.org/10.1111/J.1574-6976.2009.00188.X

Danen, E. H. J. (2009). Integrin proteomes reveal a new guide for cell motility. *Science Signaling*, *2*(89). https://doi.org/10.1126/SCISIGNAL.289PE58

Daniely, Y., Dimitrova, D. D., & Borowiec, J. A. (2002). Stress-Dependent Nucleolin Mobilization Mediated by p53-Nucleolin Complex Formation. *Molecular and Cellular Biology*, *22*(16), 6014. https://doi.org/10.1128/MCB.22.16.6014-6022.2002

Dao, K. H. T., Rotelli, M. D., Brown, B. R., Yates, J. E., Rantala, J., Tognon, C., Tyner, J. W., Druker, B. J., & Bagby, G. C. (2013). The PI3K/Akt1 pathway enhances steady-state levels of FANCL. *Molecular Biology of the Cell*, *24*(16), 2582–2592. https://doi.org/10.1091/MBC.E13-03-0144/ASSET/IMAGES/LARGE/2582FIG6.JPEG

Das, A., Vijayan, M., Walton, E. M., Stafford, V. G., Fiflis, D. N., & Asokan, A. (2022). *Epigenetic Silencing of Recombinant Adeno-associated Virus Genomes by NP220 and the HUSH Complex*.

Dasari, S., & Bernard Tchounwou, P. (2014). Cisplatin in cancer therapy: molecular mechanisms of action. *European Journal of Pharmacology*, *740*, 364. https://doi.org/10.1016/J.EJPHAR.2014.07.025

Dasika, G. K., Lin, S. C. J., Zhao, S., Sung, P., Tomkinson, A., & Lee, E. Y. H. P. (2000). DNA damage-induced cell cycle checkpoints and DNA strand break repair in development and tumorigenesis. *Oncogene 1999 18:55*, *18*(55), 7883–7899. https://doi.org/10.1038/sj.onc.1203283

Datta, A., & Brosh, R. M. (2019). Holding all the cards—how fanconi anemia proteins deal with replication stress and preserve genomic stability. In *Genes* (Vol. 10, Issue 2). MDPI AG. https://doi.org/10.3390/genes10020170

Davies, R. J. H. (1995). Ultraviolet Radiation Damage in DNA. *Biochemical Society Transactions*, *23*(2), 407–418. https://doi.org/10.1042/BST0230407

De Bont, R., & van Larebeke, N. (2004). Endogenous DNA damage in humans: a review of quantitative data. *Mutagenesis*, *19*(3), 169–185. https://academic.oup.com/mutage/article/19/3/169/1482185

Deans, A. J., & West, S. C. (2009). FANCM Connects the Genome Instability Disorders Bloom's Syndrome and Fanconi Anemia. *Molecular Cell*, *36*(6), 943–953. https://doi.org/10.1016/j.molcel.2009.12.006

Deans, A. J., & West, S. C. (2011). DNA interstrand crosslink repair and cancer. In *Nature Reviews Cancer* (Vol. 11, Issue 7, pp. 467–480). Nature Publishing Group. https://doi.org/10.1038/nrc3088

Decottignies, A. (2013). Alternative end-joining mechanisms: A historical perspective. *Frontiers in Genetics*, *4*(APR), 48. https://doi.org/10.3389/FGENE.2013.00048/BIBTEX

del Valle, J., Rofes, P., Moreno-Cabrera, J. M., López-Dóriga, A., Belhadj, S., Vargas-Parra, G., Teulé, À., Cuesta, R., Muñoz, X., Campos, O., Salinas, M., de Cid, R., Brunet, J., González, S., Capellá, G., Pineda, M., Feliubadaló, L., & Lázaro, C. (2020). Exploring the Role of Mutations in Fanconi Anemia Genes in Hereditary Cancer Patients. *Cancers*, *12*(4), 829. https://doi.org/10.3390/CANCERS12040829

Denisov, A. Y., McManus, F. P., O'Flaherty, D. K., Noronha, A. M., & Wilds, C. J. (2017). Structural basis of interstrand cross-link repair by O6-alkylguanine DNA alkyltransferase. *Organic & Biomolecular Chemistry*, *15*(39), 8361–8370. https://doi.org/10.1039/C7OB02093G

Dianov, G. L., & Parsons, J. L. (2007). Co-ordination of DNA single strand break repair. *DNA Repair*, *6*(4), 454–460. https://doi.org/10.1016/J.DNAREP.2006.10.009

Dizdaroglu, M., Rao, G., Halliwell, B., & Gajewski, E. (1991). Damage to the DNA bases in mammalian chromatin by hydrogen peroxide in the presence of ferric and cupric ions. *Archives of Biochemistry and Biophysics*, *285*(2), 317–324.

https://doi.org/10.1016/0003-9861(91)90366-Q
Douki, T., Perdiz, D., Gróf, P., Kuluncsics, Z., Moustacchi, E., Cadet, J., & Sage, E. (1999). Oxidation of guanine in cellular DNA by solar UV radiation: Biological role. *Photochemistry and Photobiology*, *70*(2), 184–190. https://doi.org/10.1111/J.1751-1097.1999.TB07988.X
Driessens, G., Harsan, L., Robaye, B., Waroquier, D., Browaeys, P., Giannakopoulos, X., Velu, T., & Bruyns, C. (2003). Micronuclei to detect in vivo chemotherapy damage in a p53 mutated solid tumour. *British Journal of Cancer 2003 89:4*, *89*(4), 727–729. https://doi.org/10.1038/sj.bjc.6601163
Dronkert, M. L. G., & Kanaar, R. (2001). Repair of DNA interstrand cross-links. *Mutation Research/DNA Repair*, *486*(4), 217–247. https://doi.org/10.1016/S0921-8777(01)00092-1
Du, C., Ma, X., Meruvu, S., Hugendubler, L., & Mueller, E. (2014). The adipogenic transcriptional cofactor ZNF638 interacts with splicing regulators and influences alternative splicing. *Journal of Lipid Research*, *55*(9), 1886. https://doi.org/10.1194/JLR.M047555
Dufour, C. (2017). How I manage patients with Fanconi anaemia. *British Journal of Haematology*, *178*(1), 32–47. https://doi.org/10.1111/BJH.14615
Dumaz, N., Drougard, C., Sarasin, A., & Daya-Grosjean, L. (1993). Specific UV-induced mutation spectrum in the p53 gene of skin tumors from DNA-repair-deficient xeroderma pigmentosum patients. *Proceedings of the National Academy of Sciences of the United States of America*, *90*(22), 10529. https://doi.org/10.1073/PNAS.90.22.10529
Duncan, T., Trewick, S. C., Koivisto, P., Bates, P. A., Lindahl, T., & Sedgwick, B. (2002). Reversal of DNA alkylation damage by two human dioxygenases. *Proceedings of the National Academy of Sciences*, *99*(26), 16660–16665. https://doi.org/10.1073/PNAS.262589799
Duquette, M. L., Zhu, Q., Taylor, E. R., Tsay, A. J., Shi, L. Z., Berns, M. W., & McGowan, C. H. (2012). CtIP Is Required to Initiate Replication-Dependent Interstrand Crosslink Repair. *PLOS Genetics*, *8*(11), e1003050. https://doi.org/10.1371/JOURNAL.PGEN.1003050
Dutta, S., Chowdhury, G., & Gates, K. S. (2007). Interstrand cross-links generated by abasic sites in duplex DNA. *Journal of the American Chemical Society*, *129*(7), 1852–1853. https://doi.org/10.1021/JA067294U/SUPPL_FILE/JA067294USI20061228_042816.PDF
Duxin, J. P., & Walter, J. C. (2015). What is the DNA repair defect underlying Fanconi anemia? *Current Opinion in Cell Biology*, *37*, 49. https://doi.org/10.1016/J.CEB.2015.09.002
Eadie, J. S., Conrad, M., Toorchen, D., & Topal, M. D. (1984). Mechanism of mutagenesis by O6-methylguanine. *Nature 1984 308:5955*, *308*(5955), 201–203. https://doi.org/10.1038/308201a0
Eker, A. P. M., Quayle, C., Chaves, I., & Van Der Horst, G. T. J. (2009). Direct DNA damage reversal: Elegant solutions for nasty problems. *Cellular and Molecular Life Sciences*, *66*(6), 968–980. https://doi.org/10.1007/S00018-009-8735-0
Elia, A. E. H., Wang, D. C., Willis, N. A., Boardman, A. P., Hajdu, I., Adeyemi, R. O., Lowry, E., Gygi, S. P., Scully, R., & Elledge, S. J. (2015). RFWD3-Dependent Ubiquitination of RPA Regulates Repair at Stalled Replication Forks. *Molecular Cell*, *60*(2), 280–293. https://doi.org/10.1016/J.MOLCEL.2015.09.011
Enoiu, M., Jiricny, J., & Schärer, O. D. (2012). Repair of cisplatin-induced DNA interstrand

crosslinks by a replication-independent pathway involving transcription-coupled repair and translesion synthesis. *Nucleic Acids Research*, *40*(18). https://doi.org/10.1093/NAR/GKS670

Essen, L. O., & Klar, T. (2006). Light-driven DNA repair by photolyases. *Cellular and Molecular Life Sciences*, *63*(11), 1266–1277. https://doi.org/10.1007/S00018-005-5447-Y/METRICS

Fahrer, J., & Kaina, B. (2017). Impact of DNA repair on the dose-response of colorectal cancer formation induced by dietary carcinogens. *Food and Chemical Toxicology*, *106*, 583–594. https://doi.org/10.1016/J.FCT.2016.09.029

Falahati, H., Pelham-Webb, B., Blythe, S., & Wieschaus, E. (2016). Nucleation by rRNA dictates the precision of nucleolus assembly. *Current Biology*, *26*(3), 277–285. https://doi.org/10.1016/j.cub.2015.11.065

Falnes, P., Johansen, R. F., & Seeberg, E. (2002). AlkB-mediated oxidative demethylation reverses DNA damage in Escherichia coli. *Nature 2002 419:6903*, *419*(6903), 178–182. https://doi.org/10.1038/nature01048

Fatyol, K., & Szalay, A. A. (2001). The p14ARF Tumor Suppressor Protein Facilitates Nucleolar Sequestration of Hypoxia-inducible Factor-1α (HIF-1α) and Inhibits HIF-1-mediated Transcription. *Journal of Biological Chemistry*, *276*(30), 28421–28429. https://doi.org/10.1074/jbc.M102847200

Feng, N., Ching, T., Wang, Y., Liu, B., Lin, H., Shi, O., Zhang, X., Zheng, M., Zheng, X., Gao, M., Zheng, Z. J., Yu, H., Garmire, L., & Qian, B. (2016). Analysis of Microarray Data on Gene Expression and Methylation to Identify Long Non-coding RNAs in Non-small Cell Lung Cancer. *Scientific Reports*, *6*. https://doi.org/10.1038/SREP37233

Feng, S., Ma, S., Li, K., Gao, S., Ning, S., Shang, J., Guo, R., Chen, Y., Blumenfeld, B., Simon, I., Li, Q., Guo, R., & Xu, D. (2022). RIF1-ASF1-mediated high-order chromatin structure safeguards genome integrity. *Nature Communications 2022 13:1*, *13*(1), 1–16. https://doi.org/10.1038/s41467-022-28588-y

Feric, M., Vaidya, N., Harmon, T. S., Mitrea, D. M., Zhu, L., Richardson, T. M., Kriwacki, R. W., Pappu, R. V., & Brangwynne, C. P. (2016). Coexisting Liquid Phases Underlie Nucleolar Subcompartments. *Cell*, *165*(7), 1686–1697. https://doi.org/10.1016/J.CELL.2016.04.047

Fiesco-Roa, M. O., Giri, N., McReynolds, L. J., Best, A. F., & Alter, B. P. (2019). Genotype-Phenotype Associations in Fanconi Anemia: A Literature Review. *Blood Reviews*, *37*, 100589. https://doi.org/10.1016/J.BLRE.2019.100589

Filipowicz, W., Pelczar, P., Pogacic, V., & Dragon, F. (1999). Structure and biogenesis of small nucleolar RNAs acting as guides for ribosomal RNA modification. *Acta Biochimica Polonica*, *46*(2), 377–389. https://doi.org/10.18388/ABP.1999_4171

Ford, E., Voit, R., Liszt, G., Magin, C., Grummt, I., & Guarente, L. (2006). Mammalian Sir2 homolog SIRT7 is an activator of RNA polymerase I transcription. *Genes & Development*, *20*(9), 1075–1080. https://doi.org/10.1101/GAD.1399706

Fradet-Turcotte, A., Canny, M. D., Escribano-Díaz, C., Orthwein, A., Leung, C. C. Y., Huang, H., Landry, M.-C., Kitevski-Leblanc, J., Noordermeer, S. M., Sicheri, F., & Durocher, D. (2013). 53BP1 is a reader of the DNA-damage-induced H2A Lys 15 ubiquitin mark. *Nature*, *498*. https://doi.org/10.1038/nature12318

Francies, F. Z., Wainwright, R., Poole, J., De Leeneer, K., Coene, I., Wieme, G., Poirel, H. A., Brichard, B., Vermeulen, S., Vral, A., Slabbert, J., Claes, K., & Baeyens, A. (2018). Diagnosis of Fanconi Anaemia by ionising radiation- or mitomycin C-induced

micronuclei. *DNA Repair*, *61*, 17–24. https://doi.org/10.1016/J.DNAREP.2017.11.001
Friedberg, E. C. (2019). Fixing Your Damaged and Incorrect Genes. *Fixing Your Damaged and Incorrect Genes*. https://doi.org/10.1142/11298
Frosina, G., Fortini, P., Rossi, O., Carrozzino, F., Raspaglio, G., Cox, L. S., Lane, D. P., Abbondandolo, A., & Dogliotti, E. (1996). Two pathways for base excision repair in mammalian cells. *Journal of Biological Chemistry*, *271*(16), 9573–9578. https://doi.org/10.1074/JBC.271.16.9573
Fu, D., & Samson, L. D. (2012). Direct repair of 3,N4-ethenocytosine by the human ALKBH2 dioxygenase is blocked by the AAG/MPG glycosylase. *DNA Repair*, *11*(1), 46–52. https://doi.org/10.1016/J.DNAREP.2011.10.004
Fugger, K., Hewitt, G., West, S. C., & Boulton, S. J. (2021). Tackling PARP inhibitor resistance. *Trends in Cancer*, *7*(12), 1102–1118. https://doi.org/10.1016/J.TRECAN.2021.08.007
Fujii, K., Miyata, Y., Takahashi, I., Koizumi, H., Saji, H., Hoshikawa, M., Takagi, M., Nishimura, T., & Nakamura, H. (2018). Differential Proteomic Analysis between Small Cell Lung Carcinoma (SCLC) and Pulmonary Carcinoid Tumors Reveals Molecular Signatures for Malignancy in Lung Cancer. *Proteomics. Clinical Applications*, *12*(6). https://doi.org/10.1002/PRCA.201800015
Fullbright, G., Rycenga, H. B., Gruber, J. D., & Long, D. T. (2016). p97 Promotes a Conserved Mechanism of Helicase Unloading during DNA Cross-Link Repair. *Molecular and Cellular Biology*, *36*(23), 2983. https://doi.org/10.1128/MCB.00434-16
Gallina, I., & Duxin, J. P. (2020). A safe fix for alcohol-derived DNA damage. *Nature 2021 579:7800*, *579*(7800), 499–500. https://doi.org/10.1038/d41586-020-00462-1
Gan, G. N., Wittschieben, J. P., Wittschieben, B., & Wood, R. D. (2007). DNA polymerase zeta (pol ζ) in higher eukaryotes. *Cell Research 2008 18:1*, *18*(1), 174–183. https://doi.org/10.1038/cr.2007.117
García-Cao, I., García-Cao, M., Martín-Caballero, J., Criado, L. M., Klatt, P., Flores, J. M., Weill, J. C., Blasco, M. A., & Serrano, M. (2002). 'Super p53' mice exhibit enhanced DNA damage response, are tumor resistant and age normally. *EMBO Journal*, *21*(22), 6225–6235. https://doi.org/10.1093/EMBOJ/CDF595
Gari, K., Décaillet, C., Delannoy, M., Wu, L., & Constantinou, A. (2008). Remodeling of DNA replication structures by the branch point translocase FANCM. *Proceedings of the National Academy of Sciences of the United States of America*, *105*(42), 16107–16112. https://doi.org/10.1073/PNAS.0804777105/SUPPL_FILE/0804777105SI.PDF
Gari, K., Décaillet, C., Stasiak, A. Z., Stasiak, A., & Constantinou, A. (2008). The Fanconi Anemia Protein FANCM Can Promote Branch Migration of Holliday Junctions and Replication Forks. *Molecular Cell*, *29*(1), 141–148. https://doi.org/10.1016/j.molcel.2007.11.032
Gates, K. S. (2009). An Overview of Chemical Processes That Damage Cellular DNA: Spontaneous Hydrolysis, Alkylation, and Reactions with Radicals. *Chemical Research in Toxicology*, *22*(11), 1747. https://doi.org/10.1021/TX900242K
Ge, X. Q., & Blow, J. J. (2010). Chk1 inhibits replication factory activation but allows dormant origin firing in existing factories. *Journal of Cell Biology*, *191*(7), 1285–1297. https://doi.org/10.1083/JCB.201007074
Gentil, A., Le Page, F., Margot, A., Lawrence, C. W., Borden, A., & Sarasin, A. (1996). Mutagenicity of a unique thymine-thymine dimer or thymine-thymine pyrimidine pyrimidone (6-4) photoproduct in mammalian cells. *Nucleic Acids Research*, *24*(10), 1837. https://doi.org/10.1093/NAR/24.10.1837

German, J., Sanz, M. M., Ciocci, S., Ye, T. Z., & Ellis, N. A. (2007). Syndrome-causing mutations of the BLM gene in persons in the Bloom's Syndrome Registry. *Human Mutation*, *28*(8), 743–753. https://doi.org/10.1002/HUMU.20501

Gharahkhani, P., Jorgenson, E., Hysi, P., Khawaja, A. P., Pendergrass, S., Han, X., Ong, J. S., Hewitt, A. W., Segrè, A. V., Rouhana, J. M., Hamel, A. R., Igo, R. P., Choquet, H., Qassim, A., Josyula, N. S., Cooke Bailey, J. N., Bonnemaijer, P. W. M., Iglesias, A., Siggs, O. M., … Wiggs, J. L. (2021). Genome-wide meta-analysis identifies 127 open-angle glaucoma loci with consistent effect across ancestries. *Nature Communications*, *12*(1). https://doi.org/10.1038/S41467-020-20851-4

Ghetti, A., Pinol-roma, S., Michael, W. M., Morandi, C., & Dreyfuss, G. (1992). hnRNP 1, the polyprimidine tract-binding protein: distinct nuclear localization and association with hnRNAs. *Nucleic Acids Research*, *20*(14), 3671–3678. https://doi.org/10.1093/NAR/20.14.3671

Ghezraoui, H., Oliveira, C., Becker, J. R., Bilham, K., Moralli, D., Anzilotti, C., Fischer, R., Deobagkar-Lele, M., Sanchiz-Calvo, M., Fueyo-Marcos, E., Bonham, S., Kessler, B. M., Rottenberg, S., Cornall, R. J., Green, C. M., & Chapman, J. R. (2018). 53BP1 cooperation with the REV7–shieldin complex underpins DNA structure-specific NHEJ. *Nature 2018 560:7716*, *560*(7716), 122–127. https://doi.org/10.1038/s41586-018-0362-1

Ghezraoui, H., Piganeau, M., Renouf, B., Renaud, J. B., Sallmyr, A., Ruis, B., Oh, S., Tomkinson, A. E., Hendrickson, E. A., Giovannangeli, C., Jasin, M., & Brunet, E. (2014). Chromosomal Translocations in Human Cells Are Generated by Canonical Nonhomologous End-Joining. *Molecular Cell*, *55*(6), 829–842. https://doi.org/10.1016/j.molcel.2014.08.002

Ghosal, G., & Chen, J. (2013). DNA damage tolerance: a double-edged sword guarding the genome. *Translational Cancer Research*, *2*(3), 107–129. https://doi.org/10.3978/J.ISSN.2218-676X.2013.04.01

Giglia-Mari, G., Zotter, A., & Vermeulen, W. (2011). DNA damage response. *Cold Spring Harbor Perspectives in Biology*, *3*(1), 1–19. https://doi.org/10.1101/CSHPERSPECT.A000745

Gjerset, R. A., & Bandyopadhyay, K. (2006). Regulation of p14ARF through subnuclear compartmentalization. *Cell Cycle (Georgetown, Tex.)*, *5*(7), 686–690. https://doi.org/10.4161/CC.5.7.2623

Gomes, B. C., Silva, S. N., Azevedo, A. P., Manita, I., Gil, O. M., Ferreira, T. C., Limbert, E., Rueff, J., & Gaspar, J. F. (2010). The role of common variants of non-homologous end-joining repair genes XRCC4, LIG4 and Ku80 in thyroid cancer risk. *Oncology Reports*, *24*(4), 1079–1085. https://doi.org/10.3892/OR_00000958

Gong, S., Chen, Y., Meng, F., Zhang, Y., Wu, H., Li, C., & Zhang, G. (2019). RCC2, a regulator of the RalA signaling pathway, is identified as a novel therapeutic target in cisplatin-resistant ovarian cancer. *FASEB Journal : Official Publication of the Federation of American Societies for Experimental Biology*, *33*(4), 5350–5365. https://doi.org/10.1096/FJ.201801529RR

González-Acosta, D., Blanco-Romero, E., Ubieto-Capella, P., Mutreja, K., Míguez, S., Llanos, S., García, F., Muñoz, J., Blanco, L., Lopes, M., & Méndez, J. (2021). PrimPol-mediated repriming facilitates replication traverse of DNA interstrand crosslinks. *The EMBO Journal*, *40*(14), e106355. https://doi.org/10.15252/EMBJ.2020106355

Goodarzi, A. A., Yu, Y., Riballo, E., Douglas, P., Walker, S. A., Ye, R., Härer, C., Marchetti, C., Morrice, N., Jeggo, P. A., & Lees-Miller, S. P. (2006). *DNA-PK autophosphorylation*

facilitates Artemis endonuclease activity. *25*(16), 3880–3889. https://doi.org/10.1038/SJ.EMBOJ.7601255
Goodfellow, S. J., & Zomerdijk, J. C. B. M. (2013). Basic mechanisms in RNA polymerase I transcription of the ribosomal RNA genes. *Sub-Cellular Biochemistry*, *61*, 211–236. https://doi.org/10.1007/978-94-007-4525-4_10/TABLES/2
Goodman, M. F., & Woodgate, R. (2013). Translesion DNA Polymerases. *Cold Spring Harbor Perspectives in Biology*, *5*(10). https://doi.org/10.1101/CSHPERSPECT.A010363
Gopalakrishnan, S., Van Emburgh, B. O., & Robertson, K. D. (2008). DNA methylation in development and human disease. *Mutation Research*, *647*(1–2), 30. https://doi.org/10.1016/J.MRFMMM.2008.08.006
Görner, W., Durchschlag, E., Wolf, J., Brown, E. L., Ammerer, G., Ruis, H., & Schüller, C. (2002). Acute glucose starvation activates the nuclear localization signal of a stress-specific yeast transcription factor. *The EMBO Journal*, *21*(1–2), 135–144. https://doi.org/10.1093/EMBOJ/21.1.135
Gradia, S., Acharya, S., & Fishel, R. (1997). The human mismatch recognition complex hMSH2-hMSH6 functions as a novel molecular switch. *Cell*, *91*(7), 995–1005. https://doi.org/10.1016/S0092-8674(00)80490-0
Graham, T. G. W., Walter, J. C., & Loparo, J. J. (2016). Two-Stage Synapsis of DNA Ends during Non-homologous End Joining. *Molecular Cell*, *61*(6), 850–858. https://doi.org/10.1016/j.molcel.2016.02.010
Gravel, S., Chapman, J. R., Magill, C., & Jackson, S. P. (2008). DNA helicases Sgs1 and BLM promote DNA double-strand break resection. *Genes & Development*, *22*(20), 2767–2772. https://doi.org/10.1101/GAD.503108
Griffiths, L. M., Swartzlander, D., Meadows, K. L., Wilkinson, K. D., Corbett, A. H., & Doetsch, P. W. (2009). Dynamic Compartmentalization of Base Excision Repair Proteins in Response to Nuclear and Mitochondrial Oxidative Stress. *Molecular and Cellular Biology*, *29*(3), 794. https://doi.org/10.1128/MCB.01357-08
Grutzen, P. J., & Andreae, M. O. (1990). Biomass Burning in the Tropics: Impact on Atmospheric Chemistry and Biogeochemical Cycles. *Science*, *250*(4988), 1669–1678. https://doi.org/10.1126/SCIENCE.250.4988.1669
Gu, G., Wang, Y., Shen, Y., Ma, Y., Yang, H., Huang, S., & Hu, L. (2022). A pan-cancer analysis of RCC2 and its interaction with HMGA2 protein in an in vitro model of colorectal cancer cells. *Experimental and Therapeutic Medicine*, *24*(6). https://doi.org/10.3892/ETM.2022.11661
Guainazzi, A., & Schärer, O. D. (2010). Using synthetic DNA interstrand crosslinks to elucidate repair pathways and identify new therapeutic targets for cancer chemotherapy. *Cellular and Molecular Life Sciences : CMLS*, *67*(21), 3683. https://doi.org/10.1007/S00018-010-0492-6
Guillotin, D., & Martin, S. A. (2014). Exploiting DNA mismatch repair deficiency as a therapeutic strategy. *Experimental Cell Research*, *329*(1), 110–115. https://doi.org/10.1016/J.YEXCR.2014.07.004
Guo, C., Fischhaber, P. L., Luk-Paszyc, M. J., Masuda, Y., Zhou, J., Kamiya, K., Kisker, C., & Friedberg, E. C. (2003). Mouse Rev1 protein interacts with multiple DNA polymerases involved in translesion DNA synthesis. *The EMBO Journal*, *22*(24), 6621–6630. https://doi.org/10.1093/EMBOJ/CDG626
Guo, Z., Qian, L., Liu, R., Dai, H., Zhou, M., Zheng, L., & Shen, B. (2008). Nucleolar Localization and Dynamic Roles of Flap Endonuclease 1 in Ribosomal DNA Replication

and Damage Repair. *Molecular and Cellular Biology*, *28*(13), 4310. https://doi.org/10.1128/MCB.00200-08

Gupta, N., Khetan, D., Chaudhary, R., & Shukla, J. S. (2020). Prospective cohort study to assess the effect of storage duration, leuko-filtration, and gamma irradiation on cell-free DNA in red cell components. *Transfus. Med. Hemother*, *47*(5), 409–419. https://doi.org/10.1159/000505937

Gupta, R., Sharma, S., Sommers, J. A., Kenny, M. K., Cantor, S. B., & Brosh, R. M. (2007). FANCJ (BACH1) helicase forms DNA damage inducible foci with replication protein A and interacts physically and functionally with the single-stranded DNA-binding protein. *Blood*, *110*(7), 2390–2398. https://doi.org/10.1182/BLOOD-2006-11-057273

Haince, J. F., Kozlov, S., Dawson, V. L., Dawson, T. M., Hendzel, M. J., Lavin, M. F., & Poirier, G. G. (2007). Ataxia telangiectasia mutated (ATM) signaling network is modulated by a novel poly(ADP-ribose)-dependent pathway in the early response to DNA-damaging agents. *Journal of Biological Chemistry*, *282*(22), 16441–16453. https://doi.org/10.1074/jbc.M608406200

Haince, J. F., McDonald, D., Rodrigue, A., Déry, U., Masson, J. Y., Hendzel, M. J., & Poirier, G. G. (2008). PARP1-dependent kinetics of recruitment of MRE11 and NBS1 proteins to multiple DNA damage sites. *Journal of Biological Chemistry*, *283*(2), 1197–1208. https://doi.org/10.1074/jbc.M706734200

Halazonetis, T. D., Gorgoulis, V. G., & Bartek, J. (2008). An oncogene-induced DNA damage model for cancer development. *Science*, *319*(5868), 1352–1355.

Hanada, K., Budzowska, M., Davies, S. L., Van Drunen, E., Onizawa, H., Beverloo, H. B., Maas, A., Essers, J., Hickson, I. D., & Kanaar, R. (2007). The structure-specific endonuclease Mus81 contributes to replication restart by generating double-strand DNA breaks. *Nature Structural & Molecular Biology*, *14*(11), 1096–1104. https://doi.org/10.1038/NSMB1313

Hanahan, D., & Weinberg, R. A. (2011). Hallmarks of cancer: the next generation. *Cell*, *144*(5), 646–674.

Hanawalt, P. C., & Spivak, G. (2008). Transcription-coupled DNA repair: Two decades of progress and surprises. *Nature Reviews Molecular Cell Biology*, *9*(12), 958–970. https://doi.org/10.1038/NRM2549

Hao, Y., Liu, X., Lu, X., Yang, X., Wang, L., Chen, S., Li, H., Li, J., Cao, J., Chen, J., Li, Y., Zhao, L., Shi, Y., Shen, C., Yan, W., He, J., Huang, J., & Gu, D. (2013). Genome-wide association study in Han Chinese identifies three novel loci for human height. *Human Genetics*, *132*(6), 681–689. https://doi.org/10.1007/S00439-013-1280-9/FIGURES/2

Harper, J. W., & Elledge, S. J. (2007). The DNA Damage Response: Ten Years After. *Molecular Cell*, *28*(5), 739–745. https://doi.org/10.1016/j.molcel.2007.11.015

Hashimoto, Y., Puddu, F., & Costanzo, V. (2011). RAD51- and MRE11-dependent reassembly of uncoupled CMG helicase complex at collapsed replication forks. *Nature Structural & Molecular Biology 2011 19:1*, *19*(1), 17–24. https://doi.org/10.1038/nsmb.2177

Hasty, P., & Montagna, C. (2014). Chromosomal rearrangements in cancer. *Https://Doi.Org/10.4161/Mco.29904*, *1*(1). https://doi.org/10.4161/MCO.29904

Hayashi, K., & Matsunaga, S. (2019). Heat and chilling stress induce nucleolus morphological changes. *Journal of Plant Research*, *132*(3), 395–403. https://doi.org/10.1007/S10265-019-01096-9/FIGURES/5

Helleday, T., Petermann, E., Lundin, C., Hodgson, B., & Sharma, R. A. (2008). DNA repair pathways as targets for cancer therapy. *Nature Reviews Cancer*, *8*(3), 193–204.

https://doi.org/10.1038/nrc2342
Hempel, W. M., Cavanaugh, A. H., Hannan, R. D., Taylor, L., & Rothblum, L. I. (2023). The Species-Specific RNA Polymerase I Transcription Factor SL-1 Binds to Upstream Binding Factor. *Https://Doi.Org/10.1128/MCB.16.2.557*, *16*(2), 557–563. https://doi.org/10.1128/MCB.16.2.557
Henle, E. S., & Linn, S. (1997). Formation, prevention, and repair of DNA damage by iron/hydrogen peroxide. *Journal of Biological Chemistry*, *272*(31), 19095–19098. https://doi.org/10.1074/jbc.272.31.19095
Hennersg, W. D., Rodriguez, L. 0, Hechte, S. M., & Haseltine, W. A. (1983). y Ray Induced Deoxyribonucleic Acid Strand Breaks. *Journal of Biological Chemistry*, *258*, 711–713. https://doi.org/10.1016/S0021-9258(18)33104-1
Hernandez-Verdun, D., Roussel, P., Thiry, M., Sirri, V., & Lafontaine, D. L. J. (2010). The nucleolus: Structure/function relationship in RNA metabolism. *Wiley Interdisciplinary Reviews: RNA*, *1*(3), 415–431. https://doi.org/10.1002/WRNA.39
Hetzer, M., Bilbao-Cortés, D., Walther, T. C., Gruss, O. J., & Mattaj, I. W. (2000). GTP hydrolysis by Ran is required for nuclear envelope assembly. *Molecular Cell*, *5*(6), 1013–1024. https://doi.org/10.1016/S1097-2765(00)80266-X
Ho, G. P. H., Margossian, S., Taniguchi, T., & D'Andrea, A. D. (2006). Phosphorylation of FANCD2 on Two Novel Sites Is Required for Mitomycin C Resistance. *Molecular and Cellular Biology*, *26*(18), 7005–7015. https://doi.org/10.1128/mcb.02018-05
Ho, T. V., & Schärer, O. D. (2010). Translesion DNA synthesis polymerases in DNA interstrand crosslink repair. *Environmental and Molecular Mutagenesis*, *51*(6), 552–566. https://doi.org/10.1002/EM.20573
Hochegger, H., Dejsuphong, D., Fukushima, T., Morrison, C., Sonoda, E., Schreiber, V., Guang, Y. Z., Saberi, A., Masutani, M., Adachi, N., Koyama, H., De Murcia, G., & Takeda, S. (2006). Parp-1 protects homologous recombination from interference by Ku and Ligase IV in vertebrate cells. *The EMBO Journal*, *25*(6), 1305–1314. https://doi.org/10.1038/SJ.EMBOJ.7601015
Hodskinson, M. R., Bolner, A., Sato, K., Kamimae-Lanning, A. N., Rooijers, K., Witte, M., Mahesh, M., Silhan, J., Petek, M., Williams, D. M., Kind, J., Chin, J. W., Patel, K. J., & Knipscheer, P. (2020). Alcohol-derived DNA crosslinks are repaired by two distinct mechanisms. *Nature*, *579*(In press), 603–608. https://doi.org/10.1038/s41586-020-2059-5
Hoeijmakers, J. H. J. (2009). DNA Damage, Aging, and Cancer. *New England Journal of Medicine*, *361*(15), 1475–1485.
Holliday, R., & Grigg, G. W. (1993). DNA methylation and mutation. *Mutation Research/Fundamental and Molecular Mechanisms of Mutagenesis*, *285*(1), 61–67. https://doi.org/10.1016/0027-5107(93)90052-H
Holliday, R., & Ho, T. (1998). Gene silencing and endogenous DNA methylation in mammalian cells. *Mutation Research - Fundamental and Molecular Mechanisms of Mutagenesis*, *400*(1–2), 361–368. https://doi.org/10.1016/S0027-5107(98)00034-7
Hölzel, M., Orban, M., Hochstatter, J., Rohrmoser, M., Harasim, T., Malamoussi, A., Kremmer, E., Längst, G., & Eick, D. (2010). Defects in 18 S or 28 S rRNA Processing Activate the p53 Pathway. *The Journal of Biological Chemistry*, *285*(9), 6364. https://doi.org/10.1074/JBC.M109.054734
Horikoshi, N., Tachiwana, H., Kagawa, W., Osakabe, A., Matsumoto, S., Iwai, S., Sugasawa, K., & Kurumizaka, H. (2016). Crystal structure of the nucleosome containing ultraviolet

light-induced cyclobutane pyrimidine dimer. *Biochemical and Biophysical Research Communications*, *471*(1), 117–122. https://doi.org/10.1016/J.BBRC.2016.01.170

Hosoya, N., & Miyagawa, K. (2014). Targeting DNA damage response in cancer therapy. *Cancer Science*, *105*(4), 370–388. https://doi.org/10.1111/CAS.12366

Housh, K., Jha, J. S., Haldar, T., Amin, S. B. M., Islam, T., Wallace, A., Gomina, A., Guo, X., Nel, C., Wyatt, J. W., & Gates, K. S. (2021). Formation and repair of unavoidable, endogenous interstrand cross-links in cellular DNA. *DNA Repair*, *98*, 103029. https://doi.org/10.1016/J.DNAREP.2020.103029

Howard, S. M., Yanez, D. A., & Stark, J. M. (2015). DNA Damage Response Factors from Diverse Pathways, Including DNA Crosslink Repair, Mediate Alternative End Joining. *PLOS Genetics*, *11*(1), e1004943. https://doi.org/10.1371/JOURNAL.PGEN.1004943

Howlett, N. G., Taniguchi, T., Durkin, S. G., D'Andrea, A. D., & Glover, T. W. (2005). The Fanconi anemia pathway is required for the DNA replication stress response and for the regulation of common fragile site stability. *Human Molecular Genetics*, *14*(5), 693–701. https://doi.org/10.1093/HMG/DDI065

Hu, K., Li, Y., Wu, W., Chen, H., Chen, Z., Zhang, Y., Guo, Y., & Dong, Y. (2018). High-performance gene expression and knockout tools using sleeping beauty transposon system. *Mobile DNA*, *9*(1). https://doi.org/10.1186/S13100-018-0139-Y

Hu, Q., Botuyan, M. V., Zhao, D., Cui, G., Mer, E., & Mer, G. (2021). Mechanisms of BRCA1–BARD1 nucleosome recognition and ubiquitylation. *Nature 2021 596:7872*, *596*(7872), 438–443. https://doi.org/10.1038/s41586-021-03716-8

Hua, L., Yan, D., Wan, C., & Hu, B. (2022). Nucleolus and Nucleolar Stress: From Cell Fate Decision to Disease Development. *Cells 2022, Vol. 11, Page 3017*, *11*(19), 3017. https://doi.org/10.3390/CELLS11193017

Huang, C., Han, Y., Wang, Y., Sun, X., Yan, S., Yeh, E. T. H., Chen, Y., Cang, H., Li, H., Shi, G., Cheng, J., Tang, X., & Yi, J. (2009). SENP3 is responsible for HIF-1 transactivation under mild oxidative stress via p300 de-SUMOylation. *The EMBO Journal*, *28*(18), 2748–2762. https://doi.org/10.1038/EMBOJ.2009.210

Huang, H., & Hopkins, P. B. (1993). DNA Interstrand Cross-Linking by Formaldehyde: Nucleotide Sequence Preference and Covalent Structure of the Predominant Cross-Link Formed in Synthetic Oligonucleotides. *Am. Chem. Soc*, *115*, 9402–9408. https://pubs.acs.org/sharingguidelines

Huang, H., Kozekov, I. D., Kozekova, A., Wang, H., Lloyd, R. S., Rizzo, C. J., & Stone, M. P. (2010). DNA Cross-links Induced by trans-4-Hydroxynonenal. *Environmental and Molecular Mutagenesis*, *51*(6), 625. https://doi.org/10.1002/EM.20599

Huang, H., Zhu, L., Reid, B. R., Drobny, G. P., & Hopkins, P. B. (1995). Solution structure of a cisplatin-induced DNA interstrand cross-link. *Science*, *270*(5243), 1842. https://doi.org/10.1126/SCIENCE.270.5243.1842

Huang, J., Liu, S., Bellani, M. A., Thazhathveetil, A. K., Ling, C., deWinter, J. P., Wang, Y., Wang, W., & Seidman, M. M. (2013). The DNA Translocase FANCM/MHF Promotes Replication Traverse of DNA Interstrand Crosslinks. *Molecular Cell*, *52*(3), 434–446. https://doi.org/10.1016/J.MOLCEL.2013.09.021

Huang, J., Zhang, J., Bellani, M. A., Pokharel, D., Gichimu, J., James, R. C., Gali, H., Ling, C., Yan, Z., Xu, D., Chen, J., Meetei, A. R., Li, L., Wang, W., & Seidman, M. M. (2019). Remodeling of Interstrand Crosslink Proximal Replisomes Is Dependent on ATR, FANCM, and FANCD2. *Cell Reports*, *27*(6), 1794-1808.e5. https://doi.org/10.1016/J.CELREP.2019.04.032

Huang, M., Ji, Y., Itahana, K., Zhang, Y., & Mitchell, B. (2008). Guanine nucleotide depletion inhibits pre-ribosomal RNA synthesis and causes nucleolar disruption. *Leukemia Research*, *32*(1), 131–141. https://doi.org/10.1016/J.LEUKRES.2007.03.025

Huang, M., Kim, J. M., Shiotani, B., Yang, K., Zou, L., & D'Andrea, A. D. (2010). The FANCM/FAAP24 complex is required for the DNA interstrand crosslink-induced checkpoint response. *Molecular Cell*, *39*(2), 259–268. https://doi.org/10.1016/j.molcel.2010.07.005

Huang, R., Yu, T., Li, Y., & Hu, J. (2018). Upregulated has-miR-4516 as a potential biomarker for early diagnosis of dust-induced pulmonary fibrosis in patients with pneumoconiosis. *Toxicol. Res (Camb.)*, *7*(3), 415–422. https://doi.org/10.1039/c8tx00031j

Huang, R., & Zhou, P. K. (2021). *DNA damage repair: historical perspectives, mechanistic pathways and clinical translation for targeted cancer therapy*. *6*(1), 1–35. https://www.nature.com/articles/s41392-021-00648-7

Huang, Y., Leung, J. W. C., Lowery, M., Matsushita, N., Wang, Y., Shen, X., Huong, D., Takata, M., Chen, J., & Li, L. (2014). Modularized Functions of the Fanconi Anemia Core Complex. *Cell Reports*, *7*(6), 1849–1857. https://doi.org/10.1016/J.CELREP.2014.04.029

Huang, Y., & Li, G. M. (2020). DNA mismatch repair in the chromatin context: Mechanisms and therapeutic potential. *DNA Repair*, *93*, 102918. https://doi.org/10.1016/J.DNAREP.2020.102918

Huang, Y., & Li, L. (2013). DNA crosslinking damage and cancer - a tale of friend and foe. *Translational Cancer Research*, *2*(3), 144–154. https://doi.org/10.3978/j.issn.2218-676X.2013.03.01

Huen, M. S. Y., & Chen, J. (2008). The DNA damage response pathways: At the crossroad of protein modifications. *Cell Research*, *18*(1), 8–16. https://doi.org/10.1038/CR.2007.109

Huertas, P., & Jackson, S. P. (2009). Human CtIP mediates cell cycle control of DNA end resection and double strand break repair. *Journal of Biological Chemistry*, *284*(14), 9558–9565. https://doi.org/10.1074/jbc.M808906200

Humphries, J. D., Byron, A., Bass, M. D., Craig, S. E., Pinney, J. W., Knight, D., & Humphries, M. J. (2009). Proteomic analysis of integrin-associated complexes identifies RCC2 as a dual regulator of Rac1 and Arf6. *Science Signaling*, *2*(87). https://doi.org/10.1126/scisignal.2000396

Hwa Yun, B., Guo, J., Bellamri, M., & Turesky, R. J. (2020). DNA Adducts: formation, biological effects, and new biospecimens for mass spectrometric measurements in humans. *Mass Spectrometry Reviews*, *39*(1–2), 55. https://doi.org/10.1002/MAS.21570

Hwang, J. W., Kim, S. N., Myung, N., Song, D., Han, G., Bae, G. U., Bedford, M. T., & Kim, Y. K. (2020). PRMT5 promotes DNA repair through methylation of 53BP1 and is regulated by Src-mediated phosphorylation. *Communications Biology 2020 3:1*, *3*(1), 1–13. https://doi.org/10.1038/s42003-020-01157-z

Ijsselsteijn, R., Jansen, J. G., & de Wind, N. (2020). DNA mismatch repair-dependent DNA damage responses and cancer. *DNA Repair (Amst.)*, *93*, 102923. https://doi.org/10.1016/j.dnarep.2020.102923

Ikeda, K., Kamisuki, S., Uetake, S., Mizusawa, A., Ota, N., Sasaki, T., Tsukuda, S., Kusayanagi, T., Takakusagi, Y., Morohashi, K., Yamori, T., Dan, S., Shiina, I., & Sugawara, F. (2015). Ridaifen G, tamoxifen analog, is a potent anticancer drug working through a combinatorial association with multiple cellular factors. *Bioorganic & Medicinal Chemistry*, *23*(18), 6118–6124. https://doi.org/10.1016/j.bmc.2015.08.001

Iliakis, G., Mladenov, E., & Mladenova, V. (2019). Necessities in the Processing of DNA

Double Strand Breaks and Their Effects on Genomic Instability and Cancer. *Cancers 2019, Vol. 11, Page 1671*, *11*(11), 1671. https://doi.org/10.3390/CANCERS11111671

Ilves, I., Petojevic, T., Pesavento, J. J., & Botchan, M. R. (2010). Activation of the MCM2-7 Helicase by Association with Cdc45 and GINS Proteins. *Molecular Cell*, *37*(2), 247–258. https://doi.org/10.1016/j.molcel.2009.12.030

Inagaki, H., Matsushima, Y., Nakamura, K., Ohshima, M., Kadowaki, T., & Kitagawa, Y. (1996). A large DNA-binding nuclear protein with RNA recognition motif and serine/arginine-rich domain. *Journal of Biological Chemistry*, *271*(21), 12525–12531. https://doi.org/10.1074/jbc.271.21.12525

Ishiai, M., Kitao, H., Smogorzewska, A., Tomida, J., Kinomura, A., Uchida, E., Saberi, A., Kinoshita, E., Kinoshita-Kikuta, E., Koike, T., Tashiro, S., Elledge, S. J., & Takata, M. (2008). FANCI phosphorylation functions as a molecular switch to turn on the Fanconi anemia pathway. *Nature Structural and Molecular Biology*, *15*(11), 1138–1146. https://doi.org/10.1038/nsmb.1504

Ivanov, E. L., & Haber, J. E. (1995). RAD1 and RAD10, but Not Other Excision Repair Genes, Are Required for Double-Strand Break-Induced Recombination in Saccharomyces cerevisiae. *MOLECULAR AND CELLULAR BIOLOGY*, *15*(4), 2245–2251.

Jackson, S. P., & Bartek, J. (2009). *The DNA-damage response in human biology and disease*. *461*(7267), 1071–1078. https://www.nature.com/articles/nature08467

Jacobs, A. L., & Schär, P. (2012). DNA glycosylases: In DNA repair and beyond. *Chromosoma*, *121*(1), 1–20. https://doi.org/10.1007/S00412-011-0347-4

Jarboui, M. A., Wynne, K., Elia, G., Hall, W. W., & Gautier, V. W. (2011). Proteomic profiling of the human T-cell nucleolus. *Molecular Immunology*, *49*(3), 441–452. https://doi.org/10.1016/J.MOLIMM.2011.09.005

Jaruga, P., & Dizdaroglu, M. (2008). 8,5′-Cyclopurine-2′-deoxynucleosides in DNA: Mechanisms of formation, measurement, repair and biological effects. *DNA Repair*, *7*(9), 1413–1425. https://doi.org/10.1016/J.DNAREP.2008.06.005

Jette, N., & Lees-Miller, S. P. (2015). The DNA-dependent protein kinase: A multifunctional protein kinase with roles in DNA double strand break repair and mitosis. *Progress in Biophysics and Molecular Biology*, *117*(2–3), 194–205. https://doi.org/10.1016/J.PBIOMOLBIO.2014.12.003

Jiang, W., Crowe, J. L., Liu, X., Nakajima, S., Wang, Y., Li, C., Lee, B. J., Dubois, R. L., Liu, C., Yu, X., Lan, L., & Zha, S. (2015). Differential phosphorylation of DNA-PKcs regulates the interplay between end-processing and end-ligation during non-homologous end-joining. *Molecular Cell*, *58*(1), 172. https://doi.org/10.1016/J.MOLCEL.2015.02.024

Jimeno, S., Fernández-Ávila, M. J., Cruz-García, A., Cepeda-García, C., Gómez-Cabello, D., & Huertas, P. (2015). Neddylation inhibits CtIP-mediated resection and regulates DNA double strand break repair pathway choice. *Nucleic Acids Research*, *43*(2), 987–999. https://doi.org/10.1093/NAR/GKU1384

Jiricny, J. (2006). The multifaceted mismatch-repair system. *Nature Rev. Mol. Cell Biol*, *7*(5), 335–346. https://doi.org/10.1038/nrm1907

Jones, R. E., Oh, S., Grimstead, J. W., Zimbric, J., Roger, L., Heppel, N. H., Ashelford, K. E., Liddiard, K., Hendrickson, E. A., & Baird, D. M. (2014). Escape from telomere-driven crisis is DNA ligase III dependent. *Cell Reports*, *8*(4), 1063–1076. https://doi.org/10.1016/j.celrep.2014.07.007

Joo, W., Xu, G., Persky, N. S., Smogorzewska, A., Rudge, D. G., Buzovetsky, O., Elledge, S. J., & Pavletich, N. P. (2011). Structure of the FANCI-FANCD2 Complex: Insights into the

Fanconi Anemia DNA Repair Pathway. *Science (New York, N.Y.)*, *333*(6040), 312. https://doi.org/10.1126/SCIENCE.1205805

Kajitani, G. S., Nascimento, L. L. de S., Neves, M. R. de C., Leandro, G. da S., Garcia, C. C. M., & Menck, C. F. M. (2021). Transcription blockage by DNA damage in nucleotide excision repair-related neurological dysfunctions. *Seminars in Cell & Developmental Biology*, *114*, 20–35. https://doi.org/10.1016/J.SEMCDB.2020.10.009

Kalab, P., Weis, K., & Heald, R. (2002). Visualization of a Ran-GTP gradient in interphase and mitotic Xenopus egg extracts. *Science*, *295*(5564), 2452–2456. https://doi.org/10.1126/SCIENCE.1068798/SUPPL_FILE/1068798S5_THUMB.GIF

Kanao, R., & Masutani, C. (2017). Regulation of DNA damage tolerance in mammalian cells by post-translational modifications of PCNA. *Mutation Research/Fundamental and Molecular Mechanisms of Mutagenesis*, *803–805*, 82–88. https://doi.org/10.1016/J.MRFMMM.2017.06.004

Kanoh, Y., Tamai, K., & Shirahige, K. (2006). Different requirements for the association of ATR-ATRIP and 9-1-1 to the stalled replication forks. *Gene*, *377*(1–2), 88–95. https://doi.org/10.1016/J.GENE.2006.03.019

Karanam, K., Kafri, R., Loewer, A., & Lahav, G. (2012). Quantitative Live Cell Imaging Reveals a Gradual Shift between DNA Repair Mechanisms and a Maximal Use of HR in Mid S Phase. *Molecular Cell*, *47*(2), 320–329. https://doi.org/10.1016/j.molcel.2012.05.052

Karanja, K. K., Cox, S. W., Duxin, J. P., Stewart, S. A., & Campbell, J. L. (2012). DNA2 and EXO1 in replication-coupled, homology-directed repair and in the interplay between HDR and the FA/BRCA network. *Cell Cycle*, *11*(21), 3983–3996. https://doi.org/10.4161/CC.22215/SUPPL_FILE/KCCY_A_10922215_SM0001.ZIP

Kasai, H., & Nishimura, S. (1984). Hydroxylation of deoxyguanosine at the C-8 position by ascorbic acid and other reducing agents. *Nucleic Acids Research*, *12*(4), 2137. https://doi.org/10.1093/NAR/12.4.2137

Kastan, M. B., & Bartek, J. (2004). Cell-cycle checkpoints and cancer. *Nature 2004 432:7015*, *432*(7015), 316–323. https://doi.org/10.1038/nature03097

Kato, N., Kawasoe, Y., Williams, H., Coates, E., Roy, U., Shi, Y., Beese, L. S., Schärer, O. D., Yan, H., Gottesman, M. E., Takahashi, T. S., & Gautier, J. (2017). Sensing and Processing of DNA Interstrand Crosslinks by the Mismatch Repair Pathway. *Cell Reports*, *21*(5), 1375–1385. https://doi.org/10.1016/J.CELREP.2017.10.032

Kavli, B., Otterlei, M., Slupphaug, G., & Krokan, H. E. (2007). Uracil in DNA-General mutagen, but normal intermediate in acquired immunity. *DNA Repair*, *6*(4), 505–516. https://doi.org/10.1016/J.DNAREP.2006.10.014

Kee, Y., & D'Andrea, A. D. (2012). Molecular pathogenesis and clinical management of Fanconi anemia. *The Journal of Clinical Investigation*, *122*(11), 3799–3806. https://doi.org/10.1172/JCI58321

Kee, Y., Kim, J. M., & D'Andrea, A. (2009). Regulated degradation of FANCM in the Fanconi anemia pathway during mitosis. *Genes & Development*, *23*(5), 555–560. https://doi.org/10.1101/GAD.1761309

Keijzers, G., Bakula, D., Petr, M. A., Madsen, N. G. K., Teklu, A., Mkrtchyan, G., Osborne, B., & Scheibye-Knudsen, M. (2019). Human Exonuclease 1 (EXO1) Regulatory Functions in DNA Replication with Putative Roles in Cancer. *International Journal of Molecular Sciences*, *20*(1). https://doi.org/10.3390/IJMS20010074

Kemp, M., & Sancar, A. (2009). DNA Distress: Just Ring 9-1-1. *Current Biology*, *19*(17), R733–R734. https://doi.org/10.1016/j.cub.2009.07.026

Kent, O. A., & Mendell, J. T. (2006). A small piece in the cancer puzzle: microRNAs as tumor suppressors and oncogenes. *Oncogene 2006 25:46*, *25*(46), 6188–6196. https://doi.org/10.1038/sj.onc.1209913

Khandelwal, N., Simpson, J., Taylor, G., Rafique, S., Whitehouse, A., Hiscox, J., & Stark, L. A. (2011). Nucleolar NF-κB/RelA mediates apoptosis by causing cytoplasmic relocalization of nucleophosmin. *Cell Death & Differentiation 2011 18:12*, *18*(12), 1889–1903. https://doi.org/10.1038/cdd.2011.79

Kidd, A. R., Snider, J. L., Martin, T. D., Graboski, S. F., Der, C. J., & Cox, A. D. (2010). The Ras-related small GTPases RalA and RalB regulate cellular survival after ionizing radiation. *International Journal of Radiation Oncology Biology Physics*, *78*(1), 205–212. /pmc/articles/PMC2922474/

Kiefer, J. (2007). Effects of ultraviolet radiation on DNA. *Chromosomal Alterations: Methods, Results and Importance in Human Health*, *9783540714149*, 39–53. https://doi.org/10.1007/978-3-540-71414-9_3/COVER

Kile, A. C., Chavez, D. A., Bacal, J., Eldirany, S., Korzhnev, D. M., Bezsonova, I., Eichman, B. F., & Cimprich, K. A. (2015). HLTF's Ancient HIRAN Domain Binds 3' DNA Ends to Drive Replication Fork Reversal. *Molecular Cell*, *58*(6), 1090–1100. https://doi.org/10.1016/j.molcel.2015.05.013

Kim, H., Yang, K., Dejsuphong, D., & D'Andrea, A. D. (2012). Regulation of Rev1 by the Fanconi anemia core complex. *Nature Structural & Molecular Biology 2012 19:2*, *19*(2), 164–170. https://doi.org/10.1038/nsmb.2222

Kim, J. M., Kee, Y., Gurtan, A., & D'Andrea, A. D. (2008). Cell cycle-dependent chromatin loading of the Fanconi anemia core complex by FANCM/FAAP24. *Blood*, *111*(10), 5215–5222. https://doi.org/10.1182/blood-2007-09-113092

Kim, J. M., Parmar, K., Huang, M., Weinstock, D. M., Ruit, C. A., Kutok, J. L., & D'Andrea, A. D. (2009). Inactivation of Murine Usp1 Results in Genomic Instability and a Fanconi Anemia Phenotype. *Developmental Cell*, *16*(2), 314–320. https://doi.org/10.1016/j.devcel.2009.01.001

Kim, T. M., Son, M. Y., Dodds, S., Hu, L., Luo, G., & Hasty, P. (2015). RECQL5 and BLM exhibit divergent functions in cells defective for the Fanconi anemia pathway. *Nucleic Acids Research*, *43*(2), 893. https://doi.org/10.1093/NAR/GKU1334

Kim, Y.-J., & M. Wilson III, D. (2011). Overview of Base Excision Repair Biochemistry. *Current Molecular Pharmacology*, *5*(1), 3–13. https://doi.org/10.2174/1874467211205010003

Kim, Y., Spitz, G. S., Veturi, U., Lach, F. P., Auerbach, A. D., & Smogorzewska, A. (2013). Regulation of multiple DNA repair pathways by the Fanconi anemia protein SLX4. *Blood*, *121*(1), 54. https://doi.org/10.1182/BLOOD-2012-07-441212

Klein Douwel, D., Boonen, R. A. C. M., Long, D. T., Szypowska, A. A., Räschle, M., Walter, J. C., & Knipscheer, P. (2014). XPF-ERCC1 Acts in Unhooking DNA Interstrand Crosslinks in Cooperation with FANCD2 and FANCP/SLX4. *Molecular Cell*, *54*(3), 460–471. https://doi.org/10.1016/J.MOLCEL.2014.03.015

Kliza, K. W., Liu, Q., Roosenboom, L. W. M., Jansen, P. W. T. C., Filippov, D. V, & Correspondence, V. (2021). Reading ADP-ribosylation signaling using chemical biology and interaction proteomics. *Molecular Cell*, *81*, 4552-4567.e8. https://doi.org/10.1016/j.molcel.2021.08.037

Kobaisi, F., Fayyad, N., Rezvani, H. R., Fayyad-Kazan, M., Sulpice, E., Badran, B., Fayyad-Kazan, H., Gidrol, X., & Rachidi, W. (2019). Signaling Pathways, Chemical and Biological Modulators of Nucleotide Excision Repair: The Faithful Shield against UV Genotoxicity.

Oxidative Medicine and Cellular Longevity, *2019*. https://doi.org/10.1155/2019/4654206
Kochetkov, N. K., & Budovskii, E. I. (1972). Photochemistry of Nucleic Acids and their Components. *Organic Chemistry of Nucleic Acids*, 543–618. https://doi.org/10.1007/978-1-4684-2973-2_8
Kondo, E., Horii, A., & Fukushige, S. (2001). The interacting domains of three MutL heterodimers in man: hMLH1 interacts with 36 homologous amino acid residues within hMLH3, hPMS1 and hPMS2. *Nucleic Acids Research*, *29*(8), 1695. https://doi.org/10.1093/NAR/29.8.1695
Kondo, N., Takahashi, A., Ono, K., & Ohnishi, T. (2010). DNA Damage Induced by Alkylating Agents and Repair Pathways. *Journal of Nucleic Acids*, *2010*. https://doi.org/10.4061/2010/543531
Korsholm, L. M., Gál, Z., Lin, L., Quevedo, O., Ahmad, D. A., Dulina, E., Luo, Y., Bartek, J., & Larsen, D. H. (2019). Double-strand breaks in ribosomal RNA genes activate a distinct signaling and chromatin response to facilitate nucleolar restructuring and repair. *Nucleic Acids Research*, *47*(15), 8019–8035. https://doi.org/10.1093/NAR/GKZ518
Korsholm, L. M., Gál, Z., Nieto, B., Quevedo, O., Boukoura, S., Lund, C. C., & Larsen, D. H. (2020). Recent advances in the nucleolar responses to DNA double-strand breaks. *Nucleic Acids Research*, *48*(17), 9449–9461. https://doi.org/10.1093/NAR/GKAA713
Kotoglou, P., Kalaitzakis, A., Vezyraki, P., Tzavaras, T., Michalis, L. K., Dantzer, F., Jung, J. U., & Angelidis, C. (2009). Hsp70 translocates to the nuclei and nucleoli, binds to XRCC1 and PARP-1, and protects HeLa cells from single-strand DNA breaks. *Cell Stress & Chaperones*, *14*(4), 391. https://doi.org/10.1007/S12192-008-0093-6
Kottemann, M. C., & Smogorzewska, A. (2013). Fanconi anemia and the repair of Watson and Crick crosslinks. *Nature*, *493*(7432), 356. https://doi.org/10.1038/NATURE11863
Krainer, A. R., Mayeda, A., Kozak, D., & Binns, G. (1991). Functional expression of cloned human splicing factor SF2: homology to rna-binding proteins, U1 70K, and drosophila splicing regulators. *Cell*, *66*(2), 383–394. https://doi.org/10.1016/0092-8674(91)90627-B
Krejci, L., Altmannova, V., Spirek, M., & Zhao, X. (2012). Homologous recombination and its regulation. *Nucleic Acids Research*, *40*(13), 5795. https://doi.org/10.1093/NAR/GKS270
Kruhlak, M., Crouch, E. E., Orlov, M., Montão, C., Gorski, S. A., Nussenzweig, A., Misteli, T., Phair, R. D., & Casellas, R. (2007). The ATM repair pathway inhibits RNA polymerase I transcription in response to chromosome breaks. *Nature 2007 447:7145*, *447*(7145), 730–734. https://doi.org/10.1038/nature05842
Kumar, A., Purohit, S., & Sharma, N. K. (2016). Aberrant DNA Double-strand Break Repair Threads in Breast Carcinoma: Orchestrating Genomic Insult Survival. *Journal of Cancer Prevention*, *21*(4), 227–234. https://doi.org/10.15430/JCP.2016.21.4.227
Kumar, D., Abdulovic, A. L., Viberg, J., Nilsson, A. K., Kunkel, T. A., & Chabes, A. (2011). Mechanisms of mutagenesis in vivo due to imbalanced dNTP pools. *Nucleic Acids Research*, *39*(4), 1360. https://doi.org/10.1093/NAR/GKQ829
Kunkel, T. A. (2004). DNA Replication Fidelity. *Journal of Biological Chemistry*, *279*(17), 16895–16898. https://doi.org/10.1074/jbc.R400006200
Kunkel, T. A. (2009). Evolving Views of DNA Replication (In)Fidelity. *Cold Spring Harbor Symposia on Quantitative Biology*, *74*, 91. https://doi.org/10.1101/SQB.2009.74.027
Kunkel, T. A. (2011). Balancing eukaryotic replication asymmetry with replication fidelity. *Current Opinion in Chemical Biology*, *15*(5), 620.

https://doi.org/10.1016/J.CBPA.2011.07.025
Kunkel, T. A., & Erie, D. A. (2005). DNA MISMATCH REPAIR. *Annu. Rev. Biochem*, *74*, 681–710. https://doi.org/10.1146/ANNUREV.BIOCHEM.74.082803.133243
Kurki, S., Peltonen, K., Latonen, L., Kiviharju, T. M., Ojala, P. M., Meek, D., & Laiho, M. (2004). Nucleolar protein NPM interacts with HDM2 and protects tumor suppressor protein p53 from HDM2-mediated degradation. *Cancer Cell*, *5*(5), 465–475. https://doi.org/10.1016/S1535-6108(04)00110-2
Kurowski, M. A., Bhagwat, A. S., Papaj, G., & Bujnicki, J. M. (2003). Phylogenomic identification of five new human homologs of the DNA repair enzyme AlkB. *BMC Genomics*, *4*, 48. https://doi.org/10.1186/1471-2164-4-48
Kutler, D. I., Auerbach, A. D., Satagopan, J., Giampietro, P. F., Batish, S. D., Huvos, A. G., Goberdhan, A., Shah, J. P., & Singh, B. (2003). High Incidence of Head and Neck Squamous Cell Carcinoma in Patients With Fanconi Anemia. *Archives of Otolaryngology–Head & Neck Surgery*, *129*(1), 106–112. https://doi.org/10.1001/ARCHOTOL.129.1.106
Lachaud, C., Moreno, A., Marchesi, F., Toth, R., Blow, J. J., & Rouse, J. (2016). Ubiquitinated Fancd2 recruits Fan1 to stalled replication forks to prevent genome instability. *Science (New York, N.Y.)*, *351*(6275), 846–849. https://doi.org/10.1126/SCIENCE.AAD5634
Laib, R. J., Stöckle, G., Bolt, H. M., & Kunz, W. (1979). Vinyl chloride and trichloroethylene: comparison of alkylating effects of metabolites and induction of preneoplastic enzyme deficiencies in rat liver. *Journal of Cancer Research and Clinical Oncology*, *94*(2), 139–147. https://doi.org/10.1007/BF00422494
Lakin, N. D., & Jackson, S. P. (1999). Regulation of p53 in response to DNA damage. *Oncogene 1999 18:53*, *18*(53), 7644–7655. https://doi.org/10.1038/sj.onc.1203015
Lambert, S., & Carr, A. M. (2005). Checkpoint responses to replication fork barriers. *Biochimie*, *87*(7), 591–602. https://doi.org/10.1016/J.BIOCHI.2004.10.020
Lambert, S., Mizuno, K., Blaisonneau, J., Martineau, S., Chanet, R., Fréon, K., Murray, J. M., Carr, A. M., & Baldacci, G. (2010). Homologous recombination restarts blocked replication forks at the expense of genome rearrangements by template exchange. *Molecular Cell*, *39*(3), 346–359. https://doi.org/10.1016/j.molcel.2010.07.015
Landau, D. A., Sun, C., Rosebrock, D., Herman, S. E. M., Fein, J., Sivina, M., Underbayev, C., Liu, D., Hoellenriegel, J., Ravichandran, S., Farooqui, M. Z. H., Zhang, W., Cibulskis, C., Zviran, A., Neuberg, D. S., Livitz, D., Bozic, I., Leshchiner, I., Getz, G., … Wu, C. J. (2017). The evolutionary landscape of chronic lymphocytic leukemia treated with ibrutinib targeted therapy. *Nature Communications 2017 8:1*, *8*(1), 1–12. https://doi.org/10.1038/s41467-017-02329-y
Langevin, F., Crossan, G. P., Rosado, I. V., Arends, M. J., & Patel, K. J. (2011). Fancd2 counteracts the toxic effects of naturally produced aldehydes in mice. *Nature 2011 475:7354*, *475*(7354), 53–58. https://doi.org/10.1038/nature10192
Larsen, D. H., Hari, F., Clapperton, J. A., Gwerder, M., Gutsche, K., Altmeyer, M., Jungmichel, S., Toledo, L. I., Fink, D., Rask, M. B., Grøfte, M., Lukas, C., Nielsen, M. L., Smerdon, S. J., Lukas, J., & Stucki, M. (2014). The NBS1-Treacle complex controls ribosomal RNA transcription in response to DNA damage. *Nature Cell Biology*, *16*(8), 792–803. https://doi.org/10.1038/ncb3007
Larson, K., Sahm, J., Shenkar, R., & Strauss, B. (1985). Methylation-induced blocks to in vitro DNA replication. *Mutation Research*, *150*(1–2), 77–84. https://doi.org/10.1016/0027-5107(85)90103-4

Lawley, P. D. (1966). Effects of Some Chemical Mutagens and Carcinogens on Nucleic Acids. *Progress in Nucleic Acid Research and Molecular Biology*, *5*(C), 89–131. https://doi.org/10.1016/S0079-6603(08)60232-9

Lawley, P. D., & Brookes, P. (1967). Interstrand cross-linking of DNA by difunctional alkylating agents. *Journal of Molecular Biology*, *25*(1), 143–160. https://doi.org/10.1016/0022-2836(67)90285-9

Leach, F. S., Nicolaides, N. C., Papadopoulos, N., Liu, B., Jen, J., Parsons, R., Peltomäki, P., Sistonen, P., Aaltonen, L. A., Nyström-Lahti, M., Guan, X. Y., Zhang, J., Meltzer, P. S., Yu, J. W., Kao, F. Ten, Chen, D. J., Cerosaletti, K. M., Fournier, R. E. K., Todd, S., … Vogelstein, B. (1993). Mutations of a mutS homolog in hereditary nonpolyposis colorectal cancer. *Cell*, *75*(6), 1215–1225. https://doi.org/10.1016/0092-8674(93)90330-S

Lee, C., Smith, B. A., Bandyopadhyay, K., & Gjerset, R. A. (2005). DNA damage disrupts the p14ARF-B23(nucleophosmin) interaction and triggers a transient subnuclear redistribution of p14ARF. *Cancer Research*, *65*(21), 9834–9842. https://doi.org/10.1158/0008-5472.CAN-05-1759

Lee, J. H., Goodarzi, A. A., Jeggo, P. A., & Paull, T. T. (2010). 53BP1 promotes ATM activity through direct interactions with the MRN complex. *The EMBO Journal*, *29*(3), 574. https://doi.org/10.1038/EMBOJ.2009.372

Legerski, R. J. (2010). Repair of DNA Interstrand Cross-links During S Phase of the Mammalian Cell Cycle. *Environmental and Molecular Mutagenesis*, *51*(6), 540. https://doi.org/10.1002/EM.20566

Lewin, B. (2004). Genes VIII. In *Chemistry & …*. Pearson Prentice Hall.

Li, G. M. (2007). Mechanisms and functions of DNA mismatch repair. *Cell Research 2008 18:1*, *18*(1), 85–98. https://doi.org/10.1038/cr.2007.115

Li, G. M., & Modrich, P. (1995). Restoration of mismatch repair to nuclear extracts of H6 colorectal tumor cells by a heterodimer of human MutL homologs. *Proceedings of the National Academy of Sciences of the United States of America*, *92*(6), 1950. https://doi.org/10.1073/PNAS.92.6.1950

Li, J., Holzschu, D. L., & Sugiyama, T. (2013). PCNA is efficiently loaded on the DNA recombination intermediate to modulate polymerase δ, η, and ζ activities. *Proceedings of the National Academy of Sciences of the United States of America*, *110*(19), 7672–7677. https://doi.org/10.1073/PNAS.1222241110/SUPPL_FILE/PNAS.201222241SI.PDF

Li, N., Wang, J., Wallace, S. S., Chen, J., Zhou, J., & D'Andrea, A. D. (2020). Cooperation of the NEIL3 and Fanconi anemia/BRCA pathways in interstrand crosslink repair. *Nucleic Acids Research*, *48*(6), 3014–3028. https://doi.org/10.1093/nar/gkaa038

Li, N., Xu, Y., Chen, H., Chen, L., Zhang, Y., Yu, T., Yao, R., Chen, J., Fu, Q., Zhou, J., & Wang, J. (2022). NEIL3 contributes to the Fanconi anemia/BRCA pathway by promoting the downstream double-strand break repair step. *Cell Reports*, *41*(6), 111600. https://doi.org/10.1016/J.CELREP.2022.111600

Li, X., Chen, M., Yuan, Y., Li, J., & Li, F. (2022). CORO1C, a novel PAK4 binding protein, recruits phospho-PAK4 at serine 99 to the leading edge and promotes the migration of gastric cancer cells. *Acta Biochimica et Biophysica Sinica*, *54*(5), 673–685. https://doi.org/10.3724/ABBS.2022044

Li, X., & Heyer, W. D. (2008). Homologous recombination in DNA repair and DNA damage tolerance. *Cell Research 2008 18:1*, *18*(1), 99–113. https://doi.org/10.1038/cr.2008.1

Liang, C. C., Zhan, B., Yoshikawa, Y., Haas, W., Gygi, S. P., & Cohn, M. A. (2015). UHRF1 Is a

sensor for DNA interstrand crosslinks and recruits FANCD2 to initiate the Fanconi Anemia pathway. *Cell Reports*, *10*(12), 1947–1956. https://doi.org/10.1016/j.celrep.2015.02.053

Liao, H., Ji, F., Helleday, T., & Ying, S. (2018). Mechanisms for stalled replication fork stabilization: new targets for synthetic lethality strategies in cancer treatments. *EMBO Reports*, *19*(9). https://doi.org/10.15252/EMBR.201846263

Lieber, M. R. (2010). NHEJ and its backup pathways in chromosomal translocations. *Nature Struct. Mol. Biol.*, *17*(4), 393–395. https://doi.org/10.1038/nsmb0410-393

Lieber, M. R., Lu, H., Gu, J., & Schwarz, K. (2007). Flexibility in the order of action and in the enzymology of the nuclease, polymerases, and ligase of vertebrate non-homologous DNA end joining: relevance to cancer, aging, and the immune system. *Cell Research 2008 18:1*, *18*(1), 125–133. https://doi.org/10.1038/cr.2007.108

Lin, H., Zhang, X., Feng, N., Wang, R., Zhang, W., Deng, X., Wang, Y., Yu, X., Ye, X., Li, L., Qian, Y., Yu, H., & Qian, B. (2018). LncRNA LCPAT1 Mediates Smoking/ Particulate Matter 2.5-Induced Cell Autophagy and Epithelial-Mesenchymal Transition in Lung Cancer Cells via RCC2. *Cellular Physiology and Biochemistry : International Journal of Experimental Cellular Physiology, Biochemistry, and Pharmacology*, *47*(3), 1244–1258. https://doi.org/10.1159/000490220

Lin, Y. J., Liao, W. L., Wang, C. H., Tsai, L. P., Tang, C. H., Chen, C. H., Wu, J. Y., Liang, W. M., Hsieh, A. R., Cheng, C. F., Chen, J. H., Chien, W. K., Lin, T. H., Wu, C. M., Liao, C. C., Huang, S. M., & Tsai, F. J. (2017). Association of human height-related genetic variants with familial short stature in Han Chinese in Taiwan. *Scientific Reports*, *7*(1). https://doi.org/10.1038/S41598-017-06766-Z

Lindahl, T. (1979). DNA Glycosylases, Endonucleases for Apurinic/Apyrimidinic Sites, and Base Excision-Repair. *Progress in Nucleic Acid Research and Molecular Biology*, *22*(C), 135–192. https://doi.org/10.1016/S0079-6603(08)60800-4

Lindahl, T. (1993). Instability and decay of the primary structure of DNA. *Nature 1993 362:6422*, *362*(6422), 709–715. https://www.nature.com/articles/362709a0

Lindahl, T., & Nyberg, B. (1972). Rate of depurination of native deoxyribonucleic acid. *Biochemistry*, *11*(19), 3610–3618. https://doi.org/10.1021/BI00769A018

Lindström, M. S., Bartek, J., & Maya-Mendoza, A. (2022). p53 at the crossroad of DNA replication and ribosome biogenesis stress pathways. *Cell Death and Differentiation*, *29*(5), 972. https://doi.org/10.1038/S41418-022-00999-W

Lirussi, L., Antoniali, G., Vascotto, C., D'Ambrosio, C., Poletto, M., Romanello, M., Marasco, D., Leone, M., Quadrifoglio, F., Bhakat, K. K., Scaloni, A., & Tell, G. (2012). Nucleolar accumulation of APE1 depends on charged lysine residues that undergo acetylation upon genotoxic stress and modulate its BER activity in cells. *Molecular Biology of the Cell*, *23*(20), 4079. https://doi.org/10.1091/MBC.E12-04-0299

Liu, A., Yoshioka, K. I., Salerno, V., & Hsieh, P. (2008). The mismatch repair-mediated cell cycle checkpoint response to fluorodeoxyuridine. *Journal of Cellular Biochemistry*, *105*(1), 245–254. https://doi.org/10.1002/JCB.21824

Liu, T., Wang, Y., Wang, Y., Cheung, S. K. K., Or, P. M. Y., Wong, C. W., Guan, J., Li, Z., Yang, W., Tu, Y., Wang, J., Ho, W. L. H., Gu, H., Cheng, A. S. L., Tsui, S. K. W., & Chan, A. M. (2022). The mitotic regulator RCC2 promotes glucose metabolism through BACH1-dependent transcriptional upregulation of hexokinase II in glioma. *Cancer Letters*, *549*. https://doi.org/10.1016/J.CANLET.2022.215914

Liu, X. F., Xiang, L., Zhou, Q., Carralot, J. P., Prunotto, M., Niederfellner, G., & Pastan, I.

(2016). Actinomycin D enhances killing of cancer cells by immunotoxin RG7787 through activation of the extrinsic pathway of apoptosis. *Proceedings of the National Academy of Sciences of the United States of America*, *113*(38), 10666–10671. https://doi.org/10.1073/PNAS.1611481113/SUPPL_FILE/PNAS.201611481SI.PDF

Liu, Y., Zhou, K., Zhang, H., Yin, Y. S., Chen, L., Xu, Z., Zhong, Y., Liu, H., Jin, L., Wei, Q., Huang, F., Lu, D., & Zhou, L. (2008). Polymorphisms of LIG4 and XRCC4 involved in the NHEJ pathway interact to modify risk of glioma. *Human Mutation*, *29*(3), 381–389. https://doi.org/10.1002/HUMU.20645

Livraghi, L., & Garber, J. E. (2015). PARP inhibitors in the management of breast cancer: Current data and future prospects. *BMC Medicine*, *13*(1), 1–16. https://doi.org/10.1186/S12916-015-0425-1/TABLES/6

Llanos, S., Clark, P. A., Rowe, J., & Peters, G. (2001). Stabilization of p53 by p14ARF without relocation of MDM2 to the nucleolus. *Nature Cell Biology 2001 3:5*, *3*(5), 445–452. https://doi.org/10.1038/35074506

Loeb, K. R., & Loeb, L. A. (2000). Significance of multiple mutations in cancer. *Carcinogenesis*, *21*(3), 379–385. https://doi.org/10.1093/CARCIN/21.3.379

Loeb, L. A., & Monnat, R. J. (2008). DNA polymerases and human disease. *Nature Reviews Genetics 2008 9:8*, *9*(8), 594–604. https://doi.org/10.1038/nrg2345

Lomax, M. E., Folkes, L. K., & O'Neill, P. (2013). Biological consequences of radiation-induced DNA damage: Relevance to radiotherapy. *Clinical Oncology*, *25*(10), 578–585. https://doi.org/10.1016/J.CLON.2013.06.007

Long, D. T., Räschle, M., Joukov, V., & Walter, J. C. (2011). Mechanism of RAD51-dependent DNA interstrand cross-link repair. *Science*, *333*(6038), 84–87. https://doi.org/10.1126/SCIENCE.1204258/SUPPL_FILE/1204258.LONG.SOM.PDF

Lopez-Martinez, D., Kupculak, M., Yang, D., Yoshikawa, Y., Liang, C.-C. C., Wu, R., Gygi, S. P., & Cohn, M. A. (2019). Phosphorylation of FANCD2 Inhibits the FANCD2/FANCI Complex and Suppresses the Fanconi Anemia Pathway in the Absence of DNA Damage. *Cell Reports*, *27*(10). /pmc/articles/PMC6581795/

Lopez-Martinez, D., Liang, C.-C. C., & Cohn, M. A. (2016). Cellular response to DNA interstrand crosslinks: the Fanconi anemia pathway. *Cellular and Molecular Life Sciences*, *73*(16), 3097–3114. https://doi.org/10.1007/s00018-016-2218-x

Lord, C. J., & Ashworth, A. (2012). The DNA damage response and cancer therapy. *Nature 2012 481:7381*, *481*(7381), 287–294. https://doi.org/10.1038/nature10760

Lou, J., Yang, Y., Gu, Q., Price, B. A., Qiu, Y., Fedoriw, Y., Desai, S., Mose, L. E., Chen, B., Tateishi, S., Parker, J. S., Vaziri, C., & Wu, D. (2021). Rad18 mediates specific mutational signatures and shapes the genomic landscape of carcinogen-induced tumors in vivo. *NAR Cancer*, *3*(1), 1–18. https://doi.org/10.1093/NARCAN/ZCAA037

Loveless, A. (1969). Possible Relevance of O–6 Alkylation of Deoxyguanosine to the Mutagenicity and Carcinogenicity of Nitrosamines and Nitrosamides. *Nature 1969 223:5202*, *223*(5202), 206–207. https://doi.org/10.1038/223206a0

Lovett, S. T. (2017). Template-switching during replication fork repair in bacteria. *DNA Repair*, *56*, 118–128. https://doi.org/10.1016/J.DNAREP.2017.06.014

Luan, Y., Tang, N., Yang, J., Liu, S., Cheng, C., Wang, Y., Chen, C., Guo, Y. N., Wang, H., Zhao, W., Zhao, Q., Li, W., Xiang, M., Ju, R., & Xie, Z. (2022). Deficiency of ribosomal proteins reshapes the transcriptional and translational landscape in human cells. *Nucleic Acids Research*, *50*(12), 6601. https://doi.org/10.1093/NAR/GKAC053

Lustig, J. P., Lugassy, G., Neder, A., & Sigler, E. (1995). Head and neck carcinoma in Fanconi's

anaemia—report of a case and review of the literature. *European Journal of Cancer Part B: Oral Oncology*, *31*(1), 68–72. https://doi.org/10.1016/0964-1955(94)00044-5
Mahaney, B. L., Meek, K., & Lees-Miller, S. P. (2009). Repair of ionizing radiation-induced DNA double strand breaks by non-homologous end-joining. *The Biochemical Journal*, *417*(3), 639. https://doi.org/10.1042/BJ20080413
Malaby, A. W., Martin, S. K., Wood, R. D., & Doublié, S. (2017). Expression and Structural Analyses of Human DNA Polymerase θ (POLQ). *Methods in Enzymology*, *592*, 103–121. https://doi.org/10.1016/BS.MIE.2017.03.026
Malinge, J. M., Giraud-Panis, M. J., & Leng, M. (1999). Interstrand cross-links of cisplatin induce striking distortions in DNA. *Journal of Inorganic Biochemistry*, *77*(1–2), 23–29. https://doi.org/10.1016/S0162-0134(99)00148-8
Malle, E., Furtmüller, P. G., Sattler, W., & Obinger, C. (2007). Myeloperoxidase: a target for new drug development? *British Journal of Pharmacology*, *152*(6), 838. https://doi.org/10.1038/SJ.BJP.0707358
Malouf, C., Loughran, S. J., Wilkinson, A. C., Shimamura, A., & Río, P. (2022). Translational research for bone marrow failure patients. *Experimental Hematology*, *105*, 18–21. https://doi.org/10.1016/j.exphem.2021.11.004
Manhart, C. M., & Alani, E. (2016). Roles for mismatch repair family proteins in promoting meiotic crossing over. *DNA Repair*, *38*, 84. https://doi.org/10.1016/J.DNAREP.2015.11.024
Maremonti, E., Brede, D. A., Olsen, A. K., Eide, D. M., & Berg, E. S. (2020). Ionizing radiation, genotoxic stress, and mitochondrial DNA copy-number variation in Caenorhabditis elegans: droplet digital PCR analysis. *Mutat. Res.*, *858–860*, 503277. https://doi.org/10.1016/j.mrgentox.2020.503277
Marians, K. J. (2018). Lesion Bypass and the Reactivation of Stalled Replication Forks. *Annual Review of Biochemistry*, *87*, 217. https://doi.org/10.1146/ANNUREV-BIOCHEM-062917-011921
Marnett, L. J. (2000). Oxyradicals and DNA damage. *Carcinogenesis*, *21*(3), 361–370. https://doi.org/10.1093/CARCIN/21.3.361
Martineau-Thuillier, S., Andreassen, P. R., & Margolis, R. L. (1998). Colocalization of TD-60 and INCENP throughout G2 and mitosis: evidence for their possible interaction in signalling cytokinesis. *Chromosoma*, *107*(6–7), 461–470. https://doi.org/10.1007/S004120050330
Massaad, M. J., Zhou, J., Tsuchimoto, D., Chou, J., Jabara, H., Janssen, E., Glauzy, S., Olson, B. G., Morbach, H., Ohsumi, T. K., Schmitz, K., Kyriacos, M., Kane, J., Torisu, K., Nakabeppu, Y., Notarangelo, L. D., Chouery, E., Megarbane, A., Kang, P. B., … Geha, R. S. (2016). Deficiency of base excision repair enzyme NEIL3 drives increased predisposition to autoimmunity. *The Journal of Clinical Investigation*, *126*(11), 4219–4236. https://doi.org/10.1172/JCI85647
Mateos-Gomez, P. A., Gong, F., Nair, N., Miller, K. M., Lazzerini-Denchi, E., & Sfeir, A. (2015). Mammalian polymerase θ promotes alternative NHEJ and suppresses recombination. *Nature 2015 518:7538*, *518*(7538), 254–257. https://doi.org/10.1038/nature14157
Matsuo, M., Nakada, C., Tsukamoto, Y., Noguchi, T., Uchida, T., Hijiya, N., Matsuura, K., & Moriyama, M. (2013). MiR-29c is downregulated in gastric carcinomas and regulates cell proliferation by targeting RCC2. *Molecular Cancer*, *12*(1). https://doi.org/10.1186/1476-4598-12-15
Matsuoka, S., Ballif, B. A., Smogorzewska, A., McDonald, E. R., Hurov, K. E., Luo, J.,

Bakalarski, C. E., Zhao, Z., Solimini, N., Lerenthal, Y., Shiloh, Y., Gygi, S. P., & Elledge, S. J. (2007). ATM and ATR substrate analysis reveals extensive protein networks responsive to DNA damage. *Science*, *316*(5828), 1160–1166. https://doi.org/10.1126/SCIENCE.1140321

Matsushima, Y., Ohshima, M., Sonoda, M., & Kitagawa, Y. (1996). A family of novel DNA-binding nuclear proteins having polypyrimidine tract-binding motif and arginine/serine-rich motif. *Biochemical and Biophysical Research Communications*, *223*(2), 427–433. https://doi.org/10.1006/bbrc.1996.0910

Mayer, E. L. (2013). Early and Late Long-Term Effects of Adjuvant Chemotherapy. *Https://Doi.Org/10.14694/EdBook_AM.2013.33.9*, *33*, 9–14. https://doi.org/10.14694/EDBOOK_AM.2013.33.9

Maynard, S., Schurman, S. H., Harboe, C., De Souza-Pinto, N. C., & Bohr, V. A. (2009). Base excision repair of oxidative DNA damage and association with cancer and aging. *Carcinogenesis*, *30*(1), 2–10. https://doi.org/10.1093/carcin/bgn250

McCulloch, S. D., & Kunkel, T. A. (2008). The fidelity of DNA synthesis by eukaryotic replicative and translesion synthesis polymerases. *Cell Research 2008 18:1*, *18*(1), 148–161. https://doi.org/10.1038/cr.2008.4

McEvoy, M. T., & Stern, R. S. (1987). Psoralens and related compounds in the treatment of psoriasis. *Pharmacology & Therapeutics*, *34*(1), 75–97. https://doi.org/10.1016/0163-7258(87)90093-3

McGowan, C. H., & Russell, P. (2004). The DNA damage response: Sensing and signaling. *Current Opinion in Cell Biology*, *16*(6), 629–633. https://doi.org/10.1016/J.CEB.2004.09.005

McKinnon, P. J. (2009). DNA repair deficiency and neurological disease. *Nature Reviews Neuroscience*, *10*(2), 100–112. https://doi.org/10.1038/NRN2559

Mckinnon, P. J., & Caldecott, K. W. (2007). *DNA Strand Break Repair and Human Genetic Disease*. https://doi.org/10.1146/annurev.genom.7.080505.115648

McStay, B. (2016). Nucleolar organizer regions: genomic 'dark matter' requiring illumination. *Genes & Development*, *30*(14), 1598. https://doi.org/10.1101/GAD.283838.116

McVey, M., Khodaverdian, V. Y., Meyer, D., Cerqueira, P. G., & Heyer, W. D. (2016). Eukaryotic DNA Polymerases in Homologous Recombination. *Annual Review of Genetics*, *50*, 393. https://doi.org/10.1146/ANNUREV-GENET-120215-035243

McVey, M., & Lee, S. E. (2008). MMEJ repair of double-strand breaks (director's cut): deleted sequences and alternative endings. *Trends in Genetics : TIG*, *24*(11), 529. https://doi.org/10.1016/J.TIG.2008.08.007

Meetei, A. R., Levitus, M., Xue, Y., Medhurst, A. L., Zwaan, M., Ling, C., Rooimans, M. A., Bier, P., Hoatlin, M., Pals, G., De Winter, J. P., Wang, W., & Joenje, H. (2004). X-linked inheritance of Fanconi anemia complementation group B. *Nature Genetics 2004 36:11*, *36*(11), 1219–1224. https://doi.org/10.1038/ng1458

Mei Kwei, J. S., Kuraoka, I., Horibata, K., Ubukata, M., Kobatake, E., Iwai, S., Handa, H., & Tanaka, K. (2004). Blockage of RNA polymerase II at a cyclobutane pyrimidine dimer and 6-4 photoproduct. *Biochemical and Biophysical Research Communications*, *320*(4), 1133–1138. https://doi.org/10.1016/j.bbrc.2004.06.066

Mekhail, K., Gunaratnam, L., Bonicalzi, M. E., & Lee, S. (2004). HIF activation by pH-dependent nucleolar sequestration of VHL. *Nature Cell Biology 2004 6:7*, *6*(7), 642–647. https://doi.org/10.1038/ncb1144

Melough, M. M., & Chun, O. K. (2018). Dietary furocoumarins and skin cancer: A review of

current biological evidence. *Food and Chemical Toxicology*, *122*, 163–171. https://doi.org/10.1016/J.FCT.2018.10.027

Mendez-Dorantes, C., Bhargava, R., & Stark, J. M. (2018). Repeat-mediated deletions can be induced by a chromosomal break far from a repeat, but multiple pathways suppress such rearrangements. *Genes & Development*, *32*(7–8), 524–536. https://doi.org/10.1101/GAD.311084.117

Meng, Y., Efimova, E. V., Hamzeh, K. W., Darga, T. E., Mauceri, H. J., Fu, Y. X., Kron, S. J., & Weichselbaum, R. R. (2012). Radiation-inducible immunotherapy for cancer: Senescent tumor cells as a cancer vaccine. *Molecular Therapy*, *20*(5), 1046–1055. https://doi.org/10.1038/mt.2012.19

Meruvu, S., Hugendubler, L., & Mueller, E. (2011). Regulation of Adipocyte Differentiation by the Zinc Finger Protein ZNF638. *The Journal of Biological Chemistry*, *286*(30), 26516. https://doi.org/10.1074/JBC.M110.212506

Meyer, S., Fergusson, W. D., Oostra, A. B., Medhurst, A. L., Waisfisz, Q., De Winter, J. P., Chen, F., Carr, T. F., Clayton-Smith, J., Clancy, T., Green, M., Barber, L., Eden, O. B., Will, A. M., Joenje, H., & Taylor, G. M. (2005). A cross-linker-sensitive myeloid leukemia cell line from a 2-year-old boy with severe Fanconi anemia and biallelic FANCD1/BRCA2 mutations. *Genes, Chromosomes and Cancer*, *42*(4), 404–415. https://doi.org/10.1002/GCC.20153

Millard, J. T., McGowan, E. E., & Bradley, S. Q. (2012). Diepoxybutane Interstrand Cross-Links Induce DNA Bending. *Biochimie*, *94*(2), 574. https://doi.org/10.1016/J.BIOCHI.2011.07.030

Millard, J. T., & White, M. M. (1993). Diepoxybutane cross-links DNA at 5'-GNC sequences. *Biochemistry*, *32*(8), 2120–2124. https://doi.org/10.1021/BI00059A034

Minca, E. C., & Kowalski, D. (2011). Replication fork stalling by bulky DNA damage: localization at active origins and checkpoint modulation. *Nucleic Acids Research*, *39*(7), 2610. https://doi.org/10.1093/NAR/GKQ1215

Mirman, Z., Lottersberger, F., Takai, H., Kibe, T., Gong, Y., Takai, K., Bianchi, A., Zimmermann, M., Durocher, D., & de Lange, T. (2018). 53BP1/Rif1/Shieldin counteract DSB resection through CST/Polα-dependent fill-in. *Nature*, *560*(7716), 112. https://doi.org/10.1038/S41586-018-0324-7

Mirman, Z., Sasi, N. K., King, A., Chapman, J. R., & de Lange, T. (2022). 53BP1–shieldin-dependent DSB processing in BRCA1-deficient cells requires CST–Polα–primase fill-in synthesis. *Nature Cell Biology 2022 24:1*, *24*(1), 51–61. https://doi.org/10.1038/s41556-021-00812-9

Missura, M., Buterin, T., Hindges, R., Hübscher, U., Kaspárková, J., Brabec, V., & Naegeli, H. (2001). Double-check probing of DNA bending and unwinding by XPA–RPA: an architectural function in DNA repair. *The EMBO Journal*, *20*(13), 3554. https://doi.org/10.1093/EMBOJ/20.13.3554

Misteli, T., & Soutoglou, E. (2009). The emerging role of nuclear architecture in DNA repair and genome maintenance. *Nature Reviews Molecular Cell Biology*, *10*(4), 243–254. https://doi.org/10.1038/NRM2651

Mitchell, D. L., & Nairn, R. S. (1989). THE BIOLOGY OF THE (6–4) PHOTOPRODUCT. *Photochemistry and Photobiology*, *49*(6), 805–819. https://doi.org/10.1111/J.1751-1097.1989.TB05578.X

Moan, J., & Peak, M. J. (1989). Effects of UV radiation on cells. *Journal of Photochemistry and Photobiology, B: Biology*, *4*(1), 21–34. https://doi.org/10.1016/1011-

1344(89)80099-5
Mollinari, C., Reynaud, C., Martineau-Thuillier, S., Monier, S., Kieffer, S., Garin, J., Andreassen, P. R., Boulet, A., Goud, B., Kleman, J.-P., & Margolis, R. L. (2003). The mammalian passenger protein TD-60 is an RCC1 family member with an essential role in prometaphase to metaphase progression. *Developmental Cell*, *5*(2), 295–307. https://doi.org/10.1016/s1534-5807(03)00205-3
Moore, H. M., Bai, B., Boisvert, F. M., Latonen, L., Rantanen, V., Simpson, J. C., Pepperkok, R., Lamond, A. I., & Laiho, M. (2011). Quantitative proteomics and dynamic imaging of the nucleolus reveal distinct responses to UV and ionizing radiation. *Molecular and Cellular Proteomics*, *10*(10), M111.009241. https://doi.org/10.1074/mcp.M111.009241
Mooser, C., Symeonidou, I. E., Leimbacher, P. A., Ribeiro, A., Shorrocks, A. M. K., Jungmichel, S., Larsen, S. C., Knechtle, K., Jasrotia, A., Zurbriggen, D., Jeanrenaud, A., Leikauf, C., Fink, D., Nielsen, M. L., Blackford, A. N., & Stucki, M. (2020). Treacle controls the nucleolar response to rDNA breaks via TOPBP1 recruitment and ATR activation. *Nature Communications 2020 11:1*, *11*(1), 1–16. https://doi.org/10.1038/s41467-019-13981-x
Morales, J. C., Li, L., Fattah, F. J., Dong, Y., Bey, E. A., Patel, M., Gao, J., & Boothman, D. A. (2014). Review of Poly (ADP-ribose) Polymerase (PARP) Mechanisms of Action and Rationale for Targeting in Cancer and Other Diseases. *Critical Reviews in Eukaryotic Gene Expression*, *24*(1), 15. https://doi.org/10.1615/CRITREVEUKARYOTGENEEXPR.2013006875
Morita, R., Nakane, S., Shimada, A., Inoue, M., Iino, H., Wakamatsu, T., Fukui, K., Nakagawa, N., Masui, R., & Kuramitsu, S. (2010). Molecular mechanisms of the whole DNA repair system: A comparison of bacterial and eukaryotic systems. *Journal of Nucleic Acids*, *2010*. https://doi.org/10.4061/2010/179594
Morrical, S. W. (2015). DNA-Pairing and Annealing Processes in Homologous Recombination and Homology-Directed Repair. *Cold Spring Harbor Perspectives in Biology*, *7*(2), a016444. https://doi.org/10.1101/CSHPERSPECT.A016444
Motegi, A., Liaw, H. J., Lee, K. Y., Roest, H. P., Maas, A., Wu, X., Moinova, H., Markowitz, S. D., Ding, H., Hoeijmakers, J. H. J., & Myung, K. (2008). Polyubiquitination of proliferating cell nuclear antigen by HLTF and SHPRH prevents genomic instability from stalled replication forks. *Proceedings of the National Academy of Sciences of the United States of America*, *105*(34), 12411–12416. https://doi.org/10.1073/PNAS.0805685105/SUPPL_FILE/0805685105SI.PDF
Motegi, A., Masutani, M., Yoshioka, K. ichi, & Bessho, T. (2019). Aberrations in DNA repair pathways in cancer and therapeutic significances. *Seminars in Cancer Biology*, *58*, 29–46. https://doi.org/10.1016/J.SEMCANCER.2019.02.005
Motnenko, A., Liang, C.-C., Yang, D., Lopez-Martinez, D., Yoshikawa, Y., Zhan, B., Ward, K. E., Tian, J., Haas, W., Spingardi, P., Kessler, B. M., Kriaucionis, S., Gygi, S. P., & Cohn, M. A. (2018). Identification of UHRF2 as a novel DNA interstrand crosslink sensor protein. *PLoS Genetics*, *14*(10), e1007643. https://doi.org/10.1371/journal.pgen.1007643
Mourón, S., Rodriguez-Acebes, S., Martínez-Jiménez, M. I., García-Gómez, S., Chocrón, S., Blanco, L., & Méndez, J. (2013). Repriming of DNA synthesis at stalled replication forks by human PrimPol. *Nature Structural & Molecular Biology 2013 20:12*, *20*(12), 1383–1389. https://doi.org/10.1038/nsmb.2719
Moynahan, M. E., & Jasin, M. (2010). Mitotic homologous recombination maintains genomic stability and suppresses tumorigenesis. *Nature Rev. Mol. Cell Biol.*, *11*(3), 196–207. https://doi.org/10.1038/nrm2851

Mozaffari, N. L., Pagliarulo, F., & Sartori, A. A. (2021). Human CtIP: A 'double agent' in DNA repair and tumorigenesis. *Seminars in Cell & Developmental Biology*, *113*, 47–56. https://doi.org/10.1016/J.SEMCDB.2020.09.001

Mukherjee, M., & Goswami, S. (2021). Identification of Key Deregulated RNA-Binding Proteins in Pancreatic Cancer by Meta-Analysis and Prediction of Their Role as Modulators of Oncogenesis. *Frontiers in Cell and Developmental Biology*, *9*. https://doi.org/10.3389/FCELL.2021.713852

Mukherjee, S., Wright, W. D., Ehmsen, K. T., & Heyer, W. D. (2014). The Mus81-Mms4 structure-selective endonuclease requires nicked DNA junctions to undergo conformational changes and bend its DNA substrates for cleavage. *Nucleic Acids Research*, *42*(10), 6511. https://doi.org/10.1093/NAR/GKU265

Muniandy, P. A., Liu, J., Majumdar, A., Liu, S. T., & Seidman, M. M. (2010). DNA interstrand crosslink repair in mammalian cells: Step by step. *Critical Reviews in Biochemistry and Molecular Biology*, *45*(1), 23–49. https://doi.org/10.3109/10409230903501819

Murfuni, I., Basile, G., Subramanyam, S., Malacaria, E., Bignami, M., Spies, M., Franchitto, A., & Pichierri, P. (2013). Survival of the Replication Checkpoint Deficient Cells Requires MUS81-RAD52 Function. *PLoS Genetics*, *9*(10). https://doi.org/10.1371/JOURNAL.PGEN.1003910

Murina, O., von Aesch, C., Karakus, U., Ferretti, L. P., Bolck, H. A., Hänggi, K., & Sartori, A. A. (2014). FANCD2 and CtIP cooperate to repair DNA interstrand crosslinks. *Cell Reports*, *7*(4), 1030–1038. https://doi.org/10.1016/j.celrep.2014.03.069

Musinova, Y. R., Kananykhina, E. Y., Potashnikova, D. M., Lisitsyna, O. M., & Sheval, E. V. (2015). A charge-dependent mechanism is responsible for the dynamic accumulation of proteins inside nucleoli. *Biochimica et Biophysica Acta (BBA) - Molecular Cell Research*, *1853*(1), 101–110. https://doi.org/10.1016/J.BBAMCR.2014.10.007

Nakamura, J., & Swenberg, J. A. (1999). Endogenous apurinic/apyrimidinic sites in genomic DNA of mammalian tissues. *Cancer Research*, *59*(11), 2522–2526.

Nakamura, J., Walker, V. E., Upton, P. B., Chiang, S., Kow, Y. W., & Swenberg, J. a. (1998). Highly Sensitive Apurinic/Apyrimidinic Site Assay Can Detect Spontaneous and Chemically Induced Depurination under Physiological Conditions. *Sites The Journal Of 20Th Century Contemporary French Studies*, *58*, 222–225.

Nakamura, K., Saredi, G., Becker, J. R., Foster, B. M., Nguyen, N. V., Beyer, T. E., Cesa, L. C., Faull, P. A., Lukauskas, S., Frimurer, T., Chapman, J. R., Bartke, T., & Groth, A. (2019). H4K20me0 recognition by BRCA1–BARD1 directs homologous recombination to sister chromatids. *Nature Cell Biology 2019 21:3*, *21*(3), 311–318. https://doi.org/10.1038/s41556-019-0282-9

Nalepa, G., & Clapp, D. W. (2018). Fanconi anaemia and cancer: an intricate relationship. *Nature Reviews Cancer 2018 18:3*, *18*(3), 168–185. https://doi.org/10.1038/nrc.2017.116

Nam, E. A., & Cortez, D. (2011). ATR signalling: more than meeting at the fork. *Biochemical Journal*, *436*(3), 527–536. https://doi.org/10.1042/BJ20102162

Nambiar, T. S., Baudrier, L., Billon, P., & Ciccia, A. (2022). CRISPR-based genome editing through the lens of DNA repair. *Molecular Cell*, *82*(2), 348–388. https://doi.org/10.1016/J.MOLCEL.2021.12.026

Nath, S., & Nagaraju, G. (2020). FANCJ helicase promotes DNA end resection by facilitating CtIP recruitment to DNA double-strand breaks. *PLOS Genetics*, *16*(4), e1008701. https://doi.org/10.1371/JOURNAL.PGEN.1008701

Neugebauer, K. M., Stolk, J. A., & Roth, M. B. (1995). A conserved epitope on a subset of SR proteins defines a larger family of Pre-mRNA splicing factors. *The Journal of Cell Biology*, *129*(4), 899–908. https://doi.org/10.1083/JCB.129.4.899

Neveling, K., Endt, D., Hoehn, H., & Schindler, D. (2009). Genotype–phenotype correlations in Fanconi anemia. *Mutation Research/Fundamental and Molecular Mechanisms of Mutagenesis*, *668*(1–2), 73–91. https://doi.org/10.1016/J.MRFMMM.2009.05.006

Ng, E. K. O., Chan, K. K., Wong, C. H., Tsui, S. K. W., Ngai, S. M., Lee, S. M. Y., Kotaka, M., Lee, C. Y., Waye, M. M. Y., & Fung, K. P. (2002). Interaction of the heart-specific LIM domain protein, FHL2, with DNA-binding nuclear protein, hNP220. *Journal of Cellular Biochemistry*, *84*(3), 556–566. https://doi.org/10.1002/jcb.10041

Nguyen, V. Q., Co, C., & Li, J. J. (2001). Cyclin-dependent kinases prevent DNA re-replication through multiple mechanisms. *Nature 2001 411:6841*, *411*(6841), 1068–1073. https://doi.org/10.1038/35082600

Ni, C., & Buszczak, M. (2023). The homeostatic regulation of ribosome biogenesis. *Seminars in Cell and Developmental Biology*, *136*, 13–26. https://doi.org/10.1016/j.semcdb.2022.03.043

Ni, W., Lin, S., Bian, S., Zheng, W., Qu, L., Fan, Y., Lu, C., Xiao, M., & Zhou, P. (2020). USP7 mediates pathological hepatic de novo lipogenesis through promoting stabilization and transcription of ZNF638. *Cell Death & Disease*, *11*(10). https://doi.org/10.1038/S41419-020-03075-8

Nie, W., Wang, B., Mi, X., Chen, J., Yu, T., Miao, J., Lin, Y., Yang, T., Ran, M., Hong, Z., Liu, X., Liang, X., Qian, Z., & Gao, X. (2021). Co-Delivery of Paclitaxel and shMCL-1 by Folic Acid-Modified Nonviral Vector to Overcome Cancer Chemotherapy Resistance. *Small Methods*, *5*(5). https://doi.org/10.1002/SMTD.202001132

Nijman, S. M. B., Huang, T. T., Dirac, A. M. G., Brummelkamp, T. R., Kerkhoven, R. M., D'Andrea, A. D., & Bernards, R. (2005). The deubiquitinating enzyme USP1 regulates the fanconi anemia pathway. *Molecular Cell*, *17*(3), 331–339. https://doi.org/10.1016/j.molcel.2005.01.008

Nik-Zainal, S., Davies, H., Staaf, J., Ramakrishna, M., Glodzik, D., Zou, X., Martincorena, I., Alexandrov, L. B., Martin, S., Wedge, D. C., Van Loo, P., Ju, Y. S., Smid, M., Brinkman, A. B., Morganella, S., Aure, M. R., Lingjærde, O. C., Langerød, A., Ringnér, M., … Stratton, M. R. (2016). *Landscape of somatic mutations in 560 breast cancer whole-genome sequences*. *534*(7605), 47–54. https://doi.org/10.1038/nature17676

Niraj, J., Färkkilä, A., & D'Andrea, A. D. (2019). The Fanconi Anemia Pathway in Cancer. *Annual Review of Cancer Biology*, *3*(1), 457. https://doi.org/10.1146/ANNUREV-CANCERBIO-030617-050422

Noordermeer, S. M., Adam, S., Setiaputra, D., Barazas, M., Pettitt, S. J., Ling, A. K., Olivieri, M., Álvarez-Quilón, A., Moatti, N., Zimmermann, M., Annunziato, S., Krastev, D. B., Song, F., Brandsma, I., Frankum, J., Brough, R., Sherker, A., Landry, S., Szilard, R. K., … Durocher, D. (2018). The Shieldin complex mediates 53BP1-dependent DNA repair. *Nature*, *560*(7716), 117. https://doi.org/10.1038/S41586-018-0340-7

O'Brien, P., Siraki, A., & Shangari, N. (2008). Aldehyde Sources, Metabolism, Molecular Toxicity Mechanisms, and Possible Effects on Human Health. *Http://Dx.Doi.Org/10.1080/10408440591002183*, *35*(7), 609–662. https://doi.org/10.1080/10408440591002183

O'Connor, T. R., Boiteux, S., & Laval, J. (1988). Ring-opened 7-methylguanine residues in DNA are a block to in vitro DNA synthesis. *Nucleic Acids Research*, *16*(13), 5879.

https://doi.org/10.1093/NAR/16.13.5879
O'Reilly, J. A., Fitzgerald, J., Fitzgerald, S., Kenny, D., Kay, E. W., O'Kennedy, R., & Kijanka, G. S. (2015). Diagnostic Potential of Zinc Finger Protein-Specific Autoantibodies and Associated Linear B-Cell Epitopes in Colorectal Cancer. *PLoS ONE*, *10*(4). https://doi.org/10.1371/JOURNAL.PONE.0123469
Ochi, T., Blackford, A. N., Coates, J., Jhujh, S., Mehmood, S., Tamura, N., Travers, J., Wu, Q., Draviam, V. M., Robinson, C. V., Blundell, T. L., & Jackson, S. P. (2015). PAXX, a paralog of XRCC4 and XLF, interacts with Ku to promote DNA double-strand break repair. *Science*, *347*(6218), 185–188. https://www.science.org/doi/10.1126/science.1261971
Ochs, F., Karemore, G., Miron, E., Brown, J., Sedlackova, H., Rask, M. B., Lampe, M., Buckle, V., Schermelleh, L., Lukas, J., & Lukas, C. (2019). Stabilization of chromatin topology safeguards genome integrity. *Nature 2019 574:7779*, *574*(7779), 571–574. https://doi.org/10.1038/s41586-019-1659-4
Ochs, F., Somyajit, K., Altmeyer, M., Rask, M. B., Lukas, J., & Lukas, C. (2016). 53BP1 fosters fidelity of homology-directed DNA repair. *Nature Structural & Molecular Biology 2016 23:8*, *23*(8), 714–721. https://doi.org/10.1038/nsmb.3251
Oestergaard, V. H., Langevin, F., Kuiken, H. J., Pace, P., Niedzwiedz, W., Simpson, L. J., Ohzeki, M., Takata, M., Sale, J. E., & Patel, K. J. (2007). Deubiquitination of FANCD2 Is Required for DNA Crosslink Repair. *Molecular Cell*, *28*(5), 798–809. https://doi.org/10.1016/j.molcel.2007.09.020
Ogawa, L. M., & Baserga, S. J. (2017). Crosstalk between the nucleolus and the DNA damage response †. *Mol. BioSyst*, *13*, 443. https://doi.org/10.1039/c6mb00740f
Orans, J., McSweeney, E. A., Iyer, R. R., Hast, M. A., Hellinga, H. W., Modrich, P., & Beese, L. S. (2011). Structures of human exonuclease 1 DNA complexes suggest a unified mechanism for nuclease family. *Cell*, *145*(2), 212–223. https://doi.org/10.1016/j.cell.2011.03.005
Owen, B. A. L., H Lang, W., & McMurray, C. T. (2009). The nucleotide binding properties of human MSH2/MSH3 are lesion-dependent and distinct from those of human MSH2/MSH6. *Nature Structural & Molecular Biology*, *16*(5), 550. https://doi.org/10.1038/NSMB.1596
Pan, G., Zhang, J., Han, Y., Chen, Y., Guo, X., Cui, X., Cheng, M., Gao, H., Wang, J., & Jiang, F. (2022). CX-5461 is a potent immunosuppressant which inhibits T cell-mediated alloimmunity via p53-DUSP5. *Pharmacological Research*, *177*, 106120. https://doi.org/10.1016/J.PHRS.2022.106120
Pang, B., Wu, N., Guan, R., Pang, L., Li, X., Li, S., Tang, L., Guo, Y., Chen, J., Sun, D., Sun, H., Dai, J., Bai, J., Ji, G., Liu, P., Liu, A., Wang, Q., Xiao, S., Fu, S., & Jin, Y. (2017). Overexpression of RCC2 Enhances Cell Motility and Promotes Tumor Metastasis in Lung Adenocarcinoma by Inducing Epithelial-Mesenchymal Transition. *Clinical Cancer Research : An Official Journal of the American Association for Cancer Research*, *23*(18), 5598–5610. https://doi.org/10.1158/1078-0432.CCR-16-2909
Papini, D., Langemeyer, L., Abad, M. A., Kerr, A., Samejima, I., Eyers, P. A., Jeyaprakash, A. A., Higgins, J. M. G., Barr, F. A., & Earnshaw, W. C. (2015). TD-60 links RalA GTPase function to the CPC in mitosis. *Nature Communications*, *6*. https://doi.org/10.1038/NCOMMS8678
Pâques, F., & Haber, J. E. (1999). Multiple Pathways of Recombination Induced by Double-Strand Breaks in Saccharomyces cerevisiae. *Microbiology and Molecular Biology Reviews*, *63*(2), 349. https://doi.org/10.1128/MMBR.63.2.349-404.1999

Paquin, K. L., & Howlett, N. G. (2018). The histone DNA repair code: H4K20me2 makes its mark. *Molecular Cancer Research : MCR*, *16*(9), 1335. https://doi.org/10.1158/1541-7786.MCR-17-0688

Paulsen, R. D., & Cimprich, K. A. (2007). The ATR pathway: Fine-tuning the fork. *DNA Repair*, *6*(7), 953–966. https://doi.org/10.1016/J.DNAREP.2007.02.015

Peak, M. J., & Peak, J. G. (1986). DNA-to-protein crosslinks and backbone breaks caused by far- and near-ultraviolet, and visible light radiations in mammalian cells. *Basic Life Sciences*, *38*, 193–202. https://doi.org/10.1007/978-1-4615-9462-8_20

Pegg, A. E. (2011). Multifaceted roles of alkyltransferase and related proteins in DNA repair, DNA damage, resistance to chemotherapy, and research tools. *Chemical Research in Toxicology*, *24*(5), 618–639. https://doi.org/10.1021/TX200031Q

Pellegrino, S., Michelena, J., Teloni, F., Imhof, R., & Altmeyer, M. (2017). Replication-Coupled Dilution of H4K20me2 Guides 53BP1 to Pre-replicative Chromatin. *Cell Reports*, *19*(9), 1819–1831. https://doi.org/10.1016/j.celrep.2017.05.016

Pelletier, J., Thomas, G., & Volarevi, S. (2017). Ribosome biogenesis in cancer: new players and therapeutic avenues. *Nature Reviews Cancer 2017 18:1*, *18*(1), 51–63. https://doi.org/10.1038/nrc.2017.104

Penzo, M., Montanaro, L., Treré, D., & Derenzini, M. (2019). The Ribosome Biogenesis—Cancer Connection. *Cells 2019, Vol. 8, Page 55*, *8*(1), 55. https://doi.org/10.3390/CELLS8010055

Pepe, A., & West, S. C. (2014). MUS81-EME2 Promotes Replication Fork Restart. *Cell Reports*, *7*(4), 1048. https://doi.org/10.1016/J.CELREP.2014.04.007

Pérez-Castro, A. J., & Freire, R. (2012). Rad9B responds to nucleolar stress through ATR and JNK signalling, and delays the G1–S transition. *Journal of Cell Science*, *125*(5), 1152–1164. https://doi.org/10.1242/JCS.091124

Perie, L., Verma, N., Xu, L., Ma, X., & Mueller, E. (2019). Transcriptional Regulation of ZNF638 in Thermogenic Cells by the cAMP Response Element Binding Protein in Male Mice. *Journal of the Endocrine Society*, *3*(12), 2326. https://doi.org/10.1210/JS.2019-00238

Perry, R. P., & Kelley, D. E. (1970). Inhibition of RNA synthesis by actinomycin D: characteristic dose-response of different RNA species. *Journal of Cellular Physiology*, *76*(2), 127–139. https://doi.org/10.1002/JCP.1040760202

Petruseva, I. O., Evdokimov, A. N., & Lavrik, O. I. (2014). Molecular mechanism of global genome nucleotide excision repair. *Acta Naturae*, *6*(20), 23–34. https://doi.org/10.32607/20758251-2014-6-1-23-34

Phillips, D. H., Hewer, A., Martin, C. N., Garner, R. C., & King, M. M. (1988). Correlation of DNA adduct levels in human lung with cigarette smoking. *Nature*, *336*(6201), 790–792. https://doi.org/10.1038/336790a0

Piccinno, R., Minneker, V., & Roukos, V. (2019). 53BP1—DNA repair enters a new liquid phase. *The EMBO Journal*, *38*(16), e102871. https://doi.org/10.15252/EMBJ.2019102871

Pilié, P. G., Tang, C., Mills, G. B., & Yap, T. A. (2019). State-of-the-art strategies for targeting the DNA damage response in cancer. *Nat. Rev. Clin. Oncol.*, *16*(2), 81–104. https://doi.org/10.1038/s41571-018-0114-z

Pires, E., Sharma, N., Selemenakis, P., Wu, B., Huang, Y., Alimbetov, D. S., Zhao, W., & Wiese, C. (2021). RAD51AP1 mediates RAD51 activity through nucleosome interaction. *The Journal of Biological Chemistry*, *297*(1), 297–298.

https://doi.org/10.1016/J.JBC.2021.100844
Poletto, M., Lirussi, L., Wilson, D. M., & Tell, G. (2014). Nucleophosmin modulates stability, activity, and nucleolar accumulation of base excision repair proteins. *Molecular Biology of the Cell*, *25*(10), 1641. https://doi.org/10.1091/MBC.E13-12-0717
Pommier, Y., Barcelo, J. M., Rao, V. A., Sordet, O., Jobson, A. G., Thibaut, L., Miao, Z. H., Seiler, J. A., Zhang, H., Marchand, C., Agama, K., Nitiss, J. L., & Redon, C. (2006). Repair of Topoisomerase I-Mediated DNA Damage. *Progress in Nucleic Acid Research and Molecular Biology*, *81*, 179. https://doi.org/10.1016/S0079-6603(06)81005-6
Poortinga, G., Hannan, K. M., Snelling, H., Walkley, C. R., Jenkins, A., Sharkey, K., Wall, M., Brandenburger, Y., Palatsides, M., Pearson, R. B., McArthur, G. A., & Hannan, R. D. (2004). MAD1 and c-MYC regulate UBF and rDNA transcription during granulocyte differentiation. *The EMBO Journal*, *23*(16), 3325. https://doi.org/10.1038/SJ.EMBOJ.7600335
Potenski, C. J., & Klein, H. L. (2014). How the misincorporation of ribonucleotides into genomic DNA can be both harmful and helpful to cells. *Nucleic Acids Research*, *42*(16), 10226. https://doi.org/10.1093/NAR/GKU773
Pourquier, P., Pilon, A. A., Kohlhagen, G., Mazumder, A., Sharma, A., & Pommier, Y. (1997). Trapping of Mammalian Topoisomerase I and Recombinations Induced by Damaged DNA Containing Nicks or Gaps. *Journal of Biological Chemistry*, *272*(42), 26441–26447. https://doi.org/10.1074/jbc.272.42.26441
Preston, B. D., Singer, B., & Loeb, L. A. (1986). Mutagenic potential of O4-methylthymine in vivo determined by an enzymatic approach to site-specific mutagenesis. *Proceedings of the National Academy of Sciences of the United States of America*, *83*(22), 8501. https://doi.org/10.1073/PNAS.83.22.8501
Qiu, S., Jiang, G., Cao, L., & Huang, J. (2021). Replication Fork Reversal and Protection. *Frontiers in Cell and Developmental Biology*, *9*, 670392. https://doi.org/10.3389/FCELL.2021.670392/BIBTEX
Quinet, A., Lemaçon, D., & Vindigni, A. (2017). Replication fork reversal: players and guardians. *Molecular Cell*, *68*(5), 830. https://doi.org/10.1016/J.MOLCEL.2017.11.022
Rajendra, E., Garaycoechea, J. I., Patel, K. J., & Passmore, L. A. (2014). Abundance of the Fanconi anaemia core complex is regulated by the RuvBL1 and RuvBL2 AAA+ ATPases. *Nucleic Acids Research*, *42*(22), 13736–13748. https://doi.org/10.1093/NAR/GKU1230
Rajendra, E., Oestergaard, V. H., Langevin, F., Wang, M., Dornan, G. L., Patel, K. J., & Passmore, L. A. (2014). The Genetic and Biochemical Basis of FANCD2 Monoubiquitination. *Molecular Cell*, *54*(5), 858–869. https://doi.org/10.1016/J.MOLCEL.2014.05.001
Ramsden, D. A., Carvajal-Garcia, J., & Gupta, G. P. (2021). Mechanism, cellular functions and cancer roles of polymerase-theta-mediated DNA end joining. *Nature Reviews Molecular Cell Biology 2021 23:2*, *23*(2), 125–140. https://doi.org/10.1038/s41580-021-00405-2
Ran, F. A., Hsu, P. D., Wright, J., Agarwala, V., Scott, D. A., & Zhang, F. (2013). Genome engineering using the CRISPR-Cas9 system. *Nature Protocols*, *8*(11), 2281–2308. https://doi.org/10.1038/nprot.2013.143
Rancourt, A., & Satoh, M. S. (2009). Delocalization of nucleolar poly(ADP-ribose) polymerase-1 to the nucleoplasm and its novel link to cellular sensitivity to DNA damage. *DNA Repair*, *8*(3), 286–297. https://doi.org/10.1016/J.DNAREP.2008.11.018
Ratti, M., Lampis, A., Ghidini, M., Salati, M., Mirchev, M. B., Valeri, N., & Hahne, J. C. (2020). MicroRNAs (miRNAs) and Long Non-Coding RNAs (lncRNAs) as New Tools for Cancer

Therapy: First Steps from Bench to Bedside. *Targeted Oncology*, *15*(3), 261–278. https://doi.org/10.1007/s11523-020-00717-x

Ravanat, J.-L., Cadet, J., & Douki, T. (2012). Oxidatively generated DNA lesions as potential biomarkers of in vivo oxidative stress. *Current Molecular Medicine*, *12*(6), 655–671. https://doi.org/10.2174/156652412800792651

Ray Chaudhuri, A., Hashimoto, Y., Herrador, R., Neelsen, K. J., Fachinetti, D., Bermejo, R., Cocito, A., Costanzo, V., & Lopes, M. (2012). Topoisomerase I poisoning results in PARP-mediated replication fork reversal. *Nature Structural & Molecular Biology*, *19*(4), 417–423. https://doi.org/10.1038/NSMB.2258

Reginato, G., & Cejka, P. (2020). The MRE11 complex: A versatile toolkit for the repair of broken DNA. *DNA Repair*, *91–92*, 102869. https://doi.org/10.1016/J.DNAREP.2020.102869

Renaudin, X., & Rosselli, F. (2020). The FANC/BRCA Pathway Releases Replication Blockades by Eliminating DNA Interstrand Cross-Links. *Genes 2020, Vol. 11, Page 585*, *11*(5), 585. https://doi.org/10.3390/GENES11050585

Rendleman, J., Shang, S., Dominianni, C., Shields, J. F., Scanlon, P., Adaniel, C., Desrichard, A., Ma, M., Shapiro, R., Berman, R., Pavlick, A., Polsky, D., Shao, Y., Osman, I., & Kirchhoff, T. (2013). Melanoma risk loci as determinants of melanoma recurrence and survival. *Journal of Translational Medicine*, *11*(1). https://doi.org/10.1186/1479-5876-11-279

Reuvers, T. G. A., Kanaar, R., & Nonnekens, J. (2020). DNA Damage-Inducing Anticancer Therapies: From Global to Precision Damage. *Cancers*, *12*(8), 1–21. https://doi.org/10.3390/CANCERS12082098

Richardson, C. D., Kazane, K. R., Feng, S. J., Zelin, E., Bray, N. L., Schäfer, A. J., Floor, S. N., & Corn, J. E. (2018). *CRISPR–Cas9 genome editing in human cells occurs via the Fanconi anemia pathway*. *50*(8), 1132–1139. https://doi.org/10.1038/s41588-018-0174-0

Río, P., Navarro, S., Guenechea, G., Sánchez-Domínguez, R., Lamana, M. L., Yañez, R., Casado, J. A., Mehta, P. A., Pujol, M. R., Surrallés, J., Charrier, S., Galy, A., Segovia, J. C., Díaz De Heredia, C., Sevilla, J., & Bueren, J. A. (2017). Engraftment and in vivo proliferation advantage of gene-corrected mobilized CD34+ cells from Fanconi anemia patients. *Blood*, *130*(13), 1535–1542. https://doi.org/10.1182/BLOOD-2017-03-774174

Robertson, A. B., Klungland, A., Rognes, T., & Leiros, I. (2009). DNA Repair in Mammalian Cells. *Cellular and Molecular Life Sciences 2009 66:6*, *66*(6), 981–993. https://doi.org/10.1007/S00018-009-8736-Z

Rocca, C. J., Soares, D. G., Bouzid, H., Henriques, J. A. P., Larsen, A. K., & Escargueil, A. E. (2015). BRCA2 is needed for both repair and cell cycle arrest in mammalian cells exposed to S23906, an anticancer monofunctional DNA binder. *Cell Cycle*, *14*(13), 2080. https://doi.org/10.1080/15384101.2015.1042632

Rochette, P. J., Therrien, J. P., Drouin, R., Perdiz, D., Bastien, N., Drobetsky, E. A., & Sage, E. (2003). UVA-induced cyclobutane pyrimidine dimers form predominantly at thymine–thymine dipyrimidines and correlate with the mutation spectrum in rodent cells. *Nucleic Acids Research*, *31*(11), 2786. https://doi.org/10.1093/NAR/GKG402

Rodrigo, R. M., Rendon, M. C., Torreblanca, J., Garcia-Herdugo, G., & Moreno, F. J. (1992). Characterization and immunolocalization of RNA polymerase I transcription factor UBF with anti-NOR serum in protozoa, higher plant and vertebrate cells. *Journal of Cell Science*, *103*(4), 1053–1063. https://doi.org/10.1242/JCS.103.4.1053

Rogers, C. M., Lee, C. Y., Parkins, S., Buehler, N. J., Wenzel, S., Martínez-Márquez, F., Takagi,

Y., Myong, S., & Bochman, M. L. (2020). The yeast Hrq1 helicase stimulates Pso2 translesion nuclease activity and thereby promotes DNA interstrand crosslink repair. *The Journal of Biological Chemistry*, *295*(27), 8945. https://doi.org/10.1074/JBC.RA120.013626

Rogers, C. M., Simmons, R. H., Fluhler Thornburg, G. E., Buehler, N. J., & Bochman, M. L. (2020). Fanconi anemia-independent DNA inter-strand crosslink repair in eukaryotes. *Progress in Biophysics and Molecular Biology*, *158*, 33–46.

Rohleder, F., Huang, J., Xue, Y., Kuper, J., Round, A., Seidman, M., Wang, W., & Kisker, C. (2016). FANCM interacts with PCNA to promote replication traverse of DNA interstrand crosslinks. *Nucleic Acids Research*, *44*(7), 3219–3232. https://doi.org/10.1093/NAR/GKW037

Román-Rodríguez, F. J., Ugalde, L., Álvarez, L., Díez, B., Ramírez, M. J., Risueño, C., Cortón, M., Bogliolo, M., Bernal, S., March, F., Ayuso, C., Hanenberg, H., Sevilla, J., Rodríguez-Perales, S., Torres-Ruiz, R., Surrallés, J., Bueren, J. A., & Río, P. (2019). NHEJ-Mediated Repair of CRISPR-Cas9-Induced DNA Breaks Efficiently Corrects Mutations in HSPCs from Patients with Fanconi Anemia. *Cell Stem Cell*, *25*(5), 607-621.e7. https://doi.org/10.1016/j.stem.2019.08.016

Roney, M. S. I., Lanagan, C., Sheng, Y. H., Lawler, K., Schmidt, C., Nguyen, N. T., Begun, J., & Kijanka, G. S. (2021). IgM and IgA augmented autoantibody signatures improve early-stage detection of colorectal cancer prior to nodal and distant spread. *Clinical and Translational Immunology*, *10*(9), 1–14. https://doi.org/10.1002/cti2.1330

Roos, W. P., & Kaina, B. (2013). DNA damage-induced cell death: From specific DNA lesions to the DNA damage response and apoptosis. *Cancer Letters*, *332*(2), 237–248. https://doi.org/10.1016/J.CANLET.2012.01.007

Rosa, J. L., Casaroli-Marano, R. P., Buckler, A. J., Vilaró, S., & Barbacid, M. (1996). p619, a giant protein related to the chromosome condensation regulator RCC1, stimulates guanine nucleotide exchange on ARF1 and Rab proteins. *The EMBO Journal*, *15*(16), 4262. https://doi.org/10.1002/j.1460-2075.1996.tb00801.x

Rosasco-Nitcher, S. E., Lan, W., Khorasanizadeh, S., & Stukenberg, P. T. (2008). Centromeric Aurora-B activation requires TD-60, microtubules, and substrate priming phosphorylation. *Science (New York, N.Y.)*, *319*(5862), 469–472. https://doi.org/10.1126/SCIENCE.1148980

Rosenberg, P. S., Greene, M. H., & Alter, B. P. (2003). Cancer incidence in persons with Fanconi anemia. *Blood*, *101*(3), 822–826. https://doi.org/10.1182/BLOOD-2002-05-1498

Rosenberg, P. S., Socié, G., Alter, B. P., & Gluckman, E. (2005). Risk of head and neck squamous cell cancer and death in patients with Fanconi anemia who did and did not receive transplants. *Blood*, *105*(1), 67–73. https://doi.org/10.1182/BLOOD-2004-04-1652

Rosenberg, P. S., Tamary, H., & Alter, B. P. (2011). How high are carrier frequencies of rare recessive syndromes? Contemporary estimates for Fanconi Anemia in the United States and Israel. *American Journal of Medical Genetics, Part A*, *155*(8), 1877–1883. https://doi.org/10.1002/AJMG.A.34087

Rothenberg, E., Grimme, J. M., Spies, M., & Ha, T. (2008). Human Rad52-mediated homology search and annealing occurs by continuous interactions between overlapping nucleoprotein complexes. *Proceedings of the National Academy of Sciences of the United States of America*, *105*(51), 20274–20279.

https://doi.org/10.1073/PNAS.0810317106/SUPPL_FILE/0810317106SI.PDF
Roy, U., & Schärer, O. D. (2016). Involvement of translesion synthesis DNA polymerases in DNA interstrand crosslink repair. *DNA Repair*, *44*, 33–41. https://doi.org/10.1016/J.DNAREP.2016.05.004
Rubbi, C. P., & Milner, J. (2003). Disruption of the nucleolus mediates stabilization of p53 in response to DNA damage and other stresses. *The EMBO Journal*, *22*(22), 6068. https://doi.org/10.1093/EMBOJ/CDG579
Rydberg, B., & Lindahl, T. (1982). Nonenzymatic methylation of DNA by the intracellular methyl group donor S-adenosyl-L-methionine is a potentially mutagenic reaction. *The EMBO Journal*, *1*(2), 211. https://doi.org/10.1002/J.1460-2075.1982.TB01149.X
Sagher, D., & Strauss, B. (1983). Insertion of Nucleotides Opposite Apurinic/Apyrimidinic Sites in Deoxyribonucleic Acid during in Vitro Synthesis: Uniqueness of Adenine Nucleotides. *Biochemistry*, *22*(19), 4518–4526. https://doi.org/10.1021/BI00288A026/ASSET/BI00288A026.FP.PNG_V03
Sakai, W., & Sugasawa, K. (2019). Importance of finding the bona fide target of the Fanconi anemia pathway. In *Genes and Environment* (Vol. 41, Issue 1). BioMed Central Ltd. https://doi.org/10.1186/s41021-019-0122-y
Sakofsky, C. J., & Malkova, A. (2017). Break Induced Replication in eukaryotes: mechanisms, functions, and consequences. *Critical Reviews in Biochemistry and Molecular Biology*, *52*(4), 395. https://doi.org/10.1080/10409238.2017.1314444
Sale, J. E. (2013). Translesion DNA Synthesis and Mutagenesis in Eukaryotes. *Cold Spring Harbor Perspectives in Biology*, *5*(3), a012708. https://doi.org/10.1101/CSHPERSPECT.A012708
Sale, J. E., Lehmann, A. R., & Woodgate, R. (2012). Y-family DNA polymerases and their role in tolerance of cellular DNA damage. *Nature Reviews Molecular Cell Biology 2012 13:3*, *13*(3), 141–152. https://doi.org/10.1038/nrm3289
Saleh-Gohari, N., Bryant, H. E., Schultz, N., Parker, K. M., Cassel, T. N., & Helleday, T. (2023). Spontaneous Homologous Recombination Is Induced by Collapsed Replication Forks That Are Caused by Endogenous DNA Single-Strand Breaks. *Https://Doi.Org/10.1128/MCB.25.16.7158-7169.2005*, *25*(16), 7158–7169. https://doi.org/10.1128/MCB.25.16.7158-7169.2005
Sanchez-Pulido, L., & Andrade-Navarro, M. A. (2007). The FTO (fat mass and obesity associated) gene codes for a novel member of the non-heme dioxygenase superfamily. *BMC Biochemistry*, *8*, 23. https://doi.org/10.1186/1471-2091-8-23
Sanij, E., & Hannan, R. D. (2009). The role of UBF in regulating the structure and dynamics of transcriptionally active rDNA chromatin. *Http://Dx.Doi.Org/10.4161/Epi.4.6.9449*, *4*(6), 374–382. https://doi.org/10.4161/EPI.4.6.9449
Sapio, R. T., Burns, C. J., & Pestov, D. G. (2021). Effects of Hydrogen Peroxide Stress on the Nucleolar Redox Environment and Pre-rRNA Maturation. *Frontiers in Molecular Biosciences*, *8*, 280. https://doi.org/10.3389/FMOLB.2021.678488/FULL
Sartori, A. A., Lukas, C., Coates, J., Mistrik, M., Fu, S., Bartek, J., Baer, R., Lukas, J., & Jackson, S. P. (2007). Human CtIP promotes DNA end resection. *Nature 2007 450:7169*, *450*(7169), 509–514. https://doi.org/10.1038/nature06337
Satoh, M. S., & Lindahl, T. (1992). Role of poly(ADP-ribose) formation in DNA repair. *Nature*, *356*(6367), 356–358. https://doi.org/10.1038/356356A0
Schipler, A., & Iliakis, G. (2013). DNA double-strand–break complexity levels and their possible contributions to the probability for error-prone processing and repair pathway

choice. *Nucleic Acids Research*, *41*(16), 7589–7605. https://doi.org/10.1093/NAR/GKT556

Schlacher, K., Christ, N., Siaud, N., Egashira, A., Wu, H., & Jasin, M. (2011). Double-Strand Break Repair Independent Role For BRCA2 In Blocking Stalled Replication Fork Degradation By MRE11. *Cell*, *145*(4), 529. https://doi.org/10.1016/J.CELL.2011.03.041

Schlacher, K., Wu, H., & Jasin, M. (2012). A Distinct Replication Fork Protection Pathway Connects Fanconi Anemia Tumor Suppressors to RAD51-BRCA1/2. *Cancer Cell*, *22*(1), 106. https://doi.org/10.1016/J.CCR.2012.05.015

Schreiber, V., Dantzer, F., Amé, J. C., & De Murcia, G. (2006). Poly(ADP-ribose): novel functions for an old molecule. *Nature Reviews Molecular Cell Biology 2006 7:7*, *7*(7), 517–528. https://doi.org/10.1038/nrm1963

Scully, R., Panday, A., Elango, R., & Willis, N. A. (2019). DNA double-strand break repair-pathway choice in somatic mammalian cells. *Nature Reviews Molecular Cell Biology 2019 20:11*, *20*(11), 698–714. https://www.nature.com/articles/s41580-019-0152-0

Sczepanski, J. T., Jacobs, A. C., & Greenberg, M. M. (2008). Self-promoted DNA interstrand cross-link formation by an abasie site. *Journal of the American Chemical Society*, *130*(30), 9646–9647. https://doi.org/10.1021/JA8030642/SUPPL_FILE/JA8030642-FILE002.PDF

Segal, A. W. (2005). How Neutrophils Kill Microbes. *Annual Review of Immunology*, *23*, 197. https://doi.org/10.1146/ANNUREV.IMMUNOL.23.021704.115653

Sejersted, Y., Hildrestrand, G. A., Kunke, D., Rolseth, V., Krokeide, S. Z., Neurauter, C. G., Suganthan, R., Atneosen-Åsegg, M., Fleming, A. M., Saugstad, O. D., Burrows, C. J., Luna, L., & Bjørås, M. (2011). Endonuclease VIII-like 3 (Neil3) DNA glycosylase promotes neurogenesis induced by hypoxia-ischemia. *Proceedings of the National Academy of Sciences of the United States of America*, *108*(46), 18802–18807. https://doi.org/10.1073/PNAS.1106880108/SUPPL_FILE/PNAS.201106880SI.PDF

Sekiguchi, M., & Matsushita, N. (2022). DNA Damage Response Regulation by Histone Ubiquitination. *International Journal of Molecular Sciences*, *23*(15). https://doi.org/10.3390/IJMS23158187

Selimoglu, R., Bettoun, A., Joffre, C., Meunier, B., & Parrini, M. C. (2014). RalA GTPase and MAP4K4 Function through NDR1 Activation in Stress Response and Apoptotic Signaling. *J Cell Biol Cell Metab*, *1*, 1. https://doi.org/10.24966/CBCM-1943/100001

Semlow, D. R., & Walter, J. C. (2021). Mechanisms of Vertebrate DNA Interstrand Cross-Link Repair. *Annual Review of Biochemistry*, *90*, 107–135. https://doi.org/10.1146/annurev-biochem-080320-112510

Semlow, D. R., Zhang, J., Budzowska, M., Drohat, A. C., & Walter, J. C. (2016). Replication-Dependent Unhooking of DNA Interstrand Cross-Links by the NEIL3 Glycosylase. *Cell*, *167*(2), 498-511.e14. https://doi.org/10.1016/j.cell.2016.09.008

Shadfan, M., Lopez-Pajares, V., & Yuan, Z. M. (2012). MDM2 and MDMX: Alone and together in regulation of p53. *Translational Cancer Research*, *1*(2), 88. https://doi.org/10.3978/j.issn.2218-676X.2012.04.02

Shav-Tal, Y., Blechman, J., Darzacq, X., Montagna, C., Dye, B. T., Patton, J. G., Singer, R. H., & Zipori, D. (2005). Dynamic Sorting of Nuclear Components into Distinct Nucleolar Caps during Transcriptional Inhibition. *Molecular Biology of the Cell*, *16*(5), 2395–2413. https://doi.org/10.1091/mbc.E04

Sherman, M. H., Bassing, C. H., & Teitell, M. A. (2011). DNA damage response regulates cell differentiation. *Trends in Cell Biology*, *21*(5), 312.

https://doi.org/10.1016/J.TCB.2011.01.004
Shigechi, T., Tomida, J., Sato, K., Kobayashi, M., Eykelenboom, J. K., Pessina, F., Zhang, Y., Uchida, E., Ishiai, M., Lowndes, N. F., Yamamoto, K., Kurumizaka, H., Maehara, Y., & Takata, M. (2012). ATR-ATRIP kinase complex triggers activation of the fanconi anemia DNA repair pathway. *Cancer Research*, *72*(5), 1149–1156. https://doi.org/10.1158/0008-5472.CAN-11-2904/650086/AM/ATR-ATRIP-KINASE-COMPLEX-TRIGGERS-ACTIVATION-OF
Shimamura, A., De Oca, R. M., Svenson, J. L., Haining, N., Moreau, L. A., Nathan, D. G., & D'Andrea, A. D. (2002). A novel diagnostic screen for defects in the Fanconi anemia pathway. *Blood*, *100*(13), 4649–4654. https://doi.org/10.1182/BLOOD-2002-05-1399
Shrivastav, M., De Haro, L. P., & Nickoloff, J. A. (2007). Regulation of DNA double-strand break repair pathway choice. *Cell Research 2008 18:1*, *18*(1), 134–147. https://doi.org/10.1038/cr.2007.111
Sidorova, J. (2017). A game of substrates: replication fork remodeling and its roles in genome stability and chemo-resistance. *Cell Stress*, *1*(3), 115. https://doi.org/10.15698/CST2017.12.114
Sijacki, T., Alcón, P., Chen, Z. A., McLaughlin, S. H., Shakeel, S., Rappsilber, J., & Passmore, L. A. (2022). The DNA-damage kinase ATR activates the FANCD2-FANCI clamp by priming it for ubiquitination. *Nature Structural & Molecular Biology 2022 29:9*, *29*(9), 881–890. https://doi.org/10.1038/S41594-022-00820-9
Simonetta, M., de Krijger, I., Serrat, J., Moatti, N., Fortunato, D., Hoekman, L., Bleijerveld, O. B., Altelaar, A. F. M., & Jacobs, J. J. L. (2018). H4K20me2 distinguishes pre-replicative from post-replicative chromatin to appropriately direct DNA repair pathway choice by 53BP1-RIF1-MAD2L2. *Https://Doi.Org/10.1080/15384101.2017.1404210*, *17*(1), 124–136. https://doi.org/10.1080/15384101.2017.1404210
Simsek, D., Brunet, E., Wong, S. Y. W., Katyal, S., Gao, Y., McKinnon, P. J., Lou, J., Zhang, L., Li, J., Rebar, E. J., Gregory, P. D., Holmes, M. C., & Jasin, M. (2011). DNA Ligase III Promotes Alternative Nonhomologous End-Joining during Chromosomal Translocation Formation. *PLOS Genetics*, *7*(6), e1002080. https://doi.org/10.1371/JOURNAL.PGEN.1002080
Singh, R. K., Kumar, S., Prasad, D. N., & Bhardwaj, T. R. (2018). Therapeutic journery of nitrogen mustard as alkylating anticancer agents: Historic to future perspectives. *European Journal of Medicinal Chemistry*, *151*, 401–433. https://doi.org/10.1016/J.EJMECH.2018.04.001
Singh, T. R., Ali, A. M., Paramasivam, M., Pradhan, A., Wahengbam, K., Seidman, M. M., & Meetei, A. R. (2013). ATR-dependent phosphorylation of FANCM at serine 1045 is essential for FANCM functions. *Cancer Research*, *73*(14), 4300–4310. https://doi.org/10.1158/0008-5472.CAN-12-3976/650793/AM/ATR-DEPENDENT-PHOSPHORYLATION-OF-FANCM-AT-SERINE
Singh, T. R., Saro, D., Ali, A. M., Zheng, X. F., Du, C. hu, Killen, M. W., Sachpatzidis, A., Wahengbam, K., Pierce, A. J., Xiong, Y., Sung, P., & Meetei, A. R. (2010). MHF1-MHF2, a Histone-Fold-Containing Protein Complex, Participates in the Fanconi Anemia Pathway via FANCM. *Molecular Cell*, *37*(6), 879–886. https://doi.org/10.1016/j.molcel.2010.01.036
Sirri, V., Urcuqui-Inchima, S., Roussel, P., & Hernandez-Verdun, D. (2008). Nucleolus: the fascinating nuclear body. *Histochemistry and Cell Biology*, *129*(1), 13. https://doi.org/10.1007/S00418-007-0359-6

Sloan, K. E., Bohnsack, M. T., & Watkins, N. J. (2013). The 5S RNP Couples p53 Homeostasis to Ribosome Biogenesis and Nucleolar Stress. *Cell Reports*, *5*(1), 237–247. https://doi.org/10.1016/j.celrep.2013.08.049

Smeaton, M. B., Hlavin, E. M., Mason, T. M. G., Noronha, A. M., Wilds, C. J., & Miller, P. S. (2008). Distortion-dependent unhooking of interstrand cross-links in mammalian cell extracts. *Biochemistry*, *47*(37), 9920–9930. https://doi.org/10.1021/BI800925E/SUPPL_FILE/BI800925E_SI_001.PDF

Smith, G. C., & Jackson, S. P. (1999). *The DNA-dependent protein kinase*. www.genesdev.org

Smith, T. A., Kirkpatrick, D. R., Smith, S., Smith, T. K., Pearson, T., Kailasam, A., Herrmann, K. Z., Schubert, J., & Agrawal, D. K. (2017). Radioprotective agents to prevent cellular damage due to ionizing radiation. *Journal of Translational Medicine*, *15*(1), 232. https://doi.org/10.1186/s12967-017-1338-x

Smogorzewska, A., Matsuoka, S., Vinciguerra, P., McDonald, E. R., Hurov, K. E., Luo, J., Ballif, B. A., Gygi, S. P., Hofmann, K., D'Andrea, A. D., & Elledge, S. J. (2007). Identification of the FANCI Protein, a Monoubiquitinated FANCD2 Paralog Required for DNA Repair. *Cell*, *129*(2), 289–301. https://pubmed.ncbi.nlm.nih.gov/17412408/

Sobeck, A., Stone, S., Landais, I., de Graaf, B., & Hoatlin, M. E. (2009). The Fanconi anemia protein FANCM is controlled by FANCD2 and the ATR/ATM pathways. *Journal of Biological Chemistry*, *284*(38), 25560–25568. https://doi.org/10.1074/jbc.M109.007690

Song, C., Liang, L., Jin, Y., Li, Y., Liu, Y., Guo, L., Wu, C., Yun, C.-H., & Yin, Y. (2018). RCC2 is a novel p53 target in suppressing metastasis. *Oncogene*, *37*(1), 8–17. https://doi.org/10.1038/onc.2017.306

Sørensen, P. D., & Frederiksen, S. (1991). Characterization of human 5S rRNA genes. *Nucleic Acids Research*, *19*(15), 4147. https://doi.org/10.1093/NAR/19.15.4147

Soria-Bretones, I., Cepeda-García, C., Checa-Rodriguez, C., Heyer, V., Reina-San-Martin, B., Soutoglou, E., & Huertas, P. (2017). DNA end resection requires constitutive sumoylation of CtIP by CBX4. *Nature Communications 2017 8:1*, *8*(1), 1–11. https://doi.org/10.1038/s41467-017-00183-6

Spielmann, H. P., Dwyer, T. J., Hearst, J. E., & Wemmer, D. E. (1995). Solution Structures of Psoralen Monoadducted and Cross-Linked DNA Oligomers by NMR Spectroscopy and Restrained Molecular Dynamics. *Biochemistry*, *34*(40), 12937–12953. https://doi.org/10.1021/BI00040A004/ASSET/BI00040A004.FP.PNG_V03

Spivak, G. (2015). Nucleotide excision repair in humans. *DNA Repair*, *36*, 13–18. https://doi.org/10.1016/J.DNAREP.2015.09.003

Srinivas, U. S., Tan, B. W. Q., Vellayappan, B. A., & Jeyasekharan, A. D. (2019). ROS and the DNA damage response in cancer. *Redox Biology*, *25*, 101084. https://doi.org/10.1016/J.REDOX.2018.101084

Stacey, S. N., Gudbjartsson, D. F., Sulem, P., Bergthorsson, J. T., Kumar, R., Thorleifsson, G., Sigurdsson, A., Jakobsdottir, M., Sigurgeirsson, B., Benediktsdottir, K. R., Thorisdottir, K., Ragnarsson, R., Scherer, D., Rudnai, P., Gurzau, E., Koppova, K., Höiom, V., Botella-Estrada, R., Soriano, V., … Stefansson, K. (2008). Common variants on 1p36 and 1q42 are associated with cutaneous basal cell carcinoma but not with melanoma or pigmentation traits. *Nature Genetics*, *40*(11), 1313–1318. https://doi.org/10.1038/NG.234

Stark, J. M., Pierce, A. J., Oh, J., Pastink, A., & Jasin, M. (2004). Genetic Steps of Mammalian Homologous Repair with Distinct Mutagenic Consequences. *Molecular and Cellular Biology*, *24*(21), 9305. https://doi.org/10.1128/MCB.24.21.9305-9316.2004

Stark, L. A., & Dunlop, M. G. (2023). Nucleolar Sequestration of RelA (p65) Regulates NF-κB-Driven Transcription and Apoptosis. *Https://Doi.Org/10.1128/MCB.25.14.5985-6004.2005*, *25*(14), 5985–6004. https://doi.org/10.1128/MCB.25.14.5985-6004.2005

Stenström, L., Mahdessian, D., Gnann, C., Cesnik, A. J., Ouyang, W., Leonetti, M. D., Uhlén, M., Cuylen-Haering, S., Thul, P. J., & Lundberg, E. (2020). Mapping the nucleolar proteome reveals a spatiotemporal organization related to intrinsic protein disorder. *Molecular Systems Biology*, *16*(8). https://doi.org/10.15252/MSB.20209469

Stern, N., Hochman, A., Zemach, N., Weizman, N., Hammel, I., Shiloh, Y., Rotman, G., & Barzilai, A. (2002). Accumulation of DNA damage and reduced levels of nicotine adenine dinucleotide in the brains of Atm-deficient mice. *Journal of Biological Chemistry*, *277*(1), 602–608. https://doi.org/10.1074/jbc.M106798200

Stewart, L., Redinbo, M. R., Qiu, X., Hol, W. G. J., & Champoux, J. J. (1998). A model for the mechanism of human topoisomerase I. *Science (New York, N.Y.)*, *279*(5356), 1534–1541. https://doi.org/10.1126/SCIENCE.279.5356.1534

Stochaj, U., & Weber, S. C. (2020). Nucleolar Organization and Functions in Health and Disease. *Cells*, *9*(3). https://doi.org/10.3390/CELLS9030526

Stonez, M. P., Cho, Y. J., Huang, H., Kim, H. Y., Kozekov, I. D., Kozekova, A., Wang, H., Minko, I. G., Lloyd, R. S., Harris, T. M., & Rizzo, C. J. (2008). Interstrand DNA Cross-links Induced by α,β-Unsaturated Aldehydes Derived from Lipid Peroxidation and Environmental Sources. *Accounts of Chemical Research*, *41*(7), 793. https://doi.org/10.1021/AR700246X

Stornetta, A., Zimmermann, M., Cimino, G. D., Henderson, P. T., & Sturla, S. J. (2017). DNA Adducts fromAnticancer Drugs as Candidate PredictiveMarkers for Precision Medicine. *Chemical Research in Toxicology*, *30*(1), 388. https://doi.org/10.1021/ACS.CHEMRESTOX.6B00380

Stults, D. M., Killen, M. W., Pierce, H. H., & Pierce, A. J. (2008). Genomic architecture and inheritance of human ribosomal RNA gene clusters. *Genome Research*, *18*(1), 13. https://doi.org/10.1101/GR.6858507

Suzuki, A., Kogo, R., Kawahara, K., Sasaki, M., Nishio, M., Maehama, T., Sasaki, T., Mimori, K., & Mori, M. (2012). A new PICTure of nucleolar stress. *Cancer Science*, *103*(4), 632. https://doi.org/10.1111/J.1349-7006.2012.02219.X

Swuec, P., Renault, L., Borg, A., Shah, F., Murphy, V. J., van Twest, S., Snijders, A. P., Deans, A. J., & Costa, A. (2017). The FA Core Complex Contains a Homo-dimeric Catalytic Module for the Symmetric Mono-ubiquitination of FANCI-FANCD2. *Cell Reports*, *18*(3), 611. https://doi.org/10.1016/J.CELREP.2016.11.013

Symington, L. S. (2016). Mechanism and Regulation of DNA End Resection in Eukaryotes. *Critical Reviews in Biochemistry and Molecular Biology*, *51*(3), 195. https://doi.org/10.3109/10409238.2016.1172552

Symington, L. S., & Gautier, J. (2011). Double-Strand Break End Resection and Repair Pathway Choice. *Https://Doi.Org/10.1146/Annurev-Genet-110410-132435*, *45*, 247–271. https://doi.org/10.1146/ANNUREV-GENET-110410-132435

Tan, W., van Twest, S., Murphy, V. J., & Deans, A. J. (2020). ATR-Mediated FANCI Phosphorylation Regulates Both Ubiquitination and Deubiquitination of FANCD2. *Frontiers in Cell and Developmental Biology*, *8*, 2. https://doi.org/10.3389/FCELL.2020.00002/BIBTEX

Tanaka, H., & Watanabe, T. (2020). Mechanisms Underlying Recurrent Genomic Amplification in Human Cancers. *Trends in Cancer*, *6*(6), 462–477.

https://doi.org/10.1016/J.TRECAN.2020.02.019
Taniguchi, T., Garcia-Higuera, I., Andreassen, P. R., Gregory, R. C., Grompe, M., & D'Andrea, A. D. (2002). S-phase-specific interaction of the Fanconi anemia protein, FANCD2, with BRCA1 and RAD51. *Blood*, *100*(7), 2414–2420. https://doi.org/10.1182/blood-2002-01-0278
Tannock, I. F. (1998). Conventional cancer therapy: promise broken or promise delayed? *The Lancet*, *351*(SUPPL.2), SII9–SII16. https://doi.org/10.1016/S0140-6736(98)90327-0
Tarsounas, M., & Sung, P. (2020). The antitumorigenic roles of BRCA1–BARD1 in DNA repair and replication. *Nature Reviews Molecular Cell Biology 2020 21:5*, *21*(5), 284–299. https://doi.org/10.1038/s41580-020-0218-z
Tateishi, S., Niwa, H., Miyazaki, J.-I., Fujimoto, S., Inoue, H., & Yamaizumi, M. (2023). Enhanced Genomic Instability and Defective Postreplication Repair in RAD18 Knockout Mouse Embryonic Stem Cells. *Https://Doi.Org/10.1128/MCB.23.2.474-481.2003*, *23*(2), 474–481. https://doi.org/10.1128/MCB.23.2.474-481.2003
Taylor, A. M. R., Groom, A., & Byrd, P. J. (2004). Ataxia-telangiectasia-like disorder (ATLD)—its clinical presentation and molecular basis. *DNA Repair*, *3*(8–9), 1219–1225. https://doi.org/10.1016/J.DNAREP.2004.04.009
Taylor, A. M. R., Rothblum-Oviatt, C., Ellis, N. A., Hickson, I. D., Meyer, S., Crawford, T. O., Smogorzewska, A., Pietrucha, B., Weemaes, C., & Stewart, G. S. (2019). Chromosome instability syndromes. *Nature Reviews Disease Primers 2019 5:1*, *5*(1), 1–20. https://doi.org/10.1038/s41572-019-0113-0
Tembe, V., & Henderson, B. R. (2007). Protein trafficking in response to DNA damage. *Cellular Signalling*, *19*(6), 1113–1120. https://doi.org/10.1016/j.cellsig.2007.03.001
Thiviyanathan, V., Somasunderam, A., Volk, D. E., Hazra, T. K., Mitra, S., & Gorenstein, D. G. (2008). Base-pairing Properties of the Oxidized Cytosine Derivative, 5-Hydroxy Uracil. *Biochemical and Biophysical Research Communications*, *366*(3), 752. https://doi.org/10.1016/J.BBRC.2007.12.010
Thoms, H. C., Loveridge, C. J., Simpson, J., Clipson, A., Reinhardt, K., Dunlop, M. G., & Stark, L. A. (2010). Nucleolar Targeting of RelA(p65) Is Regulated by COMMD1-Dependent Ubiquitination. *Cancer Research*, *70*(1), 139–149. https://doi.org/10.1158/0008-5472.CAN-09-1397
Thoms, H. C., & Stark, L. A. (2021). The NF-κB Nucleolar Stress Response Pathway. *Biomedicines*, *9*(9). https://doi.org/10.3390/BIOMEDICINES9091082
Tice, R. R., & Setlow, R. B. (1985). DNA repair and replication in aging organisms and cells. *Handbook of the Biology of Aging / Editors, C.E. Finch, E.L. Schneider, with the Assistance of Associate Editors, R.C. Adelman, G.M. Martin, E.J. Masoro*. https://doi.org/10.3/JQUERY-UI.JS
Tolley, D. A., Hargreave, T. B., Smith, P. H., Williams, J. L., Grigor, K. M., Parmar, M. K. B., Freedman, L. S., & Uscinska, B. M. (1988). Effect of intravesical mitomycin C on recurrence of newly diagnosed superficial bladder cancer: interim report from the Medical Research Council Subgroup on Superficial Bladder Cancer (Urological Cancer Working Party). *British Medical Journal (Clinical Research Ed.)*, *296*(6639), 1759. https://doi.org/10.1136/BMJ.296.6639.1759
Tomasz, M. (1995). Mitomycin C: small, fast and deadly (but very selective). *Chemistry & Biology*, *2*(9), 575–579. https://doi.org/10.1016/1074-5521(95)90120-5
Tomimatsu, N., Mukherjee, B., Catherine Hardebeck, M., Ilcheva, M., Vanessa Camacho, C., Louise Harris, J., Porteus, M., Llorente, B., Khanna, K. K. u., & Burma, S. (2014).

Phosphorylation of EXO1 by CDKs 1 and 2 regulates DNA end resection and repair pathway choice. *Nature Communications 2014 5:1*, *5*(1), 1–10. https://doi.org/10.1038/ncomms4561

Tretyakova, N., Matter, B., Jones, R., & Shallop, A. (2002). Formation of benzo[a]pyrene diol epoxide - DNA adducts at specific guanines within K-ras and p53 gene sequences: Stable isotope-labeling mass spectrometry approach. *Biochemistry*, *41*(30), 9535–9544. https://doi.org/10.1021/BI025540I/ASSET/IMAGES/LARGE/BI025540IF00007.JPEG

Trewick, S. C., Henshaw, T. F., Hausinger, R. P., Lindahl, T., & Sedgwick, B. (2002). Oxidative demethylation by Escherichia coli AlkB directly reverts DNA base damage. *Nature 2002 419:6903*, *419*(6903), 174–178. https://doi.org/10.1038/nature00908

Tripathi, V., Nagarjuna, T., & Sengupta, S. (2007). BLM helicase–dependent and –independent roles of 53BP1 during replication stress–mediated homologous recombination. *The Journal of Cell Biology*, *178*(1), 9. https://doi.org/10.1083/JCB.200610051

Tropp, B. E. (2012). *Molecular biology : genes to proteins* (4th edition.).

Truong, L. N., Li, Y., Shi, L. Z., Hwang, P. Y. H., He, J., Wang, H., Razavian, N., Berns, M. W., & Wu, X. (2013). Microhomology-mediated End Joining and Homologous Recombination share the initial end resection step to repair DNA double-strand breaks in mammalian cells. *Proceedings of the National Academy of Sciences of the United States of America*, *110*(19), 7720–7725. /pmc/articles/PMC3651503/

Tudek, B., Bioteux, S., & Laval, J. (1992). Biological properties of imidazole ring-opened N7-methylguanine in M13mp18 phage DNA. *Nucleic Acids Research*, *20*(12), 3079. https://doi.org/10.1093/NAR/20.12.3079

Tupler, R., Perini, G., & Green, M. R. (2001). Expressing the human genome. *Nature 2001 409:6822*, *409*(6822), 832–833. https://doi.org/10.1038/35057011

Ulrich, H. D. (2011). Timing and spacing of ubiquitin-dependent DNA damage bypass. *FEBS Letters*, *585*(18), 2861–2867. https://doi.org/10.1016/J.FEBSLET.2011.05.028

Unno, J., Itaya, A., Taoka, M., Sato, K., Tomida, J., Sakai, W., Sugasawa, K., Ishiai, M., Ikura, T., Isobe, T., Kurumizaka, H., & Takata, M. (2014). FANCD2 binds CtIP and regulates DNA-end resection during DNA interstrand crosslink repair. *Cell Reports*, *7*(4), 1039–1047. https://doi.org/10.1016/j.celrep.2014.04.005

Uringa, E. J., Youds, J. L., Lisaingo, K., Lansdorp, P. M., & Boulton, S. J. (2011). RTEL1: an essential helicase for telomere maintenance and the regulation of homologous recombination. *Nucleic Acids Research*, *39*(5), 1647. https://doi.org/10.1093/NAR/GKQ1045

Vacchelli, E., Galluzzi, L., Fridman, W. H., Galon, J., Sautès-Fridman, C., Tartour, E., Zitvogel, L., & Kroemer, G. (2012). Trial watch. *Https://Doi.Org/10.4161/Onci.1.2.19026*, *1*(2), 179–188. https://doi.org/10.4161/ONCI.1.2.19026

Vallur, A. C., & Maizels, N. (2010). Distinct Activities of Exonuclease 1 and Flap Endonuclease 1 at Telomeric G4 DNA. *PLOS ONE*, *5*(1), e8908. https://doi.org/10.1371/JOURNAL.PONE.0008908

van Dam, E. M., & Robinson, P. J. (2006). Ral: Mediator of membrane trafficking. *International Journal of Biochemistry and Cell Biology*, *38*(11), 1841–1847. https://doi.org/10.1016/j.biocel.2006.04.006

van Loon, B., Markkanen, E., & Hübscher, U. (2010). Oxygen as a friend and enemy: How to combat the mutational potential of 8-oxo-guanine. *DNA Repair*, *9*(6), 604–616. https://doi.org/10.1016/J.DNAREP.2010.03.004

Van Oers, J. M. M., Roa, S., Werling, U., Liu, Y., Genschel, J., Hou, H., Sellers, R. S., Modrich, P., Scharff, M. D., & Edelmann, W. (2010). PMS2 endonuclease activity has distinct biological functions and is essential for genome maintenance. *Proceedings of the National Academy of Sciences of the United States of America*, *107*(30), 13384–13389. https://doi.org/10.1073/PNAS.1008589107/-/DCSUPPLEMENTAL

van Sluis, M., & McStay, B. (2015). A localized nucleolar DNA damage response facilitates recruitment of the homology-directed repair machinery independent of cell cycle stage. *Genes & Development*, *29*(11), 1151–1163. https://doi.org/10.1101/GAD.260703.115

van Twest, S., Murphy, V. J., Hodson, C., Tan, W., Swuec, P., O'Rourke, J. J., Heierhorst, J., Crismani, W., & Deans, A. J. (2017). Mechanism of Ubiquitination and Deubiquitination in the Fanconi Anemia Pathway. *Molecular Cell*, *65*(2), 247–259. https://doi.org/10.1016/J.MOLCEL.2016.11.005

Vanni, V. S., Campo, G., Cioffi, R., Papaleo, E., Salonia, A., Viganò, P., Lambertini, M., Candiani, M., Meirow, D., & Orvieto, R. (2022). The neglected members of the family: non-BRCA mutations in the Fanconi anemia/BRCA pathway and reproduction. *Human Reproduction Update*, *28*(2), 296–311. https://doi.org/10.1093/HUMUPD/DMAB045

Varon, R., Seemanova, E., Chrzanowska, K., Hnateyko, O., Piekutowska-Abramczuk, D., Krajewska-Walasek, M., Sykut-Cegielska, J., Sperling, K., & Reis, A. (2000). Clinical ascertainment of Nijmegen breakage syndrome (NBS) and prevalence of the major mutation, 657del5, in three Slav populations. *European Journal of Human Genetics 2000 8:11*, *8*(11), 900–902. https://doi.org/10.1038/sj.ejhg.5200554

Vechtomova, Y. L., Telegina, T. A., & Kritsky, M. S. (2020). Evolution of Proteins of the DNA Photolyase/Cryptochrome Family. *Biochemistry (Moscow) 2020 85:1*, *85*(1), 131–153. https://doi.org/10.1134/S0006297920140072

Veith, S., Schink, A., Engbrecht, M., Mack, M., Rank, L., Rossatti, P., Hakobyan, M., Goly, D., Hefele, T., Frensch, M., Fischbach, A., Bürkle, A., & Mangerich, A. (2019). PARP1 regulates DNA damage-induced nucleolar-nucleoplasmic shuttling of WRN and XRCC1 in a toxicant and protein-specific manner. *Scientific Reports*, *9*(1). https://doi.org/10.1038/S41598-019-46358-7

Verma, I. M. (2004). Nuclear factor (NF)-κB proteins: therapeutic targets*. *Annals of the Rheumatic Diseases*, *63*(Suppl 2), ii57. https://doi.org/10.1136/ARD.2004.028266

Vértessy, B. G., & Tóth, J. (2009). Keeping Uracil Out of DNA: Physiological Role, Structure and Catalytic Mechanism of dUTPases. *Accounts of Chemical Research*, *42*(1), 97. https://doi.org/10.1021/AR800114W

Vieyra-Garcia, P. A., & Wolf, P. (2021). A deep dive into UV-based phototherapy: Mechanisms of action and emerging molecular targets in inflammation and cancer. *Pharmacology & Therapeutics*, *222*, 107784. https://doi.org/10.1016/j.pharmthera.2020.107784

Viguera, E., Canceill, D., & Ehrlich, S. D. (2001). Replication slippage involves DNA polymerase pausing and dissociation. *The EMBO Journal*, *20*(10), 2587. https://doi.org/10.1093/EMBOJ/20.10.2587

Vilenchik, M. M., & Knudson, A. G. (2003). Endogenous DNA double-strand breaks: Production, fidelity of repair, and induction of cancer. *Proceedings of the National Academy of Sciences of the United States of America*, *100*(22), 12871. https://doi.org/10.1073/PNAS.2135498100

Vindigni, A., & Hickson, I. D. (2009). RecQ helicases: multiple structures for multiple

functions? *HFSP Journal*, *3*(3), 153. https://doi.org/10.2976/1.3079540
Vitolo, U., Trneny, M., Belada, D., Burke, J. M., Carella, A. M., Chua, N., Abrisqueta, P., Demeter, J., Flinn, I., Hong, X., Kim, W. S., Pinto, A., Shi, Y. K., Tatsumi, Y., Oestergaard, M. Z., Wenger, M., Fingerle-Rowson, G., Catalani, O., Nielsen, T., … Sehn, L. H. (2017). Obinutuzumab or Rituximab Plus Cyclophosphamide, Doxorubicin, Vincristine, and Prednisone in Previously Untreated Diffuse Large B-Cell Lymphoma. *Journal of Clinical Oncology : Official Journal of the American Society of Clinical Oncology*, *35*(31), 3529–3537. https://doi.org/10.1200/JCO.2017.73.3402
Walker, J. R., Corpina, R. A., & Goldberg, J. (2001). Structure of the Ku heterodimer bound to DNA and its implications for double-strand break repair. *Nature 2001 412:6847*, *412*(6847), 607–614. https://doi.org/10.1038/35088000
Waltes, R., Kalb, R., Gatei, M., Kijas, A. W., Stumm, M., Sobeck, A., Wieland, B., Varon, R., Lerenthal, Y., Lavin, M. F., Schindler, D., & Dörk, T. (2009). Human RAD50 Deficiency in a Nijmegen Breakage Syndrome-like Disorder. *American Journal of Human Genetics*, *84*(5), 605–616. https://doi.org/10.1016/j.ajhg.2009.04.010
Wang, A. T., Sengerová, B., Cattell, E., Inagawa, T., Hartley, J. M., Kiakos, K., Burgess-Brown, N. A., Swift, L. P., Enzlin, J. H., Schofield, C. J., Gileadi, O., Hartley, J. A., & McHugh, P. J. (2011). Human SNM1A and XPF–ERCC1 collaborate to initiate DNA interstrand cross-link repair. *Genes & Development*, *25*(17), 1859–1870. https://doi.org/10.1101/GAD.15699211
Wang, H., Rosidi, B., Perrault, R., Wang, M., Zhang, L., Windhofer, F., & Iliakis, G. (2005). DNA Ligase III as a Candidate Component of Backup Pathways of Nonhomologous End Joining. *Cancer Research*, *65*(10), 4020–4030. https://doi.org/10.1158/0008-5472.CAN-04-3055
Wang, H., Shi, L. Z., Wong, C. C. L., Han, X., Hwang, P. Y. H., Truong, L. N., Zhu, Q., Shao, Z., Chen, D. J., Berns, M. W., Yates, J. R., Chen, L., & Wu, X. (2013). The Interaction of CtIP and Nbs1 Connects CDK and ATM to Regulate HR-Mediated Double-Strand Break Repair. *PLoS Genetics*, *9*(2). https://doi.org/10.1371/JOURNAL.PGEN.1003277
Wang, L. C., & Gautier, J. (2010). The Fanconi anemia pathway and ICL repair: implications for cancer therapy. *Critical Reviews in Biochemistry and Molecular Biology*, *45*(5), 424. https://doi.org/10.3109/10409238.2010.502166
Wang, M., Wu, W. W., Wu, W. W., Rosidi, B., Zhang, L., Wang, H., & Iliakis, G. (2006). PARP-1 and Ku compete for repair of DNA double strand breaks by distinct NHEJ pathways. *Nucleic Acids Research*, *34*(21), 6170–6182. https://doi.org/10.1093/NAR/GKL840
Wang, P., Zhang, W., Wang, L., Liang, W., Cai, A., Gao, Y., & Chen, L. (2020). RCC2 Interacts with Small GTPase RalA and Regulates Cell Proliferation and Motility in Gastric Cancer. *OncoTargets and Therapy*, *13*, 3093–3103. https://doi.org/10.2147/OTT.S228914
Wang, R., Wang, S., Dhar, A., Peralta, C., & Pavletich, N. P. (2020). DNA clamp function of the monoubiquitinated Fanconi anaemia ID complex. *Nature 2020 580:7802*, *580*(7802), 278–282. https://doi.org/10.1038/S41586-020-2110-6
Wang, S., Guo, M., Ouyang, H., Li, X., Cordon-Cardo, C., Kurimasa, A., Chen, D. J., Fuks, Z., Clifton Ling, C., & Li, G. C. (1999). *The catalytic subunit of DNA-dependent protein kinase selectively regulates p53-dependent apoptosis but not cell-cycle arrest*. www.pnas.org
Wang, S., Wang, R., Peralta, C., Yaseen, A., & Pavletich, N. P. (2021). Structure of the FA Core ubiquitin ligase closing the ID clamp on DNA. *Nature Structural & Molecular Biology*, *28*(3), 300. https://doi.org/10.1038/S41594-021-00568-8

Wang, W., Xu, B., Zhang, Z., Fang, K., & Chang, X. (2020). RCC2 Expression Stimulates ER-Positive Breast Tumorigenesis. *Journal of Oncology*, *2020*. https://doi.org/10.1155/2020/5619462

Wasserman, M. R., Schauer, G. D., O'Donnell, M. E., & Liu, S. (2019). Replication Fork Activation Is Enabled by a Single-Stranded DNA Gate in CMG Helicase. *Cell*, *178*(3), 600-611.e16. https://doi.org/10.1016/J.CELL.2019.06.032

Watanabe, K., Tateishi, S., Kawasuji, M., Tsurimoto, T., Inoue, H., & Yamaizumi, M. (2004). Rad18 guides polη to replication stalling sites through physical interaction and PCNA monoubiquitination. *The EMBO Journal*, *23*(19), 3886–3896. https://doi.org/10.1038/SJ.EMBOJ.7600383

Waters, L. S., Minesinger, B. K., Wiltrout, M. E., D'Souza, S., Woodruff, R. V., & Walker, G. C. (2009). Eukaryotic Translesion Polymerases and Their Roles and Regulation in DNA Damage Tolerance. *Microbiology and Molecular Biology Reviews*, *73*(1), 134–154. https://doi.org/10.1128/MMBR.00034-08/ASSET/7C1A9D97-7040-4080-8EF7-1F7B91B23BD8/ASSETS/GRAPHIC/ZMR0010922090004.JPEG

Waters, L. S., & Walker, G. C. (2006). The critical mutagenic translesion DNA polymerase Rev1 is highly expressed during G2/M phase rather than S phase. *Proceedings of the National Academy of Sciences of the United States of America*, *103*(24), 8971. https://doi.org/10.1073/PNAS.0510167103

Watson, P., Black, G., Ramsden, S., Barrow, M., Super, M., Kerr, B., & Clayton-Smith, J. (2001). Angelman syndrome phenotype associated with mutations in MECP2, a gene encoding a methyl CpG binding protein. *Journal of Medical Genetics*, *38*(4), 224. https://doi.org/10.1136/JMG.38.4.224

Weeks, S. E., Metge, B. J., & Samant, R. S. (2019). The nucleolus: a central response hub for the stressors that drive cancer progression. *Cellular and Molecular Life Sciences*, *76*(22), 4511. https://doi.org/10.1007/S00018-019-03231-0

West, S. C., Blanco, M. G., Chan, Y. W., Matos, J., Sarbajna, S., & Wyatt, H. D. M. (2015). Resolution of Recombination Intermediates: Mechanisms and Regulation. *Cold Spring Harbor Symposia on Quantitative Biology*, *80*, 103–109. https://doi.org/10.1101/SQB.2015.80.027649

Westdorp, K. N., Sand, A., Moorman, N. J., & Terhune, S. S. (2017). Cytomegalovirus Late Protein pUL31 Alters Pre-rRNA Expression and Nuclear Organization during Infection. *Journal of Virology*, *91*(18). https://doi.org/10.1128/JVI.00593-17

Widschwendter, M., Jiang, G., Woods, C., Müller, H. M., Fiegl, H., Goebel, G., Marth, C., Müller-Holzner, E., Zeimet, A. G., Laird, P. W., & Ehrlich, M. (2004). DNA hypomethylation and ovarian cancer biology. *Cancer Research*, *64*(13), 4472–4480. https://doi.org/10.1158/0008-5472.CAN-04-0238

Williams, H. L., Gottesman, M. E., & Gautier, J. (2012). Replication-independent repair of DNA interstrand crosslinks. *Molecular Cell*, *47*(1), 140–147. https://doi.org/10.1016/j.molcel.2012.05.001

Williamson, R. C., Cowell, C. A. M., Hammond, C. L., Bergen, D. J. M., Roper, J. A., Feng, Y., Rendall, T. C. S., Race, P. R., & Bass, M. D. (2014). Coronin-1C and RCC2 guide mesenchymal migration by trafficking Rac1 and controlling GEF exposure. *Journal of Cell Science*, *127*(19), 4292–4307. https://doi.org/10.1242/JCS.154864/-/DC1

Winterbourn, C. C. (2008). Reconciling the chemistry and biology of reactive oxygen species. *Nature Chemical Biology 2008 4:5*, *4*(5), 278–286. https://doi.org/10.1038/nchembio.85

Wojtaszek, J., Lee, C. J., D'Souza, S., Minesinger, B., Kim, H., D'Andrea, A. D., Walker, G. C., & Zhou, P. (2012). Structural basis of rev1-mediated assembly of a quaternary vertebrate translesion polymerase complex consisting of Rev1, heterodimeric polymerase (Pol) ζ, and Pol κ. *Journal of Biological Chemistry*, *287*(40), 33836–33846. https://doi.org/10.1074/jbc.M112.394841

Wolf, M., Zehentmayr, F., Niyazi, M., Ganswindt, U., Haimerl, W., Schmidt, M., Hölzel, D., & Belka, C. (2010). Long-term outcome of mitomycin C- and 5-FU-based primary radiochemotherapy for esophageal cancer. *Strahlentherapie Und Onkologie : Organ Der Deutschen Rontgengesellschaft ... [et Al]*, *186*(7), 374–381. https://doi.org/10.1007/S00066-010-2137-Y

Woods, C. G., Bundey, S. E., & Taylor, A. M. R. (1990). Unusual features in the inheritance of ataxia telangiectasia. *Human Genetics*, *84*(6), 555–562. https://doi.org/10.1007/BF00210809/METRICS

Wu, N., Ren, D., Li, S., Ma, W., Hu, S., Jin, Y., & Xiao, S. (2018). RCC2 over-expression in tumor cells alters apoptosis and drug sensitivity by regulating Rac1 activation. *BMC Cancer*, *18*(1). https://doi.org/10.1186/S12885-017-3908-Y

Wu, Q., Liu, F., Ge, M., Laster, K. V., Wei, L., Du, R., Jiang, M., Zhang, J., Zhi, Y., Jin, G., Zhao, S., Kim, D. J., Dong, Z., & Liu, K. (2022). BRD4 drives esophageal squamous cell carcinoma growth by promoting RCC2 expression. *Oncogene*, *41*(3), 347–360. https://doi.org/10.1038/S41388-021-02099-4

Wu, R. A., Semlow, D. R., Kamimae-Lanning, A. N., Kochenova, O. V., Chistol, G., Hodskinson, M. R., Amunugama, R., Sparks, J. L., Wang, M., Deng, L., Mimoso, C. A., Low, E., Patel, K. J., & Walter, J. C. (2019). TRAIP is a master regulator of DNA interstrand crosslink repair. *Nature*, *567*(7747), 267–272. https://doi.org/10.1038/s41586-019-1002-0

Wu, R., Högberg, J., Adner, M., Ramos-Ramírez, P., Stenius, U., & Zheng, H. (2020). Crystalline silica particles cause rapid NLRP3-dependent mitochondrial depolarization and DNA damage in airway epithelial cells. *Part Fibre Toxicol.*, *17*(1). https://doi.org/10.1186/s12989-020-00370-2

Xu, X., Zhou, X., Zhang, J., Li, H., Cao, Y., Tan, X., Zhu, X., & Yang, J. (2020). MicroRNA-191 modulates cisplatin-induced DNA damage response by targeting RCC2. *FASEB Journal : Official Publication of the Federation of American Societies for Experimental Biology*, *34*(10), 13573–13585. https://doi.org/10.1096/FJ.202000945R

Xuan, J., Gitareja, K., Brajanovski, N., & Sanij, E. (2021). Harnessing the Nucleolar DNA Damage Response in Cancer Therapy. *Genes 2021, Vol. 12, Page 1156*, *12*(8), 1156. https://doi.org/10.3390/GENES12081156

Yamaguchi, H., Uchihori, Y., Yasuda, N., Takada, M., & Kitamura, H. (2005). Estimation of Yields of OH Radicals in Water Irradiated by Ionizing Radiation. *Journal of Radiation Research*, *46*(3), 333–341. https://doi.org/10.1269/JRR.46.333

Yamanaka, K., Chatterjee, N., Hemann, M. T., & Walker, G. C. (2017). Inhibition of mutagenic translesion synthesis: A possible strategy for improving chemotherapy? *PLOS Genetics*, *13*(8), e1006842. https://doi.org/10.1371/JOURNAL.PGEN.1006842

Yan, S., & Michael, W. M. (2009). TopBP1 and DNA polymerase-α directly recruit the 9-1-1 complex to stalled DNA replication forks. *The Journal of Cell Biology*, *184*(6), 793. https://doi.org/10.1083/JCB.200810185

Yan, Z., Delannoy, M., Ling, C., Daee, D., Osman, F., Muniandy, P. A., Shen, X., Oostra, A. B., Du, H., Steltenpool, J., Lin, T., Schuster, B., Décaillet, C., Stasiak, A., Stasiak, A. Z., Stone, S., Hoatlin, M. E., Schindler, D., Woodcock, C. L., … Wang, W. (2010). A Histone-Fold

Complex and FANCM Form a Conserved DNA-Remodeling Complex to Maintain Genome Stability. *Molecular Cell*, *37*(6), 865–878. https://doi.org/10.1016/j.molcel.2010.01.039

Yang, C., Kim, M. S., Chakravarty, D., Indig, F. E., & Carrier, F. (2009). Nucleolin Binds to the Proliferating Cell Nuclear Antigen and Inhibits Nucleotide Excision Repair. *Molecular and Cellular Pharmacology*, *1*(3), 130. https://doi.org/10.4255/MCPHARMACOL.09.17

Yang, C., Maiguel, D. A., & Carrier, F. (2002). Identification of nucleolin and nucleophosmin as genotoxic stress-responsive RNA-binding proteins. *Nucleic Acids Research*, *30*(10), 2251. https://doi.org/10.1093/NAR/30.10.2251

Yang, F., Camp, D. G., Gritsenko, M. A., Luo, Q., Kelly, R. T., Clauss, T. R. W., Brinkley, W. R., Smith, R. D., & Stenoien, D. L. (2007). Identification of a novel mitotic phosphorylation motif associated with protein localization to the mitotic apparatus. *Journal of Cell Science*, *120*(Pt 22), 4060–4070. https://doi.org/10.1242/JCS.014795

Yang, K., Moldovan, G. L., Vinciguerra, P., Murai, J., Takeda, S., & D'Andrea, A. D. (2011). Regulation of the Fanconi anemia pathway by a SUMO-like delivery network. *Genes & Development*, *25*(17), 1847–1858. https://doi.org/10.1101/GAD.17020911

Yang, K., Yang, J., & Yi, J. (2018). Nucleolar Stress: hallmarks, sensing mechanism and diseases. *Cell Stress*, *2*(6), 125. https://doi.org/10.15698/CST2018.06.139

Yang, Y., Gao, Y., Zlatanou, A., Tateishi, S., Yurchenko, V., Rogozin, I. B., & Vaziri, C. (2018). Diverse roles of RAD18 and Y-family DNA polymerases in tumorigenesis. *Https://Doi.Org/10.1080/15384101.2018.1456296*, *17*(7), 833–843. https://doi.org/10.1080/15384101.2018.1456296

Yang, Y., & Herrup, K. (2005). Loss of Neuronal Cell Cycle Control in Ataxia-Telangiectasia: A Unified Disease Mechanism. *The Journal of Neuroscience*, *25*(10), 2522. https://doi.org/10.1523/JNEUROSCI.4946-04.2005

Yao, N. Y., & O'Donnell, M. (2010). SnapShot: The Replisome. *Cell*, *141*(6), 1088. https://doi.org/10.1016/J.CELL.2010.05.042

Yao, Y., & Dai, W. (2014). Genomic Instability and Cancer. *Journal of Carcinogenesis & Mutagenesis*, *05*(02). https://doi.org/10.4172/2157-2518.1000165

Yao, Y., Li, X., Chen, W., Liu, H., Mi, L., Ren, D., Mo, A., & Lu, P. (2020). ATM Promotes RAD51-Mediated Meiotic DSB Repair by Inter-Sister-Chromatid Recombination in Arabidopsis. *Frontiers in Plant Science*, *11*, 839. https://doi.org/10.3389/FPLS.2020.00839/BIBTEX

Yeeles, J. T. P., Poli, J., Marians, K. J., & Pasero, P. (2013). Rescuing Stalled or Damaged Replication Forks. *Cold Spring Harbor Perspectives in Biology*, *5*(5). https://doi.org/10.1101/CSHPERSPECT.A012815

Yenjerla, M., Panopoulos, A., Reynaud, C., Fotedar, R., & Margolis, R. L. (2013). TD-60 is required for interphase cell cycle progression. *Cell Cycle (Georgetown, Tex.)*, *12*(5), 837–841. https://doi.org/10.4161/CC.23821

Yi, C., & He, C. (2013). DNA repair by reversal of DNA damage. *Cold Spring Harbor Perspectives in Biology*, *5*(1). https://doi.org/10.1101/CSHPERSPECT.A012575

Yi, J. M., Eun-Jin, Hyun-Mi, Bae, J. H., Kang, K., Ahuja, N., & Yang, K. (2017). Epigenetically altered miR-1247 functions as a tumor suppressor in pancreatic cancer. *Oncotarget*, *8*(16), 26600–26612. https://doi.org/10.18632/ONCOTARGET.15722

Yilmaz, D., Furst, A., Meaburn, K., Lezaja, A., Wen, Y., Altmeyer, M., Reina-San-Martin, B., & Soutoglou, E. (2021). Activation of homologous recombination in G1 preserves centromeric integrity. *Nature 2021 600:7890*, *600*(7890), 748–753.

https://doi.org/10.1038/s41586-021-04200-z
Yokoyama, H., & Mizutani, R. (2014). Structural Biology of DNA (6-4) Photoproducts Formed by Ultraviolet Radiation and Interactions with Their Binding Proteins. *International Journal of Molecular Sciences*, *15*(11), 20321. https://doi.org/10.3390/IJMS151120321
Yonekura, S. I., Nakamura, N., Yonei, S., & Zhang-Akiyama, Q. M. (2009). Generation, biological consequences and repair mechanisms of cytosine deamination in DNA. *Journal of Radiation Research*, *50*(1), 19–26. https://doi.org/10.1269/JRR.08080
Yoon, J. H., Prakash, S., & Prakash, L. (2012). Requirement of Rad18 protein for replication through DNA lesions in mouse and human cells. *Proceedings of the National Academy of Sciences of the United States of America*, *109*(20), 7799–7804. https://doi.org/10.1073/PNAS.1204105109/SUPPL_FILE/PNAS.201204105SI.PDF
Yoshikawa, H., Komatsu, W., Hayano, T., Miura, Y., Homma, K., Izumikawa, K., Ishikawa, H., Miyazawa, N., Tachikawa, H., Yamauchi, Y., Isobe, T., & Takahashi, N. (2011). Splicing factor 2-associated protein p32 participates in ribosome biogenesis by regulating the binding of Nop52 and fibrillarin to preribosome particles. *Molecular and Cellular Proteomics*, *10*(8). https://doi.org/10.1074/mcp.M110.006148
Yu, H., Zhang, S., Ibrahim, A. N., Wang, J., Deng, Z., & Wang, M. (2019). RCC2 promotes proliferation and radio-resistance in glioblastoma via activating transcription of DNMT1. *Biochemical and Biophysical Research Communications*, *516*(3), 999–1006. https://doi.org/10.1016/J.BBRC.2019.06.097
Zamore, P. D., Patton, J. G., & Green, M. R. (1992). Cloning and domain structure of the mammalian splicing factor U2AF. *Nature*, *355*(6361), 609–614. https://doi.org/10.1038/355609A0
Zellweger, R., Dalcher, D., Mutreja, K., Berti, M., Schmid, J. A., Herrador, R., Vindigni, A., & Lopes, M. (2015). Rad51-mediated replication fork reversal is a global response to genotoxic treatments in human cells. *Journal of Cell Biology*, *208*(5), 563–579. https://doi.org/10.1083/JCB.201406099
Zeman, M. K., & Cimprich, K. A. (2013). Causes and consequences of replication stress. *Nature Cell Biology 2014 16:1*, *16*(1), 2–9. https://doi.org/10.1038/ncb2897
Zhang, J., Dewar, J. M., Budzowska, M., Motnenko, A., Cohn, M. A., & Walter, J. C. (2015). DNA interstrand cross-link repair requires replication-fork convergence. *Nature Structural & Molecular Biology*, *22*(3), 242–247. https://doi.org/10.1038/nsmb.2956
Zhang, J., & Walter, J. C. (2014). Mechanism and regulation of incisions during DNA interstrand cross-link repair. *DNA Repair*, *19*, 135–142. https://doi.org/10.1016/J.DNAREP.2014.03.018
Zhang, M., Wang, L., & Zhong, D. (2017). Photolyase: Dynamics and electron-transfer mechanisms of DNA repair. *Archives of Biochemistry and Biophysics*, *632*, 158–174. https://doi.org/10.1016/J.ABB.2017.08.007
Zhang, N., Shen, Y., Li, H., Chen, Y., Zhang, P., Lou, S., & Deng, J. (2022). The m6A reader IGF2BP3 promotes acute myeloid leukemia progression by enhancing RCC2 stability. *Experimental & Molecular Medicine*, *54*(2), 194–205. https://doi.org/10.1038/S12276-022-00735-X
Zhang, Y., & Lu, H. (2009). Signaling to p53: Ribosomal Proteins Find Their Way. *Cancer Cell*, *16*(5), 369–377. https://doi.org/10.1016/J.CCR.2009.09.024
Zhao, F., Kim, W., Kloeber, J. A., & Lou, Z. (2020). DNA end resection and its role in DNA replication and DSB repair choice in mammalian cells. *Experimental & Molecular Medicine 2020 52:10*, *52*(10), 1705–1714. https://doi.org/10.1038/s12276-020-00519-

1
Zheng, J., Lang, Y., Zhang, Q., Cui, D., Sun, H., Jiang, L., Chen, Z., Zhang, R., Gao, Y., Tian, W., Wu, W., Tang, J., & Chen, Z. (2015). Structure of human MDM2 complexed with RPL11 reveals the molecular basis of p53 activation. *Genes & Development*, *29*(14), 1524. https://doi.org/10.1101/GAD.261792.115

Zhi, G., Wilson, J. B., Chen, X., Krause, D. S., Xiao, Y., Jones, N. J., & Kupfer, G. M. (2009). Fanconi anemia complementation group FANCD2 protein serine 331 phosphorylation is important for Fanconi anemia pathway function and BRCA2 interaction. *Cancer Research*, *69*(22), 8775–8783. https://doi.org/10.1158/0008-5472.CAN-09-2312/655584/P/FANCONI-ANEMIA-COMPLEMENTATION-GROUP-FANCD2

Zhong, D. (2015). Electron transfer mechanisms of DNA repair by photolyase. *Annual Review of Physical Chemistry*, *66*, 691–715. https://doi.org/10.1146/ANNUREV-PHYSCHEM-040513-103631

Zhou, J., Chan, J., Lambelé, M., Yusufzai, T., Stumpff, J., Opresko, P. L., Thali, M., & Wallace, S. S. (2017). NEIL3 repairs telomere damage during S phase to secure chromosome segregation at mitosis. *Cell Reports*, *20*(9), 2044. http://dx.doi.org/10.1016/j.celrep.2017.08.020

Zhu, Y., Wang, G. Z., Cingöz, O., & Goff, S. P. (2018). NP220 mediates silencing of unintegrated retroviral DNA. *Nature*, *564*(7735), 278–282. https://doi.org/10.1038/s41586-018-0750-6

Zhu, Z., Chung, W. H., Shim, E. Y., Lee, S. E., & Ira, G. (2008). Sgs1 Helicase and Two Nucleases Dna2 and Exo1 Resect DNA Double-Strand Break Ends. *Cell*, *134*(6), 981–994. https://doi.org/10.1016/j.cell.2008.08.037

Ziv, Y., Bielopolski, D., Galanty, Y., Lukas, C., Taya, Y., Schultz, D. C., Lukas, J., Bekker-Jensen, S., Bartek, J., & Shiloh, Y. (2006). Chromatin relaxation in response to DNA double-strand breaks is modulated by a novel ATM-and KAP-1 dependent pathway. *Nature Cell Biology*, *8*(8), 870–876. https://doi.org/10.1038/NCB1446

Zou, L., & Elledge, S. J. (2003). Sensing DNA damage through ATRIP recognition of RPA-ssDNA complexes. *Science*, *300*(5625), 1542–1548. https://doi.org/10.1126/SCIENCE.1083430/SUPPL_FILE/ZOU.SOM.PDF